IAEA-TECDOC-1269

Isotope aided studies of atmospheric carbon dioxide and other greenhouse gases

Phase II

IAEA

January 2002

The IAEA does not normally maintain stocks of reports in this series. They are however collected by the International Nuclear Information System (INIS) as non-conventional literature. Should a document be out of print, a copy on microfiche or in electronic format can be purchased from the INIS Document Delivery Services:

INIS Clearinghouse
International Atomic Energy Agency
Wagramer Strasse 5
P.O. Box 100
A-1400 Vienna, Austria

Telephone: (43) 1 2600 22880 or 22866
Fax: (43) 1 2600 29882
E-mail: chouse@iaea.org

Orders should be accompanied by prepayment of 100 Austrian Schillings in the form of a cheque or credit card (VISA, Mastercard).

More information on the INIS Document Delivery Services and a list of national document delivery services where these reports can also be ordered can be found on the INIS Web site at http://www.iaea.org/inis/dd_srv.htm.

PLEASE BE AWARE THAT
ALL OF THE MISSING PAGES IN THIS DOCUMENT
WERE ORIGINALLY BLANK

IAEA-TECDOC-1269

Isotope aided studies of atmospheric carbon dioxide and other greenhouse gases

Phase II

INTERNATIONAL ATOMIC ENERGY AGENCY IAEA

January 2002

The originating Section of this publication in the IAEA was:

Isotope Hydrology Section
International Atomic Energy Agency
Wagramer Strasse 5
P.O. Box 100
A-1400 Vienna, Austria

ISOTOPE AIDED STUDIES OF ATMOSPHERIC CARBON DIOXIDE AND OTHER GREENHOUSE GASES — PHASE II

IAEA, VIENNA, 2002
IAEA-TECDOC-1269
ISSN 1011–4289

Printed by the IAEA in Austria
January 2002

FOREWORD

The substantial increase in atmospheric greenhouse gas concentrations and their role in global warming have become major concerns of world governments. Application of isotope techniques to label sources and sinks of CO_2 and other greenhouse gases has emerged as a potentially powerful method for reducing uncertainties in the global CO_2 budgets and for tracing pathways and interaction of terrestrial, oceanic, and atmospheric pools of carbon. As with CO_2 concentration measurements, meaningful integration of isotopes in global models requires careful attention to quality assurance, quality control and inter-comparability of measurements made by a number of networks and laboratories. To support improvements in isotope measurement capabilities, the IAEA began implementing Co-ordinated Research Projects (CRPs) in 1992. The first project, entitled Isotope Variations of Carbon Dioxide and other Trace Gases in the Atmosphere, was implemented from 1992 to 1994. A significant contribution was made towards a better understanding of the global carbon cycle and especially of the sources and sinks of carbon with data on the ^{14}C and ^{13}C content of atmospheric CO_2, pointing to a better understanding of the problem of the "missing sink" in the global carbon cycle. Important methodological developments in the field of high precision stable isotope mass spectrometry and improved data acquisition procedures emerged from work carried out within the framework of this programme. The development of pressurized gas standards and planning for an associated interlaboratory calibration were initiated. Due to the good progress and long standing nature of the required work a second CRP was initiated and implemented from 1996 to 1999. It was entitled Isotope aided Studies of Atmospheric Carbon Dioxide and Other Trace Gases — Phase II, to document the close relationship of both programmes. This publication provides an overview of the scientific outcomes of the studies conducted within Phase II of the project, which incorporate the findings of both CRPs. This report was compiled with the aid of H.A.J. Meijer, Groningen University, Netherlands, who organized the peer review. Special thanks are given to those who contributed to the peer review of the individual contributions. M. Gröning of the Isotope Hydrology Section was the IAEA officer responsible for the publication.

This publication is closely related to IAEA-TECDOC-1268, Stable Isotope Measurement Techniques for Atmospheric Greenhouse Gases, also resulting from the above mentioned projects, and providing technical information on the state of the art of the applied measurement techniques. That publication is aimed at providing useful information for laboratories, which are considering to engaging themselves in such long-term monitoring programmes.

EDITORIAL NOTE

This publication has been prepared from the original material as submitted by the authors. The views expressed do not necessarily reflect those of the IAEA, the governments of the nominating Member States or the nominating organizations.

The use of particular designations of countries or territories does not imply any judgement by the publisher, the IAEA, as to the legal status of such countries or territories, of their authorities and institutions or of the delimitation of their boundaries.

The mention of names of specific companies or products (whether or not indicated as registered) does not imply any intention to infringe proprietary rights, nor should it be construed as an endorsement or recommendation on the part of the IAEA.

The authors are responsible for having obtained the necessary permission for the IAEA to reproduce, translate or use material from sources already protected by copyrights.

CONTENTS

Summary 1

The International Atomic Energy Agency circulation of laboratory air standards for stable isotope comparisons: Aims, preparation and preliminary results 5
C. Allison, R.J. Francey, L.P. Steele

Constraining the global carbon budget from global to regional scales — The measurement challenge 25
R.J. Francey, P.J. Rayner, C.E. Allison

Atmospheric ^{14}C in urban, agricultural, mountain and costal areas in Greece 37
N. Zouridakis

Tropospheric CO_2 in Romania: Concentration and isotopic composition measurements 41
A. Tenu, F. Davidescu, V. Cucleanu

^{222}Rn and $^{14}CO_2$ concentrations in the surface layer of the atmosphere 59
K. Holý, M. Chudý, A. Šivo, M. Richtáriková, R. Böhm, A. Polášková, O. Holá, P. Vojtyla, I. Bosá

Isotope variations of carbon dioxide, methane and other trace gases in Cracow and Kasprowy, Poland 69
T. Florkowski

Monsoon signatures in trace gas records from Cape Rama, India 81
S.K. Bhattacharya, R.A. Jani, D.V. Borole, R.J. Francey, C.E. Allison, L.P. Steele, K.A. Masarie

The development of O_2/N_2 measurement capability at the CIO Groningen 91
R.E.M. Neubert, H.A.J. Meijer

The determination of $\delta^{13}C$ in atmospheric methane in the Southern Hemisphere 97
D.C. Lowe, M.R. Manning

Isotopic discrimination during nitrous oxide loss processes: An important piece of the N_2O global atmospheric budget 107
T. Rahn, M. Wahlen, Hui Zhang, G. Blake

Thermal diffusion: An important aspect in studies of static air columns such as firn air, sand dunes, and soil air 115
M. Leuenberger, C. Lang

List of Participants 129

SUMMARY

Global greenhouse gas concentration measurements are increasingly being supplemented by isotopic measurements to provide additional independent information on sources and sinks of these gases. The Co-ordinated Research Project (CRP) on Isotope-aided Studies of Atmospheric Carbon Dioxide and Other Trace Gases — Phase II was carried out during 1996–1999 to evaluate the performance of isotope labeling techniques used for estimating the fraction of greenhouse gases originating from various natural and anthropogenic sources. The project, involving 17 principal investigators from 14 countries including Australia, Ecuador, France, Germany, Greece, India, Japan, the Netherlands, New Zealand, Poland, Romania, Slovakia, Switzerland, and the United States of America, was aimed at identifying the principle benefits and drawbacks of isotope-based research, and steps required to obtain optimal benefit from the methodology in the future. This project was undertaken in continuation of a first CRP on Isotope Variations of Carbon Dioxide and Other Trace Gases in the Atmosphere (1992–1994), which involved the same group of institutions and had initiated most of the work reported here. Due to the long-term nature of the required monitoring work with required multi-annual datasets, the results presented below are mostly the outcome of work conducted within the framework of both CRPs.

Studies to date have established that isotopic signatures can be used to trace the origin of greenhouse gases, but due to atmospheric mixing, the resulting isotope signals are often subdued and sometimes approach the analytical uncertainty. A difference of 0.01‰ in $\delta^{13}C$ in CO_2 on a global scale, for example, resembles a source/sink term either from biospheric/fossil fuel or from oceanic origin of roughly 0.4 Pg of Carbon (for CO_2). Furthermore, an effective source identification of methane requires an accuracy of <0.1‰ in $\delta^{13}C$. Therefore, the contribution of isotope measurements is only valuable if measurements are performed with (i) high individual precision, using specially designed protocols, and suitable machinery (ii) high accuracy, which includes reliable long-term calibration of the laboratory, (iii) reliable inter-calibration between the different laboratories. Assessment of this latter feature requires, among other things, frequent exchange of samples and reference gases. The implementation of a laboratory inter-comparison exercise based on high-pressure cylinders called "Circulation of Laboratory Air Standards for Stable Isotope InterComparisons" (CLASSIC) was undertaken as a component of this programme, and preliminary results from the first round of inter-comparisons are presented by Allison et al. (this volume). The most important result of the exercise was to determine that substantial errors (up to 40%) may arise from computational problems related to scale conversions. Also, problems with non-linearity and scale contraction in some laboratories were also distinguished. The need for continued inter-calibration is further demonstrated by Francey et al. (this volume) who discuss a proposed world-wide inter-comparison scheme for the future.

Another issue addressed in the CRP was the world-wide coverage of monitoring stations. Although the involvement of developing countries remains limited, new groups from Europe (Greece, Romania), as well as from Ecuador and India have recently joined international efforts for monitoring the concentration and isotopic composition of greenhouse gases.

Measurement of $^{14}CO_2$ from 14 sites comprising the Greek national network are presented. Other data, mainly ^{14}C, but also CO_2 concentrations, and ^{13}C isotope measurements, are also presented for Bucharest and a remote site in Romania. Somewhat surprisingly, the ^{14}C values for the remote site are significantly above those for Bucharest only in the last year of measurements. A long time-series of $^{14}CO_2$ measurements for a densely populated area

(Bratislava) and a remote site in Slovakia are also presented which suggest that the ^{14}C signal of the Bratislava area is much closer to the European background signal after 1993 than before. This is in accordance with the trade-based numbers on fossil fuel combustion in Slovakia. The tracer ^{222}Rn is also shown to be useful for computing CO_2 fluxes from concentrations. In a comparison of an industrial zone (Krakow) with a remote, mountain station (Kasprowy), Florkowski et al. present a whole suite of measurements, namely CO_2 concentration and ^{13}C, ^{18}O and ^{14}C isotopes, CH_4 concentration and ^{13}C isotopes, and finally SF_6. For CO_2, they present a breakdown of the different components. Furthermore, based on ^{14}C, they estimate the percentage of fossil fuel-deduced CO_2 in Krakow. As in Slovakia, their results confirm the decrease of fossil fuel consumption in Eastern Europe in the 90s. A different example of a regional study is presented by Bhattacharya et al. Their monitoring station at Cape Rama is influenced by the monsoon system. During the south-west monsoon it shows oceanic "atmospheric background" features, whereas during the north-west monsoon air is transported from the Indian sub-continent. Concentrations of CO_2, CH_4, CO, N_2O and H_2 are presented, as well as the ^{13}C and ^{18}O isotopes from CO_2.

In addition to CO_2 isotopes, the highly precise measurement of atmospheric oxygen, a technique that has been developed in the past several years, has been shown to provide highly valuable additional information about the Carbon/CO_2 sources and sinks. Although actually being a concentration measurement, the measurement technique applied is identical to that for isotope ratios. At present, six labs in the world can perform these atmospheric measurements. Owing to the potential of this method, it is expected that more laboratories will develop and apply O_2 measurements as part of their atmospheric sampling networks.

Methane is also an important greenhouse gas and recent analytical improvements have enabled identification of variable source/sink patterns for methane in detailed measurements conducted at two stations in the Southern Hemisphere (Baring Head, New Zealand and Scott Base, Antarctica), as well as four voyages between New Zealand and the US west coast.

Isotope measurements are also being used to elucidate the sources and sinks of another important, anthropogenically influenced greenhouse gas, N_2O. Although sources and sinks are poorly known at the moment, early studies suggest that isotopes can help to resolve some of the important dilemmas.

Leuenberger and Lang present an evaluation study on thermodiffusion, aimed at interpretation of isotope ratio results for static air columns, such as in firn air (ice cores). Thermodiffusion corrections normally need to be applied to obtain long-time series records (e.g. CO_2 isotopes in ice cores), but the process also offers potential for direct assessment of temperature and climate changes in the past.

Overall, the studies conducted within this CRP establish that isotopic composition is a powerful marker of greenhouse gas origin. Specific problems are also identified which include subdued or weak isotopic signals, inter-laboratory uncertainty, spatial coverage in developing countries, and a lack of distinct labelling of some natural and anthropogenic sources. Importantly, the research community has already begun to address these problems by expanding global and regional networks for monitoring the isotopic composition of trace gases, by supporting comparative studies of isotopic signatures in industrialized versus non-industrialized areas, and by fostering development of new tracer techniques utilizing atmospheric O_2, methane, and N_2O. An important contribution of the CRP is the co-ordination of a first, cooperative inter-laboratory comparison exercise to improve systematic

measurement, quality assurance and quality control. These and similar activities will be required to allow high-confidence partitioning of sources and to assist in meaningful integration of global databases in the future.

This publication is closely related to IAEA-TECDOC-1268, Stable Isotope Measurement Techniques for Atmospheric Greenhouse Gases, resulting from co-ordinated work of participants of this CRP and aiming to provide the state of the art on measurement and extraction techniques. The information in that TECDOC is felt to be particularly important for laboratories planning to engage themselves in the future in monitoring activities of atmospheric greenhouse gases and it provides many links, references and contact addresses to encourage and to facilitate the establishment of further similar monitoring programmes.

THE INTERNATIONAL ATOMIC ENERGY AGENCY CIRCULATION OF LABORATORY AIR STANDARDS FOR STABLE ISOTOPE COMPARISONS: AIMS, PREPARATION AND PRELIMINARY RESULTS

C.E. ALLISON, R.J. FRANCEY, L.P. STEELE
CSIRO Atmospheric Research,
Aspendale, Victoria, Australia

Abstract. Ten air standards in high-pressure aluminium cylinders were prepared, covering a specified range of CO_2 concentration and $\delta^{13}C$ and δ^{18O} isotopic composition, to be used for laboratory intercomparisons with the primary aim of merging global atmospheric CO_2 $\delta\ ^{13}C$ data sets. After establishing the stability of the standards, five were circulated between four laboratories with established high precision global monitoring networks to quantify differences between the measurement scales used in the laboratories. Measurements of CO_2 concentration in three of the four laboratories showed agreement to better than 0.2 ppm for the five standards. Measurements of N_2O concentration reported by three of the laboratories agreed to better than 3 ppb after correction for known scaling factor differences, but a fourth laboratory reported results for two cylinders lower by about 20 ppb, contributing a $\delta\ ^{13}C$ uncertainty of about 0.012 ‰ for these two cylinders. The reported measurements of the $\delta\ ^{13}C$ and δ^{18O} of CO_2 extracted from the air in the five standards showed large offsets between the laboratories of up to 0.1‰ in $\delta\ ^{13}C$ and up to 1‰ in δ^{18O}. Analysis of the results shows that about 40% of the offsets arises from differences in the procedures used in each laboratory to calculate the $\delta\ ^{13}C$ and $\delta^{18}O$ values from the raw measurements and that the remainder arises from the pre-concentration step. Using one of the circulated standards to "normalise" the others removes most of the inter-laboratory differences but there remains a non-linear response in one or more laboratories. The differences in $\delta^{13}C$ that remain after normalisation are larger than the target precision of 0.01 ‰.

1. INTRODUCTION

Measurements of the concentration and isotopic composition of CO_2 in the atmosphere play a key role in understanding the global carbon budget. Several sample collection networks provide spatial and temporal coverage of CO_2 concentration and its stable carbon ($\delta^{13}C$) and oxygen ($\delta^{18}O$) isotopic composition [1,2,3,4]. However, there are problems in comparing the collected data to the target precision specified for budgeting studies [5] of 0.05 ppm for CO_2 concentration and 0.01‰ (per mil) for $\delta^{13}C$ [1] (no specific precision target for $\delta^{18}O$ has yet been recommended in this forum). For CO_2 concentration, the target precision is close to the internal analytical precision that is routinely obtained by most laboratories. In the most recent international World Meteorological Organization (WMO) round-robin exercise [7], eighteen laboratories measured air in sets of three high-pressure cylinders that had been analysed by one central laboratory to have CO_2 concentrations of about 342 ppm, 360 ppm

---

[1] The δ-notation is used for stable isotope composition. This notation expresses the ratio of the abundance of the heavy isotope to the abundance of the light isotope in a sample, eg ^{13}C and ^{12}C in CO_2, with respect to the same ratio in a reference material as

$$\delta^{13}C = \frac{\left(^{13}C/_{12}C\right)_{\text{Sample}}}{\left(^{13}C/_{12}C\right)_{\text{Reference}}} - 1.$$

As $\delta^{13}C$ values are very small, they are usually multiplied by 1000 and given the units "per mil" or "‰". For CO_2 the Reference is VPDB-CO_2 (realised through the preparation of NBS19 carbonate) and is usually identified by $\delta^{13}C_{VPDB}$ (see [6] for more details). Throughout this paper, $\delta^{13}C$ and $\delta^{18}O$ are used to refer to isotope measurements in general and for explicit values. Where explicit values are used, the VPDB-CO_2 standard is assumed.

and 375 ppm. Of the eighteen laboratories, only eight, six and four agreed with the central laboratory to within 0.05 ppm at these CO_2 concentrations respectively. GLOBALVIEW-CO_2 [8] is a pioneering attempt to merge CO_2 concentration data from many international laboratories; however, the GLOBALVIEW-CO_2 compilation generally does not yet incorporate intercalibration differences such as those observed in the WMO comparison. For the isotopes of atmospheric CO_2, merging data from different laboratories is even less advanced.

To address this, the International Atomic Energy Agency (IAEA) Isotope Hydrology Section established a project inside their Co-ordinated Research Project on Isotope Aided Studies of Atmospheric Carbon Dioxide and Other Trace Gases — Phase II, to produce and test a set of high-pressure air standards for interlaboratory comparisons. This project is known as CLASSIC: **C**irculation of **L**aboratory **A**ir **S**tandards for **S**table **I**sotope inter **C**omparisons [9].

The initial CLASSIC proposal was for CSIRO Atmospheric Research to prepare ten air standards: high-pressure cylinders of air with CO_2 concentration and isotopic composition bracketing that of the present atmosphere. The composition of the air in the standards was designed so that CO_2 concentration ranged from about 320 ppm to 400 ppm, $\delta^{13}C$ ranged from about –6‰ to –10‰ and $\delta^{18}O$ varied from about 0‰ to –4‰. The co-variation of $\delta^{13}C$ with CO_2 was selected to be similar to that observed in CO_2 exchange between the atmosphere and the terrestrial biosphere. Further, it was planned to vary the concentration of nitrous oxide (N_2O) in the standards to test the procedure used to correct for N_2O (co-trapped with the CO_2 in the cryogenic extraction procedures used in all four laboratories) that interferes with the $\delta^{13}C$ and $\delta^{18}O$ measurements. To this end, the ten standards were prepared as two sets of five: each set of five covering the target CO_2 concentration and isotopic composition ranges but one set having elevated N_2O concentrations. Five standards were selected for circulation from the ten prepared. Sample handling and data reporting protocols were prepared and distributed with the standards (see Section 2.3). These protocols were designed to minimise uncertainties that may arise from sample handling procedures and to elucidate uncertainties that may arise from CO_2 extraction from air, ion correction algorithms (^{17}O, N_2O) and mass spectrometer non-linearity [10, 6].

In order to make a preliminary assessment of the feasibility and effectiveness of intercalibrating stable isotope measurements with air standards in high-pressure cylinders, four laboratories with established measurement programs were selected. The four laboratories are identified in Table 1 [CSIRO:11, CMDL:4, SIO:12, TU:3]. Each of these four laboratories possess methodologies for high-precision measurement of the concentration of CO_2 and N_2O in addition to their ability to perform high-precision isotopic composition measurements on CO_2 extracted from atmospheric air. Table 1 summarizes the techniques used in each of the laboratories. Assessment of the results occurred after a complete circulation of the subset of five standards that started and finished with analysis at CSIRO.

Along with the CLASSIC standards, two low-pressure canisters of high purity CO_2 with isotopic composition close to that of atmospheric CO_2 were circulated between the four laboratories to provide isotopic measurements free from any effects that may arise from the pre-concentration step, i.e. the extraction of CO_2 from air. These canisters of CO_2, designated GS19B and GS20B, were provided by the University of Groningen [13]. The IAEA has provided a set of international reference materials, comprising NBS19 and NBS18 carbonates and VSMOW and SLAP waters, to each laboratory, independently of the gases, to use for calibration purposes. This first report describes the preparation of the ten air standards and presents the results from the first completed circulation of the five CLASSIC standards and the two low-pressure canisters of CO_2.

Table 1. Details of the laboratories involved in the initial circulation of the classic standards. For each species, the technique used in each laboratory, and the typical volume of air (at STP) required for the analysis of that species, is given.

Laboratory	Commonwealth Scientific and Industrial Research Organisation - Atmospheric Research, Aspendale, Victoria, Australia	Institute of Arctic and Alpine Research, University of Colorado, Boulder, Colorado, USA & National Oceanic and Atmospheric Administration Climate Monitoring & Diagnostics Laboratory, Boulder, Colorado, USA	Scripps Institution of Oceanography, University of California, San Diego, California, USA	Center for Atmospheric and Oceanic Studies, Tohoku University, Sendai, Japan
Code	CSIRO	CMDL	SIO	TU
Contacts	C.E. Allison & R.J. Francey	J.W.C. White & P.P. Tans	M. Wahlen	T. Nakazawa
CO_2	GC-FID[1] 30 millilitres	NDIR[2] 200 millilitres	NDIR n/a	NDIR 900 millilitres
N_2O	GC-ECD[3] 30 millilitres	GC-ECD n/a	GC-ECD 500 millilitres	GC-ECD 150 millilitres
$\delta^{13}C$ & $\delta^{18}O$	Dual Inlet IRMS[4] (Finnigan MAT252) Online extraction 50 millilitres	Dual Inlet IRMS (Fisons OPTIMA) Online extraction 400 millilitres	Dual Inlet IRMS (Fisons PRISM II) Offline extraction 5 litres	Dual Inlet IRMS (Finnigan DELTA S) Offline extraction 500 millilitres

[1] GC-FID: Gas Chromatograph - Flame Ionisation Detector

[2] NDIR: Non-Dispersive Infra-Red analyser

[3] GC-ECD: Gas Chromatograph - Electron Capture Detector

[4] IRMS: Isotope Ratio Mass Spectrometer

2. THE **CLASSIC** STANDARDS

2.1 Filling of the cylinders

Ten 29.5 litre aluminium cylinders, manufactured by Luxfer (Riverside, California, USA) were purchased from Scott-Marin (Riverside, California, USA). Each cylinder is fitted with a Ceodeux brass, packless diaphragm valve and is used with a dedicated Air Products (Allentown, Pennsylvania, USA) nickel-plated brass body, 2-stage, stainless steel diaphragm regulator. Scott Specialty Gases, Inc. (San Bernadino, California, USA) passivated the internal cylinder surfaces using their ACULIFE IV process and filled the cylinders with clean dry nitrogen for shipping to CSIRO. After receipt at CSIRO each cylinder was vented and then flushed with chemically dried air following a procedure developed for archiving air [14, 15]. In the flushing procedure, each cylinder was pressurised to about 1100 kPa and vented to atmospheric pressure four times before being filled to about 6800 kPa. The cylinders were then vented and re-pressurised to 6800 kPa and stored for between seven and twenty-eight days prior to filling, as described below.

The flushing and filling of the cylinders was done at Cape Schanck on the southern coast of Australia (38°29'S, 144°53'E). Air was collected under conditions of strong, south westerly winds from the ocean using a high-pressure compressor system built around a RIX SA-3 "Sweet Air" oil-free compressor (RIX, Emeryville, California, USA). Two drying towers, each containing about 40 g of phosphorous pentoxide, were used to chemically dry the

air during collection. Each cylinder contained a mixture of about 3200 standard litres of dry air, 800 standard litres of "CO_2-free" dry air (prepared by inserting a soda asbestos trap in series with the drying towers) and a few hundred millilitres of "spiking" CO_2 with a specific isotopic composition. Measurements of the water vapour levels in each of the standards with a Meeco Aquamatic + Moisture Analyser (Meeco, Inc., Warrington, Pennsylvania, USA) confirmed that in all cases the air standards contained water levels less than 1 ppm.

Five distinct spiking CO_2 gases were prepared by mixing two pure CO_2 gases with different isotopic compositions: one with $\delta^{13}C$ = -28.5‰ and $\delta^{18}O$ = -19.5‰ and the second with $\delta^{13}C$ = 2.27‰ and $\delta^{18}O$ = 0.60‰. Two "spikes" of each target isotopic composition were prepared and a small amount of N_2O (99%: Matheson Gas Products, East Rutherford, New Jersey, USA) was added to one of each pair. The compositions of the "spikes" are presented in Table 2.

Table 2. Composition of the CO_2 AND N_2O "spikes" added to the classic cylinders. The volumes, the $\delta^{13}C$ and the $\delta^{18}O$ values are nominal.

CYLINDER	Volume of CO_2 Added (ml)	$\delta^{13}C$ ‰	$\delta^{18}O$ ‰	Volume of N_2O added (µl)
CA01648	0	-	-	0
CA01609	160	2.27	0.60	0
CA01631	230	-7.09	-5.52	0
CA01672	300	-12.09	-8.78	0
CA01608	370	-15.19	-10.81	0
CA01632	440	-17.31	-12.19	0
CA01664	160	2.27	0.60	400
CA01691	230	-7.09	-5.52	400
CA01638	300	-12.09	-8.78	160
CA01660	370	-15.19	-10.81	400
CA01685	440	-17.31	-12.19	400

The CO_2 spikes were transferred, using liquid nitrogen, into a 300 ml stainless steel cylinder (Whitey Co., Highland Heights, Ohio, USA), fitted with two high-pressure valves (Autoclave Engineers, Erie, Pennsylvania, USA). This cylinder was inserted into the high-pressure stream of the compressor system and the contents flushed into the target cylinder with about 200 litres of dry air. The variation of $\delta^{13}C$ with CO_2 concentration, from standard to standard, was designed to be -0.05 ‰ per ppm, similar to that observed for CO_2 exchange between the atmosphere and C-3 plants [16]. A specific $\delta^{18}O$ variation with CO_2 concentration was not attempted. One extra cylinder, CA01648, an ACULIFE treated cylinder also, was filled with un-modified dry air from the sampling site for reference purposes. After filling, each cylinder was transported to CSIRO, fitted with a dedicated regulator and allowed to equilibrate for about 7 days before the water vapour content, trace gas concentrations and the carbon and oxygen isotopic composition of the CO_2 were measured. The analytical procedures used for the analyses have been described elsewhere [11, 17].

2.2 Logistic problems associated with circulating the cylinders

There are a number of problems associated with circulating high-pressure cylinders between laboratories. One is the cost of shipping, which is unavoidable, but needs to be addressed in future exercises to spread the shipping costs equally amongst the participating laboratories. Also, high-pressure cylinders are classified as dangerous goods and must be shipped with the regulator removed from the cylinder, introducing a further procedure that could affect the measurements when the regulators are removed and re-attached.

Instrumental problems were the major source of circulation delays during the first CLASSIC circulation. Two laboratories had lengthy delays due to instrument breakdowns and laboratory relocations. In total, the first circulation took nearly twenty months, almost twice as long as initially anticipated. It is expected that the second circulation of the CLASSIC standards (see below) will proceed much faster.

An unexpected, and serious, problem occurred involving a leak that developed across the main canister valve of GS19B. This resulted in the CO_2 becoming contaminated with air after only two laboratories had analysed the CO_2. Inability to measure this sample has compromised the planned comparison of isotope measurements, in each laboratory, using CO_2 samples obtained independently of the pre-concentration steps.

2.3 Protocols

A set of protocols for sampling and reporting results was distributed with the standards to ensure consistent treatment at each laboratory. The protocols recommended:

As soon as possible after arrival, the cylinders are stored at the laboratory temperature to acclimatise.

- As soon as possible, the regulator and laboratory-supplied transfer-line are fitted to the cylinder. The regulator and transfer-line should then be pressurised and leak-tested.
- After leak-testing, the regulator delivery pressure is set to 10 psig and the transfer-line flushed and then capped. The cylinder valve is then opened to pressurise the regulator to full cylinder pressure and then closed. (The effectiveness of the maintenance of this pressure can be used as a confirmatory leak test).
- The regulator and transfer line are vented to atmospheric pressure and then re-pressurised three times every day for one week before the first analysis.
- All analytical techniques used and details of the relevant calibration scales are to be reported.
- Raw $\delta 45$ and $\delta 46$ values[2] are reported against the laboratory working gas (CO_2 in the reference variable volume).
- Assigned $\delta^{13}C$ and $\delta^{18}O$ values for each CLASSIC standard are reported, including full corrections, and, if applicable, details of calibration of the measurements against working air standards.

Reporting sheets were provided to facilitate compliance with the protocols.

2.4 Circulation of the standards

The five circulating CLASSIC standards were analysed at CSIRO on several occasions between filling in 1995 and December 1996 when they were shipped to CMDL. The standards

[2] $\delta 45$ and $\delta 46$ are the measured quantities before conversion to $\delta^{13}C$ and $\delta^{18}O$. For a more complete description see [6].

were analysed at CMDL in April 1997 and then shipped to SIO. The standards were analysed at SIO in December 1997 and then shipped to TU in early 1998. The standards were analysed at TU in May 1998 and returned to CSIRO where they were re-analysed in August 1998.

2.5 Measurement scales

This work does not establish a unique calibration scale, nor does it clarify the relationship between any one laboratory and an international calibration scale; however, some information on individual laboratory measurement scales is presented as background. In the detailed laboratory intercomparisons, the information provided by individual laboratories on their link to international calibration scales is not used.

CSIRO and CMDL report CO_2 concentration (mixing ratio) using the WMO X93 scale and TU use a scale based on gravimetrically prepared standards that is very close to the WMO X93 scale. Previous measurements by CSIRO, CMDL and TU using high-pressure cylinders of air have shown that CO_2 measurements made on these scales agree to within ±0.04 ppm at ambient CO_2 levels (360 ppm). Details of the CO_2 measurement scale used at SIO were not reported.

CSIRO measurements of N_2O concentration are based on the CMDL measurement scale with an observed scale factor of 0.9986 (CMDL/CSIRO) that produces agreement to about 0.4 ppb at current ambient levels (about 313 ppb). A scaling factor between CSIRO and SIO of 0.99252 (SIO/CSIRO) has also been established previously. No details of the N_2O measurement scale used at TU were reported.

All laboratories report measurements of $\delta^{13}C$ and $\delta^{18}O$ using the international VPDB-CO_2 scale [6].

3. RESULTS

3.1 Stability of the standards

3.1.1 Initial analyses

The eleven standards were analysed soon after filling and occasionally until November 1996 when all standards were analysed prior to the five selected standards being despatched. Table 3 presents the average concentration for all species (except H_2O and H_2) and the CO_2 isotopic composition during the analysis period. The H_2O content was measured only once, shortly after filling. For H_2, the initial measured concentration in each cylinder is given and the quantity in parentheses is the annual increase of H_2 in that cylinder. These large, variable growth rates of H_2 have been observed in other ACULIFE treated cylinders used at CSIRO, but they have not been associated with storage problems for CO_2 and its isotopic composition [18].

The analyses show that the targets for trace gas concentration and CO_2 isotopic composition were achieved. The variation of $\delta^{13}C$ with CO_2 concentration is about -0.05 ‰ per ppm, as planned, and the variation of $\delta^{18}O$ with CO_2 concentration is about -0.04 ‰ per ppm. Also given in Table 3 are the usual precision limits for the analytical techniques used at CSIRO and the target precision for $\delta^{13}C$ and CO_2. From these results we consider the air in the cylinders to be stable for CO_2 and $\delta^{13}C$.

Table 3. Results of the analysis by CSIRO of the ten prepared cylinders, and the cylinder of dried, natural Cape Schanck air (CA01648), from the time of filling to the commencement of the classic circulation in November 1996. The five cylinders selected for circulation are indicated by bold type. Numbers in parentheses are the standard deviation of all analyses, except for H_2, where the number in parentheses is the annual rate of increase of h_2 concentration. the final section of the table presents the analytical precision for the measurement techniques and the target precision for $\delta^{13}C$ and CO_2. for N_2O, the analytical precision increases from 0.3 ppb at ambient levels to 3 PPB at concentrations greater than 340 PPB due to linearity corrections made in extrapolating the calibration.

CYLINDER	$\delta^{13}C$ ‰	$\delta^{18}O$ ‰	CO_2 ppm	N_2O ppb	CH_4 ppb	H_2 ppb	CO ppb	H_2O ppm
CA01648	-7.846(0.009)	-1.264 (0.079)	358.74 (0.19)	311.77 (0.18)	1695.9 (3.1)	531.8 (106.1)	104.7 (0.5)	0.22
CA01609	-6.799 (0.021)	-1.259 (0.117)	320.02 (0.17)	311.82 (0.30)	1696.0 (1.9)	528.3 (19.1)	109.0 (0.6)	0.14
CA01631	**-7.752 (0.024)**	**-2.153 (0.110)**	**336.49 (0.06)**	**311.66 (0.10)**	**1694.4 (1.0)**	**530.9 (8.8)**	**107.4 (0.5)**	**0.30**
CA01672	**-8.717 (0.022)**	**-2.751 (0.139)**	**355.15 (0.08)**	**312.02 (0.30)**	**1693.5 (1.0)**	**533.2 (34.7)**	**110.6 (0.5)**	**0.28**
CA01608	**-9.606 (0.013)**	**-3.586 (0.063)**	**378.78 (0.07)**	**312.05 (0.37)**	**1689.0 (1.1)**	**549.0 (70.3)**	**118.6 (0.5)**	**0.25**
CA01632	-10.480 (0.016)	-4.289 (0.039)	396.18 (0.11)	311.71 (0.13)	1689.2 (0.7)	541.5 (66.2)	133.0 (0.8)	0.25
CA01664	**-6.681 (0.021)**	**-0.963 (0.062)**	**323.04 (0.08)**	**403.17 (0.42)**	**1695.0 (0.8)**	**528.7 (41.0)**	**98.9 (0.3)**	**0.91**
CA01691	-7.757 (0.012)	-2.085 (0.068)	339.39 (0.06)	393.82 (0.37)	1694.6 (0.7)	530.0 (5.6)	110.4 (0.1)	0.24
CA01638	-8.709 (0.030)	-2.869 (0.116)	353.33 (0.06)	341.60 (0.38)	1690.8 (0.5)	541.8 (70.5)	114.2 (0.6)	0.23
CA01660	-9.518 (0.037)	-3.581 (0.075)	375.25 (0.33)	404.10 (0.20)	1688.8 (0.5)	539.6 (58.0)	128.8 (1.1)	0.14
CA01685	**-10.421 (0.017)**	**-4.381 (0.105)**	**394.52 (0.03)**	**408.77 (0.46)**	**1689.3 (0.7)**	**540.9 (12.8)**	**135.4 (0.7)**	**0.27**
Analytical Precision	0.03	0.06	0.06	0.3 (3)	3.0	3.0	1.0	
TARGET	0.01		0.05					

Five standards were chosen for circulation using the criteria that the full range of CO_2 concentrations is represented and that two of the cylinders with elevated N_2O concentration were included. These standards are indicated by bold typeface in Table 3.

The isotopic compositions of GS19B and GS20B measured at CSIRO in November 1996 are given in Table 4. CSIRO has separate canisters of both of these gases (designated GS19 and GS20) that have been analysed over many years and were analysed with GS19B and GS20B in November 1996. The isotopic compositions of GS19 and GS20 are also summarised in Table 4. Both sets of these "GS" standards have isotopic compositions near the middle of the range covered by the CLASSIC air standards. Also given in Table 4 are the isotopic compositions assigned to the CO_2 gases in these canisters [13].

Table 4. Isotopic compositions of the pure CO_2 gases measured in November 1996. (standard deviation in parentheses). The isotopic composition assigned to these two CO_2 gases are given in bold typeface [13].

Cylinder	$\delta^{13}C$ (‰)	$\delta^{18}O$ (‰)
GS19	-7.534 (.008)	-0.705 (.026)
GS19B	-7.509 (.019)	-0.655 (.031)
GS19	**-7.502 (.025)**	**-0.193 (.040)**
GS20	-8.615 (.011)	-1.429 (.025)
GS20B	-8.610 (.013)	-1.434 (.030)
GS20	**-8.622 (.025)**	**-0.991 (.040)**

3.1.2 Analysis of the non-circulating standards at CSIRO: 1996–1998

The six non-circulated standards were analysed once during the circulation of the CLASSIC standards, in August 1997, and then in 1998 when the circulating standards returned to CSIRO. All results from the analysis of these standards and the GS19 and GS20 canisters are summarised in Table 5. The differences between measurements before and after the circulation period are given in column 6. For CO_2 there is variation in excess of the analytical precision of 0.06 ppm. For N_2O the measured differences are within the analytical precision. (At concentrations less than 340 ppb the analytical precision is 0.3 ppb but the extrapolation techniques used to extend the calibration scale to higher concentrations cause the analytical precision to decrease to 3 ppb). Measured $\delta^{13}C$ differences between 1996 and 1998 show variation of less than the analytical precision of 0.03 ‰. Measured $\delta^{18}O$ differences between 1996 and 1998 are generally within the 0.06 ‰ analytical precision although one cylinder, CA01691, shows a considerably larger difference. Measurements of GS19 and GS20 show slight increases of both $\delta^{13}C$ and $\delta^{18}O$ from 1996 to 1998. For GS19, $\delta^{13}C$ increases by 0.024 ‰ and $\delta^{18}O$ increases by 0.047 ‰, while for GS20, $\delta^{13}C$ increases by 0.025 ‰ and $\delta^{18}O$ increases by 0.027 ‰. These increases are less than the analytical precision for these species.

While small changes in the composition of individual standards over the two-year period cannot be excluded, the results suggest that, on average, the standards are stable to the analytical precision.

3.1.3 Analysis of the circulating standards at CSIRO: 1996–1998

The results of the CSIRO analysis of the five circulating CLASSIC standards and the GS19B GS20B canisters are presented in Table 6. Analysis at CSIRO in 1996 is identified as CSIRO(1) and analysis at CSIRO in August 1998 is identified as CSIRO(2). The differences between analyses in these two periods are given in column 8 of Table 6. The scatter in the differences for CO_2, N_2O, $\delta^{13}C$ and $\delta^{18}O$ is similar to that observed in the non-circulated standards and for these standards also, we conclude that they are stable for N_2O, CO_2 and the stable isotopes to within the analytical precision. (Although we again note that small changes in composition of individual standards may have occurred over the two-year period).

Table 5. CO_2 and N_2O concentrations, and the CO_2 stable isotopic composition of the non-circulated classic cylinders. The numbers in parentheses are the standard deviation of the measurements made on the cylinder during the analysis period. The values for GS19 and GS20 are from measurements in 1996 when the GS19B and GS20B canisters were analysed.

		1996 (1995-96 average)	1997	1998	Difference (1998-1996)	Difference (1998-1997)
CO_2	CA01648	358.74 (.19)	358.70 (.06)	358.67 (.04)	-0.07	-0.03
(ppm)	CA01609	320.02 (.17)	320.06 (.06)	320.13 (.05)	0.11	0.07
	CA01691	339.39 (.06)	339.28 (.11)	339.46 (.09)	0.07	0.18
	CA01638	353.33 (.06)	353.22 (.05)	353.24 (.05)	-0.09	0.02
	CA01660	375.25 (.33)	375.44 (.07)	375.67 (.12)	0.42	0.23
	CA01632	396.18 (.11)	396.27 (.04)	396.33 (.04)	0.15	0.06
N_2O	CA01648	311.77 (.18)	311.57 (.21)	311.84 (.39)	0.07	0.27
(ppb)	CA01609	311.82 (.30)	311.71 (.28)	311.64 (.49)	-0.18	-0.07
	CA01691	393.82 (.37)	394.02 (.58)	393.70 (.56)	-0.12	-0.32
	CA01638	341.60 (.38)	342.04 (.43)	342.22 (.43)	0.62	0.18
	CA01660	404.10 (.20)	404.67 (.33)	404.32 (.67)	0.22	-0.35
	CA01632	311.71 (.13)	311.87 (.28)	312.06 (.41)	0.35	0.19
$\delta^{13}C_{VPDB}$	CA01648	-7.846 (.009)	-7.845 (.005)	-7.859 (.006)	-0.013	-0.014
(‰)	CA01609	-6.799 (.021)	-6.784 (.026)	-6.782 (.005)	0.017	0.002
	CA01691	-7.757 (.012)	-7.747 (.005)	-7.757 (.011)	0.000	-0.010
	CA01638	-8.709 (.030)	-8.679 (.011)	-8.721 (.013)	-0.012	-0.042
	CA01660	-9.518 (.037)	-9.499 (.013)	-9.513 (.017)	0.005	-0.014
	CA01632	-10.480 (.016)	-10.447 (.011)	-10.460 (.007)	0.020	-0.013
	GS19	-7.534 (.008)	-7.517 (.005)	-7.510 (.012)	0.024	0.007
	GS20	-8.615 (.011)	-8.580 (.012)	-8.590 (.020)	0.025	-0.010
$\delta^{18}O_{VPDB}$	CA01648	-1.264 (.079)	-1.182 (.033)	-1.259 (.057)	0.005	-0.077
(‰)	CA01609	-1.259 (.117)	-1.143 (.095)	-1.236 (.053)	0.023	-0.093
	CA01691	-2.085 (.068)	-2.109 (.084)	-2.236 (.073)	-0.151	-0.127
	CA01638	-2.869 (.116)	-2.721 (.026)	-2.795 (.004)	0.074	-0.074
	CA01660	-3.581 (.075)	-3.440 (.039)	-3.565 (.044)	0.016	-0.125
	CA01632	-4.289 (.039)	-4.329 (.039)	-4.241 (.023)	0.048	0.088
	GS19	-0.705 (.026)	-0.662 (.015)	-0.658 (.014)	0.047	0.004
	GS20	-1.429 (.025)	-1.404 (.022)	-1.402 (.026)	0.027	0.002

Table 6. Results reported by all laboratories from the analysis of the circulated classic cylinders. The reported N_2O concentrations from CMDL and SIO have been corrected for scale difference as described in section 2.4. The numbers in parentheses are the standard deviation of the measurements made on the cylinder during the analysis period in each laboratory. Nr indicates no value was reported. The CSIRO(2)-CSIRO(1) difference values are the difference between the analyses at CSIRO.

	Cylinder	CSIRO(1) 1995-96 Avg	CMDL Apr1997	SIO Dec1997	TU May1998	CSIRO(2) Aug1998	CSIRO(2) - CSIRO(1)
CO_2	CA01664	323.04 (0.08)	323.19 (NR)	323 (NR)	323.10 (.01)	323.11 (.05)	0.07
(ppm)	CA01631	336.49 (0.06)	336.59 (NR)	337 (NR)	336.55 (.01)	336.57 (.04)	0.08
	CA01672	355.15 (0.08)	355.19 (NR)	355 (NR)	355.23 (.01)	355.19 (.06)	0.04
	CA01608	378.78 (0.07)	378.87 (NR)	379 (NR)	378.84 (.01)	378.77 (.05)	-0.01
	CA01685	394.52 (0.03)	394.64 (NR)	395 (NR)	394.45 (.03)	394.53 (.06)	0.01
N_2O	CA01664	403.17 (0.42)	384.64 (NR)	403.32 (NR)	403.2 (1.2)	403.38 (.55)	0.21
(ppb)	CA01631	311.66 (0.10)	311.12 (NR)	311.73 (NR)	313.0 (1.4)	311.85 (.22)	0.19
	CA01672	312.02 (0.30)	312.12 (NR)	311.73 (NR)	309.6 (0.3)	311.62 (.30)	-0.40
	CA01608	312.05 (0.37)	311.97 (NR)	311.63 (NR)	310.0 (0.7)	311.66 (.72)	-0.39
	CA01685	408.77 (0.46)	390.38 (NR)	408.56 (NR)	408.2 (0.9)	408.13 (.23)	-0.64
$\delta^{13}C_{VPDB}$	CA01664	-6.681 (0.021)	-6.645 (.010)	-6.561 (.009)	-6.667 (.028)	-6.657 (.025)	0.024
(‰)	CA01631	-7.752 (0.024)	-7.759 (.012)	-7.655 (.016)	-7.803 (.019)	-7.741 (.017)	0.011
	CA01672	-8.717 (0.022)	-8.765 (.010)	-8.649 (.011)	-8.794 (.012)	-8.715 (.014)	0.002
	CA01608	-9.606 (0.013)	-9.641 (.011)	-9.508 (.014)	-9.668 (.023)	-9.597 (.013)	0.009
	CA01685	-10.421 (0.017)	-10.531 (.010)	-10.411 (.007)	-10.578 (.003)	-10.437 (.017)	-0.016
	GS19B	-7.509 (0.011)	-7.517	n/a	n/a	n/a	n/a
	GS20B	-8.610 (0.009)	-8.624	-8.589	-8.637	-8.610 (.016)	0.000
$\delta^{18}O_{VPDB}$	CA01664	-0.963 (0.062)	-0.824 (.033)	0.068 (.035)	-0.110 (.013)	-0.983 (.045)	-0.020
(‰)	CA01631	-2.153 (0.110)	-2.000 (.028)	-1.089 (.029)	-1.323 (.035)	-2.076 (.030)	0.077
	CA01672	-2.751 (0.139)	-2.843 (.017)	-1.934 (.034)	-2.131 (.013)	-2.789 (.017)	-0.038
	CA01608	-3.586 (0.063)	-3.576 (.022)	-2.685 (.025)	-2.859 (.014)	-3.670 (.047)	-0.084
	CA01685	-4.381 (0.105)	-4.376 (.013)	-3.509 (.026)	-3.707 (.029)	-4.348 (.032)	0.033
	GS19B	-0.655 (0.028)	-0.790	n/a	n/a	n/a	n/a
	GS20B	-1.434 (0.023)	-1.580	-0.935	-0.966	-1.445 (.012)	-0.011

Of the two pure CO_2 canisters only GS20B was re-analysed at CSIRO due to the leaking valve on GS19B. The differences in both $\delta^{13}C$ and $\delta^{18}O$ of GS20B between 1996 and 1998 are negligible, 0.000 ‰ and -0.011 ‰ respectively, indicating this canister was stable and not compromised during the circulation.

3.1.4 Summary of stability

The analyses at CSIRO over the three years indicate that all CLASSIC standards are stable within the analytical precision of the techniques used. For CO_2 and $\delta^{13}C$, differences between the 1996 and 1998 measurements at CSIRO are close to the desired precision targets of 0.05 ppm and 0.01 ‰ respectively. The $\delta^{18}O$ results indicate agreement at close to the analytical precision, 0.06 ‰, although the scatter in these measurements is greater than expected.

3.2 Reported results from the four laboratories

The results reported by the four laboratories are presented in Table 6. For CO_2 concentrations, the agreement is good, better than 0.1 ppm for all laboratories except SIO. The lack of agreement with SIO arises, most probably, from the reported concentrations being rounded to the nearest integer giving a precision of 1 ppm for these measurements, much poorer than the anticipated precision.

For N_2O there is good agreement (range of 0.6 ppb) for the ambient level N_2O standards (CA01631, CA01672 and CA01608) between CSIRO, CMDL and SIO. (The N_2O concentrations have been adjusted using the scale factors given in Section 2.5). The TU measurements of the ambient concentration standards are up to 2 ppb different from the other laboratory measurements. For the elevated N_2O standards the agreement is good (range of 0.6 ppb) for all laboratories except CMDL whose reported values are low by about 20 ppb. Subsequent investigation by CMDL has revealed a problem with calibration during the analysis of these standards and that the "correct" concentrations should be about 400 ppb [19]. The reported $\delta^{13}C$ and $\delta^{18}O$ for the five standards are plotted in Figure 1. There are large differences in the reported $\delta^{13}C$ values, far greater than the desired target for $\delta^{13}C$ of 0.01 ‰. The range in reported $\delta^{13}C$ values increases from 0.12 ‰ for cylinder CA01664 to 0.16 ‰ for cylinder CA01685. The ranges in reported $\delta^{18}O$ values are much larger, decreasing from 1.05 ‰ to 0.87 ‰ for the same standards. These differences could originate from a number of sources including the procedures used to convert measurements onto the VPDB-CO_2 scale, different corrections for the presence of N_2O and differences in the pre-concentration step that includes the cryogenic extraction and normalisation using air standards. The impacts of these are explored below.

3.3 Calibration scale offsets

The two canisters of high purity CO_2, GS19B and GS20B, were included to determine the relative performance of the laboratory calibration procedures without the complications associated with the pre-concentration step, i.e. the extraction of CO_2 from air. Results from the analysis of GS19B and GS20B are given in Table 6. The isotopic composition of GS20B, as reported by all laboratories, is shown in Figure 1 (dashed line) with the measurements of the nearest air standards, CA01672 for $\delta^{13}C$ and CA01631 for $\delta^{18}O$. (Even though the measurements of GS19B at CSIRO and CMDL are consistent with the measurements of

GS20B in these laboratories, they are not considered valid as the leaking valve could have influenced these measurements).

The range of the reported $\delta^{13}C$ values is much less for GS20B than for the CLASSIC standards, 0.048 ‰ compared with more than 0.12 ‰. For $\delta^{18}O$, the range of reported GS20B values is 0.645 ‰ compared with about 1 ‰ for the CLASSIC standards. The range of the reported GS20B $\delta^{13}C$ values is larger than the precision target for merging data and the analytical precision of the measurements. If these differences were observed to be consistent across a range of isotopic compositions, which was the intended use of GS19B, they could be used to correct the reported isotopic compositions of the CLASSIC standards thereby reducing the scatter. The second circulation of the CLASSIC standards will include a second pure CO_2 sample to assess further the calibration scale offsets indicated by GS20B.

The measurements of GS20B suggest that 40% of the difference in the reported isotopic compositions of the CLASSIC standards arises from the conversion onto the VPDB-CO_2 scale. The remaining difference arises from the specific procedures applied to the CLASSIC standards, i.e. the pre-concentration step, the N_2O correction and, where applicable, the calibration to air standards.

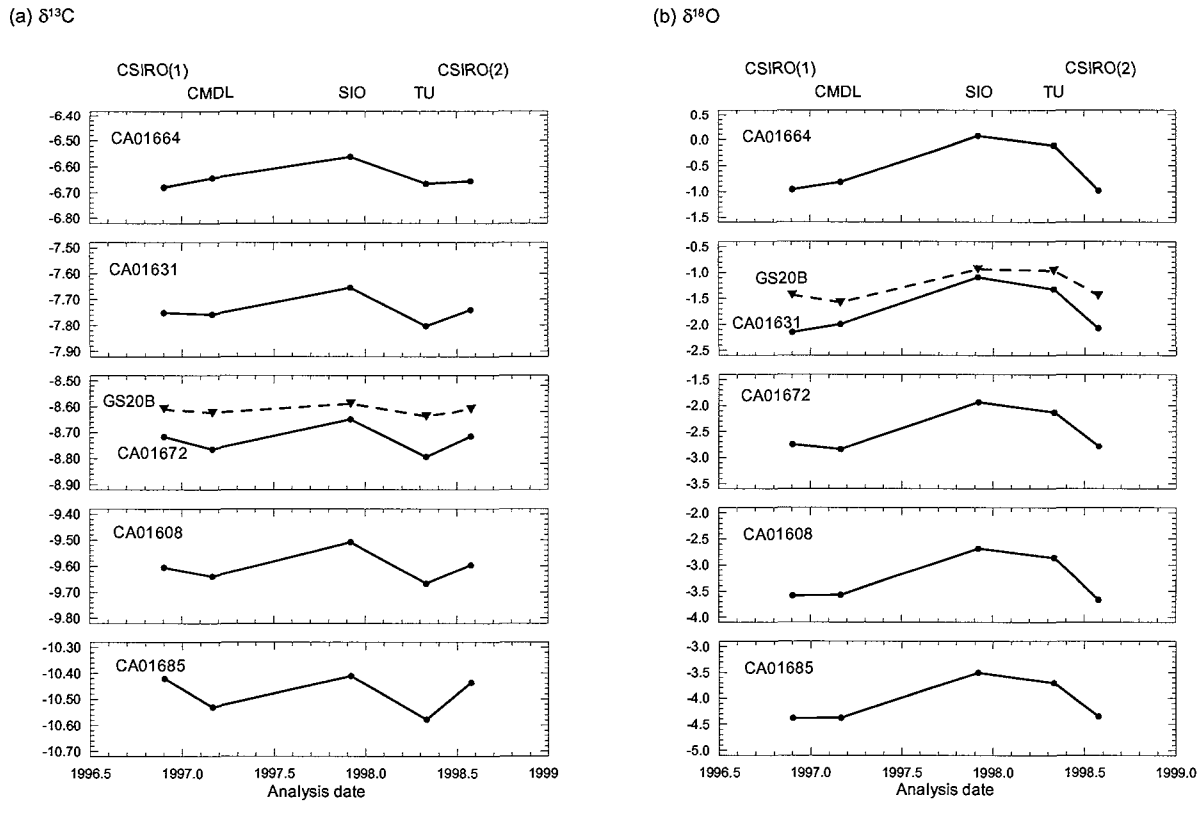

Figure 1. Measured isotopic composition of the CO_2 in the five circulated CLASSIC standards (solid lines) and GS20B (dashed line). (a) $\delta^{13}C$. (b) δ^{18O}.

3.4 N_2O correction

The N_2O correction [*20*] is applied in a similar fashion in each laboratory as:

$$\delta^{13}C \text{ (corrected)} = \delta^{13}C + A \cdot (N_2O/CO_2), \text{ and}$$
$$\delta^{18}O \text{ (corrected)} = \delta^{18}O + B \cdot (N_2O/CO_2),$$

where A is the N_2O correction factor for contribution to the measured $\delta^{13}C$ and B is the N_2O correction factor for contribution to the measured $\delta^{18}O$. The correction factors, A and B, have been determined experimentally by each laboratory and range from 0.248 to 0.283, and from 0.358 to 0.425, respectively. The magnitude of the applied corrections in the laboratories varies between 0.012 ‰ and 0.044 ‰ for $\delta^{13}C$ and between 0.014 ‰ and 0.082 ‰ for $\delta^{18}O$. Differences in A and B reflect the different relative ionisation efficiencies of CO_2 and N_2O in each mass spectrometer, and the assumed isotopic composition of atmospheric N_2O. Variation in the relative ionisation efficiency of ± 5 % would lead to an error of ± 0.011 ‰ and ± 0.015 ‰ in $\delta^{13}C$ and $\delta^{18}O$ respectively, much less than the observed differences.

Small differences in the reported N_2O and CO_2 concentrations, of a few ppb or a few ppm respectively, are not significant. For instance, CMDL reported concentrations almost 20 ppb lower than CSIRO for the two elevated N_2O standards but if the CMDL concentrations are increased by 20 ppb, $\delta^{13}C$ and $\delta^{18}O$ would increase by only 0.012 ‰ and 0.021 ‰ respectively. The reported $\delta^{13}C$ and $\delta^{18}O$ from CMDL for the analyses of these standards were not corrected for this as the changes affected only two standards, were much smaller than the range of differences observed for these standards, and would not change the range of reported compositions for these standards. The N_2O corrections are not considered to be a significant source of difference at this stage.

3.5 The pre-concentration step

The pre-concentration step can be monitored using working air standards, high-pressure cylinders of air with CO_2 isotopic composition that has been assigned following repeated extraction and analysis. The working air standards are analysed for $\delta^{13}C$ and $\delta^{18}O$ in exactly the same manner as the CLASSIC standards. The difference between the measured and the assigned isotopic composition of CO_2 extracted from the working air standards is used to correct for variations in the extraction step and the subsequent analysis. We refer to using working air standards in this fashion as "normalisation". Normalisation can also correct for short-term variations in instrument performance. In their calibration strategies, CSIRO, CMDL and TU routinely extract, and analyse, CO_2 from working air standards at the same time as samples are processed while SIO uses CO_2 extracted from air standards during separate CO_2 extraction sessions. To assess the pre-concentration effects further, one of the CLASSIC standards was used to normalise, i.e. correct for pre-concentration effects, the other four CLASSIC standards. This allows the consistent use of working air standards for all laboratories and applies a single N_2O correction procedure and VPDB-CO_2 scale conversion.

First, cylinder CA01672 was selected as the working air standard because its $\delta^{13}C$ isotopic composition was close to that of GS20B. The CSIRO measurements made in 1998 were arbitrarily used to assign the "true" composition of CA01672 as N_2O = 311.62 ppb, CO_2 = 355.19 ppm, $\delta^{13}C$ = -8.715 ‰ and $\delta^{18}O$ = -2.789 ‰. Next, the reported δ45 and δ46 from each laboratory were used to produce a set of "relative" δ45 and δ46 differences, Δ45 and Δ46, that express the relative isotopic composition difference between each cylinder and CA01672 without any normalisation that may have been applied by the laboratories. Finally, the CSIRO procedures [6, 1] for N_2O correction, using a relative ionisation efficiency of 0.72,

and conversion onto the VPDB-CO_2 scale were used to convert the Δ45 and Δ46 into $\delta^{13}C$ and $\delta^{18}O$. These final values still contain laboratory-specific influences but we make the assumption that these influences are consistent through the measurements reported for each laboratory and are handled equally for all standards by the normalisation.

The relationship to produce the relative delta values was derived from:

$$\delta(2\text{-}R) = \delta(1\text{-}R) + \Delta(2\text{-}1) + \delta(1\text{-}R)*\Delta(2\text{-}1)/1000, \quad (1)$$

where δ(1-R) is the delta value of gas 1 measured against the reference gas, δ(2-R) is the delta value of gas 2 with respect to the reference gas and Δ(2-1) is the delta value of gas 2 measured against gas 1. Rearrangement gives the relative difference between cylinders, Δ(2-1), as:

$$\Delta(2\text{-}1) = 1000*(\delta(2\text{-}R) - \delta(1\text{-}R))/(1000+\delta(1\text{-}R)). \quad (2)$$

For CSIRO(1), the raw δ45 and δ46 are from measurements made in November 1996, not from the entire pre-circulation analysis period, to avoid introducing errors from different instrument behaviour over such a long period of time. The raw δ45 and δ46 values, the calculated Δ45 and Δ46 values, and the calculated $\delta^{13}C$ and $\delta^{18}O$ values for all standards are given in Table 7 and the $\delta^{13}C$ and $\delta^{18}O$ are plotted in Figure 2. Also plotted in Figure 2 are the reported isotopic compositions (light symbols).

Table 7. The "raw" δ45 and δ46 reported by each laboratory, the "relative" δ45 and δ46 with respect to CA01672 in each laboratory and the "consistent" $\delta^{13}C_{VPDB}$ and $\delta^{18}O_{VPDB}$ after applying the consistent corrections (see text) to the "relative" δ45 and δ46.

	Cylinder	CSIRO(1)	CMDL	SIO	TU	CSIRO(2)
Raw δ45	CA01664	-0.106	30.303	35.489	3.096	-0.131
(‰)	CA01631	-1.064	29.253	34.454	2.068	-1.102
	CA01672	-2.009	28.261	33.464	1.135	-2.037
	CA01608	-2.851	27.378	32.609	0.300	-2.876
	CA01685	-3.713	26.449	31.638	-0.648	-3.749
Raw δ46	CA01664	12.161	38.254	28.049	3.889	12.313
(‰)	CA01631	11.106	37.157	26.981	2.794	11.334
	CA01672	10.429	36.315	26.132	2.004	10.626
	CA01608	9.782	35.584	25.384	1.293	9.755
	CA01685	8.874	34.680	24.454	0.355	8.969
Relative δ45	CA01664	1.907	1.986	1.959	1.959	1.910
(‰)	CA01631	0.947	0.965	0.958	0.932	0.937
(wrt CA01672)	CA01672	0.000	0.000	0.000	0.000	0.000
	CA01608	-0.844	-0.859	-0.827	-0.834	-0.841
	CA01685	-1.707	-1.762	-1.767	-1.781	-1.715
Relative δ46	CA01664	1.714	1.871	1.868	1.881	1.669
(‰)	CA01631	0.670	0.812	0.827	0.788	0.701
(wrt CA01672)	CA01672	0.000	0.000	0.000	0.000	0.000
	CA01608	-0.640	-0.705	-0.729	-0.710	-0.862
	CA01685	-1.539	-1.578	-1.635	-1.646	-1.640
Consistent	CA01664	-6.661	-6.582	-6.610	-6.611	-6.656
$\delta^{13}C_{VPDB}$	CA01631	-7.723	-7.709	-7.717	-7.743	-7.735
(‰)	CA01672	-8.715	-8.715	-8.715	-8.715	-8.715
	CA01608	-9.600	-9.614	-9.580	-9.588	-9.589
	CA01685	-10.430	-10.487	-10.490	-10.505	-10.435
Consistent	CA01664	-0.947	-0.790	-0.793	-0.780	-0.992
$\delta^{18}O_{VPDB}$	CA01631	-2.105	-1.963	-1.948	-1.986	-2.074
(‰)	CA01672	-2.789	-2.789	-2.789	-2.789	-2.789
	CA01608	-3.446	-3.511	-3.534	-3.515	-3.667
	CA01685	-4.263	-4.301	-4.359	-4.369	-4.363

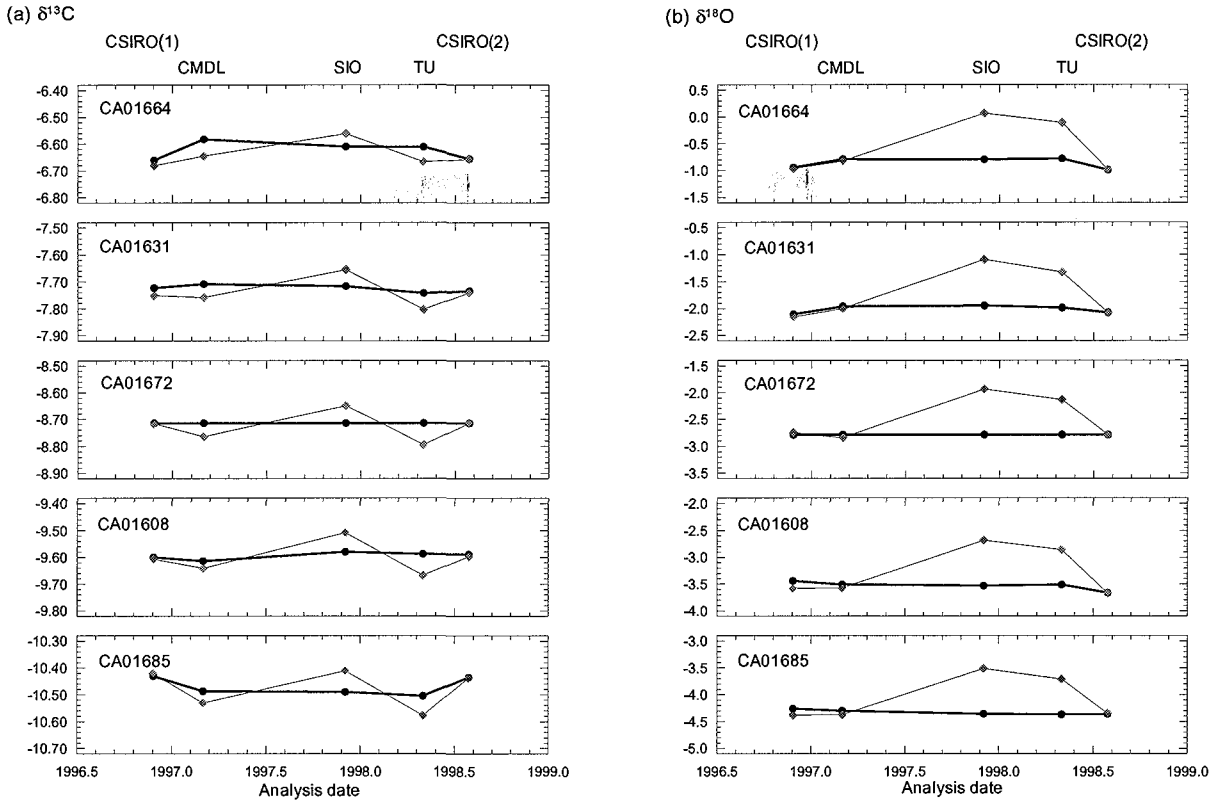

Figure 2. Isotopic composition of the CO_2 in the five circulated CLASSIC standards after normalisation to cylinder CA01672. (a) $\delta^{13}C$. (b) $\delta^{18}O$. The lighter lines in each panel are the "un"-normalised measurements transferred from Figure 1.

With the large mean offsets between laboratories removed, the ranges of $\delta^{13}C$ and $\delta^{18}O$ for each standard have decreased to 0.055‰, on average, for $\delta^{13}C$ and to 0.174‰, on average, for $\delta^{18}O$. The maximum $\delta^{13}C$ differences are for cylinders CA01664 and CA01685, the most positive and the most negative standards, with most of the differences being due to the CSIRO measurements. (These two cylinders have the highest N_2O concentrations of the five circulated CLASSIC cylinders but the N_2O contribution to these $\delta^{13}C$ differences should be negligible). The average of the CSIRO measurements for cylinder CA01664 is 0.058 ‰ more negative than the average from the other three laboratories and the average of the CSIRO measurements for CA01685 is 0.061 ‰ more positive than the average of the other three laboratories. For $\delta^{18}O$, the maximum difference is observed for cylinders CA01608 and CA01664 with most of the differences arising from the CSIRO measurements.

In Figure 3, the difference between the cylinder $\delta^{13}C$ and $\delta^{18}O$ values calculated for each standard in each laboratory and the average value calculated for each standard is shown. There is a clear indication of significantly different behaviour in the CSIRO measurements, i.e. the CSIRO measurements have a different linearity compared to the other laboratories. We have previously discussed some of the processes that could cause this [21,10] and believe that the CSIRO measurements are affected by mixing of the sample and reference gases in the ion source region of the mass spectrometer. The result of this mixing is an apparent "scale contraction", with measured isotope ratio differences being slightly smaller than they should be. We expect this mixing to occur to some degree in all dual-inlet, isotope ratio mass spectrometers but the CSIRO measurements may be more susceptible because of the small sample size used for analysis. In CSIRO, and possibly in the other laboratories, further

information on past scale contractions may exist in the extensive data archives and a CSIRO study to this end is underway.

4. PRELIMINARY CONCLUSIONS

A suite of ten air standards, high-pressure cylinders of modified marine air, has been prepared and the stability of the air in these standards has been established. The results of the first circulation of five of the standards show interlaboratory differences in $\delta^{13}C$ that are much larger than the target precision of 0.01 ‰ and preclude merging global data sets of $\delta^{13}C$ at this stage. Using one of the CLASSIC standards to normalise the measurements of the others has reduced the differences but they remain larger than the precision targets.

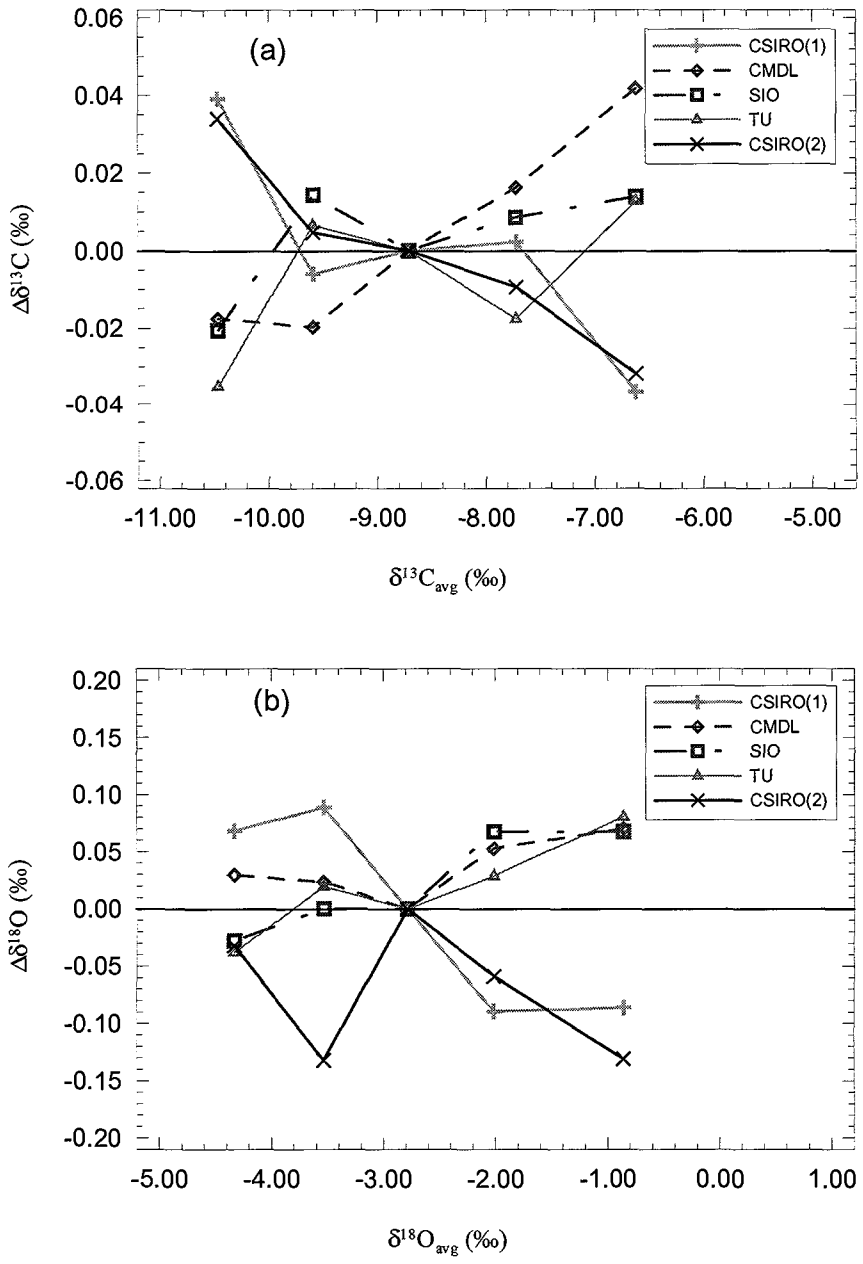

Figure 3. Difference between the normalised isotopic composition for each cylinder, for each laboratory, and the average for that cylinder from all laboratories plotted against the average value for that cylinder: (a) $\delta^{13}C$, (b) $\delta^{18}O$.

Analysis of the canister of pure CO_2, GS20B, showed that about 40% of the difference in the reported isotopic compositions could be due to the conversion onto the VPDB-CO_2 scale. (In order to determine if this is simply a result of the calculation procedures, the test data suggested by [6] should be processed by each of the participating laboratories. Any inconsistencies that might be identified can then be investigated). The source of the remaining differences is not clear, but there appears to be a measurement scale contraction in at least one laboratory (CSIRO) that is being investigated further.

Some required improvements to intercalibration through the CLASSIC circulation are evident. Firstly, the circulation of the CLASSIC standards should take less than one year. The first circulation took almost two years, more than one year longer than anticipated. The circulation time needs to be reduced to provide information on intercalibration issues at a higher frequency. Secondly, a canister of pure CO_2 has been prepared to replace GS19B to allow more information about each laboratories calibration scale to be obtained, independently of the pre-concentration procedures. Thirdly, the results from the five standards initially circulated indicate that there is little intercalibration offset arising from the different N_2O/CO_2 ratios in them. One, or more, of the previously un-circulated standards could be used to test this observation.

The second CLASSIC circulation, commencing in 1999, will provide more information on the stability of the standards, the cylinder-to-cylinder variation measured in each laboratory and the calibration strategies used in the laboratories. Further in the future, it is proposed that the suite of CLASSIC standards play a key supporting role in the GLOBALHUBS strategy [5]. While the CLASSIC high-pressure standards check intercalibration with high precision, they are circulated with low frequency and cannot provide information on the time-scale that a high frequency flask intercomparison program, such as that in operation between CSIRO and NOAA [22], is able to. The GLOBALHUBS strategy includes aspects of CLASSIC and flask intercomparisons and will also allow access by a greater number of laboratories to well characterised air for comparison purposes.

ACKNOWLEDGEMENTS

This work has been partially funded by the IAEA Technical Contract No. 9720/R0 and Renewal Contract 9720/R1 and by CSIRO Atmospheric Research. The strong support of Kaz Rozanski, Manfred Gröning and Klaus Fröhlich of the IAEA is acknowledged. The willing participation of the four laboratories, especially represented by Takakiyo Nakazawa, Martin Wahlen and Jim White, has been, and continues to be, necessary for the successful circulation of the CLASSIC standards. Finally, the large number of people in the four laboratories who have contributed to the preparation, analysis and circulation of the CLASSIC standards are gratefully acknowledged: Alane Bollenbacher, Tom Conway, Lisa Cooper, Scott Coram, Bruce Deck, Fred de Silva, Ed Dlugokencky, Candice Urban Evans, K. Ishijima, Ray Langenfelds, Ken Masarie, Jesse Smith, Darren Spencer, Pieter Tans, Bruce Vaughn, T. Watai and Ni Zhang.

REFERENCES

[1] FRANCEY, R.J., C.E. ALLISON AND E.D. WELCH, "The 11-year high precision in situ CO_2 stable isotope record from Cape Grim, 1982-1992", in Baseline Atmospheric Program (Australia) 1992, edited by A.L. Dick and P.J. Fraser, p 16-25, Bureau of Meteorology and CSIRO, Division of Atmospheric Research, Melbourne, Australia, 1995a.

[2] KEELING, C.D., T.P. WHORF, M. WAHLEN AND J. VAN DER PLICHT, "Interannual extremes in the rate of rise of atmospheric carbon dioxide since 1980", Nature, 375, 666-670, 1995.

[3] NAKAZAWA, T., S. MORIMOTO, S. AOKI AND M. TANAKA, "Temporal and spatial variations of the carbon isotopic ratio of atmospheric carbon dioxide in the western Pacific region", J. Geophys. Res. - Atm, 102, 1271-1285, 1997.

[4] TROLIER, M., J.W.C. WHITE, P.P. TANS, K.A. MASARIE AND P.A. GEMERY, "Monitoring the isotopic composition of atmospheric CO_2 - measurements from the NOAA global air sampling network", J. Geophys. Res. - Atm., 101, 25897-25916, 1996.

[5] FRANCEY, R.J., P.J. RAYNER AND C.E. ALLISON, "Constraining the global carbon budget from global to regional scales – the measurement challenge", this volume.

[6] ALLISON, C.E., R.J. FRANCEY AND H.A.J. MEIJER, "Recommendations for the reporting of stable isotope measurements of carbon and oxygen in CO_2 gas", in Reference and Intercomparison Materials for Stable Isotopes of Light Elements, IAEA-TEDOC-825, Edited by K. Rozanski, Vienna, p155-162, 1995.

[7] PETERSON, J., P. TANS, AND D. KITZIS, "CO_2 Round-Robin Reference Gas Intercomparison" in Report of the Ninth WMO Meeting of Experts on Carbon Dioxide Concentration and Related Tracer Measurement Techniques, Aspendale, Victoria, Australia, 1-4 September 1997, edited by R. Francey, World Meteorological Organization, Geneva, 1999.

[8] GLOBALVIEW-CO_2: Cooperative Atmospheric Data Integration Project - Carbon Dioxide. CD-ROM, NOAA CMDL, Boulder, Colorado [Also available on Internet via anonymous FTP to ftp.cmdl.noaa.gov, Path: ccg/co2/GLOBALVIEW], 1999.

[9] FRANCEY, R.J., C.E. ALLISON AND L.P. STEELE, "Circulation of laboratory air standards for stable isotope intercomparisons", IAEA CRP on Isotope Aided Studies of Carbon Dioxide and Other Trace Gases, Phase II, IAEA, Vienna, 1996a.

[10] ALLISON, C.E. AND R.J. FRANCEY, "High precision stable isotope measurements of atmospheric trace gases", in Reference and Intercomparison Materials for Stable Isotopes of Light Elements, IAEA-TEDOC-825, edited by K. Rozanski, International Atomic Energy Agency, Vienna, p131-153, 1995.

[11] FRANCEY, R.J., L.P. STEELE, R.L. LANGENFELDS, M.P. LUCARELLI, C.E. ALLISON, D.J. BEARDSMORE, S.A. CORAM, N. DEREK, F.R. DE SILVA, D.M. ETHERIDGE, P.J. FRASER, R.G. HENRY, B. TURNER, E.D. WELCH, D.A. SPENCER AND L.N. COOPER, "Global Atmospheric Sampling Laboratory (GASLAB): Supporting and Extending the Cape Grim Trace Gas Programs", in Baseline Atmospheric Program (Australia) 1993. (Ed. R.J. Francey, A.L. Dick and N. Derek) Bureau of Meteorology and CSIRO Division of Atmospheric Research, p 8-29, 1996b.

[12] WHORF, T.P., C.D. KEELING AND M. WAHLEN, "A comparison of CO2 and 13/12c seasonal amplitudes in the northern hemisphere", CMDL 23, 153-156, 1996.

[13] MEIJER, H.A.J., "The isotopic composition of the Groningen GS-19 and GS-20 pure CO_2 standards", in Reference and intercomparison materials for stable isotopes of light elements, IAEA-TECDOC-825, p 81-83, International Atomic Energy Agency, Vienna, 1995.

[14] WEEKS, I.A., R.J. FRANCEY, D.J. BEARDSMORE AND L.P. STEELE, "Studies in air archiving techniques. Part 2: filling high-pressure cylinders with baseline air", in Baseline Atmospheric Program (Australia) 1990 (Ed. S.R. Wilson and J.L. Gras) Bureau of Meteorology and CSIRO Division of Atmospheric Research, p 16-23, 1992.

[15] LANGENFELDS, R.L., R.J. FRANCEY, L.P. STEELE, R.F. KEELING, M.L. BENDER, M. BATTLE, AND W.F. BUDD, "Measurements of O2/N2 ratio from the Cape Grim Air Archive and three independent flask sampling programs", in Baseline Atmospheric Program (Australia) 1996, edited by J.L. Gras, N. Derek, N.W. Tindale, and A.L. Dick, p 57-70, Bureau of Meteorology and CSIRO Atmospheric Research, Melbourne, Australia, 1999.

[16] PEARMAN, G.I. AND P. HYSON, "Activities of the Global Biosphere as Reflected in Atmospheric CO_2 Records", J. Geophys. Res., 85(C8), 4468-4474, 1980.

[17] ALLISON, C.E. AND R.J. FRANCEY, "$\delta^{13}C$ of atmospheric CO_2 at Cape Grim: The *in situ* record, the flask record, air standards and the CG92 calibration scale", in Baseline Atmospheric Program (Australia) 1996, edited by J.L. Gras, N. Derek, N.W. Tindale and A.L. Dick, p. 45-56, Bureau of Meteorology and CSIRO Atmospheric Research, Melbourne, Australia, 1999.

[18] LANGENFELDS, R.L., private communication, 1994

[19] WHITE, J.W.C., private communication, 1999

[20] MOOK, W.G. AND S. VAN DER HOEK, "The N_2O correction in the carbon and oxygen isotopic analysis of atmospheric CO_2", Isotope Geoscience, 1, 237-242, 1983.

[21] FRANCEY, R.J. AND C.E. ALLISON, "The trend in atmospheric $\delta^{13}CO_2$ over the last decade", in Report of the Final Meeting of the Coordinated Research Programme on Isotope Variations of Carbon Dioxide and Other Trace Gases in the Atmosphere, Ed. K. Rozanski, IAEA, Vienna, 7-10 November 1994.

[22] MASARIE, R.L. LANGENFELDS, K.A., C.E. ALLISON, T.J. CONWAY, E.J. DLUGOKENCKY, R.J. FRANCEY, P.C. NOVELLI, L.P. STEELE, P.P. TANS, B. VAUGHN, J.W.C. WHITE, "NOAA/CSIRO Flask Air Intercomparison Experiment: A strategy for directly assessing consistency among atmospheric measurements made by independent laboratories", J. Geophysical Research 106, D17 (2001) 20445-20464.

CONSTRAINING THE GLOBAL CARBON BUDGET FROM GLOBAL TO REGIONAL SCALES — THE MEASUREMENT CHALLENGE

R.J. FRANCEY, P.J. RAYNER, C.E. ALLISON
CSIRO Atmospheric Research, Aspendale, Victoria;
Centre for Southern Hemisphere Meteorology, Clayton, Victoria

Australia

Abstract: The Global Carbon Cycle can be modelled by a Bayesian synthesis inversion technique, where measured atmospheric CO_2 concentrations and isotopic compositions are analysed by use of an atmospheric transport model and estimates of regional sources and sinks of atmospheric carbon. The uncertainty associated to carbon flux estimates even on a regional scale can be improved considerably using the inversion technique. In this approach, besides the necessary control on the precision of atmospheric transport models and on the constraints for surface fluxes, an important component is the calibration of atmospheric CO2 concentration and isotope measurements. The recent improved situation in respect to data comparability is discussed using results of conducted interlaboratory comparison exercises and larger scale calibration programs are proposed for the future to further improve the comparability of analytical data.

The long lifetime and rapid mixing of CO_2 in the atmosphere provides a large scale integration of surface fluxes, while, with sufficient measurement precision, a signature of individual surface source or sink regions can still be detected. The 3-dimensional Bayesian synthesis inversion technique was introduced to global carbon cycle modelling by Enting [1]. Measurements of atmospheric CO_2 mixing ratios and stable carbon isotope ratios from globally distributed sampling sites for selected years were interpreted using an atmospheric transport model to determine regional sources and sinks of atmospheric carbon. The inversion process is inherently unstable, and requires additional constraints, in this case the spatial distribution of known sources and sinks, and prior estimates of the surface fluxes. When those prior estimates are independently and rigorously determined, the Bayesian technique provides a promising framework within which the various studies of regional carbon fluxes (and associated process information) can be reconciled with changes in the global atmospheric carbon content. A particular advantage is the potential for systematic treatment of uncertainty in the various components of the inversion. The application to global carbon budgeting is still in the early stages of development.

Recently, Rayner [2] developed a 3D time-dependent inversion model to determine interannual variability in the regional terrestrial and oceanic uptake of fossil fuel CO_2 over the last two decades. The Rayner [2] study is used here, as a benchmark against which the potential for improved precision and spatial resolution of flux estimates from atmospheric composition measurements is explored.

In the Rayner study [2], extended records of monthly average concentrations of CO_2 in background air measured at 12 or 25 selected sites in the NOAA/CMDL (Climate Monitoring and Diagnostics Laboratory) global flask-sampling network were employed. Partitioning of carbon between oceanic and terrestrial reservoirs used $^{13}C/^{12}C$ in CO_2 from one site and used a new determination at the same site (Cape Grim) of the trend in O_2/N_2 over two decades [3,4]. The small number of selected sites for CO_2, can be compared to the current number of global sampling sites which approaches 100, many with decadal records and longer. For $^{13}C/^{12}C$, at least two global sampling networks have made measurements from several sites since the early 1980's [5,6], yet only one site record was used. In the case of O_2/N_2 there is no

other reliable information available over this time frame. The limited site selections for the Rayner study [2] reflect a very real concern about the quality and intercalibration of records from different measurement laboratories.

Figure 1 is adapted from Rayner et al. [2], and illustrates the uncertainty allocated to prior flux estimates (Figure 1a) and the modified uncertainties resulting from the inversion of the atmospheric measurements (Figure 1b). The grid-scale of the inversion model has dimensions of 8° latitude × 10° longitude. The numbers refer to flux uncertainties (in Gt $C \cdot a^{-1}$) representative over 25 larger aggregated areas selected as characteristic source regions for the prior source estimates.

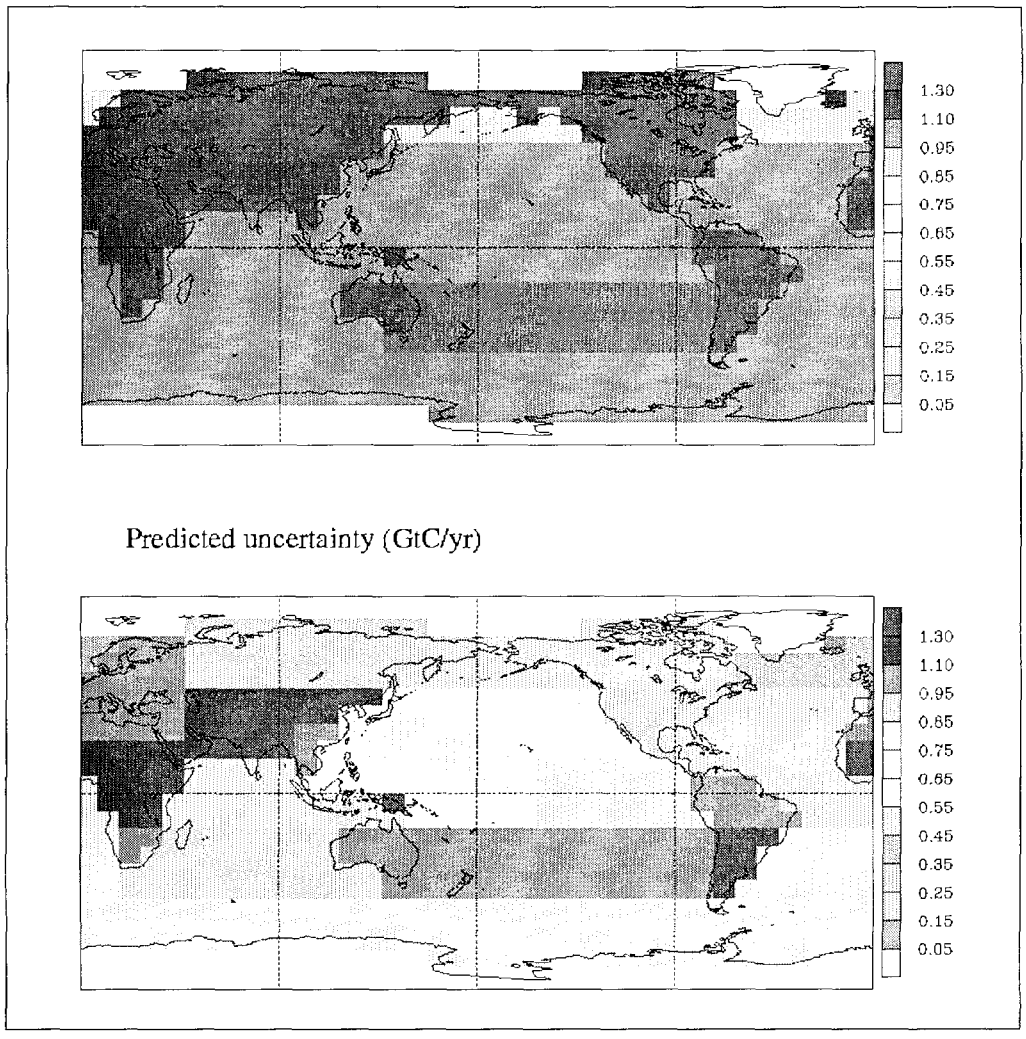

Figure 1. Prior and predicted estimates of uncertainty in air-surface fluxes of CO_2 as the result of a 3D Bayesian synthesis inversion of atmospheric CO_2, $\delta^{13}C$ and O_2/N_2 data from selected sites for the period 1980–1995 [2].

A reduction in uncertainty in a region from Fig. 1a to 1b indicates that effective constraints are imposed by the atmospheric measurements, and it is no coincidence that the larger improvements occur in regions best represented by atmospheric sampling sites (for example, North America compared to South America). There are still regions of the globe where uncertainties are relatively large (~±1 Gt $C \cdot a^{-1}$, compared to global fossil fuel emissions of around 6 Gt $C \cdot a^{-1}$). Even where uncertainties appear relatively small, e.g. North America at ±0.5 Gt $C \cdot a^{-1}$, this should be viewed against the net derived sink in this study of 0.3 Gt $C \cdot a^{-1}$

and the total fossil source of ~1.6 Gt $C \cdot a^{-1}$. Uncertainties are often reduced when regions are aggregated, but even regions in Figure 1 are too large for many policy needs.

The potential advantages of the atmospheric inversion approach compared to more conventional on-the-surface carbon accounting methods are that: firstly, flux estimates are firmly bounded by the global growth rate of atmospheric CO_2, perhaps the best determined of all inputs to a global carbon budget. Secondly, if the regional uncertainties can be reduced to levels small enough to detect important changes in net continental emissions and uptakes, then atmospheric monitoring provides an opportunity for continuous, relatively low cost, globally consistent monitoring. The Kyoto Protocol, 1997 and more recently, COP4 of the UN Framework Convention on Climate Change, Buenos Aires, November 1998, present a new and urgent challenge to the atmospheric community to provide and monitor regional carbon fluxes for verification and/or regulatory purposes.

Of the three broad inputs to the Bayesian synthesis inversion, namely atmospheric transport models, surface flux constraints and atmospheric measurements, all have experienced rapid progress over the last few years. In the atmospheric transport area, the problem of estimating GCM model error is significant. However progress has occurred: (a) with increasing availability of analysed wind fields [7] (permitting an examination of the impact of inter-annual variation in transport on measured parameters) and (b) with identification of model differences in the on-going series of TRANSCOM model comparisons (e.g. [8,9]). Considerable research effort is now focussed on "bridging the scale gap" between the typical grid cells of the transport models and the volume of atmosphere represented by the atmospheric measurement at surface sites. This research introduces boundary layer and regional transport models, direct flux measurement campaigns and vertical profiling of CO_2 and related trace species. Significant remaining uncertainties are perceived, for example in the representation of mass transport in the tropical areas.

A flood of new information is also emerging on the interaction between terrestrial ecosystems and the atmosphere with process oriented campaigns focussed on major ecosystems such as the Amazon and Siberia. Recent perspectives and a summary of the advances in knowledge of the understanding of the role of the terrestrial biosphere in the global carbon cycle is provided by [10,11]. The situation is similar for the interaction with the worlds oceans. Extensive on-going surveys of ocean parameters are elucidating air-sea gas exchange constraints on carbon uptake by the oceans [12,13], while similar constraints are emerging from the development of ocean general circulation models, e.g. [14,15]. The formal integration of the information on terrestrial and oceanic fluxes as additional constraints in the Bayesian inversion framework is in its infancy. Even with these various streams of information, the carbon cycle remains an under-determined system which requires more and better calibrated measurements.

The rest of this contribution concentrates on recent and potential progress in the measurement of atmospheric CO_2 mixing ratios and related species. The challenge for such measurement programs is to monitor, with high precision, the temporal changes and/or spatial gradients of CO_2 and related species. Conventional methodologies for monitoring atmospheric CO_2, developed over the past 40 years, show a number of shortcomings when examined in the light of the requirements for improved estimates of regional fluxes from baseline atmospheric composition measurements.

Measurements of carbon dioxide mixing ratios are made at over 100 globally distributed "baseline" sites (i.e. fixed or mobile sites for which measurements reflect CO_2 behaviour over large spatial scales). The requirement for large scale representation has heavily influenced global sampling strategies in so far as the great majority of sampling sites is located to access marine boundary layer air. In fact, for the smaller sampling networks, zonal representation was a common assumption. Furthermore, data are still generally selected to

reinforce the marine boundary layer bias, though this is changing. Most results are now reported to one or more data banks, including the Carbon Dioxide Information Analysis Center (CDIAC) World Data Centre — A, for Atmospheric Trace Gases, established in 1982 by the Oak Ridge National Laboratory, Tennessee, USA and the World Meteorological Organisation (WMO) World Data Centre for Greenhouse Gases (WDCGG) in the Japan Meteorological Agency, established in 1990. In late 1995, a Co-operative Atmospheric Data Integration Project (CADIP-CO_2) was commenced in NOAA Climate Monitoring and Diagnostics Laboratory (CMDL), USA, using data from much the same sources, with the aim of providing an integrated "globally-consistent" data set, GLOBALVIEW-CO_2, for modelling studies. At the heart of GLOBALVIEW is a data extension and integration technique [16] which addresses difficulties such as those related to missing data or introduction of new stations, however inter-laboratory calibration remains a problem.

Around 17 different laboratories from 12 nations are involved in the measurement and reporting of CO_2 data to these data banks. Historically, the WMO has taken responsibility for the intercalibration of measurements in different laboratories. Primary activities have involved the establishment of a Central Calibration Laboratory to maintain and provide access to "primary" CO_2-in-air standards measured with high precision manometric techniques, and initiation of blind "round-robin" intercalibrations involving the circulation of high pressure cylinders containing CO_2-in-air among participating laboratories. In addition the WMO has provided a forum of "CO_2 Measurement Experts", now held every two years to assess progress and plan future activities, with each meeting resulting in a WMO technical report.

Results from two recent WMO CO_2 round robins are summarised in Figure 2, adapted from WMO technical reports (Pearman, 1993; Peterson, 1997). As an example of the procedure, the most recent round-robin, (b), was proposed at the July 1995 8th WMO CO2-Experts Meeting in Boulder, USA, and was completed in time for an initial assessment at the 9th Meeting of Experts on the Measurement of Carbon Dioxide Concentration and Associated Tracers (endorsed by International Atomic Energy Agency), Aspendale, Australia, 1–4 September 1997. NOAA CMDL prepared three sets of three cylinders of air with nominal CO_2 mixing ratios of 345, 360 and 375 ppm. Each set was distributed to one of three groups of around 8 laboratories (in North America & the Southern Hemisphere, Asia, and Europe). A target inter-laboratory precision of 0.05 ppm was identified by this community to achieve a "network precision" of 0.1 ppm. This precision is appropriate for the merging of data from different sites to estimate regional fluxes via synthesis inversion studies [17]. This level of precision is comparable to that of an individual measurement in the better operational systems; the "target" precision of 0.05 ppm refers more to the requirement for precise average temporal values (e.g. annual or seasonal) and for precise large-scale values (e.g. GCM grid scale to hemispheric). Note that Figure 2 results usually represent the average of multiple measurements on a cylinder.

The most important point to be drawn from Figure 2 is that there are significant (>0.05 ppm) and variable calibration differences between laboratories, which are not currently accounted for in the CDIAC and WDCGG data bases, or in the GLOBALVIEW data assimilation. Another general observation is that there is a significant overall improvement going from the first to second round-robin (while the actual laboratories are not identified, the identification of country is sufficient to make this inference). However, in the second, more precise, intercalibration a new concern about linearity emerges, with a majority of participants measuring lower than the low mixing ratio tank and higher than the high mixing ratio tank. The fact that the degree of "non-linearity" varies widely suggests that this in an issue for many laboratories; it also argues for an independent verification of both the manometric technique and the scale propagation, e.g. by using gravimetric dilution techniques.

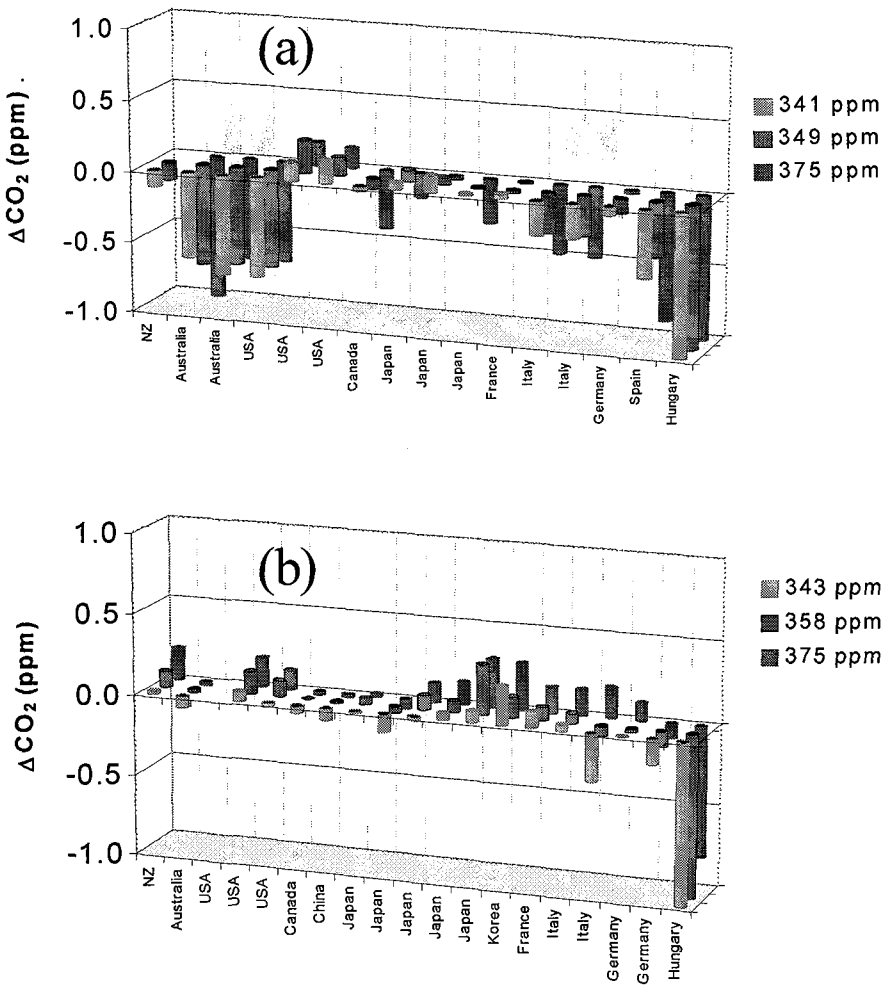

Figure 2. WMO round robin intercalibrations of CO_2 measurement laboratories (identified by country only). Plotted are measured differences from mixing ratios assigned by NOAA CMDL. (a) is for a circulation conducted between 1991-93, and (b) between 1995-97.

The unsatisfactory situation for CO_2 mixing ratio intercalibration is also evident for $\delta^{13}C$ of CO_2. The International Atomic Energy Agency (IAEA) conducts a co-operative research program on "Isotope-aided Studies of Atmospheric Carbon Dioxide and Other Greenhouse Gases" with an objective of providing whole air standards for the measurement of greenhouse gas isotopes. Figure 3 shows preliminary results from the first circulation of "CLASSIC" (Circulation of Laboratory Air Standards for Stable Isotope inter-Comparisons) standards, where the initial round-robin has been restricted to 4 laboratories with the longest involvement in sampling the background atmosphere from a network of stations. Here the community has set a required target precision of 0.01 ‰ for temporal or large-scale averages, which is even more demanding than the case with CO_2 mixing ratios since typical precision on an individual measurement is around 0.03 ‰.

Preliminary results of this round robin are given in Figure 3 [18]. Measured differences are reported with respect to initial measurements conducted at CSIRO in November 1996. CSIRO (2) refers to CSIRO measurements conducted after circulation in July 1998, confirming the stability of the tank standards. Measurements on pure CO_2 samples scatter between ~±0.02‰, outside the required target. For the analyses of the whole-air

standards the situation is much worse, with reported values scattered over a range of almost ±0.1‰, suggesting serious differences between pre-treatments to extract CO_2 from air. Furthermore, there also appears to be a linearity problem with the CSIRO measurement compared to the other three laboratories.

The situation is even more serious than indicated by the round-robin comparisons. Since 1992, with the aim of confirming our ability to merge data from two different measuring laboratories, CMDL and CSIRO commenced an "operational intercalibration" (also referred to as the ICP, Inter-Comparison Program, also the "flask-air-sharing" comparison). Both CSIRO and CMDL networks collect pairs of flasks 3–4 times per month, from the Cape Grim station on the north-west tip of Tasmania. Approximately twice per month, one of a pair of CMDL flasks has been routinely routed through CSIRO's GASLAB for analysis prior to analysis in CMDL and Institute for Alpine and Arctic Research, University of Colorado (INSTAAR, for the isotopic measurements on CMDL flask samples). The process is facilitated by the unusually small sample requirements for precise analysis in GASLAB [19]. Once per month, the results of the multi-comparisons (CO_2, CH_4, CO, N_2O, H_2, $\delta^{13}C$, $\delta^{18}O$) in both routine flask sampling of Cape Grim air from each laboratory and from the ICP flasks are automatically processed, and reported via ftp in both laboratories [20].

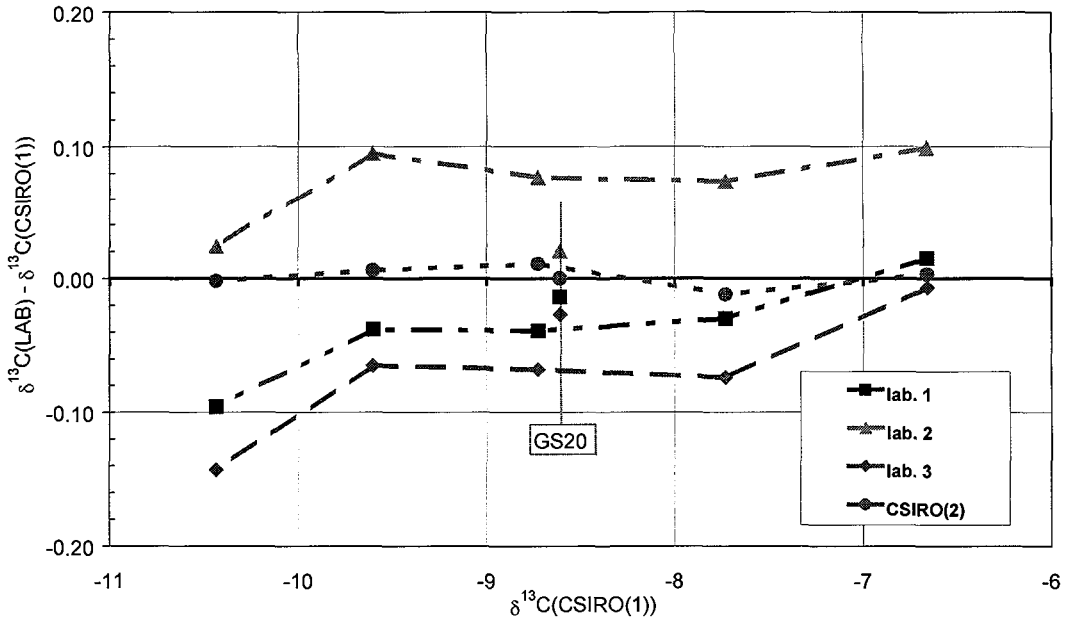

Figure 3. IAEA round robin intercalibrations of $\delta^{13}C$ of CO_2 using both pure CO_2 (GS20) and whole air in high pressure cylinders (in which $\delta^{13}C$ is related to CO_2 mixing ratio difference from ambient values by ~ –0.05‰ ppm^{-1}). USA and Japanese measurement laboratories are identified by number only. Plotted are measured differences from $\delta^{13}C$ assigned by CSIRO prior to circulation. CSIRO(2) refers to analyses after circulation.

No systematic influence of GASLAB measurements on CMDL flasks has been detected. Figure 4 shows the results of the ICP flask comparisons for CO_2 and for $\delta^{13}C$. Compared to cylinder inter-comparisons, the precision on the ICP comparisons is low (individual measurements) but the frequency is high. The CO_2 results are startling. The Australian calibration scale was established to within ~0.01 ppm at ambient CO_2 mixing ratios by repeated analysis of 10 cylinders initially characterised by CMDL. Return of a subset of the cylinders after two years confirmed this agreement to within a few hundredths of a ppm, as

have comparisons of other cylinders. Despite this agreement in calibration scales (see also Figure 2b, Australia), there is a consistent mean difference (CSIRO-CMDL) in the ICP flasks of 0.17 ± 0.17 ppm.

The reason for this offset in flasks compared to high pressure cylinders is not yet fully understood. However, development of a low flow (15 mL·min^{-1}), high precision (~7 ppb) and highly stable NDIR CO_2 analyser at CSIRO (G. Da Costa and L.P. Steele, in preparation) has provided clues that implicate high pressure regulators as a likely contributor to such offsets.

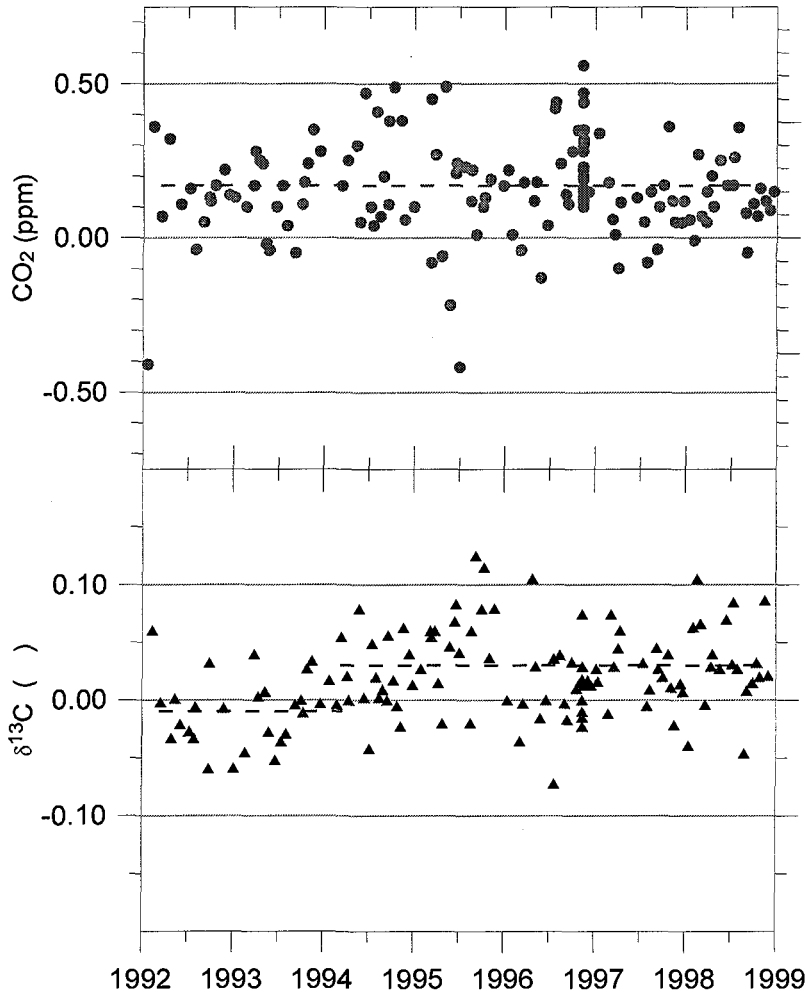

Figure 4: (CSIRO-INSTAAR) measured differences on Cape Grim air from the same flask as a function of flask collection date, for CO_2 (circles) and $\delta^{13}C$ (triangles).

The $\delta^{13}C$ comparison in Figure 4 illustrates another advantage of the ICP. The (CSIRO-INSTAAR) difference begins at close to zero, or slightly negative, and early in 1994 jumps to a positive value. After 1994, the difference is consistent with high pressure cylinder inter-comparisons included in Figure 3. The discrepancy between the laboratories, if applied globally, translates in a partitioning error of around 1 Gt C·a^{-1} between the two laboratories. The continuity of the ICP data has permitted detection of the onset of the problem with reasonable accuracy, and the identification of possible contributing factors which occurred around this time.

It is clear that such unanticipated discrepancies between results from different measuring laboratories are a major obstacle for high precision merging of data sets. The merging is highly desirable from the point of view of maintaining adequate spatial monitoring of global trends and for identification of regional source/sink changes from atmospheric inversion techniques. From this perspective, we conclude this paper by outlining an international calibration strategy which aims to overcome identified shortcomings in the present methods. The strategy is also aimed at providing frequent, low-cost access to a constantly monitored international calibration scale, which is currently not an option, particularly for new laboratories from developing countries. It grows out of the IAEA CLASSIC strategy, and we call it here "CLASSIC-AL" (CLASSIC for All Laboratories). While CLASSIC specifically targets CO_2 stable isotopes, CLASSIC-AL is seen as providing calibration for the majority of long-lived trace gas species in ambient air.

Since high freight costs and long delays are a major constraint on circulating high-pressure standards for round-robin exercises, CLASSIC-AL is structured around 4 geographically distributed "HUB" Laboratories (e.g. USA, Europe, Japan, Australia), see Figure 5. Here, the Australian HUB is allocated a special "CORE" role based on its ability to prepare high pressure standards and high quality, low-pressure sub-samples from high pressure cylinders, to quickly assess regulator effects on CO_2, to produce state-of-the art precision measurements on a wide range of key trace gas species using unusually small sample sizes and its established pioneering role in operational intercalibrations with CMDL/INSTAAR, as well as Japanese, French, German, Canadian and New Zealand laboratories. Other laboratories might also wish to be considered for some or all of this central role, though at least initially, there is a requirement for uniformity of methodology, best achieved through one laboratory.

A common HUB scale is maintained by a variety of approaches:

1. An upgraded CLASSIC rotation between the HUB laboratories is conducted at least once per year. With upgraded and certified regulators, CO_2, $\delta^{13}C$, $\delta^{18}O$, CH_4, N_2O, CO, H_2 , etc. can be established to high precision (e.g. CO_2 ~±0.01 ppm, $\delta^{13}C$ ~ ±0.01 ‰) with respect to the CORE laboratory scale for air standards covering the full range of anticipated clean air values. The CLASSIC high-pressure cylinders are accompanied by a range of pure-CO_2 standards for the isotope measurements. The CLASSIC rotation, though relatively cumbersome and expensive, provides a long standard lifetime (decades for the air standards, and many decades for CO_2 isotope standards). It also provides precise detector response information from both air and pure CO_2 standards.

2. It introduces "CLASSIC JNR" exchanges between the CORE laboratory and the other three HUB laboratories. The containers are high-quality, electropolished, four-litre stainless steel filled at 1-4 bar pressure by decanting from high-pressure cylinder air standards comprising CO_2-free air (CO_2 stripped from ambient Southern Hemisphere marine boundary layer air) plus ~360 ppm of GS20 (or equivalent, with near ambient CO_2 isotopic ratios). The CLASSIC JNR air standards provide moderate to high precision (e.g. CO_2 ~ ±0.01 to 0.03 ppm, $\delta^{13}C$ ~ ±0.01 to 0.03 ‰, depending on required sample size), and have moderate frequency (~4 per year). Possible complications related to high-pressure regulators are avoided.

3. It maintains/upgrades flask air-sharing (ICP) programs for Cape Grim samples and introduces new ICP programs where they become possible. This is seen as a verification step. It uses exact sample methodology, has high frequency (2-4 per month), but with lower precision (e.g. CO_2 ~ ±0.1 ppm, $\delta^{13}C$ ~ ±0.03 ‰).

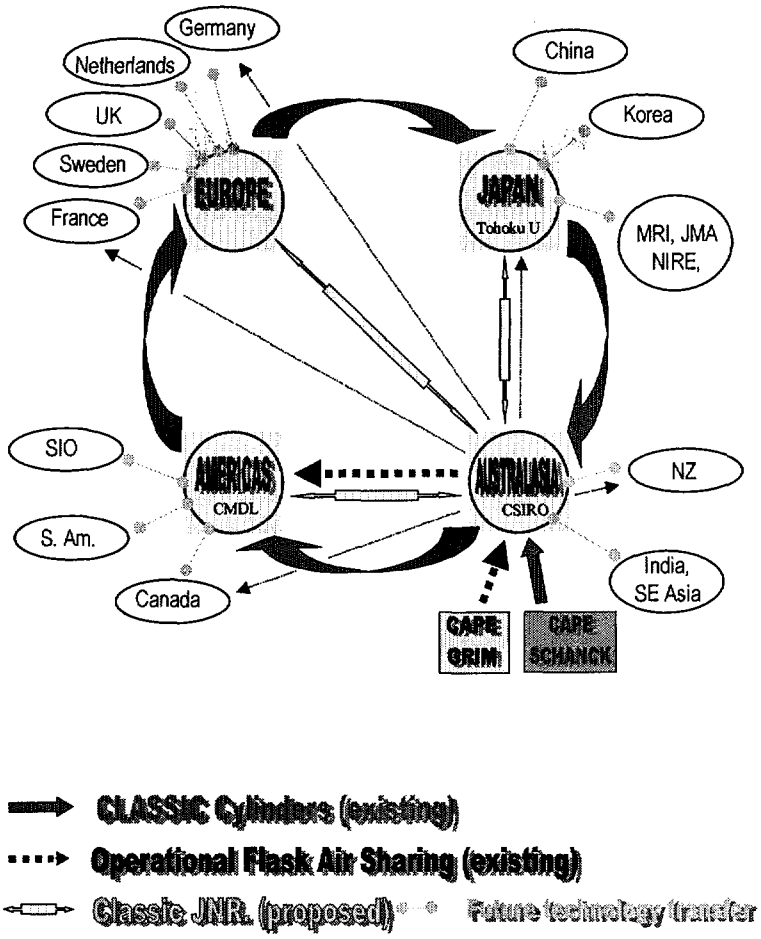

Figure 5. Proposed CLASSIC-AL international calibration strategy for laboratories measuring long-lived atmospheric trace gases in air. Identification of laboratories is nominal only.

4. The CORE laboratory prepares and provides each HUB laboratory with calibrated high-pressure cylinders of Southern Hemisphere marine boundary layer air, plus CLASSIC JNR type containers and the technology to decant into these for frequent provision to regional laboratories to propagate and maintain the HUB scale.

5. The HUB structure permits rapid assessment and dissemination of community-approved calibration scale adjustments (e.g. arising from new manometric or gravimetric determinations), or of new methods (e.g. "continuous flow" technology for $\delta^{13}C$, D. Lowe, NIWA, NZ, personal communication).

Initial funding is required to establish the CORE and HUB capability in existing advanced laboratories, and to secure their long-term involvement. Once the HUB scale is established quite modest regional funding is expected to maintain operation and access. The current strategy is to seek endorsement from WMO and IAEA, and a commitment to continue their roles for planning, assessment and dissemination of results, with particular encouragement to laboratories from developing countries. Coordinated establishment costs and regional operating costs are being sought from international funding bodies with a charter to support atmospheric composition/climate change research.

We speculate here on the improvements to atmospheric inversion studies of air-sea and air-land carbon fluxes that might flow from more effective global calibration strategies for CO_2, $\delta^{13}C$ and O_2/N_2. A realistic ambition for the precision of year-to-year and large spatial scale differences over the next 5 years for >100 station networks, i.e. using merged data from different measurement laboratories, is close to an order of magnitude improvement (0.2 to 0.02 ppm, 0.2 to 0.02 ‰ for CO_2, $\delta^{13}C$ respectively). For O_2/N_2, perhaps 20-50 sites might contribute to similar precision improvements. With parallel improvements in atmospheric transport and surface flux parameterization, surface fluxes on current GCM grid scales may be improved from current levels of ~1 Gt $C \cdot a^{-1}$ to better than 0.1 Gt $C \cdot a^{-1}$.

ACKNOWLEDGEMENTS

Colleagues at CSIRO Atmospheric Research and the CRC for Southern Hemisphere Meteorology have contributed greatly to the results and perspectives aired here. Paul Steele provided valuable comments on this manuscript. We thank the IAEA for support in developing the CLASSIC-AL strategy, the WMO for permission to include round-robin results in press and CMDL and INSTAAR for the use of ICP results.

REFERENCES

[1] ENTING, I.G., C.M. TRUDINGER, R.J. FRANCEY, A synthesis inversion of the concentration and $\delta^{13}C$ of atmospheric CO_2. Tellus **47B**, 1995, 35-52.

[2] RAYNER, P.J., I.G. ENTING, R.J. FRANCEY, R.L. LANGENFELDS, Reconstructing the recent carbon cycle from atmospheric CO_2, $\delta^{13}C$ and O_2/N_2 observations. Tellus **51B**, 1999, 213-232.

[3] LANGENFELDS, R.L., R.J. FRANCEY, L.P. STEELE, M. BATTLE, R.F. KEELING, W.F. BUDD, Partitioning of the global fossil CO2 sink using a 19-year trend in atmospheric O2. GRL (submitted)

[4] LANGENFELDS, R.L., R.J. FRANCEY, L.P. STEELE, R.F. KEELING, M.L. BENDER, M. BATTLE, W.F. BUDD, Measurements of O2/N2 ratio from the Cape Grim Air Archive and three independent flask sampling programs. Baseline 96, 1999 (in press)

[5] FRANCEY R.J., P.P. TANS, C.E. ALLISON, I.G. ENTING, J.W.C. WHITE, M. TROLIER, Changes in the oceanic and terrestrial carbon uptake since 1982. Nature 373, 1995, 326-330.

[6] KEELING, C.D., T.P. WHORF, M. WAHLEN, J. VAN DER PLICHT, Interannual extremes in the rate of rise of atmospheric carbon dioxide since 1980. Nature 375, 1995, 666-670.

[7] TRENBERTH, K., Global Analyses from ECMWF and Atlas of 1000 to 10 mb Circulation Statistics, CGD, NCAR Report TN-373+STR 205 pp., June 1992. For a copy please contact Kevin Trenberth at (303)497-1318. (NTIS # PB92 218718/AS).

[8] LAW, R.M., P.J. RAYNER, A.S. DENNING, D. ERICKSON, I.Y. FUNG, M. HEIMANN, S.C. PIPER, M. RAMONET, S. TAGUCHI, J.A. TAYLOR, C.M. TRUDINGER, I.G. WATTERSON, Variations in modelled atmospheric transport of carbon dioxide and consequences for CO2 inversion. Glob. Biogeochem. Cyc. 10, 1996, 483-496.

[9] DENNING, A.S., M. HOLZER, K.R. GURNEY, M. HEIMANN, R.M. LAW, P.J. RAYNER, I.Y. FUNG, S.-M. FAN, S. TAGUCHI, P. FRIEDLINGSTEIN, Y. BALKANSKI, J. TAYLOR, M. MAISS, I. LEVIN, Three-dimensional transport and concentration of SF6: A model intercomparison study (TransCom 2). Tellus 51B, 1999, 266-297.

[10] SCHIMEL, D. S., Terrestrial ecosystems and the carbon cycle. Global Change Biology, 1, 1995, 77-91.

[11] LLOYD, J., Current perspectives on the terrestrial carbon cycle. Tellus 51B, 1999, 336-342.

[12] TAKAHASHI, T., R. A. FEELY, R. WEISS, R. H. WANNINKHOF, D. W. CHIPMAN, S. C. SUTHERLAND, T. T. TAKAHASHI, Global air-sea flux of CO2: an estimate based on measurements of sea-air pCO2 difference. Proc. Nat. Acad. Sci., 94, 1997, 8292-8299.

[13] HEIMANN, M., E. MAIER-REIMER, On the relations between the oceanic uptake of CO2 and its carbon isotopes. Glob. Biogeochem. Cyc., 10, 1996, 89-110.

[14] ORR, J.C., On ocean carbon-cycle model comparison. Tellus 51B, 1999, 509-510.

[15] SARMIENTO, J.L., T.M.C. HUGHES, R.J. STOUFFER, S. MANABE, Simulated response of the ocean carbon cycle to anthropogenic climate warming. Nature, 393, 1998, 245-249.

[16] MASARIE, K.A., P.P. TANS, Extension and integration of atmospheric carbon dioxide data into a globally consistent measurement record. J. Geophys. Res., 100, 1995, 11593-11610.

[17] WMO, Environmental Pollution Monitoring and Research Programme, No. 51. Report of the NBS/WMO Expert meeting on Atmospheric Carbon Dioxide Measurement Techniques, Gaithersburg, MD, USA, June 1987, World Meteorological Organization, Geneva.

[18] ALLISON, C.E., R.J. FRANCEY, L.P. STEELE, The IAEA Circulation of Laboratory Air Standards for Stable Isotope Comparisons: aims, preparation and preliminary results, IAEA TECDOC (this issue).

[19] FRANCEY, R.J., L.P. STEELE, R.L. LANGENFELDS, M.P. LUCARELLI, C.E. ALLISON, D.J. BEARDSMORE, S.A. CORAM, N. DEREK, F. DE SILVA, D.M. ETHERIDGE, P.J. FRASER, R.J. HENRY, B. TURNER, E.D. WELCH, Global Atmospheric Sampling Laboratory (GASLAB): supporting and extending the Cape Grim trace gas programs, Baseline Atmospheric Program (Australia) 1993, (eds. R.J. Francey, A.L. Dick and N. Derek), Bureau of Meteorology and CSIRO Division of Atmospheric Research, Melbourne, 1996, pp. 8-29.

[20] MASARIE, K.A., P.P. TANS, GLOBALVIEW-CO2: An update. WMO Experts Report, 1999 (in press).

ATMOSPHERIC ^{14}C IN URBAN, AGRICULTURAL, MOUNTAIN AND COASTAL AREAS IN GREECE

N. ZOURIDAKIS
Isotope Hydrology Laboratory, Institute of Physical Chemistry,
NCSR "Demokritos", Aghia Paraskevi, Athens, Greece

Abstract. In this study, we present the values of the atmospheric ^{14}C concentration that were measured in Athens and other places in the Greek region in a 2-year period. The sampling was performed by collection of air using a ventilated intake stack. The measurements of the radioactivity were performed by the Liquid Scintillation method.

1. INTRODUCTION

It is common knowledge that the concentration of the natural ^{14}C in the atmosphere has been significantly modified by two effects: Firstly, by the emission of CO_2 from fossil fuel combustion that lacks of radioactive carbon and causes a reduction to its concentration (Suess effect) and secondly, by the nuclear weapon tests mainly in the Northern Hemisphere during the '60s that gave out a significant amount of ^{14}C. These two contradictory effects caused a great variation of the value of the ^{14}C concentration.

Today, after the treaty that banned the weapon tests in the atmosphere, we can observe a continuous reduction of the ^{14}C values. Many laboratories have performed measurements on these effects from their very beginning and they still carry out measurements of the value of ^{14}C concentration in various countries worldwide [1-5].

This project presents the ^{14}C measurements so far in the Greek region. We think it is important to perform such measurements in Greece for the following reasons: 1) to gain experience of such measurements (to know how), 2) to study the pollution of the atmosphere above Athens or other cities in Greece, 3) to study the regional variations in ^{14}C concentration that may occur in various sites of the Greek region, as the geography of Greece can provide many different morphologies: high mountains, seaside areas, regions with vegetation or regions completely barren.

2. PROCEDURE AND METHOD

The experiment that is presented was carried out by the Isotope Hydrology Laboratory of NCSR 'DEMOKRITOS'. Our main aim is to define the concentration of the atmospheric ^{14}C in the Greek region today. For this reason we established 13 similar sampling stations at different sites in Greece (Fig.1).

Four stations were placed in the region of Athens (Ippokratus st., Kipseli, Egaleo and Demokritos), two in South Greece (Pelloponese, Crete), two in North Greece (Kavala, Komotini) and one in Central Greece (Sofades - Thessalia). In addition, in May of '98 we placed three more stations at the height of 1000-1500 meters in North Greece (mountain Grammos), in Central Greece (mountain Dirfis) and in Crete (mountain Idi), and one more station on the mountain Troodos in Cyprus.

The first 9 stations started functioning altogether on 15 May 1997 and the sampling of the atmospheric CO_2 lasted for a month. The experiment was repeated in October 1997, in May 1998 and the last sampling procedure will be completed in October '98. The stations in Kavala and Komotini (North Greece) did not function during the second year, while during the second semester of the same year there were not any samples from four other stations (Egaleo, Thessalia, Diros and Troodos in Cyprus).

Fig. 1: Sites of the sampling stations 1-13. The station 14 in Cyprus is not displayed.

Sample No.	Site of sample
1	Athens
2	Athens
3	Athens
4	Athens
5	Kavala
6	Komotini
7	Thessalia
8	Rethimno
9	Diros
10	Ptolemaida
11	Mount. Grammos
12	Mount. Dirfis
13	Mount. Idi
14	Mount. Troodos (Cyprus)

A crucial point in our project was the choice of suitable sites for the station establishment and their attendance by reliable observers. The majority of the observers were colleague teachers in Secondary and Higher Education. All the stations were placed at a height of over 5 meters above the ground and were protected from additional sources of CO_2 like chimneys, fires, etc. The atmospheric CO_2 was trapped by $Ca(OH)_2$ and produced $CaCO_3$. The $Ca(OH)_2$ solution is made of 50g $Ca(OH)_2$ dissolved in 15 liter distilled water. The $Ca(OH)_2$ used contained less than 3% $CaCO_3$. The 15 liter $Ca(OH)_2$ solution was placed in a plastic pot and the atmospheric air was piped into it via an electric pump. The pump had an air flow of 9-10 liter/h and according to our measurements the reaction was completed in about 21 days if the air contained about 0.3% CO_2 and in 12,5 days if the air contained about 0.5% CO_2. The amount of $CaCO_3$ that we finally took was 60-65 g. 10 g from this $CaCO_3$ were used in order to be converted into C_6H_6 using the usual method [6]. The β-radiation measurements of the samples were performed by the Liquid Scintillator method. The Liquid Scintillator equipment of the Laboratory is a Tricarb 2560 TR/XL of the Packard Company, having an efficiency of 90%. The measurements were taken in low level counter mode and the standard of ^{14}C that was used came from the Laboratoire d'Oceanographie Dynamique et de Climatologie (L.O.D.Y.C.) of the University of Pierre and Marie Curie and its radioactivity was 1760 dpm. The background measured in the 10.8-81 keV region is around 0.67 cpm. The vials that were used for the measurements had a volume of 20 ml.

3. RESULTS AND CONCLUSIONS

The results of this experimental procedure ($\delta^{13}C$ and $\Delta^{14}C$ values) are listed in Table 1. The $\delta^{13}C$ values have been measured for the $CaCO_3$ samples and are given in PDB. The $\Delta^{14}C$ values were calculated from the equation: [7]

$$\Delta\ ^{14}C = \delta\ ^{14}C - 2\times(\delta\ ^{13}C+25) \times (1+\delta\ ^{14}C/1000)$$

with

$$\delta\ ^{14}C = 1000\times(A_e - A_0)/A_0$$

where A_e: the radioactivity of the sample in % value compared to that of a sample of 1950,
$A_0 = 100$ % : the radioactivity of a sample of 1950 in % value compared to itself.

TABLE 1. MEASUREMENTS OF THE $\delta\ ^{13}C$ AND $\Delta\ ^{14}C$ VALUES [IN‰] IN THE GREEK REGION IN THE YEARS 1997 AND 1998

Sample No.	Spring 1997		Autumn 1997		Spring 1998		Autumn 1998	
	$\delta^{13}C$	$\Delta\ ^{14}C$	$\delta^{13}C$	$\Delta\ ^{14}C$	$\delta^{13}C$	$\Delta\ ^{14}C$	$\delta^{13}C$	$\Delta\ ^{14}C$
1	-13.1	28 ± 3	-15.2	18 ± 3	-12.3	23 ± 3	-14.9	10 ± 2
2	-14.3	34 ± 3	-14.8	20 ± 3	-14.3	26 ± 3	-17.4	31 ± 3
3	-16.0	68 ± 4	-16.3	55 ± 4	-16.4	60 ± 4	—	—
4	-15.1	81 ± 5	-15.7	56 ± 4	-15.5	82 ± 6	-15.6	51 ± 4
5	-13.5	70 ± 5	-13.8	67 ± 5	—	—	—	—
6	-16.4	76 ± 5	-18.5	77 ± 5	—	—	—	—
7	-14.5	90 ± 6	-14.1	71 ± 5	-14.4	89 ± 6	-14.4	73 ± 4
8	-13.5	87 ± 6	-13.4	66 ± 5	-13.6	88 ± 6	—	—
9	—	—	—	—	-13.5	85 ± 6	—	—
10	—	—	—	—	-14.8	68 ± 6	-14.2	39 ± 4
11	—	—	—	—	-13.3	85 ± 6	-13.4	66 ± 5
12	—	—	—	—	-13.7	85 ± 6	-13.6	77 ± 4
13	—	—	—	—	-13.3	92 ± 6	-13.3	68 ± 5
14	—	—	—	—	-13.4	92 ± 6	—	—

From this table, one can observe that the measurements follow the local and seasonal variations of the ^{14}C concentration. As a result, in the center of Athens, where there is a great release of "dead" CO_2 due to oil combustion, the values of the ^{14}C concentration are lower than the ones in and out of the town region. In addition, there is a distinguishable difference between the values during spring and winter.

By placing a lot of stations all over Greece, we aim to discriminate different values of $^{14}CO_2$ between coastal and non-coastal regions, between regions with and without vegetation, in the center of large cities (Athens) and in industrial regions (Ptolemaida); we would also like to examine the seasonal effect on our measurements (spring - autumn).

Our measurements are in good agreement with the influence of different factors such as CO_2 absorption in coastal areas and in areas with plenty of vegetation. The observed differences are not completely accurate and acceptable due to the small number of measurements. However, the $\Delta^{14}C$ values for the clean stations (Mountain Idi and Mountain Troodos) for the years 1997 and 1998 are in good agreement with the values of Levin I. and Kromer B. [8] for the years 1995 and 1996.

In general, all the measurements show a clear differentiation in the values, not only between industrial areas and country, but between spring and autumn as well.

4. FUTURE PROSPECTS

In the future we are going to run the project by using only three stations: one in the center of Athens in order to observe the effects of the inactive CO_2 on the values of ^{14}C concentration, one on a high mountain (like mountain Idi in Krete) that is considered as a clean station and one in the plain of Thessalia in the central Greece. The sampling will be carried out monthly during the whole year, so that the differences due to the seasonal cycle can be observed.

ACKNOWLEDGEMENTS

This research was supported by the International Atomic Energy Agency. The author thanks J. F. Saliege of the Oceanographie Dynamique Laboratory of the Pierre et Marie Curie University for the $\delta^{13}C$ measurements.

REFERENCES

[1] LEVIN, I., et al., "The continental European Suess effect", Radiocarbon, **31** No.3 (1989) pp. 431-440.

[2] LEVIN, I., et al., "Radiocarbon in atmospheric carbon dioxide and methane: Global distribution and trends", In Taylor, R. E., Long, A. and Kra, R. S., eds, Radiocarbon after four decades: An Interdisciplinary Perspective, New York (1992), Spinger – Verlag: 503-517.

[3] MEIJER, H. A. J., VAN DER PLICHT, J., GISLEFOSS, J.S., and NYDAL, R., "Comparing long-term atmospheric ^{14}C and ^{3}H records near Groningen, Netherlands, Fruholmen, Norway and Izana, Canary Islands ^{14}C stations", Radiocarbon **37** No.1 (1995) pp. 39-50.

[4] NYDAL, R., and LÖVSETH, K., "Carbon-14 measurements in atmospheric CO_2 from Northern and Southern Hemisphere sites, 1962-1993.", ORNL/CDIAC-93, NPD-057, Oak Ridge National Laboratory, Oak Ridge, Tennessee (1996).

[5] KUC, T., "Changes of carbon isotopes in atmospheric CO_2 of the Krakow region in the last five years", In Long, A., Kra, R. S. and Srdoč, D., eds, Proceedings of the 13th International ^{14}C Conference, Radiocarbon, **31** No.3 (1989) pp. 441-447.

[6] TAMMERS, M. A., "Carbon-14 dating with the liquid scintillation counter: total synthesis of the benzene solvent", Science, **132** (1960) pp. 668-669.

[7] STUIVER, M. and POLLACH, M.A. "Discussion: Reporting of ^{14}C data", Radiocarbon 19, 355-363 (1977).

[8] LEVIN, I., KROMER, B., "Twenty years of atmospheric $^{14}CO_2$ observations at Schauinsland station, Germany", Radiocarbon, **39** No.2 (1997) pp. 205-218.

TROPOSPHERIC CO_2 IN ROMANIA: CONCENTRATION AND ISOTOPIC COMPOSITION MEASUREMENTS[1]

A. TENU, F. DAVIDESCU, V. CUCULEANU
National Institute of Meteorology and Hydrology, Bucharest, Romania

Abstract. Monthly atmospheric CO_2 samples were collected at Bucharest (during the last seven years) and Cernavoda (during the last four years) in order to determine the carbon isotopes, ^{13}C and ^{14}C. The radiocarbon activity, expressed as $\Delta^{14}C$, range generally from –80 to 380 ‰. The highest values are measured at Cernavoda — a station located near to a nuclear power plant — in the last part (May–November) of 1998. The Bucharest series of tropospheric $\Delta^{14}C$ activities includes 83 values covering the interval 1992–1998. These data permit to discuss level, seasonal variation, trend of evolution and also the integration of this station in the framework of regional and global ^{14}C evolution. Besides the carbon isotope measurements, the first quantitative CO_2 determinations carried out in Romania, at Bucharest, for the years 1996 and 1997 are available. The values are expressed as ppmv. The annual mean values are 375–379 ppmv, with minimum and maximum hourly values of 328 (July) and 507 (December) ppmv, respectively. The existence of seasonal and daily variations was also discerned.

1. INTRODUCTION

The measurement of the ^{14}C activity and of the ^{13}C content in atmospheric CO_2 in Romania started in 1991 within the framework of national research regarding "Current Climatic Changes", extended later to the "Impact of Natural and Anthropic Processes on Atmosphere and Hydrosphere", both developed by the National Institute of Meteorology and Hydrology (NIMH). Since July 1997, as a part of the Co-ordinated Project "Isotope-aided studies of atmospheric carbon dioxide and other greenhouse gases–Phase 2", an IAEA Research Project concerning "Carbon isotope composition of atmospheric CO_2 in Romania" also started in NIMH.

The measurements of CO_2 concentration started in Romania in 1996, also within the framework of the above mentioned NIMH project, Impact of Natural and Anthropic Processes on Atmosphere and Hydrosphere.

The extreme eastern points of Central Europe for which measurements of these isotopes and CO_2 concentration have been published until 1997 year were Krakow-Poland [1, 2], Bratislava-Slovakia [3, 4] and Zagreb-Croatia [5]. By the results recently presented in an IAEA Symposium [6], the data from Romania represents a significant extension towards the inside of the continent.

2. SAMPLING LOCATIONS

The carbon isotope measurements for atmospheric CO_2 were related to two locations: Bucharest City and Cernavoda area, with the start of those determinations in 1992 and 1995, respectively.

The quantitative CO_2 monitoring started in 1996 in the Bucharest City also, but in the station named Afumati. Some specifications are given below for the sampling points.

The *Bucharest city* site (44° 25' N, 26° 06' E, 82 m a.s.l.), is situated on a large flat plain area; the air composition characterizes a large town area — surface about 400 km^2 and approximately 2.3 million inhabitants — and particular (predominant northern winds in the cold season) dynamic climate conditions. The sampling point for isotopic composition was

[1] The work was partially performed within the framework of IAEA 9721 Research Contract.

located close to the boundary of the city, inside an empty room (two windows were permanently open), situated at the top of a tower at about 17 m above the ground level. The monitoring point for CO_2 measurements is situated in the most north-eastern part of the Bucharest City area at about 150 m next to a busy road and very close to a small coal heating plant.

The *Cernavoda area* (44°21' N, 28°03' E and 37 m a.s.l) is also situated in the Romanian Plain but about 160 km East of Bucharest. The Cernavoda town and the close nuclear power plant are situated near to the right bank of the Danube River; the sampling is made inside a meteorological shelter.

3. EXPERIMENTAL PROCEDURES

The sampling of carbon dioxide for subsequent analysis of its isotopic composition is made by static absorption, in about one liter of diluted (0.5 N) NaOH, in a 900 cm^2 plastics tray, for 14 days, during the first half of each month. The Na_2CO_3 formed in this way absorbs 4 g carbon, sufficient for the analysis of both carbon isotopes. It is known that such procedures as absorbing carbon dioxide in a basic solution cause considerable fractionation [7]; consequently, the $\delta^{13}C$ values do not represent the true atmospheric ^{13}C level.

During the preparation procedure, the CO_2 is extracted from the basic solution in a vacuum system by adding hydrochloric or sulphuric acid.

The ^{14}C activity is measured using the liquid scintillation technique with benzene obtained by the CO_2 conversion; a LS 5801 Beckman counter is used.

The ^{14}C results are expressed as $\Delta^{14}C$ [8], referred to the – decay corrected –95% NBS oxalic acid activity and adjusted to $\delta^{13}C = -25$ ‰. As the sampling procedure was not quantitatively, each ^{14}C activity expressed as $\delta^{14}C$ was corrected by its individual $\delta^{13}C$ value. The precision of a single $\Delta^{14}C$ value is assumed to be ±5‰.

The ^{13}C / ^{12}C ratio is measured by mass spectrometry from small aliquots of the CO_2 gas. The mass spectrometers used in this study were Varian-MAT-250 and Atlas, installed at Ramnicu Valcea Institute and Cluj-Napoca Institute, respectively. Values are given relative to the VPDB standard; the overall precision is typically ±0.1‰.

For the CO_2 concentration determination, the sampling is made by continuously aspiration of air at about 10 m above the ground level. A non-dispersive infrared (NDIR) monitor was used with the gas filter correlation technique and a Thermo Environmental Instruments analyzer, type GFC, model 41 H. Each 5 minutes a measurement of 12 seconds is made and every half-hour the average values are stored on a computer hard-disk. The sensivity is about 0.2 ppmv and the detection limit of 0.005 ppmv.

4. EXPERIMENTAL RESULTS

The isotopic results refer to the Bucharest and Cernavoda stations while the quantitative CO_2 measurements refer only to the Bucharest-Afumati station.

As ^{14}C activities, the *Bucharest series* (Table I) include 83 values, covering 83 months in the interval 1991–1998; from February 1992 until November 1998 the series is practically continuous. In order to obtain comparable isotopic results, ^{14}C (pMC) and $\delta^{13}C$ were determined while $\delta^{14}C$ and $\Delta^{14}C$ were successively calculated. The last six $\Delta^{14}C$ values are provisional because calculated by a $\delta^{13}C$ evaluated as an average of previous 11 measured results. They were taken into consideration only in the discussion of isotopic results on local framework.

TABLE I. TROPOSPHERIC $\Delta^{14}C$ ACTIVITIES AT THE BUCHAREST STATION (* MISSING VALUE; $\Delta^{14}C$ EVALUATED BY THE $\delta^{13}C$ AVERAGE VALUE OF ADJACENT MONTHS OR INTERVAL)

Sample no.	Sampling interval Year/month	$\delta^{13}C$ [‰]	$\Delta^{14}C$ [‰]
P-114	91.05	–15.0	64
P-121	92.02	*	124
P-123	92.03	*	117
P-125	92.04	–18.3	177
P-127	92.05	–19.3	82
P-129	92.06	–23.5	214
P-131	92.07	–21.2	80
P-133	92.08	–23.4	107
P-135	92.09	–18.2	192
P-137	92.10	–23.4	169
P-139	92.11	–19.3	197
P-141	92.12	–21.1	115
P-143	93.01	–22.2	74
P-145	93.02	–22.9	256
P-147	93.03	–19.0	134
P-149	93.04	–22.9	173
P-151	93.05	–20.9	148
P-153	93.06	* –21.8	98
P-155	93.07	–23.1	120
P-157	93.08	–18.3	85
P-159	93.09	–19.9	63
P-161	93.10	–20.0	111
P-163	93.11	–21.1	99
P-165	93.12	–20.0	122
P-167	94.01	–19.4	190
P-169	94.02	–22.9	140
P-171	94.03	–19.3	130
P-173	94.04	–21.2	162
P-175	94.05	–22.2	150
P-177	94.06	–18.2	157
P-179	94.07	–21.3	139
P-181	94.08	–19.6	145
P–183	94.09	–13.6	125
P-- 185	94.10	* –15.4	123
P-187/P-187	94.11	–21.7	121
P-189/P-189	94.12	–15.7	116
P-191/P-191	95.01	–16.4	75
P-193/P-193	95.02	–15.9	115
P-195/P-195	95.03	–16.4	167
P-197/P-197	95.04	–14.4	179
P–199	95.05	–9.3	199
P-201	95.06	–13.0	206
P-203	95.07	–13.5	140
P-205	95.08	–14.2	131
P-207	95.09	–13.0	125
P-209	95.10	–15.6	24
P-211	95.11	–14.8	148
P-213	95.12	–23.9	134
P-215	96.01	–17.3	*
P-217	96.02	–18.0	41
P-219	96.03	–17.5	124
P-221	96.04	–12.7	138
P-223	96.05	–12.7	130

TABLE I (cont.)

P-225	96.06	–11.3	88
P-227	96.07	–10.5	37
P-229	96.08	–12.2	48
P-231	96.09	–17.8	30
P-233	96.10	–10.5	22
P-235	96.11	–20.8	102
P-237	96.12	–15.0	–26
P-239	97.01	–39.5	–21
P-241	97.02	–24.7	–77
P-243	97.03	-23.8	32
P-245	97.04	–24.0	170
P-247	97.05	–24.3	83
P-249	97.06	* –17.1	68
P-251	97.07	–9.9	53
P-253	97.08	–6.4	48
P-255	97.09	–15.8	29
P-257	97.10	–15.3	87
P-259	97.11	–16.3	53
P-261	97.12	–16.3	153
P-263	98.01	–18.1	157
P-265	98.02	–13.6	–17
P-267	98.03	–13.2	32
P-269	98.04	–12.4	19
P-271	98.05	–10.1	88
P-273	98.06	* –14.3	214
P-275	98.07	* –14.3	188
P-277	98.08	* –14.3	200
P-279	98.09	* –14.3	150
P-281	98.10	* –14.3	93
P-283	98.11	* –14.3	174

The *Cernavoda series* (Table II) includes 44 samples, covering 44 months in the interval April 1995–November 1998; after July 1996 the results refer to the nuclear power plant functioning stage. All the results were similarly treated as above. The last six $\Delta^{14}C$ values are provisional because calculated by a $\delta^{13}C$ evaluated as an average of previous 9 measured results. They were taken into consideration only in the discussion of isotopic results on local framework. Some of these results were previously published, too [9].

CO_2 concentration was measured in tropospheric air at Bucharest-Afumati station and refer to 1996 and 1997 years. While for 1996 the monitored interval cover only 5 months (23 June to 14 October) and totalize 5,056 determinations, the 1997 year had all the months covered by monitoring; even if there are some gaps, among them one of 22 days for the month of May, the general continuity may be considered satisfactory. The total annual determinations number is of 14,653 that means a coverage degree which reaches about 84%.

As it is not useful to reproduce the entire data base, Table III shows the average monthly and annual CO_2 contents for the entire mentioned period while Table IV includes the main statistical monthly parameters for 1997 CO_2 determinations.

TABLE II. TROPOSPHERIC Δ ^{14}C ACTIVITIES AT THE CERNOVODA STATION. (* MISSING VALUE; $\Delta^{14}C$ EVALUATED BY THE $\delta^{13}C$ AVERAGE VALUE OF ADJACENT MONTHS OR INTERVAL)

Sample no.	Sampling interval Year/month	$\delta^{13}C$ [‰]	$\Delta^{14}C$ [‰]
P-198	95.04	-18.3	171
P-200	95.05	-16.2	211
P-202	95.06	-10.4	143
P-204	95.07	–14.2	129
P-206	95.08	–14.4	121
P-208	95.09	–15.4	44
P-210	95.10	–14.6	113
P-212	95.11	–19.6	131
P-214	95.12	–21.4	45
P-216	96.01	* –18.3	81
P-218	96.02	–15.3	50
P-220	96.03	–18.1	143
P-222	96.04	–17.7	248
P-224	96.05	–16.8	219
P-226	96.06	–14.7	125
P-228	96.07	–14.8	121
P-230	96.08	–23.5	103
P-232	96.09	–28.3	85
P-234	96.10	–26.7	7
P-236	96.11	–19.7	66
P-238	96.12	* –20.0	–86
P-240	97.01	* –19.5	17
P-242	97.02	–19.0	–39
P-244	97.03	–21.8	65
P-246	97.04	–21.6	–52
P-248	97.05	–25.7	27
P-250	97.06	* –20.0	86
P-252	97.07	* –20.0	108
P-254	97.08	* –20.0	142
P-256	97.09	–14.4	108
P-258	97.10	–15.4	85
P-260	97.11	–15.8	25
P-262	97.12	–15.5	84
P-264	98.01	–17.5	132
P-266	98.02	–12.8	123
P-268	98.03	–10.3	45
P-270	98.04	–15.6	90
P-272	98.05	–13.3	929
P-274	98.06	* –14.5	391
P-276	98.07	* –14.5	253
P-278	98.08	* –14.5	266
P-280	98.09	* –14.5	240
P-282	98.10	* –14.5	378
P-284	98.11	* –14.5	278

TABLE III. AVERAGE MONTHLY AND ANNUAL CO_2 CONTENTS (ppmv) OF ATMOSPHERIC AIR IN BUCHAREST — AFUMATI STATION (- NOT MEASURED; * MISSING VALUE)

Month	1996	1997
January	-	388.6
February	-	380.4
March	-	385.8
April	-	379.2
May	-	361.8
June	386.2	373.1
July	384.3	379.8
August	379.8	364.6
September	380.3	371.2
October	362.5	370.7
November	*	375.3
December	*	373.7
Annual average	378.6	375.4

TABLE IV. MONTHLY STATISTICAL PARAMETERS FOR 1997 CO_2 DETERMINATIONS AT BUCHAREST — AFUMATI STATION

Month	No. determ.	Max. value	Min. value	Average	St.dev.	Median	Mode	Kurt	Skew
J	834	444	359	389	15	387	381	1.2	0.9
F	1344	445	350	380	13	378	368	3.1	1.4
M	1488	445	358	386	11	385	383	1.0	0.5
A	1364	424	354	379	11	379	377	-0.2	0.2
M	432	394	349	362	8	360	356	2.5	1.5
J	1440	505	341	373	27	365	352	4.0	1.9
J	1104	493	328	380	25	372	359	2.1	1.4
A	1152	493	341	365	19	359	349	9.3	2.5
S	1367	438	345	371	15	369	361	1.2	1.0
O	1200	437	341	371	17	368	363	0.7	0.9
N	1440	494	335	375	21	369	366	6.7	2.3
D	1488	507	347	374	22	368	362	11.1	2.9

Average — arithmetic mean of the values. **St.dev** — a measure of how widely values are dispersed from the average value. Standard deviation uses the following formula: $\sqrt{\frac{n\sum x^2-(\sum x)^2}{n(n-1)}}$ **Median** — the number in the middle of set of numbers. **Mode** — the most frequently occurring value in an array or range of data. **Kurt** (kurtosis) — characterizes the relative peakedness or flatness of a distribution compared with the normal distribution. Positive kurtosis indicates a relatively peaked distribution. Negative kurtosis indicates a relatively flat distribution. Kurtosis is defined as: $\left[\frac{n(n+1)}{(n-1)(n-2)(n-3)}\sum\left(\frac{xi-\bar{x}}{s}\right)\right]-\frac{3(n-1)^2}{(n-2)(n-3)}$ where: s is the sample standard deviation. **Skew** (skewness) — characterizes the degree of asymmetry of a distribution around its mean. Positive skewness indicates a distribution with an asymmetric tail extending toward more positive values. Negative skewness indicates a distribution with an asymmetric tail extending toward more negative values. The equation for skewness is defined as: $\frac{n}{(n-1)(n-2)}\sum\left(\frac{xi-\bar{x}}{s}\right)^3$

5. DISCUSSION OF THE RESULTS

5.1. Isotopic results.

It is known that the present atmospheric ^{14}C activity at any place is a balance between natural activity, additional anthropogenic activities, dilution by fossil-fuel carbon dioxide, local sources of $^{12}CO_2$ (e.g. mofette) and exchange between the reservoirs. In this context, important factors are latitude, altitude, distance from the ocean and the regional dynamic pattern of the atmosphere.

The seasonal variation is mainly attributed to a seasonally varying contribution of fossil fuel CO_2 at the measurement site with a largest contribution in the winter half year. Secondary causes are [13]:

- biospheric CO_2 flux in the atmosphere, with a higher ^{14}C level in summer months;
- stratospheric intrusions of air enriched in ^{14}C into the troposphere (max. in July).

The decline of radiocarbon content in the atmosphere is the consequence of bomb ^{14}C that is still equilibrated with the world oceans and the biosphere, as well as an ongoing input of ^{14}C-free fossil fuel CO_2.

5.1.1. On the local framework.

As already mentioned, the Bucharest series includes observations practically continuously covering 82 months during the 1992—1998 period, while the Cernavoda series is much shorter, with only 44 observation months. Fig. 1, giving the time variation of the $\Delta^{14}C$ values at the two stations, supplies the following information regarding their variability:

(a) First of all, a random variation of the values with time is emphasized, shown by sometimes significant jumps between the adjacent information steps. This is well illustrated for the Bucharest station in 1992.

(b) It can also be noticed that there is a periodical variability with an annual cyclicity due to some natural or anthropic factors acting seasonally. This variability is much more clearly revealed for both stations in Fig. 2, where multiannual mean values were used. The histograms are similar, with maximum values during the April-May period, with a trend for the appearance of a second – but less accentuated – maximum, in November.

(c) Finally, Fig. 1 also suggests the existence in the interval 1992–1997 of a multiannual trend which, for both stations, is a decreasing one. After a relatively constant period during the 1992–1994 period, emphasized also by the annual mean values (Table V), during the following three years a rapid decrease followed (some values $\Delta^{14}C$ are even negative) accompanied by a marked variability.

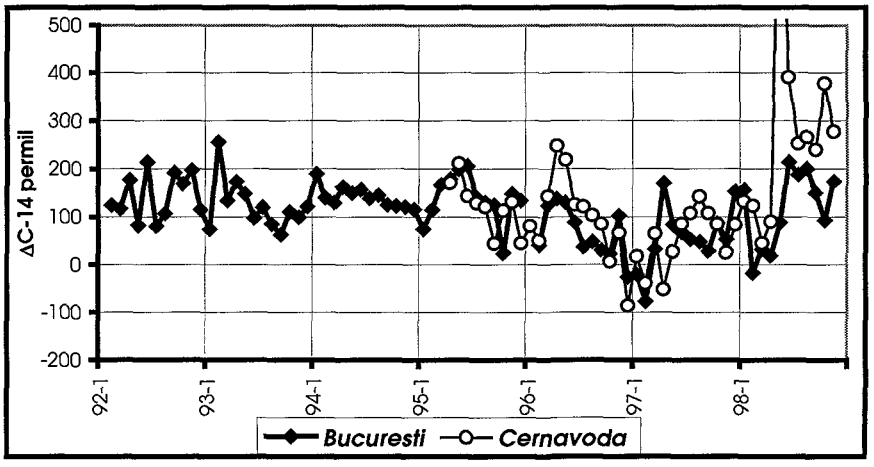

Figure 1. $\Delta^{14}C$ time-variation in Romania.

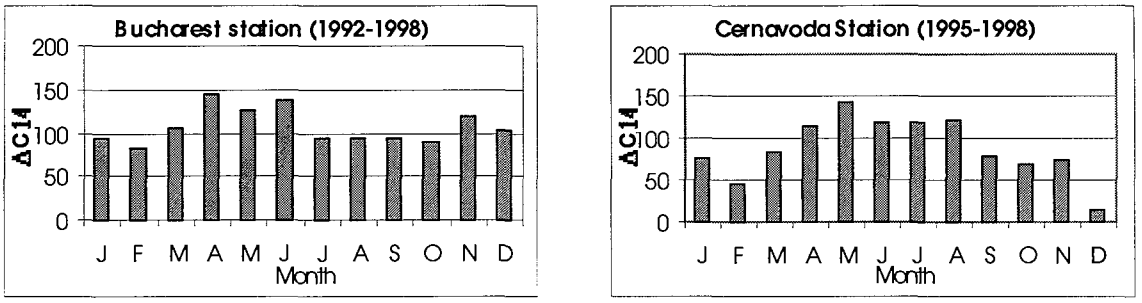

Figure 2. Monthly multiannual averages of $\Delta^{14}C$ in tropospheric air (Romania).

TABLE V. ANNUAL $\Delta^{14}C$ AVERAGES[1)] FOR BUCHAREST (B) AND CERNAVODA (C) STATIONS

Year	(B)	(C)
1992	141	-
1993	124	-
1994	142	-
1995	137	★124
1996	68	97
1997	57	55
1998	✷ 56	✷101

1) ★- values obtained by extrapolation; ✷ — values for the first 5 months.

Trying a quantification of the decrease rate with time (linear trend of monthly values) it can be noticed that the Bucharest series (1992–1997) has decreased by about 18‰/year while over the period 1995–1997 the Cernavoda series has emphasized a much higher decreasing rate, of about 53‰/year.

Very interesting, but not yet clarified because the $\Delta^{14}C$ values are provisional, is the fact that during 1998 year seems to occur an radiocarbon increasing at both stations, higher at Cernavoda starting in May ($\Delta^{14}C$ = 929 ‰) the values remain all over 240 permil until the end of the year. This very strong growth in May and even the subsequent high values can be in relation with the activity of Cernavoda nuclear power plant but, a reliable conclusion will be possible only later, after the ^{13}C measurements and a longer period of observations.

Another aspect followed by the interpretation of the radiocarbon data was the correlation degree between the two stations. The diagram in Fig. 1 emphasizes, from the qualitative point of view, the existence of a good correlation for 1995 as well as decreases/increases that are in agreement as concerning the season — even if they cannot be correlated as amplitudes — during the following years, 1996–1998. The moving average curves (Fig. 3) calculated on 4-month time lags, so that the seasonal variations should not become dim, show a much better agreement of the maximum and minimum values for the two stations than the curves in Fig. 1. However, the correlation of the two stations, Bucharest and Cernavoda (Fig. 4) with a strength of only R = 0.36 suggests that the local conditions, though not very different, impose a separate monitoring.

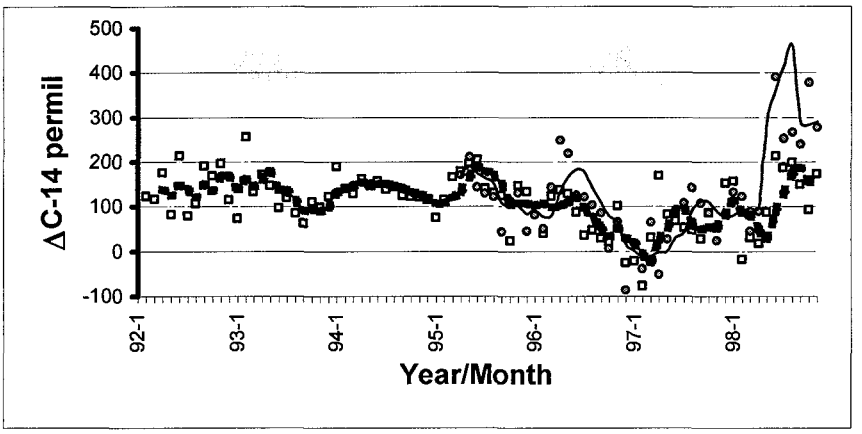

Figure 3. Four months moving average of $\Delta^{14}C$ time variation (dotted line — Bucharest series; continuous line — Cernavoda series).

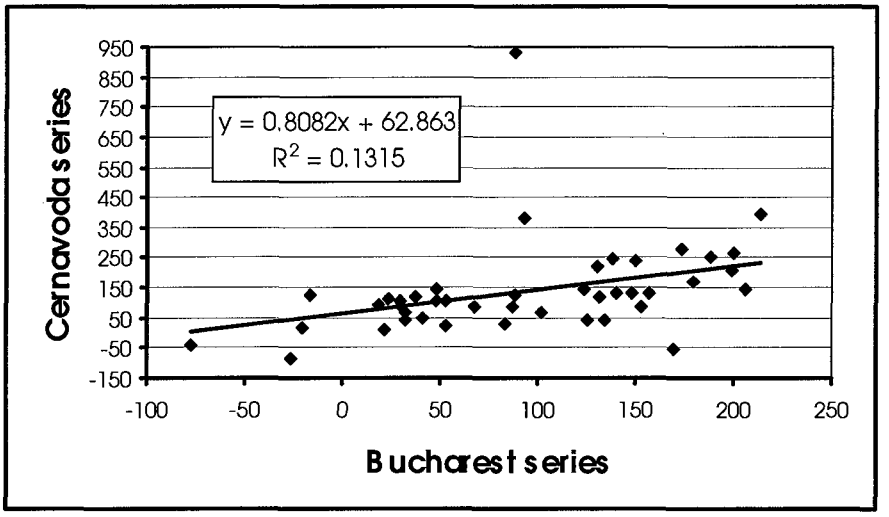

Figure 4. $\Delta^{14}C$ linear correlation between Bucharest and Cernavoda series.

5.1.2. On the regional framework

The Bucharest series, as the longest measurement range performed in Romania, permit to discuss their integration in the framework of regional and global ^{14}C evolution. Only the reliable results, from February 1992 till May 1998 were taken into consideration; the last six provisional values (June–November 1998) were excluded.

The following aspects will be discussed: activity level, seasonal variation and trend evolution.

Yearly means (Table V) of the ^{14}C activity level in Bucharest lie in the range of 57 −142 ‰. This level seems to be constant enough during the 1992–1995 period and strongly descendent after 1996.

In order to evaluate the absolute level of these results at a global scale, the diagram in Fig. 5 was carried out using some experimental data for Vermunt-Austria [10], for Wellington, New Zealand and [11] and for Krakow, Poland [12], published in a numeric form.

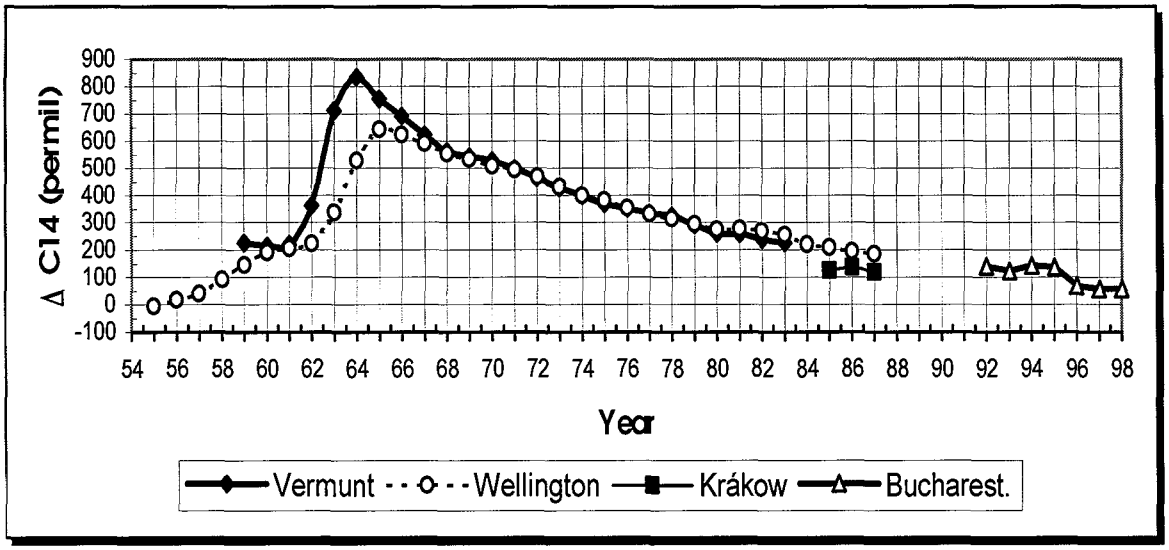

Figure 5. Time-variation of $\Delta^{14}C$ yearly means for some experimental data.

TABLE VI. THE RANGE OF MAXIMUM ANNUAL DIFFERENCES FOR MONTHLY $\Delta^{14}C$‰

Station	Interval	$\Delta^{14}C$ range	Obs.
Wellington, New Zealand	1966–1977	22 58	
Vermunt, Austria	1966–1982	20.....62	101 for 1966
Krákow, Poland	1985–1987	98.....106	
Bucharest, Romania	1992–1997	74.....247	

By their position in this diagram, our results from 1992–1995 interval are in continuity and in a good agreement with the Vermunt and Wellington series but are situated at the same absolute level as the samples collected in Poland in the 1985–87 interval, $\Delta^{14}C \cong 120–140$ ‰. On the other hand, the three last values (1996–1998) are very low, situated near 60–70‰ $\Delta^{14}C$.

The annual amplitude at Bucharest of the monthly $\Delta^{14}C$ values, calculated as the difference between maximum and minimum values, generally is large (usually between 100 and 200 ‰) and varies strongly from year to year (247 ‰ in the 1997 year and only 74 ‰ in the 1994). Table VI shows the range of yearly differences for Bucharest and for other three stations on the globe. The great annual amplitudes and the large range found at Bucharest may be explained, partially at least, by the inside continent position and by the low elevation of the sampling point.

The existence of a seasonal variation, sometimes more obvious (1995), at other times rather attenuated (1994) is also observed for the Bucharest station [6]. The monthly multiannual histogram of $\Delta^{14}C$ (Fig. 2a) emphasizes very clearly, for the entire interval 1992–1998, the presence of this phenomenon. Generally, the maximum value is migratory in the first half of the year while the minimum is generally placed in the second half. Moreover, the average of ^{14}C activity for the first half of each year is higher than the same value for the second half year.

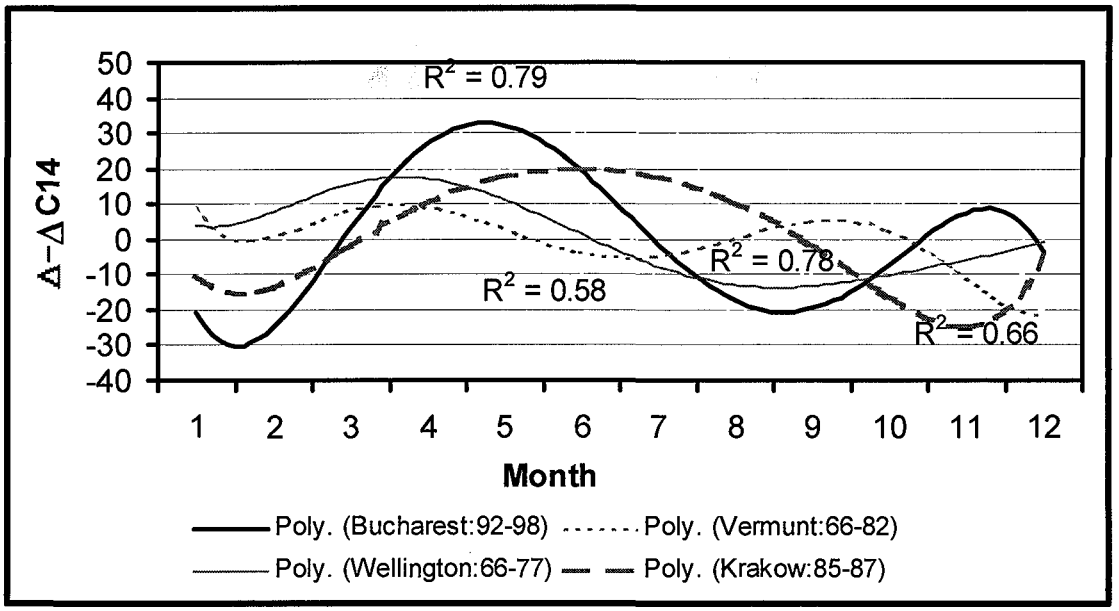

Figure 6. Seasonal-polynomial trend of multiannual monthly $\Delta^{14}C$ means.

In order to compare the seasonality between different sites, the mean seasonal cycles for four stations (Bucharest, Vermunt, Krákow and Wellington) were calculated using a polynomial equation of the order of 6 (Fig. 6), with $R^2 > 0.58$ for all curves. The following steps were observed for all stations:

(1) the selection of the years with as complete as possible data series in the observation intervals mentioned in Table VI (excluding 1974–75 for Vermunt);

(2) the calculation of the monthly multiannual means and of the multiannual average;

(3) the calculation of Δ-$\Delta^{14}C$ by the difference of these previous values.

A first observation on Fig. 6 refers to the fact that the curves for Bucharest and Krákow show, during the last months of the years, an additional inflexion that we attribute to the shorter observation series. However, it must be noticed that even for a station as Vermunt, with a long determination period, two clear maximum values along the year are emphasized. As Fig. 6 reveals, there are significant differences between the seasonality of the four stations in amplitude and phase. From the amplitude point of view, the Bucharest station is similar to the Krákow one, the other two stations having lower amplitudes due to accountable reasons (altitude or geographical position). But these two stations, Bucharest and Krákow, though situated in the approximately similar conditions, have some peculiarities: a larger shape of the Krákow curve for the maximum, accompanied by an about two-month phase difference and inverse trend in the last months of the year. It is interesting to emphasize the similarity of the Bucharest and Wellington curves, corresponding very well as seasonality of the maximum and minimum values, of course less as amplitude. We would like to precise once more that the Wellington curve in Fig. 6 corresponds to 1966–1977 period. At this station an unusual change phenomenon in the seasonal cycle was revealed [11]; since 1980 onwards the maximum is placed in the July-August and the minimum in January. It must be noticed that by adding the last values determined at the Bucharest station, the shape of the polynomial curve has not been significantly modified as compared to the previous [6] and R^2 has increased from 0.61 to 0.79. In order to evaluate our yearly results as the trend evolution, Fig. 7 was elaborated using the multiannual background ^{14}C activity level in Europe.

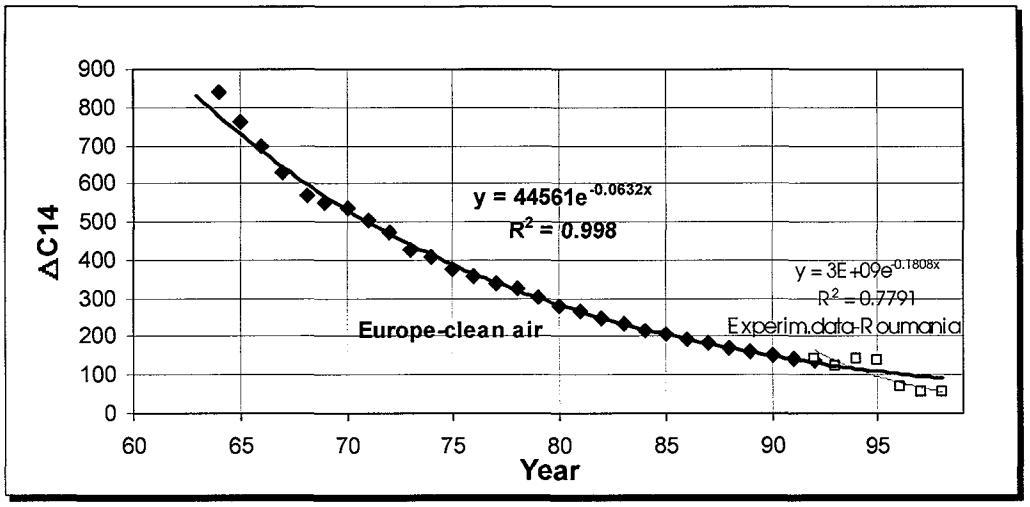

Figure 7. Exponential trendline for $\Delta^{14}C$ in the Central European atmosphere.

"Europe-clean air" represents a synthetic series which may be considered as representative background $\Delta^{14}C$ level for the mid-latitude of continental Northern Hemisphere, more precisely for the Central Europe. It is mainly constituted on the basis of the combination of two high altitude stations data: Vermunt-Austria (47°N, 10°E, 1800 m a.s.l), for the interval 1959–1983 [10] and Jungfraujoch in the Swiss Alps (47°N, 8°E, 3450 m a.s.l) for the interval 1986–1991, extrapolated later by calculation to the 1977–1992 period [14]. This level, undisturbed by local fossil fuel contamination, is higher by about 6‰ than other stations situated at lower altitude in Germany but a deviation of 60‰ in Georgia [3] was mentioned in the interval 1977–1980.

As can be seen in Fig. 7, the trendline for Europe-clean air in the interval 1964–1992 may be well approximated by an exponential trendline equation, $y = 44561 \times e^{-0.0632x}$ (with $R^2 = 0.998$). According to this last equation, the ^{14}C activity expressed as $\Delta^{14}C$ shows a steady and approximately exponential decrease of about $T^{1/2} = 11$ years.

As Figure 7 shows, the experimental data at Bucharest overlap the extrapolated exponential trendline for 1992–1995 interval in contrast to the expectation that the means of 1994 and 1995 to be a few units lower and therefore located below this line. For the years 1996–1998, the mean values are situated much below the expected ones.

5.2. CO_2 concentration

The previously presented results of the CO_2 measurements in Bucharest (section 4.2.) provide a complete series only for 1997. The data of this type constitute time series with values that can be ultimately admitted as discrete. It is known that the graphic shape of such a series (Fig. 8) is the result of several variability's with natural or anthropic causes acting at the planetary, regional or local level. The analysis of the dynamics and behavior of such series is relatively complicated from the mathematical point of view. This fact, added to the relatively limited extent of our series, have led to an exclusive approach at general statistical analysis.

The annual mean values (Table III) coming only from 1996 and 1997 have values of 375–379 ppmv. We think that these values are enhanced compared to other European regions and reflect the continental character of the station with significant fossil fuel burning in the area. However, the contents measured are much below those recorded for the NW of China, 410–550 ppmv [15]. The incomplete monthly data for 1996 (see Table III) make it risky to discuss on the decrease of the mean value of 1997 although this could be a reality and it could be related to the diminishing activity in the thermo-power plants.

The data series corresponding to 1997 allows a more complete analysis of an annual sequence. Table IV presents the monthly statistical parameters for this year; only two observations will be underlined as compared to the tabled values, that is:

- the fact that the minimum and maximum values recorded in 1997 were 328 ppmv (July) and 507 ppmv (December), respectively;
- the monthly (maximum-minimum) range is, for seven months in a year, located between 50 and 100 ppmv and for the other five months (June, July, August and November, December), at values above 150 ppmv.

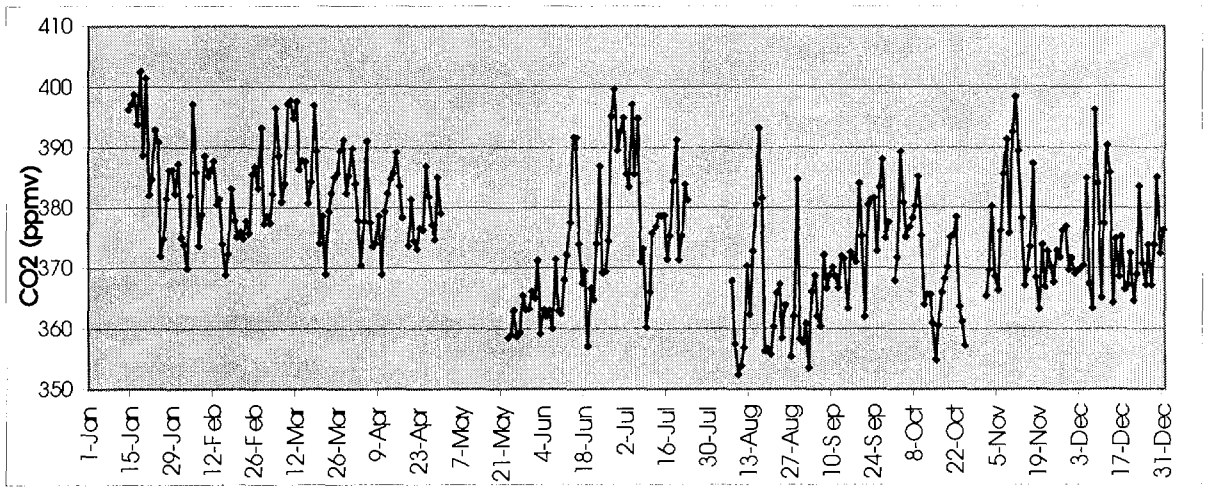

Figure 8. Variation of the CO_2 daily-average values at Bucharest-Afumati station (1997 year).

Fig. 9 shows the monthly distribution frequency of the values grouped into classes. The general asymmetry character of the distributions is normal for a natural component that shows a threshold concentration. On the other hand, the right asymmetry noticed for CO_2 at Bucharest-Afumati station may be attributed to natural or anthropogenic carbon dioxide short-time releases; this type of asymmetry is emphasized also by skew parameter (Table IV) that shows, for Romania, the greatest asymmetry (skew >2) for three months, August, November and December.

As regarding the seasonal variation of CO_2, it must be noticed that the diagram of the daily mean values (Fig. 8) does not very clearly reflect this phenomenon; the fact that this can be a peculiar characteristic of 1997 must not be excluded. The histogram in Fig. 10 illustrates more clearly the cyclic character of the phenomenon: higher monthly mean contents in the winter (January-April) when in Bucharest there are massive burning of fossil fuels for heating.

As regarding the daily variation of CO_2, Fig. 11, carried out by all the 1997 values, shows the existence of an extremely ordered (the polynomial correlation coefficient, $R^2 = 0.98$) and well marked distribution (about 20 ppmv range) with maximum and minimum values placed at 5–6 and 16–17 hourly intervals respectively. It must be mentioned that the similar diagram for 1996 is in total agreement with that in Fig. 11. The above mentioned image, that does not take into consideration the monthly or seasonal peculiarities, has been detailed for each separate month by using the hourly mean values; for the four seasons have been chosen only the characteristic months for exemplification (Fig. 12). The approximation of experimental distribution have been drawn by the polynomial curves. These diagrams allow us to retrieve useful observations not only for the daily cycle but also for its variability (shape, values, amplitudes) along a year. Only a few of them will be mentioned here.

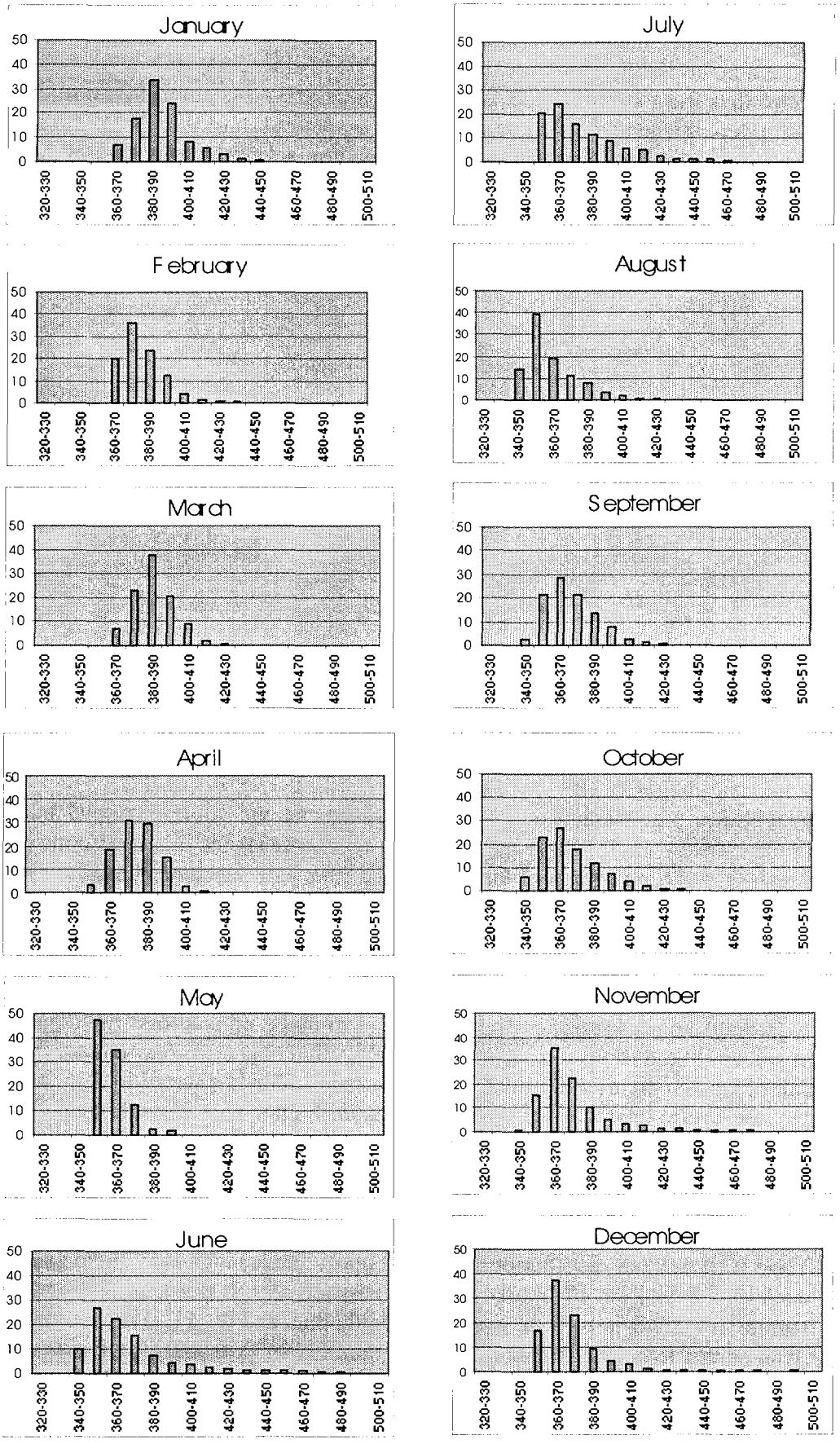

Figure 9. Monthly distribution frequency of CO_2 value classes for Bucharest-Afumati station in the 1997 year.

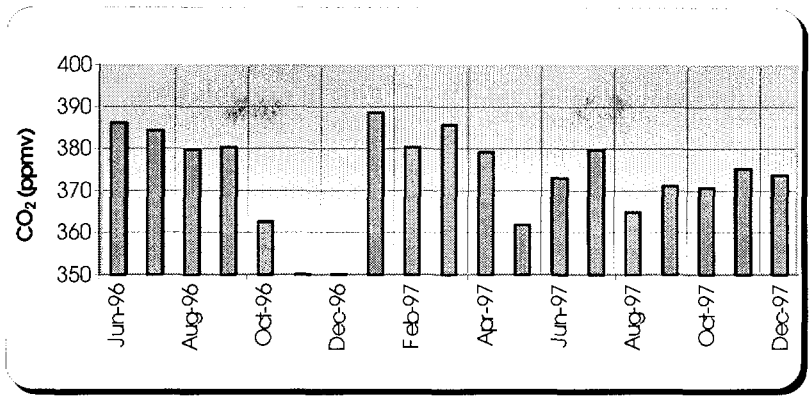

Figure 10. Histogram of CO_2 monthly average contents in atmospheric air at Bucharest-Afumati station (1996–1997).

A first aspect to which we shall refer will be the curve shape. By comparing the distribution curves of the experimental values in the four months (Fig. 12) with the annual curve (Fig. 11) it can be noticed that:

- The curves of April and July are smooth and approximately identical with the annual curve; all these curves show — for 24 hours — a single maximum and minimum.
- The January and October curves, however, are irregular and present an additional small maximum placed towards the evening (20–21 hourly interval). We interpret the irregularities as a sign of anthropogenic, instantaneous influences and the evening maximum as being obviously related to the urban heating time table. During the last part of October 1997, earlier than other years, Bucharest experienced low air temperature requiring some dwelling heating.
- Finally, we must remark a very large minimum for the July, undoubtedly a consequence of the day-light duration.

A second aspect to which we shall refer is that of some parameters, the seasonal variation of which is synthesized on Table VII. Two aspects are to be especially remarked:

- The large value of the maximum and of the amplitude for July and the small ones for October which are a natural consequence of the vegetation period stages and of a reduced anthropic CO_2 contribution;
- The daily moments of the maximum and minimum values are maintained about the same, that is in the morning (3–6 a.m.) and in the afternoon (2–5 p.m.) respectively, except the maximum for January when this is shifted towards 9–10 a.m.

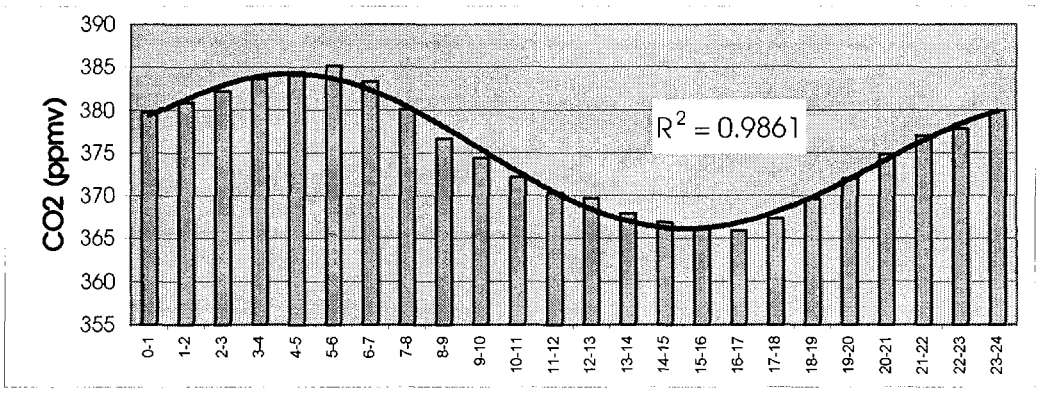

Figure 11. Global diurnal variation for 1997 CO_2 contents in tropospheric air at Bucharest-Afumati station.

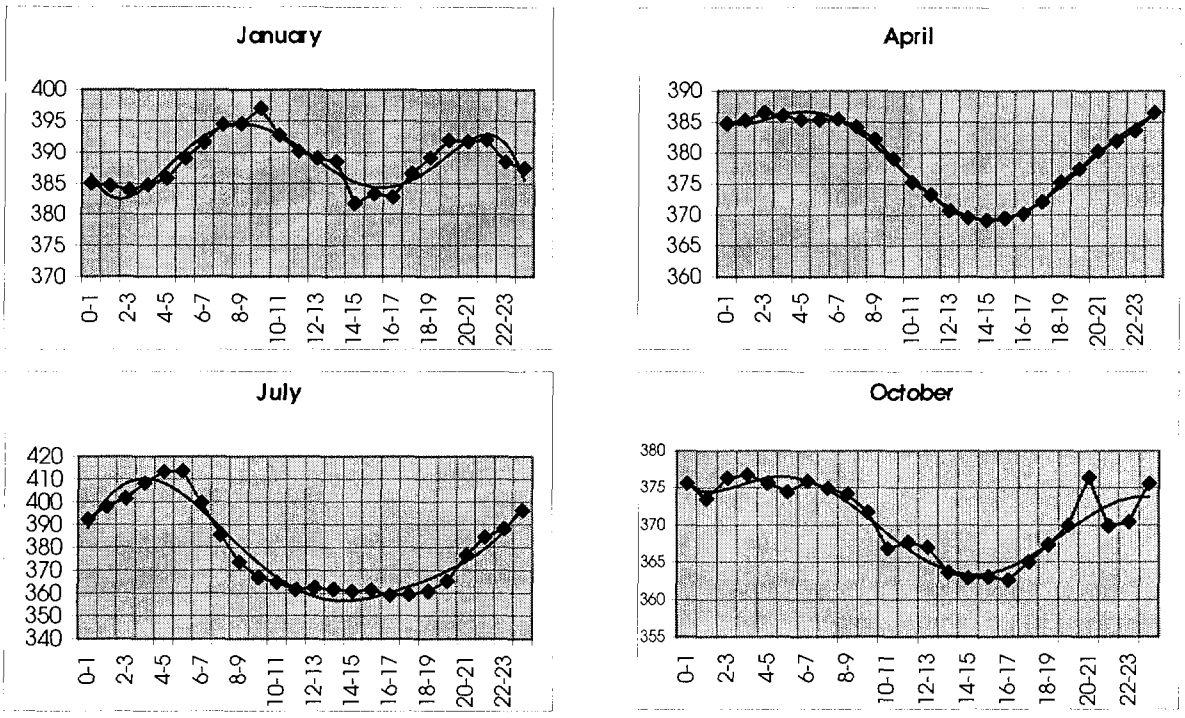

Figure 12. Annual variation of CO_2 diurnal cycle for seasonal characteristic months at Bucharest-Afumati station in the 1997 year.

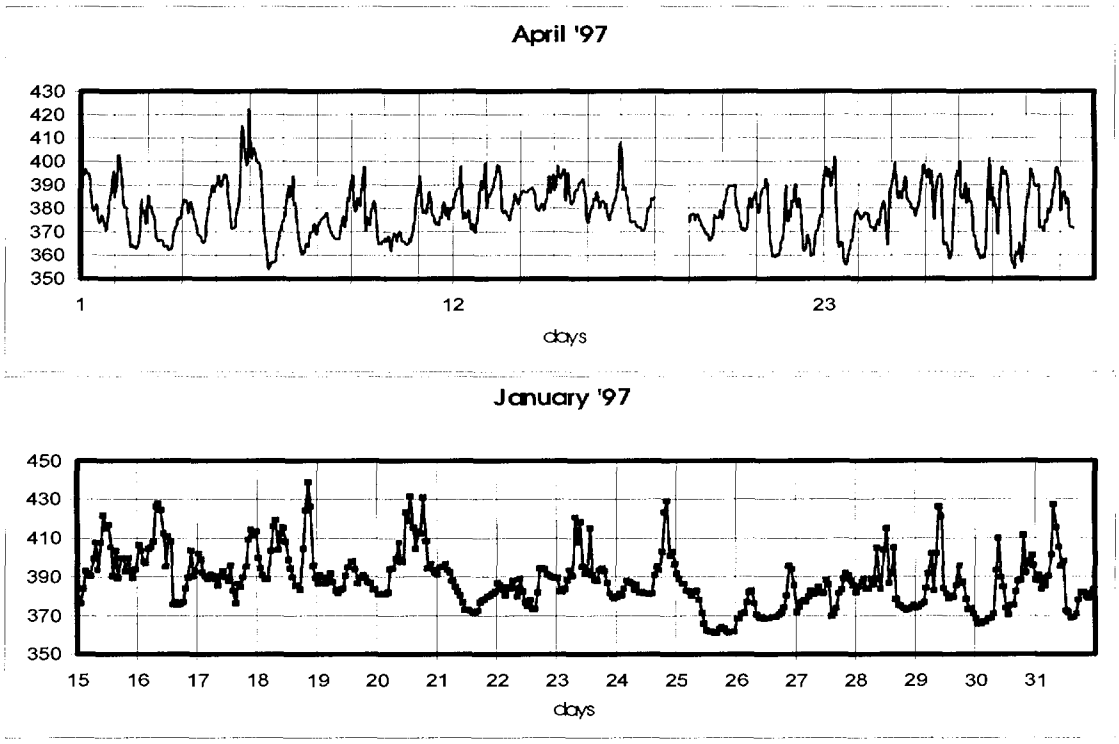

Figure 13. Hourly CO_2 variation during two seasonal characteristic months.

TABLE VII. SYNTHETIC TABLE ABOUT THE CO_2 (PPMV) DIURNAL CYCLE IN CHARACTERISTIC SEASONAL MONTHS (BUCHAREST-AFUMATI STATION, 1997)

Month	Max		Min		Amplitude
	Value	Time	Value	Time	
January	397	9–10	381	14–15	16
April	386	2–3	369	14–15	17
July	413	4–6	359	16–17	54
October	377	3–4	363	16–17	14

The diagrams in Fig. 12 have been detailed by carrying out the hourly variation curves of the CO_2 values for each separate month. In this case too, only two characteristic months have been chosen for exemplification (Fig. 13), one for each of the two above mentioned half-years, that is January (interval 15–31) and April (the entire month). The regularity of the maximum and minimum moments sequence for April or the appearance of some entirely non-typical days, such as the 20^{th} of January, confirms the existence every year of two halves when the CO_2 variability is governed by various causes.

6. CONCLUSIONS

Related to the ***radiocarbon activity***, two continuous monthly measurement series were obtained in Romania. At Bucharest station — a sampling point that characterizes a large town area — the level and evolution trend for 1992–1995 interval correspond satisfactorily to the same parameters in Central Europe. An important decrease of $\Delta^{14}C$ values was recorded for the following. three years. An early maximum seasonally phase placed in the spring (instead of the summer) was found as a local peculiarity. For Cernavoda station, a sampling point close to a nuclear power plant, a similar multiannual and seasonal evolution as Bucharest station was established. Some higher values in April–May 1996 (just in the plant testing period) and especially during 1998 are probably due to the nuclear power plant releases.

Related to the ***CO_2 contents***, the first results obtained in Romania, at Bucharest-Afumati station over two-years period are presented and discussed. The main findings are: A mean value for the 5 month period (June–October) in 1996 of 379 ppmv and a yearly mean of 375 ppmv in 1997. The maximal and minimal values in 1997 were measured in December with 507 ppmv and in June with 328 ppmv, respectively. For both years a very ordered and well marked diurnal cycle was found. Seasonal differences of diurnal cycles were discerned from the data. During winter months the fossil fuel emission influence due to heating can be seen.

REFERENCES

[1] KUC, T, (1991) — "Concentration and carbon isotopic composition of atmospheric CO_2 in southern Poland". Tellus, **43 B**, pp. 373–378.

[2] ZIMNOCH, M., (1994) — "Monitoring of isotopic composition of atmospheric carbon dioxide in Krakow-recent results". Final Report of IAEA-CRP — "Isotope variations of carbon dioxide and other trace gases in the atmosphere", IAEA, Vienna.

[3] POVINEC, P., SIVO, A., CHUDY, M., BURCHULADZE, A., PAGAVA, S., TOGONIDZE, G., ERISTAVI, I., (1986) — "Seasonal variations of anthropogenic radiocarbon in the atmosphere." Nuclear Instruments & Methods in Physics Research, **B17/5,6** , pp. 556–559.

[4] CHUDY, M., HOLY, K., RICHTARIKOVA, M., SIVO, A., VOJTYLA, P., (1994)– "Variation of 14C, 85Kr and 222Rn in the Bratislava air". Final Report of IAEA-CRP– "Isotope variations of carbon dioxide and other trace gases in the atmosphere", IAEA, Vienna.

[5] OBELIC, B., HORVATINCIC, N., KRAJCAR-BRONIC, I., (1993) - "^{14}C and tritium activity in the atmosphere". Applications of isotopes techniques in studying past and current environmental changes in the hydrosphere and the atmosphere, IAEA-SM-329, Extended synopses, pp. 7–8.

[6] TENU, A., DAVIDESCU, F., (1998) — "Carbon isotope composition of atmospheric CO_2 in Romania". Isotope Techniques in the Study of Environmental Change, Proc of Intern. Symp on Isotope Techniques in the Study of Past and Current Environmental Changes in the Hydrosphere and the Atmosphere, IAEA, Vienna, pp. 19–26.

[7] CRAIG, H., (1953) — "The geochemistry of the stable carbon isotopes". Geochim. and Cosmochim. Acta, **3**, pp. 53–92.

[8] BROECKER, W.S., OLSON, E.A., (1961) — "Lamont Radiocarbon Measurements VIII ". Radiocarbon, **3,** pp.176–204.

[9] DAVIDESCU, F., (1996) — "Monitoringul izotopilor carbonului in CO_2 atmosferic din zona C.N.E. Cernavoda". Mediul Inconjurator, **7** , nr.1, pp. 15–19.

[10] LEVIN, I., KROMER, B., SCHOH-FISCHER, H., BRUNS, M., MÜNNICH, M., BERDAU, D., VOGEL, J.C., MÜNNICH, K. O., (1985) — "25 years of tropospheric ^{14}C observations in Central Europe". Radiocarbon, **27**, pp. 1–19.

[11] MANNING, H.R., LOWE, D.C., MELHUISH, W.H., SPARKS, R. J., WALANCE, G., (1990) — "The use of radiocarbon measurements in atmospheric studies". Radiocarbon, **32**, pp. 37–58.

[12] KUC, T., (1989) — "Changes of carbon isotopes in atmospheric CO_2 of the Krakow region in the last five years". Radiocarbon, **31,** pp. 441–447.

[13] LEVIN, I., SCHUCHARD, J., KROMER, B., MÜNNICH, K. O., (1989) — "The continental European Suess effect". Radiocarbon, **31**, pp. 431–440.

[14] LEVIN, I., GRAUL, R., TRIVETT, N. B. A., (1995)- "Long-term observations of atmospheric CO_2 and carbon isotopes at continental sites in Germany". Tellus, **47 B**, pp. 23–34.

[15] XU, Y., ZHANG, L., (1993) — "The character of the concentration and isotopic ratios of the atmospheric CO_2 in the north western China". Applications of isotopes techniques in studying past and current environmental changes in the hydrosphere and the atmosphere, IAEA-SM-329, Extended Synopses, Vienna, 19–23 April, pp. 162.

^{222}Rn AND $^{14}CO_2$ CONCENTRATIONS IN THE SURFACE LAYER OF THE ATMOSPHERE

K. HOLÝ*, M. CHUDÝ*, A. ŠIVO*, M. RICHTÁRIKOVÁ*, R. BÖHM*, A. POLÁŠKOVÁ*, O. HOLÁ**, P. VOJTYLA*, I. BOSÁ*

* Faculty of Mathematics and Physics, Comenius University
** Faculty of Chemical Technology, Slovak Technical University

Bratislava, Slovakia

Abstract. Long-term monitoring of the $\Delta^{14}C$ in the atmospheric near-ground CO_2 has been realized in Bratislava and Zlkovce, situated near the nuclear power plant Jaslovske Bohunice. Until 1993, the monthly mean $\Delta^{14}C$ values showed a high variability. The annual means of $\Delta^{14}C$ were about 30‰ higher at Zlkovce than in highly industrialised Bratislava. An important change in the behaviour of the ^{14}C data has occurred since 1993. The records from both stations show the similar course, mainly due to the fact that there do not occur deep winter minima in Bratislava. This behaviour corresponds to the lower values of the total fossil fuel CO_2 emissions in the years after 1993 when compared to the previous years. At present, both sets of data show that the ^{14}C concentration is about 10% above the natural level. Since 1987 also the ^{222}Rn concentration in the surface layer of the atmosphere has been measured in Bratislava. These measurements provided an extensive set of the ^{222}Rn data characteristic for the inland environment with high level of atmospheric pollution. The seasonal and daily variations of the ^{222}Rn concentration were observed. The investigation of the relation between the monthly mean diurnal courses of the ^{222}Rn concentration and the atmospheric stability proved a high correlation between them. The ^{222}Rn data were used to interpret the anomalous $\Delta^{14}C$ values in the surface layer of the atmosphere.

1. INTRODUCTION

Two human activities have increased the ^{14}C level in the atmosphere: nuclear bomb tests and the development of nuclear industry, but the latter to a lesser degree. Approximately in the year 1963, the ^{14}C concentration from nuclear bomb tests reached the peak value of about 100% above the natural level in the atmosphere of the northern hemisphere [1]. After the nuclear moratorium for the atmospheric tests, the ^{14}C concentration in the atmosphere has decreased because of the exchange processes between the atmosphere and the other carbon reservoirs [2–6]. There is also another anthropogenic effect caused by the fossil fuel combustion, which changes the ^{14}C concentration in the atmosphere [2,7]. This effect is well seen through the $^{14}CO_2$ seasonal variations. In annual $\Delta^{14}C$ courses, the winter minima are observed mainly as a consequence of the emission of the ^{14}C free fossil fuel CO_2 into the atmosphere (Suess effect) [8]. However, the annual courses of $\Delta^{14}C$ are the result of the simultaneous influence of various factors from which also the atmospheric mixing conditions can change the ^{14}C concentration on a significant level [5]. Therefore, it is clear that these conditions should be checked to take them into account at the interpretation of the ^{14}C data and at their comparison from the different stations.

As it seems, the ^{222}Rn can be an appropriate means for the solution of the last mentioned problems. It was found out that the ^{222}Rn concentration in the surface layer of the atmosphere was controlled by the vertical mixing. In the last years, some progress has been achieved in the determination of some characteristics of the atmosphere on the basis of the ^{222}Rn concentration measurements, for example at the determination of an equivalent mixing height or an exchange coefficient [9–11]. The parallel measurements of the ^{222}Rn and ^{14}C in the atmosphere have been used already for the determination of the fossil fuel CO_2 flux densities to the atmosphere [5].

In this contribution, the results of the long-term measurements of the atmospheric $^{14}CO_2$ in samples from two stations of Slovakia are presented and the influence of the anthropogenic CO_2 emissions on the ^{14}C concentration is discussed. Further, the results of the ^{222}Rn monitoring in Bratislava station in the surface layer of the atmosphere are shown. On the basis of the continually collected ^{222}Rn data the seasonal changes of the mean daily ^{222}Rn waves and of the monthly mean ^{222}Rn concentrations are analysed and their relation to the atmospheric stability is described. Partially the ^{222}Rn data are also used at the interpretation of the $\Delta^{14}C$ courses.

2. SAMPLING SITES

Samples of ^{14}C in the form of the carbon dioxide have been collected at two sites in Slovakia: in Bratislava (48°9' N, 17°7' E, 164 m a.s.l.) and at the field sampling station Zlkovce (48°29' N, 17°40' E, 162 m a.s.l.). The samples from Bratislava (0.5 million inhabitants) correspond to the highly industrialised region. There is another big source of pollution in this region besides Bratislava. It is Vienna (1.5 million inhabitants) approximately 50 km WNW from Bratislava. The prevailing winds in Bratislava are northwest and northeast winds (secondary maximum) [12].

Zlkovce is situated approximately 60 km NE from Bratislava in a flat agricultural area. The nearest pollution sources that can influence the ^{14}C concentration in the atmosphere are the nuclear power plant Jaslovske Bohunice, approximately 5 km WNW from Zlkovce and the industrial city of Trnava (70 thousand inhabitants), located 15 km from the station in the SW direction. The prevailing winds in this region are northwest and southeast (secondary maximum) [13].

The measurements of the ^{222}Rn in the surface layer of the atmosphere were carried out in the campus of the Faculty of Mathematics and Physics in Bratislava. The sampling place for radon measurement has been only 40 m from the place where the samples of the atmospheric CO_2 have been collected.

3. METHODS

For the carbon isotope measurements, the monthly large-volume samples of atmospheric CO_2 have been continuously collected at a height of 15 m above the ground surface by the dynamic absorption of CO_2 in NaOH solution [14].Then, CH_4 was prepared from the sample for filling the low-level proportional counter, which was used for the counting of the ^{14}C decays [15].

A few ml of CO_2 liberated from the sample in the form of $BaCO_3$ were analysed using a mass spectrometer for the determination of the isotopic ratio of $^{13}C/^{12}C$. The $\delta^{13}C$ values were calculated relative to the VPDB standard. The precision of $\delta^{13}C$ values is on the level of $\pm$ 0.1‰. The $\delta^{14}C$ values were calculated relative to NBS oxalic acid activity and their standard deviations are on the level of $\pm$ 6 ‰. Results are presented in this contribution as $\Delta^{14}C$ values and they were obtained from $\delta^{14}C$ values by the correction on the isotopic fractionation.

The $\delta^{14}C$ data measured in Bratislava in the time interval from 1996 to 1999 were corrected using the measured $\delta^{13}C$ values in the same period. Other data measured in Bratislava and at Zlkovce were corrected using the average $\delta^{13}C$ value of –11‰.

The ^{222}Rn was measured at the height 1.5 m above the ground surface by two methods [16]. In the first one, the short-term samples of radon were trapped in the activated charcoal. For the counting of radon separated from the charcoal, a small-volume scintillation chamber of the Lucas type was used. In the second method, the ^{222}Rn has been monitored continuously

using the large-volume scintillation chamber. The monitor allows obtaining of almost 80% of the radon data in the surface layer of the atmosphere with uncertainties less than 30% in the counting interval of 2 hours.

4. RESULTS AND DISCUSSION

4.1. ^{222}Rn results

Radon was measured in Bratislava from 1987 on and since 1991 it has been monitored continuously. On the basis of the measured data mainly the mean daily and annual courses of the ^{222}Rn activity concentration have been analysed [17, 18] in order to reveal only the basic atmospheric variables inducing the radon behaviour. The mean ^{222}Rn daily courses month by month and the mean annual course of the ^{222}Rn activity concentration are shown in Fig. 1. All the significant features of the behaviour of the ^{222}Rn concentration in the surface layer of the atmosphere are clearly visible.

The monthly mean diurnal courses of the ^{222}Rn activity concentration show a quasi-harmonic behaviour. The maximum radon activity concentrations are measured in the early-morning hours, usually between 4–6 a.m., when the vertical mixing of the air in the surface layer of the atmosphere is restricted due to the air temperature inversion. In the afternoon, usually between 2–4 p.m., the minimum radon activity concentrations are measured, corresponding to the maximum of the vertical mixing of the air during a day.

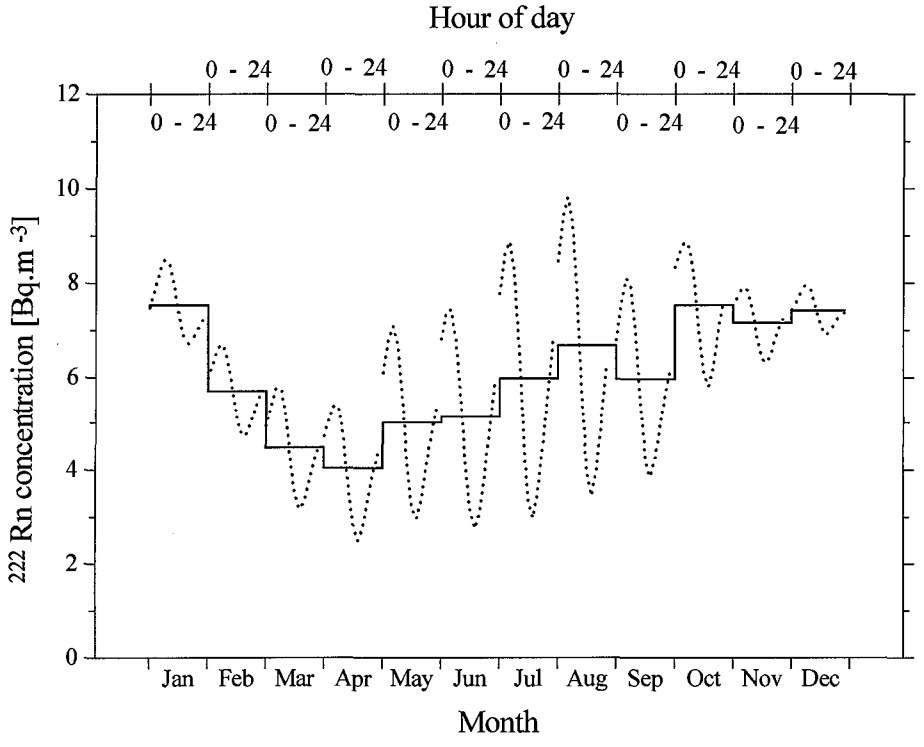

Figure 1. The mean annual course (histogram) and the monthly mean diurnal courses (dotted curves) of the ^{222}Rn activity concentration in the surface layer of the atmosphere in Bratislava. Both types of courses were obtained by summation of the radon data from years 1993–1998.

The maximum amplitudes of the daily pattern, corresponding to 3 $Bq.m^{-3,}$ are reached in the summer months from June to August. The low atmospheric stability of the atmosphere in the afternoon and well generated nocturnal radiation inversion, together create conditions for big changes of the ^{222}Rn concentration during a day in the mentioned months.

The amplitudes of the daily cycles are small (approximately 0.8 $Bq.m^{-3}$) at the end of the autumn and during the winter months. It can be ascribed to small differences between the intensity of the vertical mixing of the air at night and during the day in this period.

The analysis of the monthly mean diurnal cycles of the ^{222}Rn activity concentration showed, that in the first approximation their amplitudes are in proportion to the global solar radiation irradiating the Earth's surface [17, 19]. This relation discussed also in the previous works [20] confirms that it is predominantly this part of the vertical mixing which is governed by the solar heating, that influences the characteristics of the mean daily radon cycles significantly.

The influence of the wind speed on the ^{222}Rn activity concentration need not be the same under all meteorological conditions. However, the reverse proportion between the monthly mean of the wind speed and the monthly mean of the radon activity concentration with high correlation (correlation coefficient $R > 0.82$ for successive years 1993–1998) was found out[21]. This dependence is connected to the fact, that periodic changes of the daily wind speed are the same as the daily ^{222}Rn cycles caused by the daily periodic course of the radiation and thermal balance in the surface layer of the atmosphere [12]. High-speed wind (more than 5 $m.s^{-1}$) which goes along with the non-periodic changes of the weather, almost effaces the daily radon cycles also during the summer days and moreover significantly cuts down the radon activity concentrations in the winter months.

The annual course of the monthly mean values of the radon activity concentration also presented in Fig.1, shows the minimum values in the spring months (April) and maximum values in the autumn and winter months. It follows from the daily courses that the high ^{222}Rn monthly means in the winter months are caused mainly by the high radon concentrations in minima of the daily radon cycles. This is caused by the fact that during the winter months the relatively stable temperature stratification in the surface layer of the atmosphere often persists during the day.

The low monthly mean of the ^{222}Rn activity concentration in April is caused by the low concentrations of the ^{222}Rn during days as well as nights. It is in a good agreement with the biggest vertical temperature gradients during twenty-four-hours and with the smallest occurrence of the inversions in the atmospheric boundary layer in this month (of the whole year) [22].

On the basis of the ^{222}Rn data measured in 1997 there was studied also the relation between the daily courses of the ^{222}Rn activity concentrations and the daily courses of the atmospheric stability indexes calculated according to Turner's method [23]. It was found out, that the monthly mean diurnal courses of the radon activity concentration and the monthly mean courses of the atmospheric stability were approximately the same. The correlation between both courses is at a maximum if one is shifted with respect to the other in order to remove the approximately 2 hour delay (on an average the correlation coefficient is then about 0.98). This study demonstrates that the atmospheric stability indexes can be determined directly on the basis of the radon activity concentrations.

In Fig.2, the monthly means of the radon activity concentrations for the years 1987–1999 are shown. The spring minima and maxima occurring in various months of the second half-year can be seen in the annual ^{222}Rn courses for all the years. The individual years differ from each other quite considerably. The amplitudes of the annual courses vary from 2.9 Bq m^{-3} (1995) to 1.2 $Bq{\cdot}m^{-3}$ (1998). The last four years show a decreasing trend of these amplitudes, predominantly as a consequence of the decreasing of the radon activity

concentrations in the year's maxima. Simultaneously, a shift of the year's maxima from the late autumn and winter months towards the summer months is observed. This effect is due to the lowering of the radon activity concentrations in the minima of the daily cycles of the autumn and winter months (October–January) with only mild decrease of amplitudes of the daily ^{222}Rn waves. It indicates the lowering of the stability of the surface layer of the atmosphere in this period in comparison to the previous years. The reason of such behaviour of the atmospheric stability and therefore also of the ^{222}Rn concentrations could be found in the decrease of the solid pollution in the atmosphere during late autumn and winter months in the last years.

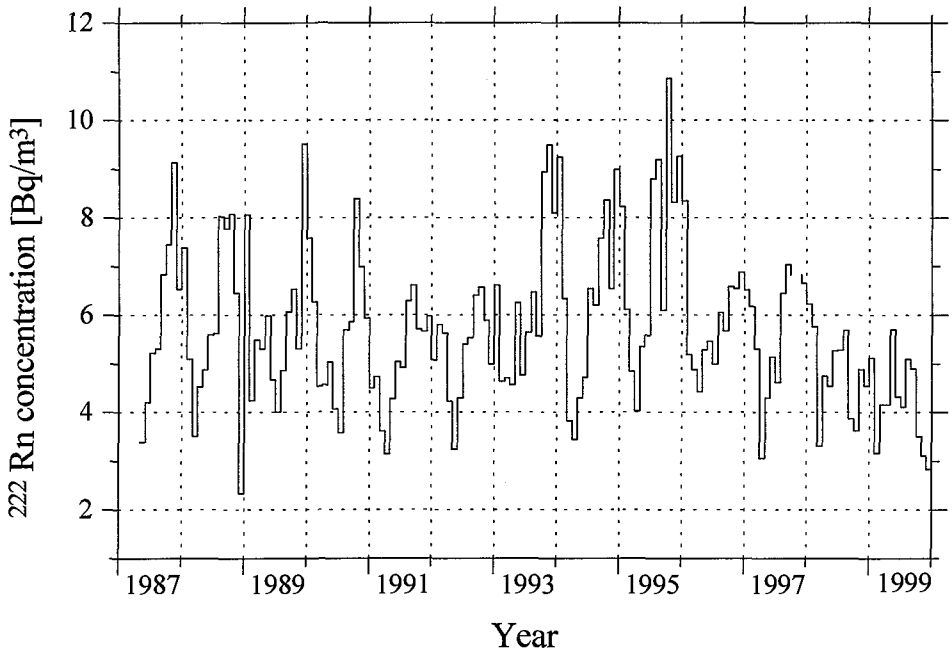

Figure 2. The monthly mean values of the ^{222}Rn activity concentration in the surface layer of the atmosphere in Bratislava.

4.2. $\Delta^{14}C$ results

The ^{14}C activity in atmospheric CO_2 has been measured in Bratislava since 1967 [24]. In Fig.3 the results of the regular ^{14}C measurements in Bratislava are shown in the time period from 1984 to 1999 and at Zlkovce in the time interval from 1987 to 1999. For a comparison, the dashed line in Fig.3 shows the long-term trend of annual mean $\Delta^{14}C$ in background air over Europe. From the point of the variability of data it is possible to divide the $\Delta^{14}C$ courses in Fig.3 into two different periods: the period until 1993 and the period after 1993. The first one is characterized by the expressive minima of the $\Delta^{14}C$ in the winter months and by the relative maxima of the $\Delta^{14}C$ in the early summer months. Very low and sometimes even negative $\Delta^{14}C$ values were measured mainly in January and February as a consequence of the high input of ^{14}C free fossil fuel CO_2 into the atmosphere (Suess effect). The relative increases of $\Delta^{14}C$ in spring and early summer months are caused rather by the depletion of the atmospheric ^{14}C in winter months than by the injection of the stratospheric air into the troposphere.

According to the expectation, the Suess minima of $\Delta^{14}C$ are not as distinct at Zlkovce as they are in Bratislava, although they can be identified. The cause is that the sampling

station Zlkovce is not situated directly in the large city area. However, some pollution by fossil fuel CO_2 can be expected from the near city of Trnava.

In the data from Bratislava and Zlkovce, we can see also some monthly mean $\Delta^{14}C$ values that are far above the background trend line. It refers for example to two peaks: in March 1989 and May 1990, when the high values of $\Delta^{14}C$ were measured simultaneously in Bratislava and at Zlkovce. In these months, the occurrence of NE and ENE winds up to 50% from the direction of Jaslovske Bohunice was also recorded in Bratislava. However, high $\Delta^{14}C$ values do not always coincide in these two stations. This is documented for example by the high $\Delta^{14}C$ values measured in April, May and July 1991 only at Zlkovce. In these months, the NWN wind direction was prevailing in Bratislava (NE/ NWN ≈0.1) and therefore the probability of the transport of pollutants between both the stations is small. Such responses of the stations are in accordance with the expectation that $\Delta^{14}C$ excesses are of technogenic origin (from the nuclear power plant).

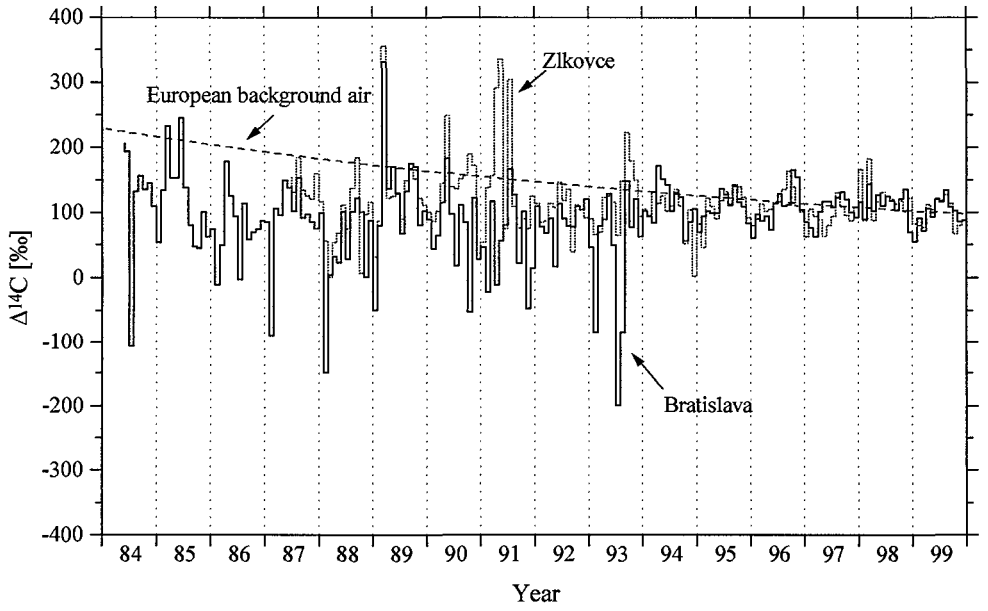

Figure 3. The monthly mean values of the $\Delta^{14}C$ in atmospheric CO_2 in Bratislava and at Zlkovce. The dashed line represents the long-term trend of the annual mean $\Delta^{14}C$ in the background air over Europe. For the years 1984 –1992 the trend line was calculated according to the equation: $y=6\times10^{11}x^{-4.8937}$, where y is the annual mean value of $\Delta^{14}C$ in the atmospheric CO_2 and x is the calendar year [6]. The trend line was also extrapolated to 1993–1999 by means of the same calculation.

In the same period some Suess minima of $\Delta^{14}C$ occurred in Bratislava also in summer months. It could be seen most distinctly in July and August 1993. Because the worse atmospheric mixing conditions were not confirmed by the distinctly higher ^{222}Rn concentrations in these months (see Fig. 2), this effect could be ascribed to the local increase of the emissions of the fossil fuel CO_2 as well as to the transport of CO_2 from the distant sources (for example Vienna). The second source of the pollution is probable too, because the NW wind direction was prevailing in these months (above 70%).

The behaviour of the $\Delta^{14}C$ values has changed after 1993. There are no significant maxima and minima and the records from both the stations show a similar course. However,

the correlation plot of the $\Delta^{14}C$ data from both the sampling sites measured in the time period from 1994 to 1999 shows that the correlation coefficient is only about 0.5. Two reasons could cause the mentioned behaviour. The first one–the concentration of the fossil fuel CO_2 in the atmosphere was lower than in preceding years. This could be confirmed also by the calculations of the fossil fuel CO_2 emissions in Slovakia for the years 1990–1998 [25, 26]. Just according to these calculations the total fossil fuel CO_2 emissions dropped of about 28% in the period of 1990–1994 in comparison with the year 1990, when the total CO_2 emissions from fossil fuel combustion were 57 Tg per year. Since 1994 this emission has been on the constant level, equal approximately to 41 Tg per year. The other cause could be connected with the enhanced dilution of the atmospheric pollution. As it follows from the radon data in Fig.2, this influence is also possible, but only in the years 1996–1999, when in Bratislava the concentrations of ^{222}Rn measured were lower than in the previous years.

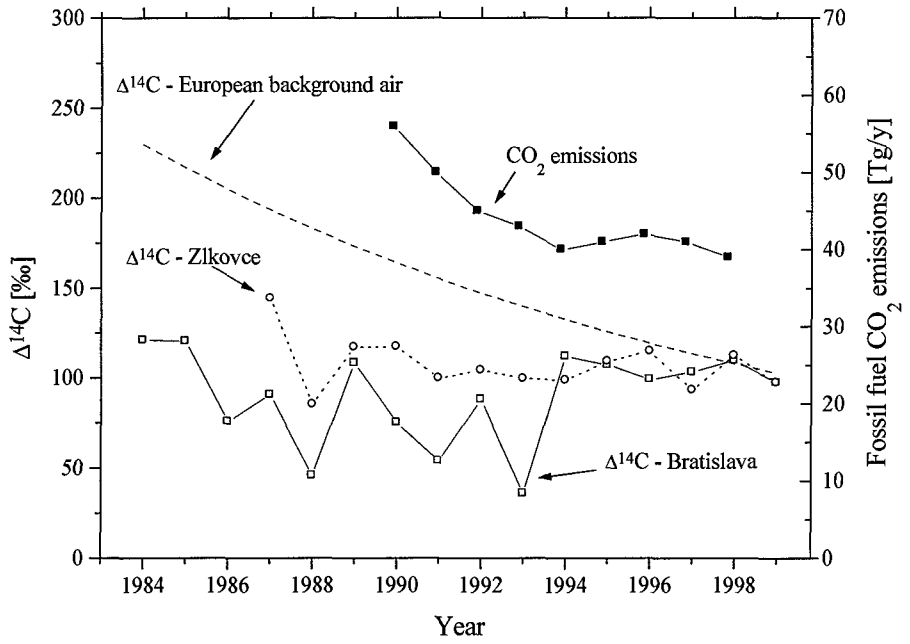

Figure 4. The annual mean values of the $\Delta^{14}C$ in the atmospheric CO_2 in Bratislava and at Zlkovce. The monthly mean $\Delta^{14}C$ values above trendline in Fig. 3 were not taken into calculations of the annual mean $\Delta^{14}C$ because of the elimination of the influence of the technogenic ^{14}C on the $\Delta^{14}C$ courses. The dashed line represents the annual mean $\Delta^{14}C$ in the background air over Europe like in Fig. 3. The dark curve represents the total CO_2 emissions from fossil fuel combustion in Slovakia estimated according to the IPCC methodology [25, 26].

In Fig. 4, the courses of the annual mean $\Delta^{14}C$ measured in Bratislava and at Zlkovce are shown. The annual mean $\Delta^{14}C$ courses for both stations are significantly below the trend of the annual mean $\Delta^{14}C$ in background air over Europe. This is a consequence of the big and variable amount of fossil fuel CO_2 in the atmosphere. However, in the last years, the measured $\Delta^{14}C$, for the two sites, moves much closer to the European background $\Delta^{14}C$ trend line.

Before 1994 the annual mean values of $\Delta^{14}C$ in atmospheric CO_2 collected in Bratislava were on average about 50% lower and at Zlkovce about 20% in comparison with the $\Delta^{14}C$ background level. At that time, the $\Delta^{14}C$ at Zlkovce were about 30‰ higher than in Bratislava. If we assume that the big source of the CO_2 emissions represents the highly

industrialized Bratislava, then the last mentioned results show that the sites with various levels of fossil fuel CO_2 emissions can well be distinguish using the $\Delta^{14}C$ data.

Since 1994 there were no longer such marked differences in annual mean $\Delta^{14}C$ courses between the two stations. This is mainly caused by the increasing and smoothing of the annual mean $\Delta^{14}C$ in Bratislava. In our opinion it clearly confirms the decreasing of the amount of the fossil fuel CO_2 in Bratislava's atmosphere and it is in an agreement with the calculated trend of the fossil fuel CO_2 emissions in Slovakia. In the years 1994–1999 the annual means of $\Delta^{14}C$ in both the localities are approximately only 10% below the trend line for the $\Delta^{14}C$ in European background air. For more details, however, the course of the annual mean $\Delta^{14}C$ in background air over Europe derived from the $\Delta^{14}C$ observations must be taken into account as well.

5. CONCLUSION

Extensive sets of the ^{222}Rn and $\Delta^{14}C$ data have been obtained in an inland environment with the variable pollution of the atmosphere.

The seasonal and daily variations of the ^{222}Rn concentrations were observed. The monthly mean diurnal courses of the ^{222}Rn concentration have a quasi-harmonic shape with an amplitude of up to 3 $Bq.m^{-3}$ in the summer months. During the winter months the amplitudes of the daily cycles are small and sometimes cannot be identified. A high correlation has been found between the monthly mean diurnal waves of the ^{222}Rn concentration and the atmospheric stability indexes. It gives an opportunity to use the ^{222}Rn as a tracer of the distribution of the CO_2 and other pollutants in the surface layer of the atmosphere.

A high variability of the monthly mean $\Delta^{14}C$ in the atmospheric CO_2 was observed at two not very distant stations until 1993. In this period the annual mean values of the $\Delta^{14}C$ in Bratislava (with heavily polluted atmosphere) were about 50% lower and at Zlkovce about 20% lower when compared with $\Delta^{14}C$ in European background air. After 1993 there has been no deep winter minima in the $\Delta^{14}C$ courses and annual mean $\Delta^{14}C$ were in both sites approximately only 10% below the $\Delta^{14}C$ background level. The $\Delta^{14}C$ behaviour in the last years provides a unique and independent qualitative evidence of the decrease of fossil fuel CO_2 emissions (though only on the regional level). Until now the decrease of the CO_2 emissions in Slovakia has been documented only with the calculation by means of the IPCC method on the basis of the economic statistics.

ACKNOWLEDGEMENTS

This study was funded by the Scientific Grant Agency of the Ministry of Education of the Slovak Republic (VEGA project No. 1/4194/97) and by the International Atomic Energy Agency, Vienna, Austria (Res. Contract No. 9093/RO).

REFERENCES

[1] NYDAL, R., LÖVSETH, K., Distribution of radiocarbon from nuclear tests, Nature, Vol. 206, (1965) 1029–1031.

[2] LEVIN, I., MÜNNICH, K., WEISS, W., The effect of anthropogenic CO_2 and ^{14}C sources on the dilution of ^{14}C in atmosphere, Radiocarbon, Vol. 22, (1980) 379–391.

[3] BURCHULADZE, A.A., et al., Anthropogenic ^{14}C variations in atmospheric CO_2 and wines, Radiocarbon, Vol. 31, (1989) 771–776.

[4] HESSHAIMER, V., HEIMANN, V., LEVIN, I., Radiocarbon evidence for a smaller oceanic carbon dioxide sink than previously believed, Nature, Vol. 370, (1994) 201–203.
[5] LEVIN, I., GRAUL, R., TRIVETT, N.B.A., Long-term observations of atmospheric CO_2 and carbon isotopes at continental sites in Germany, Tellus, 47 B, (1995) 23–34.
[6] TENU, A., DAVIDESCU, F., "Carbon isotope composition of atmospheric CO_2 in Romania", Isotope Techniques in the Study of Environmental Change (Proc. Symp. Vienna, 1998), IAEA, Vienna (1998) 19–26.
[7] SEGL, M., et al., Anthropogenic ^{14}C variations, Radiocarbon, Vol. 25, (1983) 583–592.
[8] LEVIN, I., et al., The continental European Suess-Effect, Radiocarbon, Vol. 31, (1989) 431–440.
[9] BOSÁ, I., The ^{222}Rn Volume Activity in Outdoor Atmosphere and its Relation to the Atmospheric Stability, Diploma thesis, (HOLÝ, K. - Supervisor), Faculty of Math. and Phys., Com. Univ., Bratislava (1999) 77 p, In Slovak.
[10] SESANA, L., et al., ^{222}Rn as a tracer of atmospheric motions: a study in Milan, Radiat. Prot. Dosim., Vol. 78, (1998) 65–71.
[11] GUEDALIA, D., et al., Monitoring of the atmospheric stability above an urban and suburban site using solar and radon measurements, J. Appl. Meteor., Vol. 19, (1980) 839–848.
[12] OTRUBA J., "Circulation conditions in the region of Bratislava". Climat and bioclimat of Bratislava, VEDA, Bratislava (1979), 83–116, In Slovak.
[13] Atlas of the Slovak Republic, Slovak Academy of Sciences, Bratislava (1980), 296 p.
[14] POVINEC, P., et al., The rapid method of carbon-14 counting in atmospheric carbon dioxide, Int. J., Appl. Rad. Isotopes, Vol. 19, (1968) 877–881.
[15] POVINEC, P.,et al., Bratislava radiocarbon measurements, Radiocarbon, Vol.15, (1973) 443–450.
[16] BELÁŇ, T., et al.,"Investigation of radionuclide variations in the Bratislava air", Rare Nuclear Processes (Proc. of 14th Europhysics Conf. on Nucl. Phys., POVINEC, P., Ed.), World Scientific Publishing, Singapore (1992) 345–366.
[17] HOLÝ, K., et al., "Variations of ^{222}Rn concentration in the Bratislava air", IRPA 9 (Proc. of 1996 Int. Cong. on Rad. Prot.), Vol. 2, Vienna (1996) 176-178.
[18] HOLÝ, K., et al., "Results of long-term measurement of ^{222}Rn concentrations in outdoor atmosphere", Radiation Protection in Neighbouring Countries of Central Europe (Proc. of IRPA Reg. Symp., SABOL, J., Ed.), Sess. 2, Prague (1997) 121–124.
[19] CHUDÝ, M., et al., Investigation of ^{3}H, ^{14}C, ^{85}Kr and ^{222}Rn Variations in the Bratislava Air, Final Report for the IAEA, RC No. 5609/RB, Report UK-JF-119/95, Bratislava (1995) 53 p.
[20] GARZON, L., et al., The universal Rn wave an approach, Health Physics, Vol.51, No.2 (August), (1986) 185–195.
[21] HOLÝ, K., et al., Investigations of ^{14}C and ^{222}Rn variations in atmosphere and soil in Slovakia, Final Report for the IAEA, RC No. 9093 RB, Report UK-JF-129/99, Bratislava (1999), 109 p.
[22] TOMLAIN, J., CIMBAKOVA, M., Temperature and wind fields in conditions of Slovakia. Final Report No. A-12-531-804–04/03, Faculty of Math. and Physics, Bratislava (1988) 185 p. In Slovak.
[23] TURNER, D.B., A diffusion model for an urban area, J. Appl. Meteorol., Vol. 3, (1964) 83.
[24] POVINEC, P., et al., Seasonal variations of anthropogenic radiocarbon in the atmosphere, Nucl. Instr. and Methods, Vol. 317, (1986) 556–559.

[25] The Second National Communication on Climate Change, Ministry of Environment, Bratislava (1997) 97 p.
[26] MARECKOVA, K., et al., Arrangement of the international duties of Slovakia– Evaluation of pollution of the atmosphere and its global risks. Report of the Slovak Hydrometeorological Institute, Bratislava (2000), In Slovak.

ISOTOPE VARIATIONS OF CARBON DIOXIDE, METHANE AND OTHER TRACE GASES IN CRACOW AND KASPROWY, POLAND

T. FLORKOWSKI
Department of Environmental Physics, Faculty of Physics and Nuclear Techniques,
University of Mining and Metallurgy,
Cracow, Poland

Abstract. Seasonal variations of concentration and isotopic composition of the atmospheric trace gases CO_2, CH_4 and SF_6 are presented for a three years period in two stations in Poland. The station in Cracow represents a polluted urban area with strong contributions of anthropogenic local sources, while the other one is located 80 km away in the High Tatra mountains at Kasprowy Wierch representing a nearly undisturbed clean station. Trends of the concentration and isotopic signatures are discussed and a separation of the CO_2 concentration in three components of anthropogenic, biogenic and background origin is presented.

1. INTRODUCTION

Studies of temporal variations of CO_2, CH_4 and SF_6 in the atmosphere at two stations located in Poland have been continued. One station is situated in the High Tatra mountains at Kasprowy Wierch (49°N, 20°E, 1980 m.a.s.l., 300 m above the tree line). This place is considered a "clean" station, with small influence from local sources of trace gases. The second station is located in Cracow, in a polluted urban area with a strong contribution of anthropogenic gases originating from local sources (coal burning, car traffic, leakages from city gas network, landfills) and from a large industrial district located ca. 80 km west from Cracow (Silesia district). Both stations are equipped with automatic gas chromatographs which provide continuous measurements of trace gas concentrations. Air is also sampled into 100 l Aluminium-PE bags and to glass and metal flasks. Recently, the Kasprowy station was equipped with a sampling device to collect two-weekly composite samples of CO_2 for ^{14}C analysis. This type of sampling has been performed in Cracow since 1976.

Standards for concentration measurements were kindly provided by the Institute of Environmental Physics, Heidelberg, Germany. Also, certain isotope ratio measurements ($\delta^{13}C$ and $\delta^{18}C$ of atmospheric CO_2) are done in parallel in Heidelberg.

2. CARBON DIOXIDE

Fig. 1 shows the record of the CO_2 concentration at Kasprowy station for the period from September 1994 to December 1997. The amplitude of seasonal variations of the CO_2 concentration is about 32 ppm, with the lowest values in July/August (334 ppm) and the highest in March (376 ppm). The available record is still too short to reveal any unambiguous long-term trend.

The comparison of continuous GC measurements with the weekly integrated samples from the bag collection system does not reveal any systematic offset in the measured CO_2 concentration (Fig. 2) — with the mean difference between GC and bag samples being equal to 1 ± 1.5 ppm.

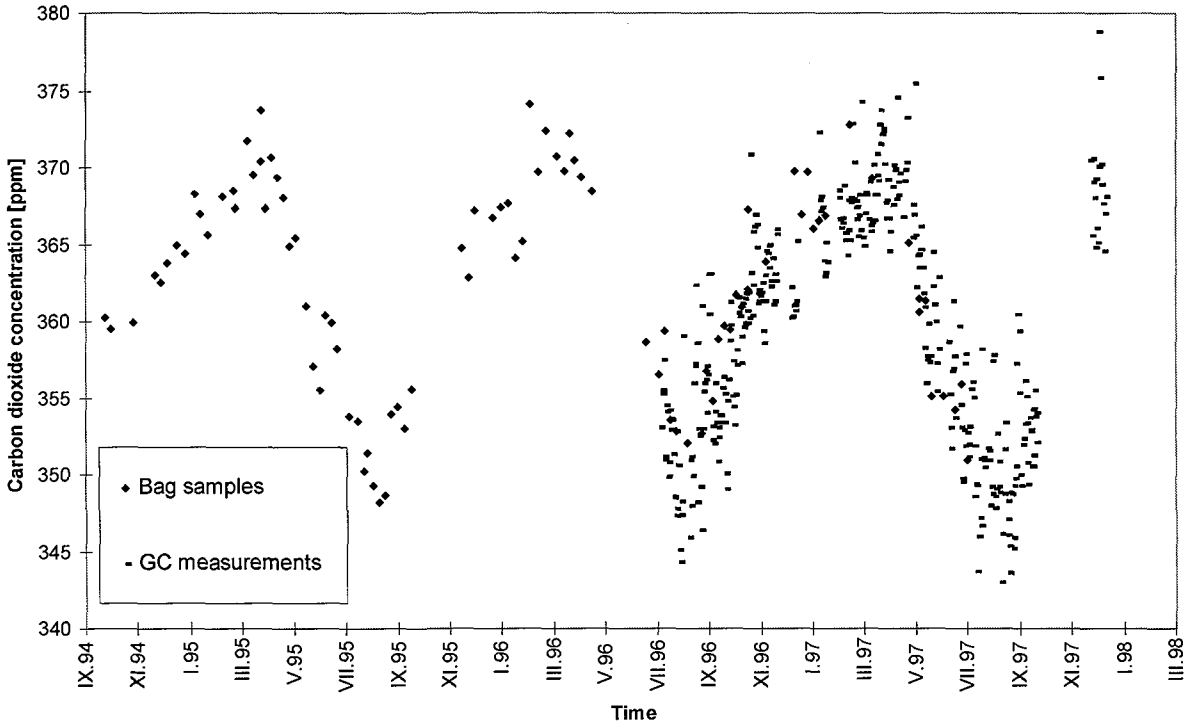

Fig. 1. The CO_2 concentration record from Kasprowy Wierch station. The bag samples were measured at the Institute of Environmental Physics, University Heidelberg, Germany.

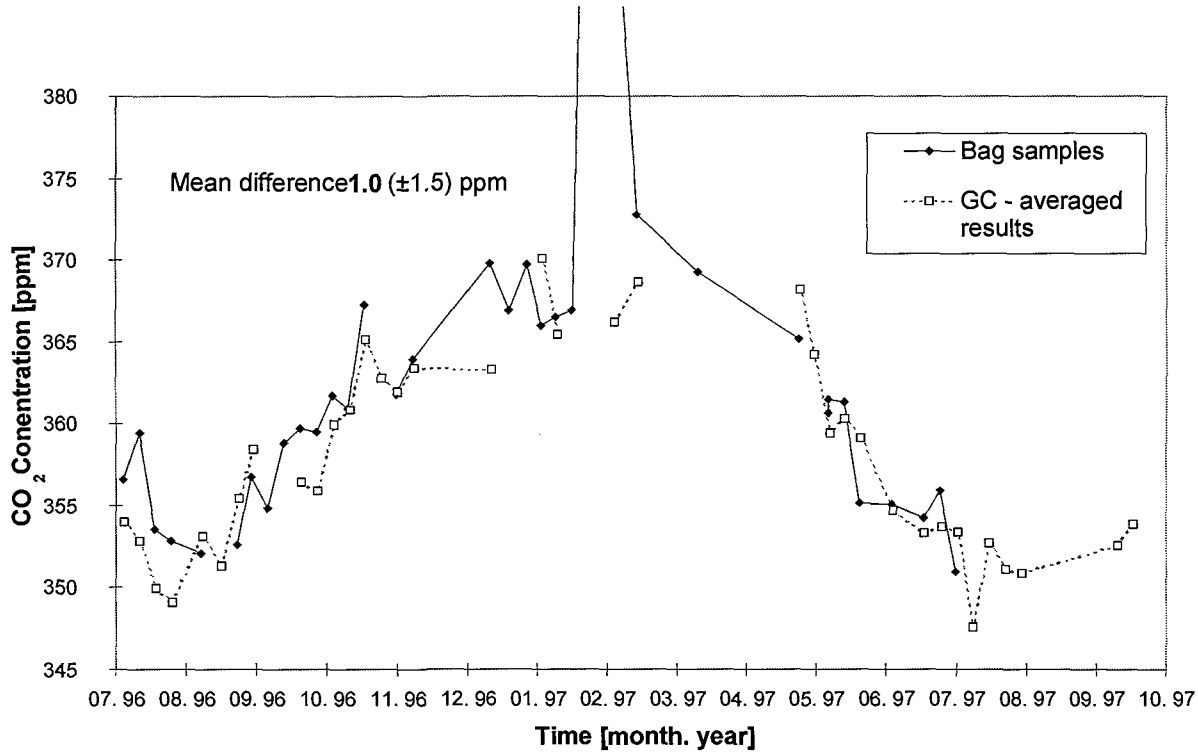

Fig. 2. The comparison of the weekly averages of CO_2 concentration at Kasprowy Wierch measured in-situ (quasi-continuous) and weekly averages from bag samples.

The urban area of Cracow is characterised by frequent temperature inversions. This fact, in connection with a relatively large flux of biogenic carbon dioxide, leads to a much more pronounced diurnal amplitude of the CO_2 concentration in Cracow, when compared with Kasprowy (Fig. 3a). The mean amplitude in Cracow is equal 90 ± 40 ppm whereas at Kasprowy it usually does not exceed 10 ppm. The minimum values of the CO_2 concentration recorded in Cracow in August 1997 are equal 351 ± 5 ppm, slightly higher than the regional background represented by Kasprowy data (345 ± 4 ppm) for the same period.

The carbon isotopic composition of atmospheric CO_2 together with concentration data was used to identify the origin of atmospheric CO_2 in Cracow. The correlation between $\delta^{13}C$ and the reciprocal concentration was applied to derive the $\delta^{13}C$ of the mean local CO_2 source in Cracow for the period April 93–January 94. Its result is –22.2‰. The corresponding value for Kasprowy (March 95–March 96) is –25.8‰. Fig. 4 presents a comparison between bi-weekly mean $\delta^{13}C$ values for Schauinsland, Germany [1], bi-weekly mean $\delta^{13}C$ values for Cracow (weekly composite samples [2]) and spot samples collected in Cracow. The spot samples indicate that during periods of good vertical mixing of the lower atmosphere, the observed $\delta^{13}C$ values are close to those observed in "clean" areas. However, the bi-weekly means for the $\delta^{13}C$ data are significantly more negative than corresponding Schauinsland data due to relatively strong surface fluxes of CO_2 of anthropogenic and biogenic origin. The contribution of biogenic, anthropogenic and "clean" CO_2 to the total measured CO_2 concentration in Cracow on the diurnal time scale was calculated using isotope and mass balance equations:

$$c_{tot} = c_{bg} + c_{bio} + c_{ant}$$

$$c_{tot} \cdot \delta^{13}C_{tot} = c_{bg} \cdot \delta^{13}C_{bg} + c_{bio} \cdot \delta^{13}C_{bio} + c_{ant} \cdot \delta^{13}C_{ant}$$

$$c_{tot} \cdot \delta^{18}O_{tot} = c_{bg} \cdot \delta^{18}O_{bg} + c_{bio} \cdot \delta^{18}O_{bio} + c_{ant} \cdot \delta^{18}O_{ant}$$

where:

c_{tot}, $\delta^{13}C_{tot}$, $\delta^{18}O_{tot}$ — measured concentration and isotopic composition of atmospheric CO_2;

$\delta^{13}C_{bg}$, $\delta^{13}C_{bio}$, $\delta^{13}C_{ant}$ — carbon isotope composition of individual components (background, biospheric and anthropogenic);

$\delta^{18}O_{bg}$, $\delta^{18}O_{bio}$, $\delta^{18}O_{ant}$ — oxygen isotope composition of individual components (background, biospheric and anthropogenic);

c_{bg}, c_{bio}, c_{ant} — calculated contribution of individual components to the total measured CO_2 concentration .

The three following assumptions were made in deriving the contribution of individual components using the above equations:

- the measured atmospheric CO_2 concentration consists of three components: the background, biogenic CO_2 and anthropogenic CO_2;
- the isotope composition of individual components is constant during the analysed period;
- the concentration and isotope composition of carbon and oxygen of atmospheric carbon dioxide is measured.

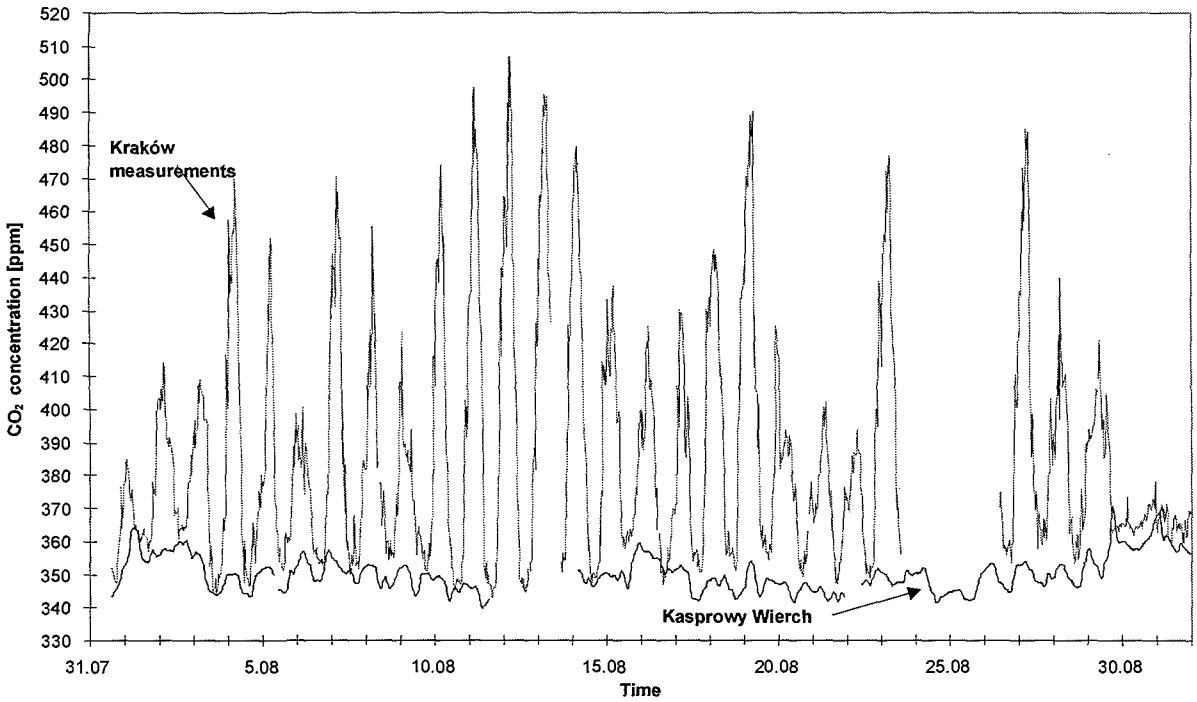

Fig. 3a. Carbon dioxide at Kasprowy Wierch and in Cracow (August 1997). Both graphs3a and 3b show quasi-continuous GC measurements.

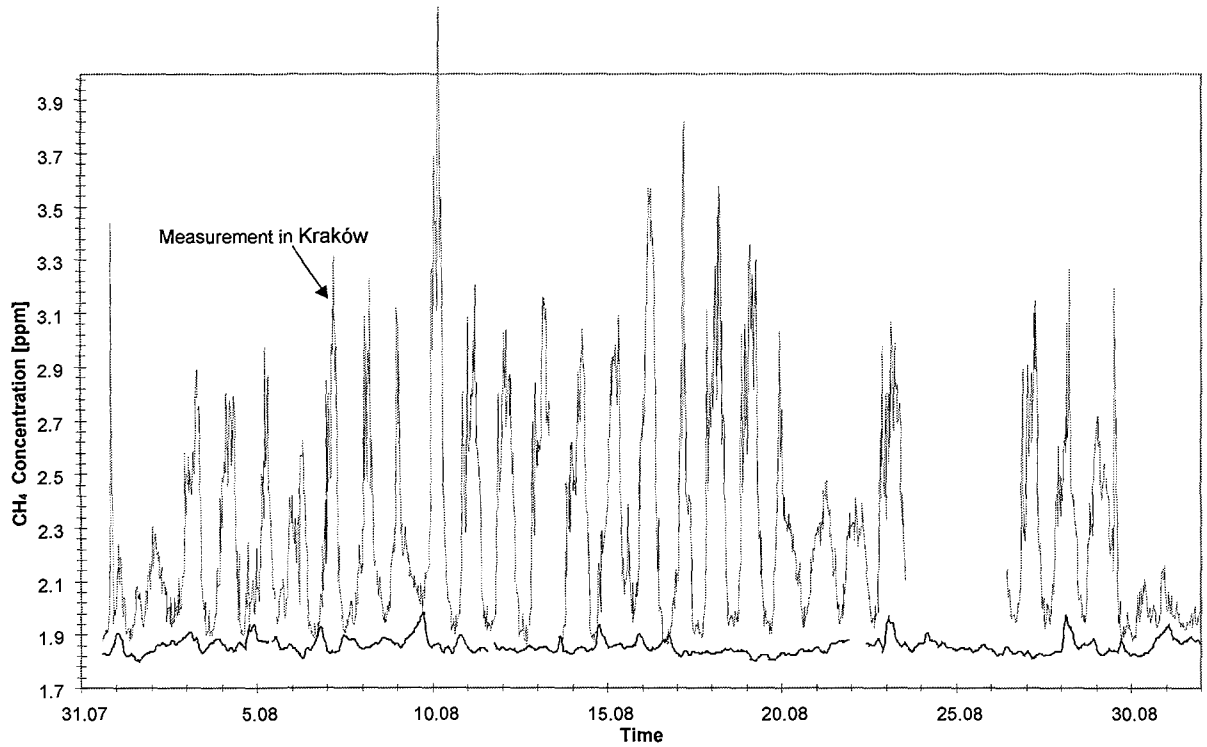

Fig. 3b. Methane (b) at Kasprowy Wierch and in Cracow (August 1997). Both graphs3a and 3b show quasi-continuous GC measurements.

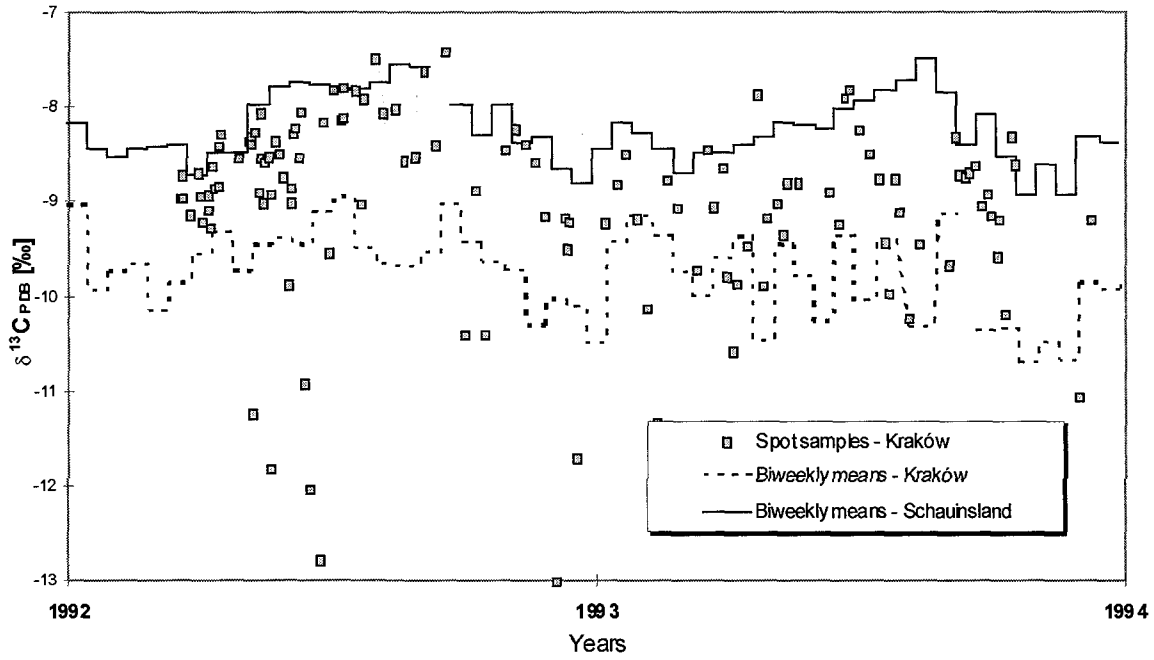

Fig. 4. Carbon isotopic composition of atmospheric CO_2 in Cracow and at Schauinsland. For details, see text.

Figs 5a and 5b show typical diurnal variations of the total CO_2 concentration and its components during the summer and winter periods, calculated using the above discussed mass balance approach [3].

It is apparent from Fig. 5a (summer) that during night hours the biogenic component was dominating while during the day the anthropogenic component plays the most important role. The contribution of anthropogenic CO_2 reaches ca. 20 ppm. This result is consistent with similar calculations based on the radiocarbon data [2]. The calculated background CO_2 concentration is 354 ppm, in good agreement with concentrations observed at Kasprowy station. In winter (Fig. 5b), the anthropogenic component dominates.

3. RADIOCARBON IN CO_2

Systematic measurements of the carbon isotope composition in tropospheric CO_2 are being carried out since 1983. The sampling point is located in Cracow (53°3'N, 19°54'E), ca. 25 m above the ground level (on the roof of the Faculty building), in an area bordering recreation and sport grounds and the university campus.

Atmospheric CO_2 is continuously sampled by sorption in a molecular sieve in bi-weekly intervals. The sampled air (usually ca. 15 m^3) is pumped through a molecular sieve container, and after thermal desorption more than 5 dm^3 of CO_2 is obtained in which $\delta^{14}C$ and $\delta^{13}C$ are measured [4], [2].

For carbon isotopic measurements ($\delta^{14}C$, $\delta^{13}C$), we use liquid scintillation spectrometers (LSC, TRI-CARB Canberra-Packard), and mass spectrometers (VG Micromass 602 C, and Finnigan Mat DELTA S), respectively. The measurement uncertainty (1σ for single measurement) is ±8‰ for $\delta^{14}C$, and ±0.09‰ for $\delta^{13}C$.

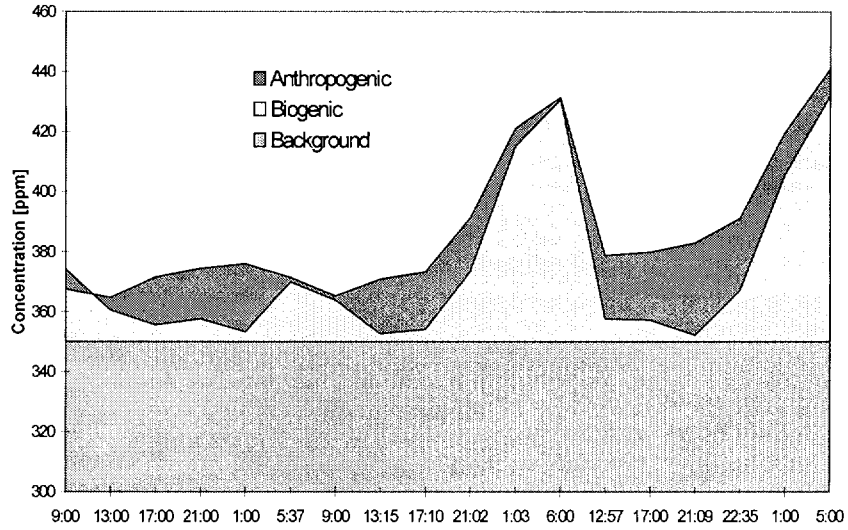

Fig. 5a. The calculated contribution of three components of the measured CO_2 concentration in the Cracow atmosphere during summer diurnal changes.

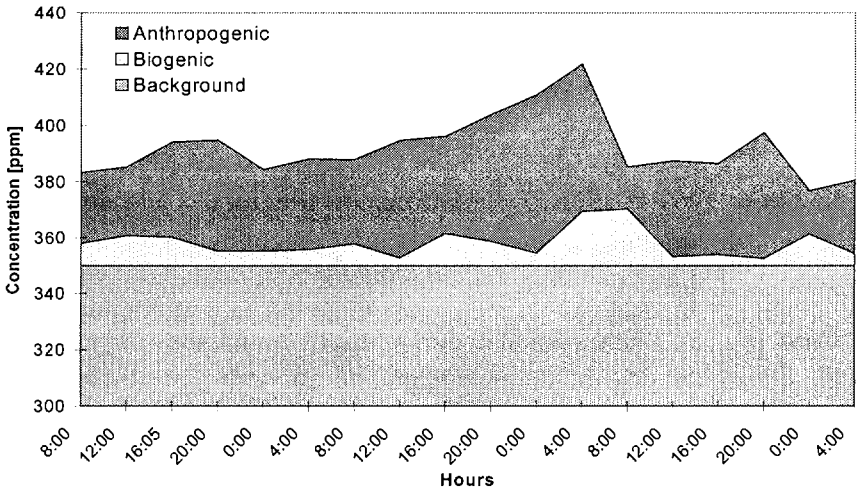

Fig. 5b. The calculated contribution of three components of the measured CO_2 concentration in the Cracow atmosphere during winter diurnal changes.

Radiocarbon results are reported as $\delta^{14}C$ in per mil versus NBS Oxalic Acid (Contemporary Standard for Carbon-14-Dating Laboratories) following the generally accepted notation [5]. The stable carbon isotope ratio, $^{13}C/^{12}C$ is reported as $\delta^{13}C$ per mil deviation from the primary standard VPDB [6], [7]. N_2O was not determined and a N_2O correction was not applied. Both $\delta^{14}C$ and $\delta^{13}C$ are generally decreasing with time ($\Delta\delta^{14}C$ = –92‰, $\Delta\delta^{13}C$ = –0.24‰ in a 12 year interval), however, radiocarbon results point to a local minimum in February 1991. The observed decrease of $\delta^{13}C$ falls well into a straight line.

The atmospheric ^{14}C activity of air at Cracow is systematically lower than reported in the background fit for Schauinsland, Germany [8] (Fig. 6). The difference reaches 44 ‰ in January 1983, showing a decreasing tendency to 41‰ in January 1993. However, this difference was significantly minimised in further years by the local minimum of $\delta^{14}C$ observed at Cracow as well as by its following small increase. The noticed effect is most probably of regional importance as a result of the remarkable lowering of fossil fuel consumption for industrial purposes since the early 90s (Fig. 7).

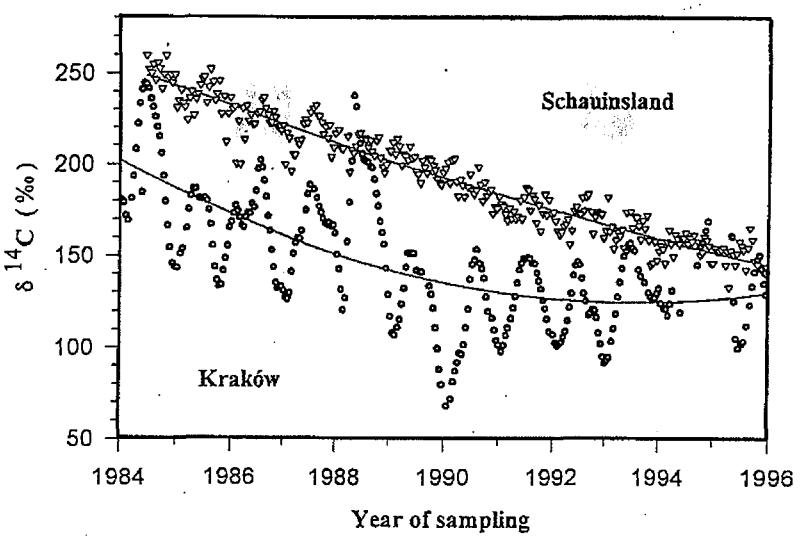

Fig. 6. Radiocarbon in atmospheric CO_2 in Cracow and at Schauinsland.

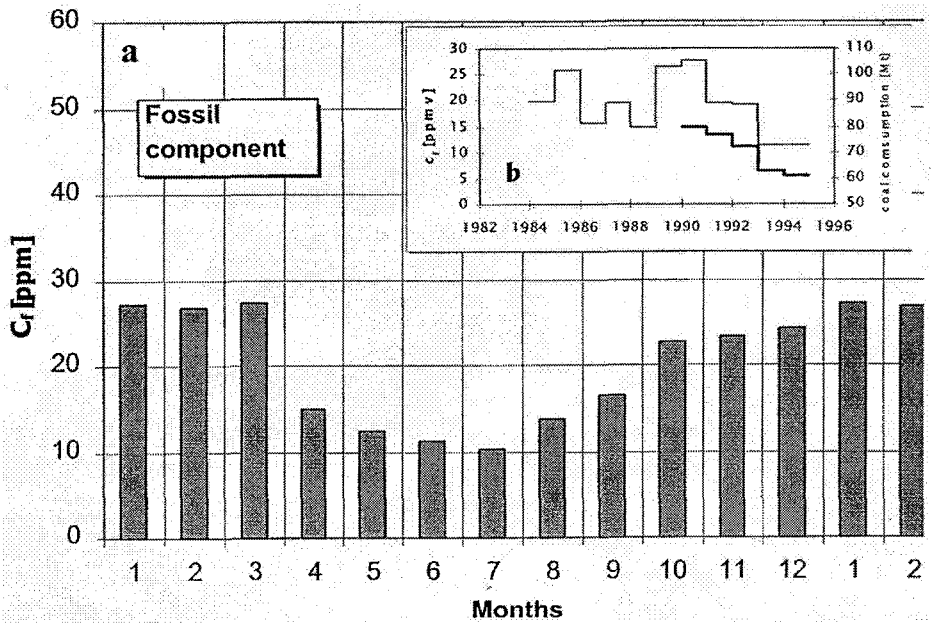

Fig. 7a, b. Calculated fossil component in atmospheric CO_2 in Cracow.

The $\delta^{13}C$ mean value at Cracow in 1983–1994 shows a systematic linear decrease with a slope of 0.02‰/a, from –9.6‰ in January 1983. This value is ca. 1.7‰ more negative than for uncontaminated marine air, and ca. 0.95‰ more negative compared to Schauinsland data [8].

The highest values of $\delta^{14}C$ and $\delta^{13}C$ observed in the summer months (June, July) reach 24.8‰ ($\delta^{14}C$) and +3.3‰ ($\delta^{13}C$) above the respective trend while the lowest values of $\delta^{13}C$ appear in November (–0.3‰) gradually increasing till summer. The peak-to-peak difference close to 0.71‰ confirms the high fossil fuel effect with overlapped biogenic activity. In case of $\delta^{14}C$, the minimum (–30.5‰) is observed four months later, in February/March.

4. METHANE

The measurements of methane were undertaken with the main aim of providing high-quality concentration and isotope data ($\delta^{13}CH_4$) for two sites in southern Poland, in the city of Cracow and in Kasprowy as a part of the ongoing efforts towards a better characterisation of the regional budget of methane for the European continent. The following specific objectives were formulated with respect to measurements of methane:

- characterisation of the temporal variability of the atmospheric CH_4 concentration (background level, diurnal and seasonal changes) in Cracow, representing heavily polluted urban environment, typical for eastern European cities,
- identifying major sources of atmospheric methane in Cracow and their characteristic $\delta^{13}C$ values,
- characterisation of the temporal variability of the atmospheric CH_4 concentration at a high-altitude continental site in Central Europe, relatively free of local influences (Kasprowy),
- determination of the $\delta^{13}C$ signature of the regional CH_4 source mix in central Europe from concentration and $\delta^{13}CH_4$ measurements.

The CH_4 concentration was measured using a GC system based on a HP5890 Gas Chromatograph. Standards were supplied by the Institut fuer Umweltphysik, University of Heidelberg, Germany. They are calibrated with respect to the NOAA scale [8]. The $\delta^{13}CH_4$ of air samples was measured in Cracow using an extraction/conversion line of the New Zealand type [9] and analysis by isotope ratio mass spectrometry. The overall reproducibility of the method is around 0.1‰ for the air sample of 20 litres. Details of the analytical protocol are reported in [10].

The following modes of sampling were used:
- spot sampling (50 litres of air collected in stainless steel containers) used in Cracow for both concentration and $\delta^{13}C$ measurements,
- quasi-continuous GC based monitoring used at the Kasprowy station (frequency of sampling: every 30 minutes)
- integrated sampling used at the Kasprowy station, parallel to the GC-based monitoring (one-week and one-month composite samples collected in alu-bags).

Fig. 8 shows the record of methane concentration at the Kasprowy station. From September 1994 until July 1996 only integrated bag samples were collected. The analysis of bag samples was done in the Institute of Environmental Physics in Heidelberg. Later the GC system was operated in parallel. Fig. 3b illustrates diurnal changes of the CH_4 concentration in Cracow and Kasprowy Wierch.

The average concentration of CH_4 in Cracow for the period from March 1996 to March 1997 was 2.464 ± 0.109 ppm (1σ of the mean), based on 52 equally distributed spot measurements performed at 6:00 and 15:00 hours, respectively. Averaging only the values representing maximum intensity of vertical mixing (15:00) yields 2.028 ± 0.050 ppm. The mean concentration of CH_4 derived from the same period for Kasprowy station, based on monthly

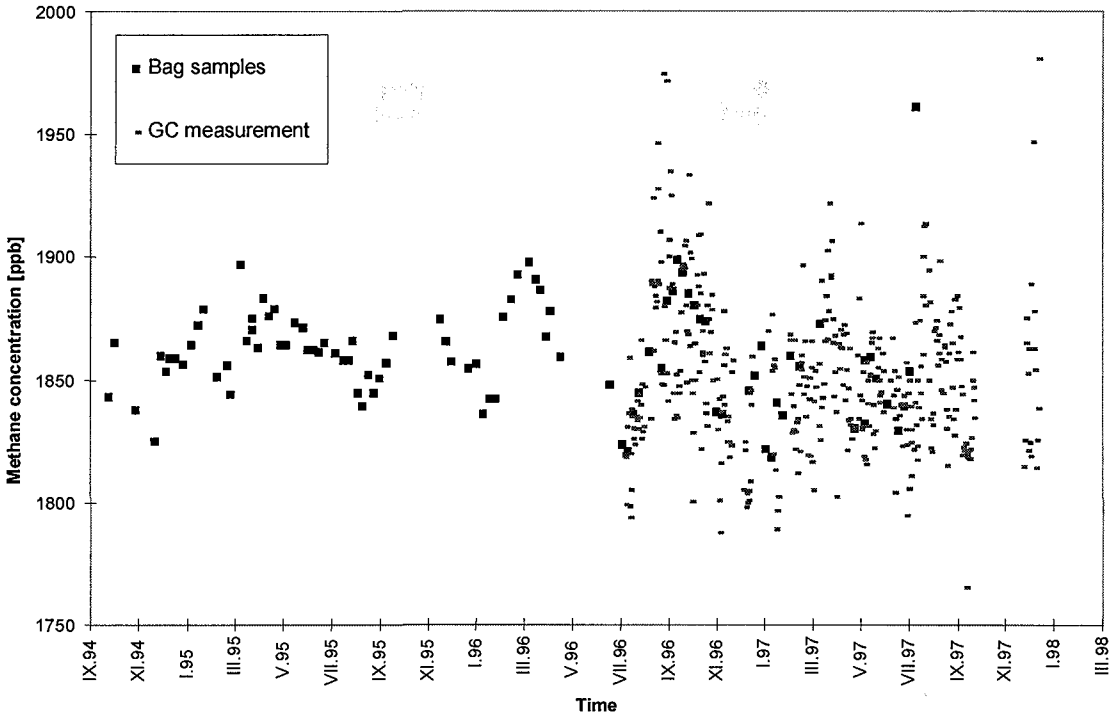

Fig. 8. The CH_4 concentration record from Kasprowy Wierch station. The bag samples were measured at the Institute of Environmental Physics, University Heidelberg, Germany.

vertical mixing, the average CH_4 level in the Cracow atmosphere is elevated with respect to the regional background represented by the Kasprowy data by around 170 ppb. This elevated methane background in the Cracow atmosphere is most likely due to relatively large sources of this gas located ca. 100 km west of the city (large urban centers of the Silesia district, with numerous coal mines and heavy industry).

The average amplitude of daily variations of CH_4 concentration in Cracow atmosphere for the above-mentioned period is 0.911 ± 0.210 ppm. It was derived as a mean difference of the measured CH_4 concentration at 6:00 hours and 15:00 hours. The derived amplitude was used to assess the average flux density of CH_4 for the Cracow metropolitan area assuming the average height of the inversion layer in Cracow equal to ca. 100 meters and the average catchment area for diurnal mixing within the lower atmosphere equal to around 230 km^2. The estimated flux density is equal to about 0.7 g CH_4 /km^2 s which corresponds to the annual emission of CH_4 in the order of 2.5×10^7 m^3/year. This estimate agrees well with independent assessments of leakages from the city gas network (around 2×10^7 m^3/year).

A linear regression of $\delta^{13}CH_4$ versus the reciprocal concentration data available for Cracow (Fig. 9a) yields the average $\delta^{13}C$ signature of the local source mix of methane (leakages from the city gas network, cars, landfills) to be –54.0±0.3‰. This is very close to the mean $\delta^{13}CH_4$ value obtained for methane distributed in the city network (–54.4 ± 0.6‰ — average of nine independent determinations carried out over a two-year period). This similarity confirms earlier suggestions that leakages from the city gas network constitute a major methane source in this environment.

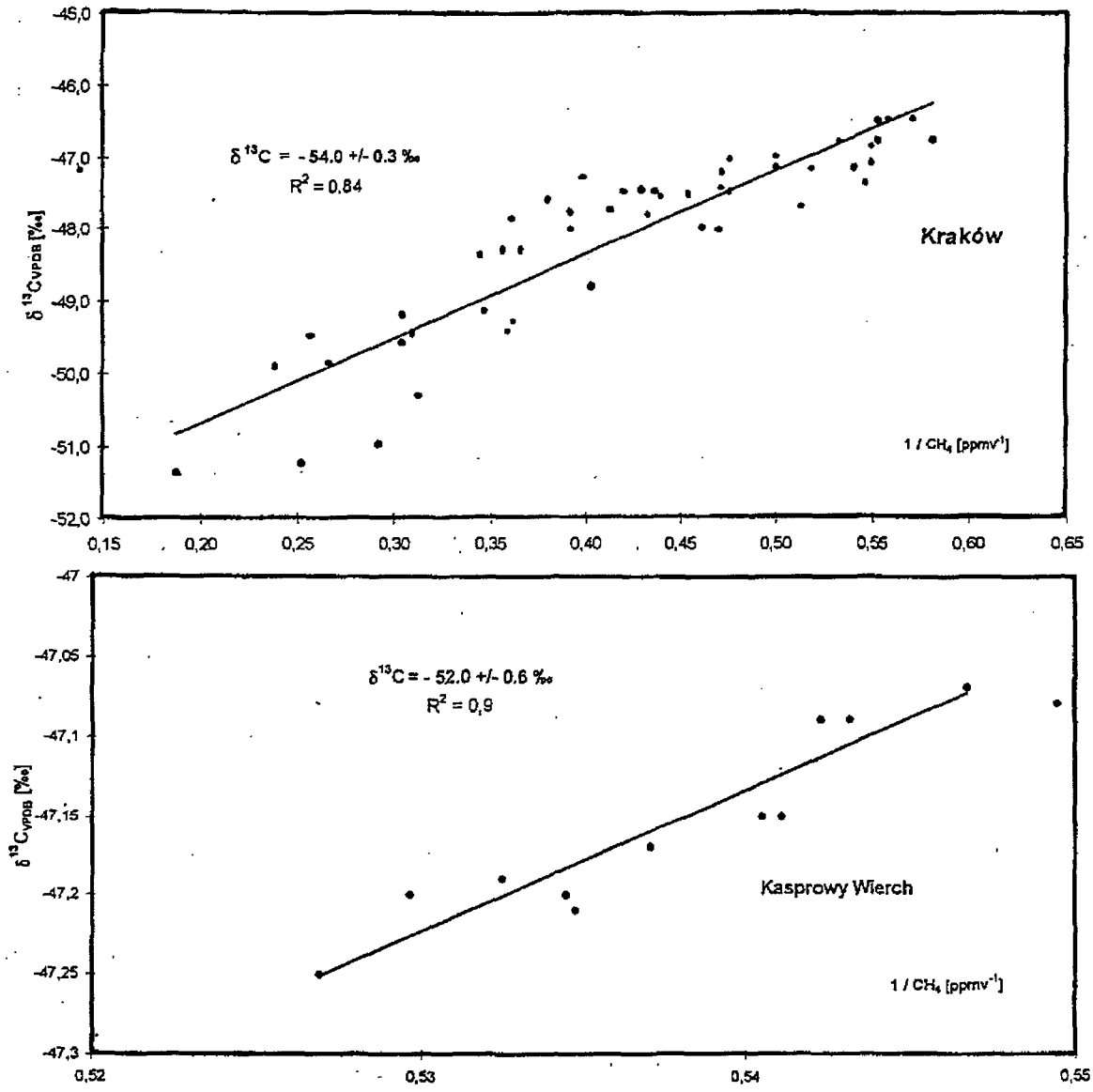

Fig. 9. The correlation between $\delta^{13}C$ and inverse concentration for the Cracow (a) and Kasprowy Wierch (b) atmosphere.

The average $\delta^{13}C$ signature of the regional source mix for Kasprowy, derived in a analogous way to Cracow data, is equal to –52.0 ± 0.6‰ (Fig. 9b). A very similar $\delta^{13}C$ value is obtained when the concentration and $\delta^{13}CH_4$data for Kasprowy are compared with the analogous data available for the station Izana, Canary Islands [1], representing undisturbed marine air entering the European continent from the Atlantic Ocean. In this case, the derived $\delta^{13}C$ value (–53.5 ± 07‰) represents the average net source of methane, integrated over the distance from the Atlantic coast to Kasprowy. The fact that both estimates agree very well suggests that the influence of local sources of CH_4 on the data being gathered at Kasprowy station is negligible. A first interpretation of those data is given in [11].

5. SULPHUR HEXAFLUORIDE (SF_6)

Measurements of sulphur hexafluoride on Kasprowy Wierch are done by gas chromatography with an ECD detector without a sample enrichment procedure. The reproducibility of a single

analysis on the level of 0.05 pptv allows to observe changes of SF_6 concentration as low as 0.02 ppt on a daily average scale. The record of the SF_6 concentration at the Kasprowy Wierch station for a 1.5-year period covering the second part of 1996 and almost the whole of 1997 shows a slight seasonality with minimal values in summer and maximal ones in winter (Fig. 10). An increase of about 0.15 ppt appeared between July 1996 and July 1997. Such concentration changes are not of a daily character but occasionally sudden increases are observed more than 0.5 ppt over the background level (Fig. 11). Because these changes are not connected to the local meteorological conditions, an origin from remote sources is expected. There is no evident correlation with the methane or carbon dioxide concentration. For 1997, the annual mean SF_6 mixing ratio on Kasprowy Wierch air was 4.24 ppt.

The result of a comparison between GC measurements and bag samples showed a mean difference of 0.06 ± 0.06 ppt.

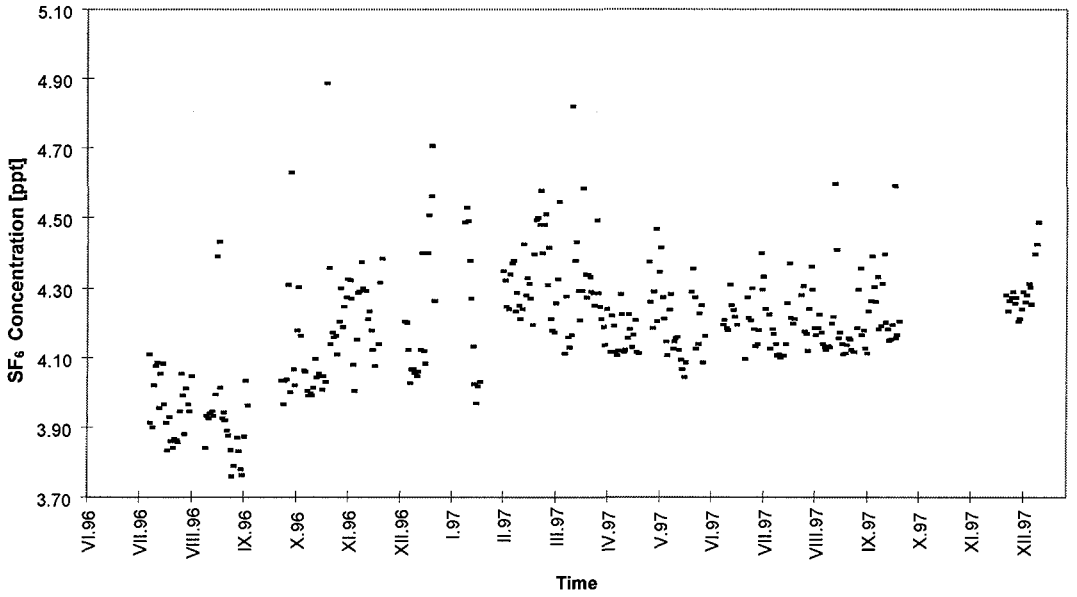

Fig. 10. SF_6 concentration measured by GC at Kasprowy Wierch.

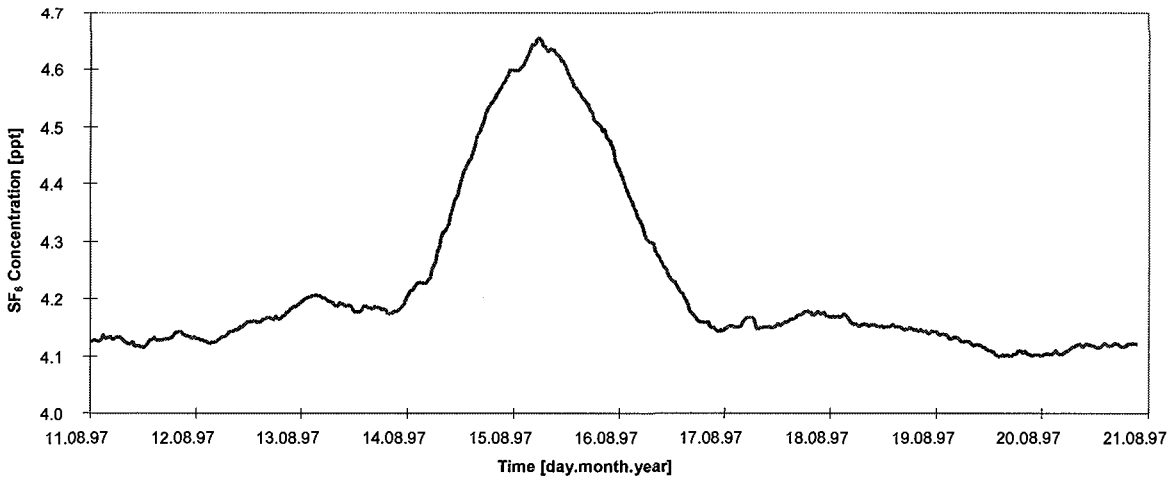

Fig. 11. Incidental increase of SF_6 concentration observed in August 1997 on Kasprowy Wierch

REFERENCES

[1] LEVIN I., (1997), European methane. Regional methane budget in south-west Germany derived from atmospheric observations. Final Report from EU Environment Program Contract #EV5V-CT94-0413, E.Nisbet, I.Levin, G.P.Wyers, A.Roddy (Eds.), Brussels, pp.72–114

[2] KUC,T.,(1991), Concentration and carbon isotopic composition of atmospheric CO_2 in southern Poland, Tellus 43B, pp.373–378

[3] ZIMNOCH M., (1997), Isotope composition of CO_2 in the environment, PhD Thesis, University of Mining and Metallurgy, Krakow, 105 pp. (in Polish).

[4] FLORKOWSKI T., GRABCZAK J., KUC T. ,RÓŻAŃSKI K., (1975), Determination of radiocarbon in water by gas or liquid scintillation counting: Nukleonika, 20, no. 11–12, 1053–1066.

[5] STUIVER M. ,POLLACH H., (1977), Discussion: Reporting of ^{14}C data: Radiocarbon, 19, no. 3, 355–363.

[6] COPLEN T. B., (1995), Reporting of stable carbon, hydrogen, and oxygen isotopic abundances, in: Reference and intercomparison materials for stable isotopes of light elements IAEA-TECDOC-825, 31–34.

[7] ALLISON C. E., FRANCEY R. J. AND MEIJER H. A., (1995), Recommendations for the reporting of stable isotope measurements of carbon and oxygen in CO_2 gas, in: Reference and intercomparison materials for stable isotopes of light elements IAEA-TECDOC-825, 155–162.

[8] LEVIN I., KROMER B., (1997), Twenty years of high precision observations at Schauinsland station, Germany, Radiocarbon, Proc. 16-th Int. Radiocarbon Conference, Groningen, the Netherlands, June 15–20, 1997.

[9] LOWE D.C., BRENNINKMEIJER C.A.M., BRAILSFORD G.W., LASSEY K.R., GOMEZ A.J., (1994), Concentration and ^{13}C records of atmospheric methane in New Zealand and Antarctica: Evidence for changes in methane sources. J.Geophys.Res., 99(D8), 16913–16925

[10] MIROSŁAW J., (1997), Isotope ratios of methane in Krakow atmosphere, PhD Thesis, University of Mining and Metallurgy, Krakow, 123 pp. (in Polish).

[11] FLORKOWSKI T., KORUS A.,MIROSŁAW J., NĘCKI J., NEUBERT R., SCHMIDT M., ZIMNOCH M. (1998), Isotopic composition of CO_2 and CH_4 in the heavily polluted urban atmosphere and in the remote mountain area (Southern Poland), Paper IAEA -SM–349/5 Isotope Techniques in the Study of Past and Current Environmental Changes in the Hydrosphere and the Atmosphere, IAEA Vienna.

MONSOON SIGNATURES IN TRACE GAS RECORDS FROM CAPE RAMA, INDIA

S.K. BHATTACHARYA[1], R.A. JANI[1], D.V. BOROLE[2], R.J. FRANCEY[3], C.E. ALLISON[3], L.P. STEELE, K.A. MASARIE[4]

[1] Physical Research Laboratory, Ahmedabad, India
[2] National Institute of Oceanography, Goa, India
[3] CSIRO Atmospheric Research, Aspendale, Australia
[4] NOAA/CMDL, Boulder, Colorado, United States of America

Abstract. Concentrations of trace gases CO_2, CH_4, CO, N_2O and H_2, and the stable carbon and oxygen isotopic composition of CO_2 have been measured in air samples collected from Cape Rama, a coastal station on the west coast of India, since 1993. The data show clear signatures of continental and oceanic air mass resulting in complex seasonal variation of trace gas characteristics. The regional atmospheric circulation in the Indian Ocean and Arabian Sea undergoes biannual reversal in low-level winds associated with the yearly migration of the inter-tropical convergence zone (ITCZ). From June to September, the wind is from the equatorial Indian Ocean to the Indian subcontinent (southwest monsoon) and brings in pristine marine air. From December to February, dry continental winds blow from the northeast and transport continental emissions to the ocean (northeast monsoon). Detailed transport and chemical modelling will be necessary to interpret these records, however the potential to identify and constrain the regional trace gas emissions appears to be high.

1. INTRODUCTION

The large-scale atmospheric circulation in the Indian Ocean and Arabian Sea region is characterized by biannual reversal in low-level winds associated with the Indian monsoon [1]. This flow pattern is largely driven by the temperature gradient between the land mass (Indian subcontinent) and the ocean as a result of differential solar heating, which changes seasonally [2]. In the winter months, the atmosphere over the continent cools faster relative to the ocean, forming a region of general subsidence, which causes a dry northeasterly flow (NE monsoon). In contrast, the intense heating in summer months (April-May) results in the development of heat lows over the northern landmass reversing the circulation; this causes a moisture rich south-westerly flow that brings torrential rains over India during June to September (SW monsoon). During the transition period between the NE monsoon (December-February) and the SW monsoon (June-September), zonal temperature gradients and easterlies in the tropical Indian Ocean are weak and the inter-tropical convergence zone (ITCZ) is located typically at about 10° S. At this time, the cross-equatorial monsoon flow from the continent meets the Southern Hemisphere air at the ITCZ. The effect of these two monsoons on the biogeochemistry of the Arabian Sea and the Bay of Bengal is well known [3, 4]. The productivity on the land also changes drastically in response to the monsoon system. It is therefore expected that the two monsoon systems must have an important effect on the concentration and isotopic composition of atmospheric CO_2, and the concentration of other trace gases. Air sampling at Cape Rama contributes to a global atmospheric composition study [5] and, given the potential for global impacts originating in the poorly sampled tropical/sub-tropical regions, data from this site provide valuable constraints on global forcing from these regions. Preliminary results of this study are presented here.

2. SAMPLING SITE

After some preliminary exploration we were able to find an excellent site at Cape Rama on the west coast of India (Figure 1) about 80 km south of Panaji, Goa. The sampling location is on flat rocky terrain, about 60 m above sea level and overlooks the sea. The site is devoid of any vegetation over a scale of 50 m on all sides and is at least a few hundred metres away from sparse habitation.

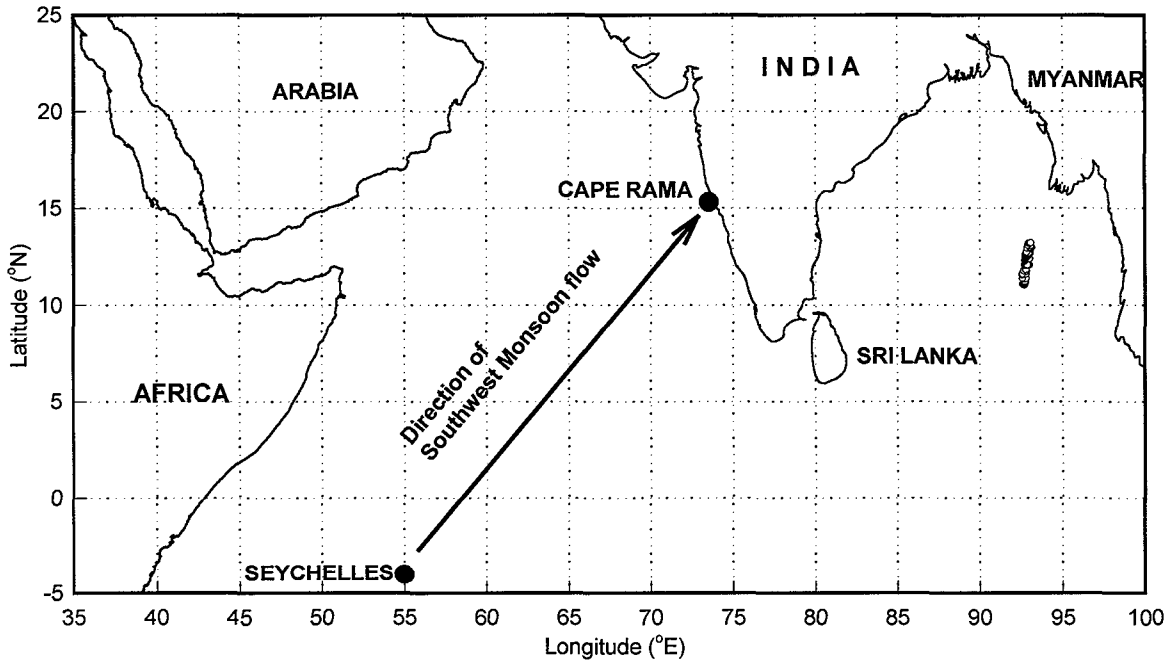

Figure 1. Locations of the Cape Rama and Seychelles air sampling stations. The general direction of wind flow during the SW monsoon is from Seychelles to Cape Rama.

The meteorological data from Panaji show that on this part of the west coast, the wind in the afternoon (sampling time) is onshore all year round. In the summer (SW) monsoon period, this flow direction matches the general large-scale flow and, therefore, air samples collected during this period (June to September) represent tropical oceanic air mass averaging a large-scale equatorial regime. In the winter (NE) monsoon period, the zonal wind direction is offshore and matches with the morning local wind. However, the same air mass recirculates as a sea breeze in the afternoon after mixing over a large oceanic fetch. Therefore, air samples collected in the afternoon during the winter monsoon period (December to February) represent an air mass with integrated continental signatures. The wind speed at the time of sampling is moderate, generally about 4 to 6 ms^{-1} but increasing to 10 to 12 ms^{-1} at the peak of SW monsoon.

3. EXPERIMENTAL METHOD

Air samples are collected in 500 ml glass flasks at a pressure of 190 kPa (absolute) using a specially designed portable flask pump unit that chemically dries the air using $MgClO_4$, and incorporates digital wind speed and wind direction monitors. The air-intake is 6 metres above ground and two flasks are pressurised, one after another, during each site visit. Each flask is flushed with dried air for about 10 minutes before filling. After filling, the flasks

are returned to CSIRO Atmospheric Research's GASLAB (Global Atmospheric Sampling LABoratory) in Aspendale for determination of the concentrations of trace gases CO_2, CH_4, CO, N_2O and H_2 by gas-chromatographic methods. Subsequently, the carbon and oxygen isotopic ratios in CO_2 are determined using an automatic cryogenic extraction system coupled to a Finnigan Mat 252 mass-spectrometer with external precisions of 0.015 ‰ and 0.050 ‰ for $\delta^{13}C$ and $\delta^{18}O$ measurements respectively. Further details of GASLAB operation are given in Francey et al. [5].

4. RESULTS AND DISCUSSIONS

Regular sampling at Cape Rama started in February 1993 and, since then, continuous bi-monthly samples have been collected. The data from 1993 through 1998 are presented here in the form of time series plots (Figures 2 to 9). For each species, we produced a smooth fit to the data by applying a Fast Fourier Transform (FFT) routine to convert data into the frequency domain, applying a low-pass filter and then applying an inverse FFT to get back to the time domain [6]. The filter effectively removes variations with periods less than 80 days. Smoothed data from Cape Rama (15.1°N, 73.8°E) are compared to smoothed CSIRO data from Mauna Loa (19.5°N, 155.6°W, representing zonal Northern Hemisphere marine-air), and smoothed NOAA-CMDL measurements [7, 8] from Seychelles (4.7°S, 55.2°E), which is directly upwind of Cape Rama during SW monsoons, and downwind in NE monsoons. For the purpose of our discussion, the data from the two networks are assumed to be on comparable scales.

4.1 Carbon dioxide and its isotopes

In Figure 2, the Cape Rama CO_2 mixing ratio (thick line) is compared to a smooth curve fitted to CSIRO Mauna Loa data (thin line) and to the Seychelles data (grey line). The Seychelles data exhibit small seasonality and a relatively low overall growth rate from 1993 through 1995 with stronger growth from 1995 through 1999. The Cape Rama trends are consistent with this but exhibit a strong seasonal variation with peak-to-peak amplitude of 10–15 ppm. The Cape Rama seasonality appears particularly large in 1993/94 and 1997/98, although this is not reflected in either the Mauna Loa or Seychelles curves.

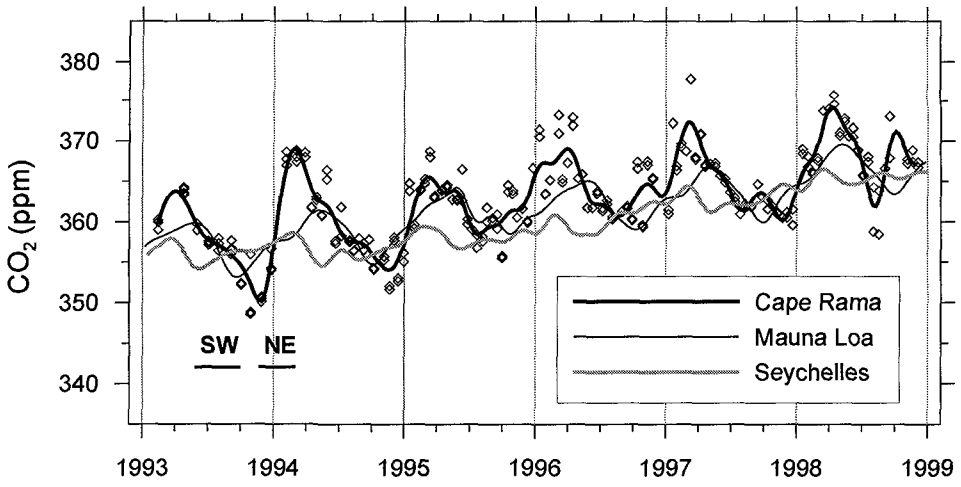

Figure 2. Measured concentration of CO_2 (diamonds) in air samples collected at Cape Rama, along with the smoothed fit to the data points (thick line). Periods of SW monsoon and NE monsoon are indicated. Smoothed fits to the Seychelles (grey line) and Mauna Loa (thin line) data are given for comparison.

Annually, the highest mixing ratio is observed in February-March, towards the end of the NE monsoon, while the lowest mixing ratio occurs in October, soon after the end of the SW monsoon. During the SW monsoon, the CO_2 concentrations observed at Cape Rama agree well with those observed at Seychelles. This is expected as the air mass reaching Cape Rama at that time is from the equatorial zone carrying pure marine air from the direction of Seychelles [2]. The wind speed is also moderately high during the SW monsoon, which minimizes any possible effect due to the upwelling in the Arabian Sea at this time.

In October-November, Cape Rama CO_2 concentrations are generally close to those at Seychelles, although in 1993, 1994 and 1997, the Cape Rama concentrations are lower than those at Seychelles. From October-November until February-March, Cape Rama values increase sharply to values much higher than the Seychelles, particularly in 1993–94 and 1997–98. During this period, Northern Hemisphere values are also increasing (as shown in the Mauna Loa record), however the Cape Rama increases are more rapid and of larger amplitude. These increases to well above Southern Hemisphere values are generally consistent with increases observed in the Northern Hemisphere. This transport of Northern Hemisphere continental air towards the equator has also been observed during ship-based studies of tropospheric trace constituents over the Indian Ocean [9]. The Cape Rama /Seychelles differences are also consistent with regional net (photosynthetic) uptake in October-November, followed by net winter respiration, which may explain the year-to-year variability observed in the CO_2 record. Late 1994 and late 1997 have been identified as periods of enhanced biomass burning in tropical regions [10] that may have contributed to the Cape Rama seasonality in these years, although full transport modelling with global network data will be necessary to more accurately separate regional causes from long-range transport.

The anti-correlation between the Cape Rama $\delta^{13}C$-CO_2 (Figure 3) and CO_2 mixing ratio on the seasonal timescale favours a strong biogenic contribution, and excludes a strong oceanic contribution. Regression analysis of each year's data from 1993 to 1998 yields coefficients of –0.0433, –0.0478, –0.0476, –0.0467, –0.0551 and –0.0408 ‰ ppm^{-1}, respectively. While the magnitudes of the year-to-year differences in coefficients are of marginal significance, it is suggestive that the largest values (most negative) occur in 1994 and 1997, the years of enhanced biomass burning, and the lowest values (most positive) occur in the immediately following years. Such a pattern would be expected if a higher proportion of C3 photosynthetic material were involved in global exchange in 1994 and, particularly, 1997 followed by an increased C4 proportion in the subsequent year. This pattern is expected if wild fires convert tropical forest to savannah. Climatic-induced changes in the photosynthetic fractionation factors might also contribute.

The $\delta^{18}O$-CO_2 values (Figure 4) exhibit a complex seasonal behaviour, with relatively steady values, close to Southern Hemisphere values observed at other GASLAB sites, during the SW monsoon. A small decrease in $\delta^{18}O$-CO_2 is observed at the end of the SW monsoon and is followed by a rapid increase to a maximum value at the beginning of the NE monsoon. This seasonal pattern breaks down in 1998, possibly an artefact due to deteriorating flask storage (under further investigation).

The $\delta^{18}O$-CO_2 values in the SW monsoon period show a general decline of around 0.5 ‰ from 1993 to 1996, followed by a flattening/reversal that has been observed elsewhere in the CSIRO global network. The sharp positive peak in the NE monsoon period is most easily explained by an isotopic exchange with leaf water, which is significantly enriched compared to soil water, particularly in conditions of high evapotranspiration (low relative humidity).

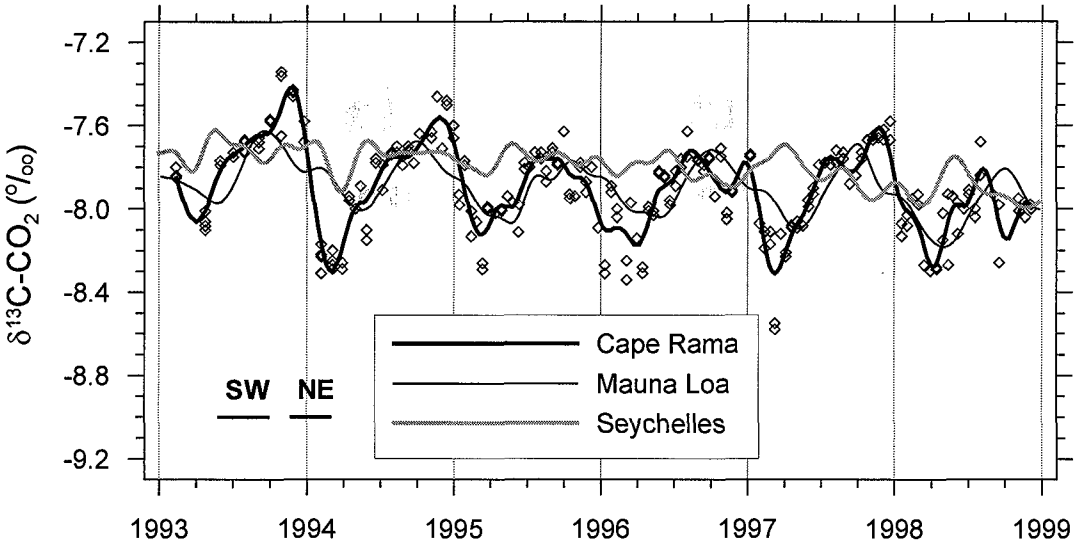

Figure 3. Measured $\delta^{13}C$-CO_2 (diamonds) in air samples collected at Cape Rama, along with the smoothed fit to the data points (thick line). Periods of SW monsoon and NE monsoon are indicated. Smoothed fits to the Seychelles (grey line) and Mauna Loa (thin line) data are given for comparison.

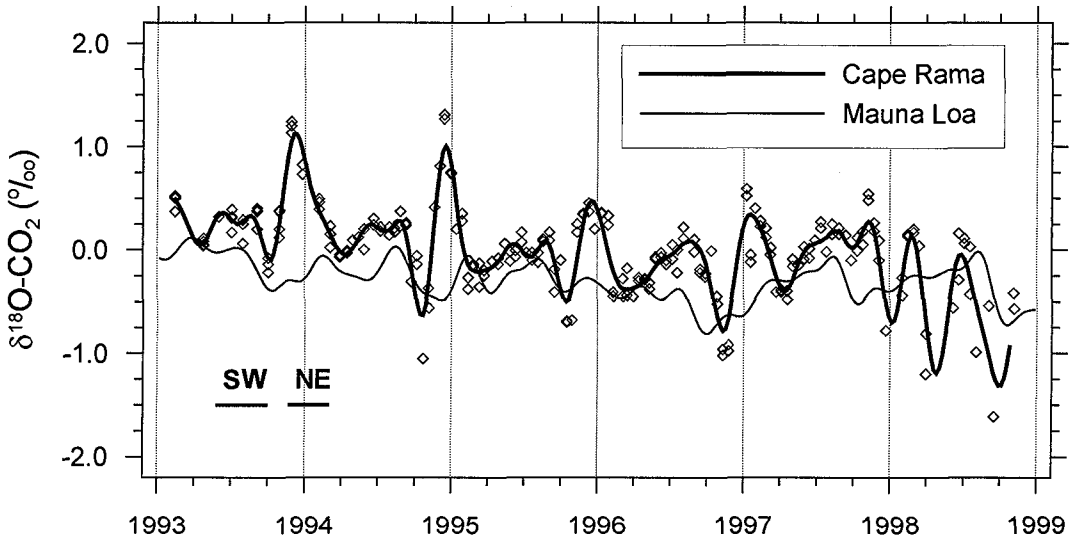

Figure 4. Measured $\delta^{18}O$-CO_2 (diamonds) in air samples collected at Cape Rama, along with the smoothed fit to the data points (thick line). Periods of SW monsoon and NE monsoon are indicated. A smoothed fit to the Mauna Loa data (thin line) is given for comparison.

4.2 Methane, Carbon monoxide and Hydrogen

Variations in mixing ratios of CH_4 and CO at Cape Rama are shown in Figures 5 and 6, along with smooth curves fitted to the Mauna Loa and Seychelles data. As expected, the Cape Rama and Seychelles values are quite similar for both gases during the SW monsoon period for all years, 1993 to 1998, but the Cape Rama data show significant increases during the NE monsoon period. Over the whole season, Cape Rama growth rates for CH_4 and CO are remarkably similar (Figure 7).

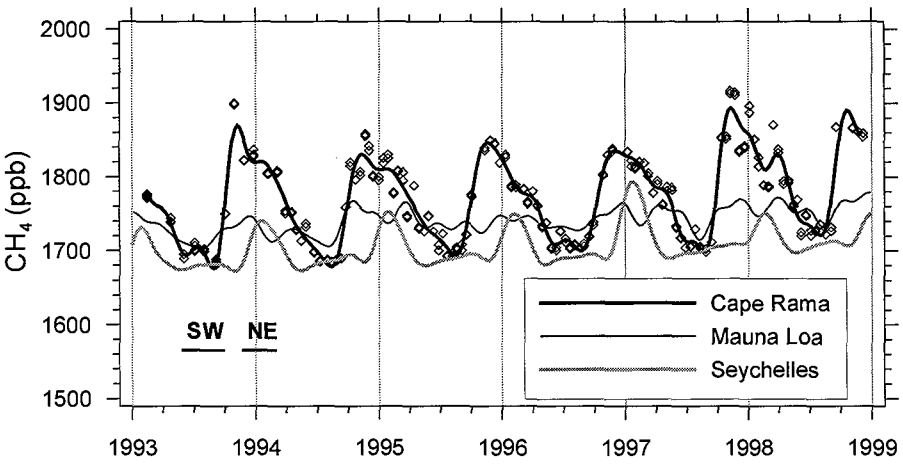

Figure 5. Measured concentration of CH_4 (diamonds) in air samples collected at Cape Rama, along with the smoothed fit to the data points (thick line). Periods of SW monsoon and NE monsoon are indicated. Smoothed fits to the Seychelles (grey line) and Mauna Loa (thin line) data are given for comparison.

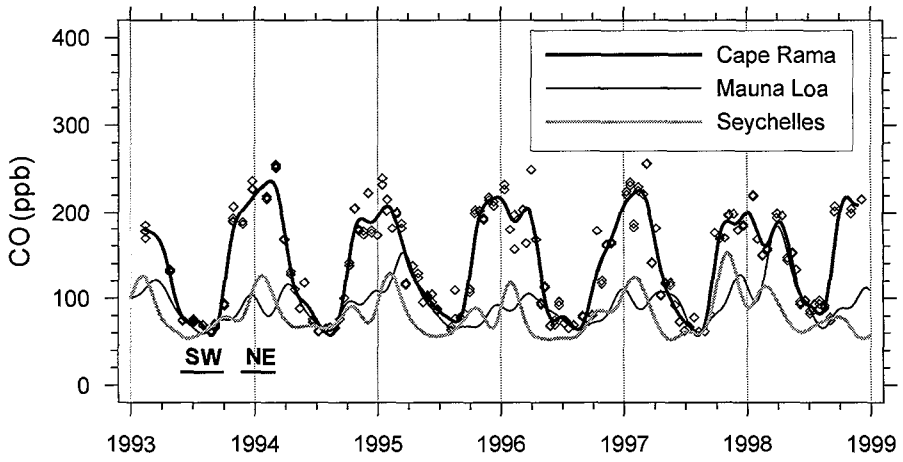

Figure 6. Measured concentration of CO (diamonds) in air samples collected at Cape Rama, along with the smoothed fit to the data points (thick line). Periods of SW monsoon and NE monsoon are indicated. Smoothed fits to the Seychelles (grey line) and Mauna Loa (thin line) data are given for comparison.

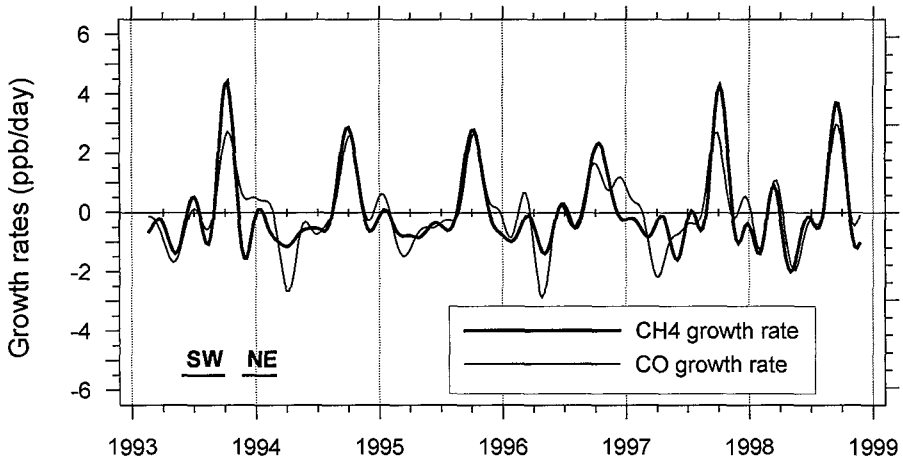

Figure 7. Growth rates of CH_4 (thick line) and CO (thin line) in air samples collected at Cape Rama. Periods of SW monsoon and NE monsoon are indicated.

The mixing ratios start to increase strongly just after the SW monsoon when the origin of the air mass is from the northwest or north-northwest direction, carrying partly continental air. CH_4 peaks at the beginning of the NE monsoon and then steadily decreases through to the beginning of the next SW monsoon. The highest CO values are obtained throughout the NE monsoon, characterizing high emission from Indian subcontinent.

The post SW monsoon increase in CH_4 and CO is also clear in the Seychelles data but occurs later, in early December (i.e. during the NE monsoon in India), when the continental air first arrives at Seychelles. At this time, the ITCZ position probably coincides with the Seychelles latitude (4°S) and the winter continental air starts to flow over it. Subsequently, during the northward migration of the ITCZ as it moves past Seychelles, the supply of continental air is cut off and the equatorial marine value is returned there. Cape Rama continues to have higher mixing ratios until June as it still continues to receive the continental air. The net result is that the peaks in CH_4 and CO at Seychelles are flanked on both sides by the peaks at Cape Rama, and the peak value observed at Seychelles is less, due to dilution by marine air.

Again, modelling of atmospheric transport and chemistry will be required to understand the contributions of these interacting species from large-scale transport, local surface sources and sinks and chemical modification within the atmosphere.

During the NE monsoon, H_2 steadily increases at Cape Rama (Figure 8), before returning to relatively steady values at the beginning of the SW monsoon. Since continental regions are usually considered a sink for H_2, this is surprising behaviour, suggesting that the increasing H_2 and decreasing CH_4 are linked.

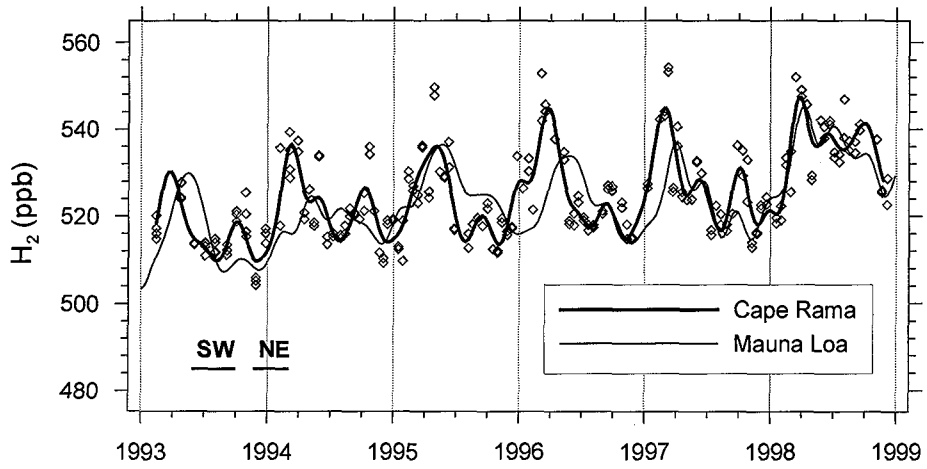

Figure 8. Measured concentration of H_2 (diamonds) in air samples collected at Cape Rama, along with the smoothed fit to the data points (thick line). Periods of SW monsoon and NE monsoon are indicated. A smoothed fit to the Mauna Loa data (thin line) is given for comparison.

4.3 Nitrous oxide

The N_2O mixing ratio (Figure 9) does not show a consistent significant seasonal cycle at the available measurement precision. From 1993 to mid-1995, the mean value remained close to 313 ppb, but after that it increased steadily reaching 318 ppb in 1998. The interannual variation of the N_2O is very similar to that observed for CO_2, although the sources and sinks for these two gases are thought to be quite different.

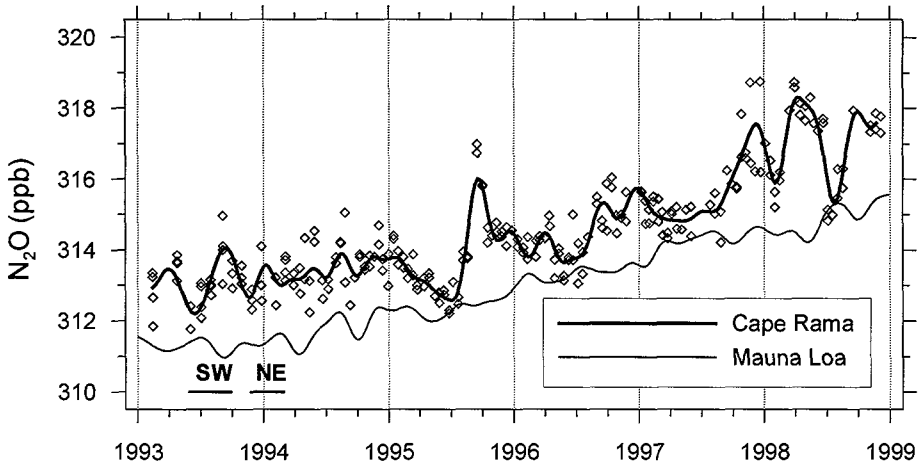

Figure 9. Measured concentration of N_2O (diamonds) in air samples collected at Cape Rama, along with the smoothed fit to the data points (thick line). Periods of SW monsoon and NE monsoon are indicated. A smoothed fit to the Mauna Loa data (thin line) is given for comparison.

5. FUTURE PERSPECTIVES

Atmospheric trace gas studies initiated by the Physical Research Laboratory (PRL), Ahmedabad and the National Institute of Oceanography, Goa, in collaboration with CSIRO Atmospheric Research, Aspendale, and with the help and sponsorship of the International Atomic Energy Agency (IAEA), are providing important time series for the first time in a monsoonal zone of the equatorial belt. Enhanced levels of methane during the NE monsoon period are thought to be due to various continental sources and, considering the agricultural practices in the Indian subcontinent, it seems that rice cultivation and cattle rumination are the main sources. To estimate the relative contribution of these sources, we have set up a methane extraction line at PRL to convert methane to carbon dioxide for isotopic analysis. This line has recently become operational and the first measurements to characterize the source signatures are being planned. As an offshoot of these initiatives, some important investigations of oxygen isotopic anomalies in atmospheric CO_2 have been made and further investigations are being planned. These combined efforts are expected to be of great value in understanding the budget of the greenhouse gases in the earth's atmosphere.

ACKNOWLEDGEMENT

Several scientists and administrative personnel from CSIRO Atmospheric Research (Aspendale), PRL (Ahmedabad) and NIO (Goa) contributed significantly towards the success of the program outlined above. The trace gas measurements are crucially dependent on the sophisticated methods and equipment developed and maintained in CSIRO GASLAB. In this context, we are extremely thankful to Ms. Lisa Cooper, Mr. Darren Spencer, Mr. Ray Langenfelds and Mr. Scott Coram. PRL are grateful to CSIRO Atmospheric Research for the scientific gift of the methane extraction line. Special thanks are due to the personnel at NOAA-CMDL, Boulder, Colorado, for providing the Seychelles data. We are also grateful for financial help received from the India-Australia Exchange Program and the Department of Science, Industry and Tourism, Australia, at various stages. We finally thank the Director of PRL, Chief of Division of CSIRO Atmospheric Research, and the Administrative Head at IAEA for encouragement and financial help to carry out this work.

REFERENCES

[1] RAO, Y.P., South-West Monsoon, Meteorol. Monograph, No. 1, India Meteorological Dept. 1976

[2] CADET, D., Meteorology of the Indian summer monsoon, Nature, 279, 261–267, 1979.

[3] LAL, D. (Editor), Biogeochemistry of the Arabian Sea, Proceedings of the Indian Academy of Sciences, Bangalore, India, 1994.

[4] QASIM, S.Z., Oceanography of the northern Sea, Deep Sea Res., Pt A, 29(9), 1041–1068, 1982.

[5] FRANCEY, R.J., STEELE, L.P., LANGENFELDS, R.L., LUCARELLI, M.P., ALLISON, C.E., BEARDSMORE, D.J., CORAM, S.A., DEREK, N., DE SILVA, F.R., ETHERIDGE, D.M., FRASER, P.J., HENRY, R.J., TURNER, B., WELCH, E.D., SPENCER, D.A., COOPER, L.N., Global Atmospheric Sampling Laboratory (GASLAB): supporting and extending the Cape Grim trace gas programs. In: Baseline Atmospheric Program Australia. 1993 R. J. Francey, A. L. Dick and N. Derek (editors). Department of the Environment, Sport and Territories, Bureau of Meteorology in cooperation with CSIRO Division of Atmospheric Research. p. 8–29.

[6] THONING, K.W., TANS, P.P., KOMHYR, W.D., Atmospheric carbon dioxide at Mauna Loa Observatory, 2, Analysis of the NOAA/GMCC data, 1974–1985, J. Geophys. Res., 94, 8549–8565, 1989.

[7] (a) CONWAY, T.J., TANS, P.P., WATERMAN, L.S., THONING, K.W., KITZIS, D.R., MASARIE, K.A., ZHANG, N., Evidence for interannual variability of the carbon cycle from the NOAA/CMDL global air sampling network, J. Geophys. Res., **99**, 22831–22855, 1994.

(b) DLUGOKENCKY, E.J., STEELE, L.P., LANG, P.M., MASARIE, K.A., MARTIN, R.C., The growth rate and distribution of atmospheric methane, J. Geophys. Res, 99, 17021–17043, 1994.

(c) NOVELLI, P.C., MASARIE, K.A., LANG, P.M., Distributions and recent trends of carbon monoxide in the lower troposphere, J. Geophys. Res., 103, 19015–19033, 1998.

[8] TROLIER, M., WHITE, J.W.C., TANS, P.P., MASARIE, K.A., GEMERY, P.A., Monitoring the isotopic composition of atmospheric CO_2 - measurements from the NOAA global air sampling network, J. Geophys. Res., 101, 25897–25916, 1996.

[9] RHOADS, K.P., KELLEY, P., DICKERSON, R.R., CARSEY, T.P., FARMER, M., SAVOIE, D.L., PROSPERO, J.M., Composition of the troposphere over the Indian Ocean during the monsoonal transition, J. Geophys. Res., 102, 18981–18995, 1997.

[10] MATSUEDA, H., INOUE, H. Y., Aircraft measurements of trace gases between Japan and Singapore in October of 1993, 1996 and 1997, Geophys. Res. Lett., 26, 2413–2416, 1999.

THE DEVELOPMENT OF O_2/N_2 MEASUREMENT CAPABILITY AT THE CIO GRONINGEN

R.E.M. NEUBERT, H.A.J. MEIJER
Centrum voor IsotopenOnderzoek, Groningen University, Netherlands

Abstract. The measurement capability for high-precision atmospheric O_2 concentration measurements, with a precision high enough to be of use on global carbon cycle studies, has been established at the CIO, and O_2/N_2 ratios can now in principle routinely be determined. The technique has already found a number of applications, such as soil air analysis, firn air analysis, diurnal cycles for the determination of apparent stoichiometric ratios CO_2 : O_2, and last but not least regular aircraft sampling as well as ground-based campaign work in the EU project Eurosiberian Carbonflux.

1. INTRODUCTION

In order to trace the fate of anthropogenic produced CO_2, as well as better understand natural variations of the Global Carbon Cycle, different efforts have been undertaken: In the first place the precise and continuous measurement of atmospheric CO_2 concentrations [1] to get a picture of the interannual, seasonal and regional variations, as well as of the secular increase; later on the ratio of the stable carbon isotopes was investigated to learn about the partitions of CO_2 taken up by respectively oceans and land biosphere [2,3,4] and in parallel the $\delta^{18}O$ of CO_2 could be analyzed. This isotope ratio tells us about the activity of the land biosphere [5,6,7]. The decrease of atmospheric $^{14}CO_2$, brought into the atmosphere by nuclear bomb tests in addition to the natural level, is still used successfully to trace the paths of atmospheric CO_2 into the reservoirs ocean and land biosphere [8,9]. Statistics of (fossil) fuel usage are used to define the anthropogenic CO_2 source [10,11,12], and historic trace gas data are unraveled from firn air measurements [13]. Nowadays a lot of conclusions are drawn applying computer simulations on the global datasets [14,15,16]. However, the puzzle remained incomplete.

In the late 1980's a new method was developed by R.F. Keeling [17]. The changes of the atmospheric oxygen concentration are inverse to those of the CO_2 concentration in case of Carbon burning, photosynthesis and biospheric release of CO_2. CO_2 uptake by the oceans, however, is not accompanied by a release of oxygen, apart from smaller seasonal effects [18]. Combining global atmospheric CO_2 and O_2-measurements with fuel burning statistics, and using a certain ratio of molecules O_2 used per molecule CO_2 produced for fuel-burning and biological processes resp. (the so-called stoichiometric ratio), the partitioning of ocean versus land biosphere CO_2 uptake can be made [19].

In order to be helpful for global carbon cycle research, the atmospheric oxygen concentration needs to be determined with a precision of a fraction of a ppm, concurrently with CO_2 concentration measurements. Such an oxygen measurement on an absolute basis is very difficult indeed: the atmospheric oxygen concentration is close to 21 %, so 1 ppm absolute precision at this level would mean a ratio of $1:(0.21 \cdot 10^6) = 4.7 \cdot 10^{-6}$. However, the very successful *relative* measurement technique of Isotope Ratio Mass Spectrometry (IRMS) can be used to determine the relative oxygen concentration with the required precision [20].

2. INSTRUMENTAL

The principle of the mass spectrometric technique is that molecular oxygen and molecular nitrogen are treated as if they were each other's "isotopes". The ratio O_2/N_2 of a sample, determined by measuring the ion beams at the mass/charge ratio m/z = 28 (N_2) and

m/z = 32 (O_2), is compared to the same ratio of an atmospheric air sample as reference gas. In analogy to stable isotope measurements, results are reported as relative deviations form a reference material; whereas for stable isotopes these relative deviations are expressed as "per mil" (‰), for the O_2 N_2 ratio the "per meg" (= 0.001 per mil) is in use. 1 ppm change in oxygen concentration is thus in our atmospheric situation equivalent to 4.7 per meg [21]. As described by Bender et al.[20], measuring different non-ideal gases with different thermodynamic properties, instead of different isotopomers of the same gas, has its own difficulties.

At the CIO, a Micromass Optima IRMS (Micromass Ltd., Manchester, UK) is dedicated to this goal. Its build-up and cup design even permits to measure, apart from the O_2/N_2 ratio, the Ar N_2 ratio, as well as the stable isotope ratios $^{16}O^{18}O/^{16}O^{16}O$ ($\delta^{18}O$ of O_2) and $^{14}N^{15}N/^{14}N^{14}N$ ($\delta^{15}N$ of N_2) at the same time.

The instrument was developed in close cooperation between the CIO and the manufacturer and the machine was the first one to measure all of the above-mentioned signals (resp. ratios) really simultaneously, without switching the working parameters like the magnetic field. It is in use since September 1997. The primarily aimed-at precision for the O_2/N_2 ratios is achieved (although improvement is always possible and desirable).

The long-term accuracy of the results depends to a great deal on the quality of the different standard gases that are available in the laboratory in high pressure cylinders, and which are under permanent monitoring and control.

3. RESULTS

As an example for the CIO's newly achieved capability to do oxygen concentration measurements in atmospheric air with the required precision, the results of one diurnal cycle are presented here (Figure 1).

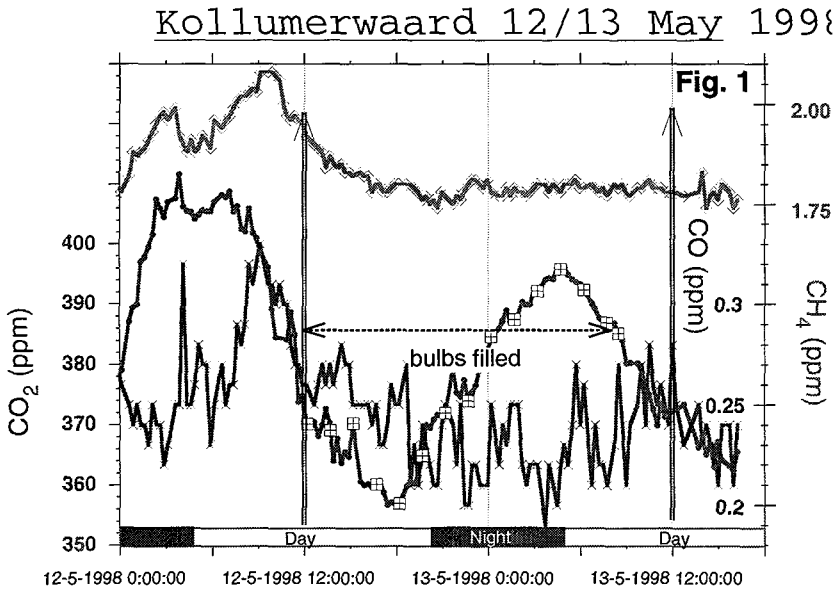

Figure 1: A diurnal cycle as observed for the concentrations of CO_2 (circles, left-hand scale), CH_4 (diamonds, right hand scale) and CO (crosses, right hand scale) at the station Kollumerwaard, close to the dutch North Sea coast nearby Groningen. Concurrently with the concentration measurements 10 l glass bulbs were filled one after the other, at the time indicated by the squares on the CO_2 concentration line.

During the time from 12 May 1998, 12:00 until 13 May 1998, 12:00, 15 glass bulbs of 10 liter volume each were filled at the station Kollumerwaard, close to the Dutch North Sea coast nearby Groningen. The air was sampled at 7 m height and dried cryogenically at –60°C. One after the other the bulbs were flushed at about 3 $l \cdot min^{-1}$ during 90 minutes, resulting in spot samples of a few minutes integration time every 90 minutes.

The concentrations of CO_2, CH_4 and CO were measured using a gas chromatographic system (GC-FID) by KEMA (Dutch Electricity Companies' Joint Research Institute) four times per hour on air from the same inlet as used by the bulb system [22].

Back in our laboratory the bulb air was first analyzed for O_2/N_2 ratios with the dedicated mass spectrometer. The measurements were done with respect to a laboratory working standard gas and are reported here on this internal scale, as no international scale is available yet. Meanwhile we have built up the capability to do high-precision concentration measurements of CO_2, CH_4 and CO on air samples in our lab on the same samples as for O_2/N_2 analysis. For the diurnal cycle shown here, however, we use interpolations of the KEMA CO_2 results (preliminary internal scale) as our bulb CO_2 concentration data.

After the nighttime peak on 12-5-1998, the CO_2 concentration decreased until 18:00 local time and then increased until 04:30 the next morning, when the daily decrease started again (see Figure 1). What we observe here is the result of changing mixing-heights and -intensities in the near-ground atmosphere layer, i.e. accumulation of (near-) ground produced trace gases during night time and their mixing and dilution to higher layers after sunrise. The sampled air record includes a CO_2 concentration variation of about 40 ppm.

As there is no concurrent accumulation of methane or CO during the nighttime or early morning of 13 May (in contrast to the night before), the conclusion is that the CO_2 does not (or only for a minor part) originate from fossil fuel burning, which is always connected with CO- and CH_4- emissions, but originates from biogenic sources. This is also supported by measurements of the $^{14}CO_2$-activity (Fig. 2(a), right scale, visible $\pm 1\sigma$-uncertainty bars). In the range of the measurement uncertainties there is almost no variation visible, whereas for a pure fossil fuel contribution (no $^{14}CO_2$ at all) we would expect a variation of about –3‰ per ppm CO_2 admixed. These methods were applied earlier [23,24], to quantify the biogenic vs. fossil fuel derived CO_2 partitions and to investigate e.g. the ratio of CO : CO_2 emissions of fossil fuel burning and the $\delta^{13}C$ of the regional fossil fuel CO_2 source.

Fig. 2(b) shows the CO_2 concentrations together with the results of our oxygen concentration measurements, given as $\delta O_2/N_2$, the deviation of the ratio O_2/N_2 from the ratio of our working standard. Note that the oxygen scale is reversed, in order to make the anti-parallel behavior more obvious, as an increase of CO_2 means a decrease of O_2.

Figure 3 shows the good correlation between CO_2- and O_2 concentrations. We find a slope of (–7.3±0.4) permeg O_2 per ppm CO_2, which means a stoichiometric ratio of 1.53 mol O_2 used up per mol CO_2 produced. This is different from the mean value used on a global scale up to now and further investigations will show in which range this stoichiometric ratio varies regionally and seasonally.

The measurement accuracy of ±5 permeg $\delta O_2/N_2$ achieved is clearly sufficient for the resolution of this kind of diurnal cycle investigations with a variation of about 300 permeg. Meanwhile sampling started for longtime series a/o at the meteorological station Kasprowy Wierch (High Tatra Mountains in Poland) in cooperation with UMM Krakow, at Spitzbergen in cooperation with NILU and MISU Stockholm, at Mace Head in Ireland in cooperation with LSCE Paris and University of Galway, and onboard of aircrafts in the frame of the EU-project Eurosiberian Carbonflux.

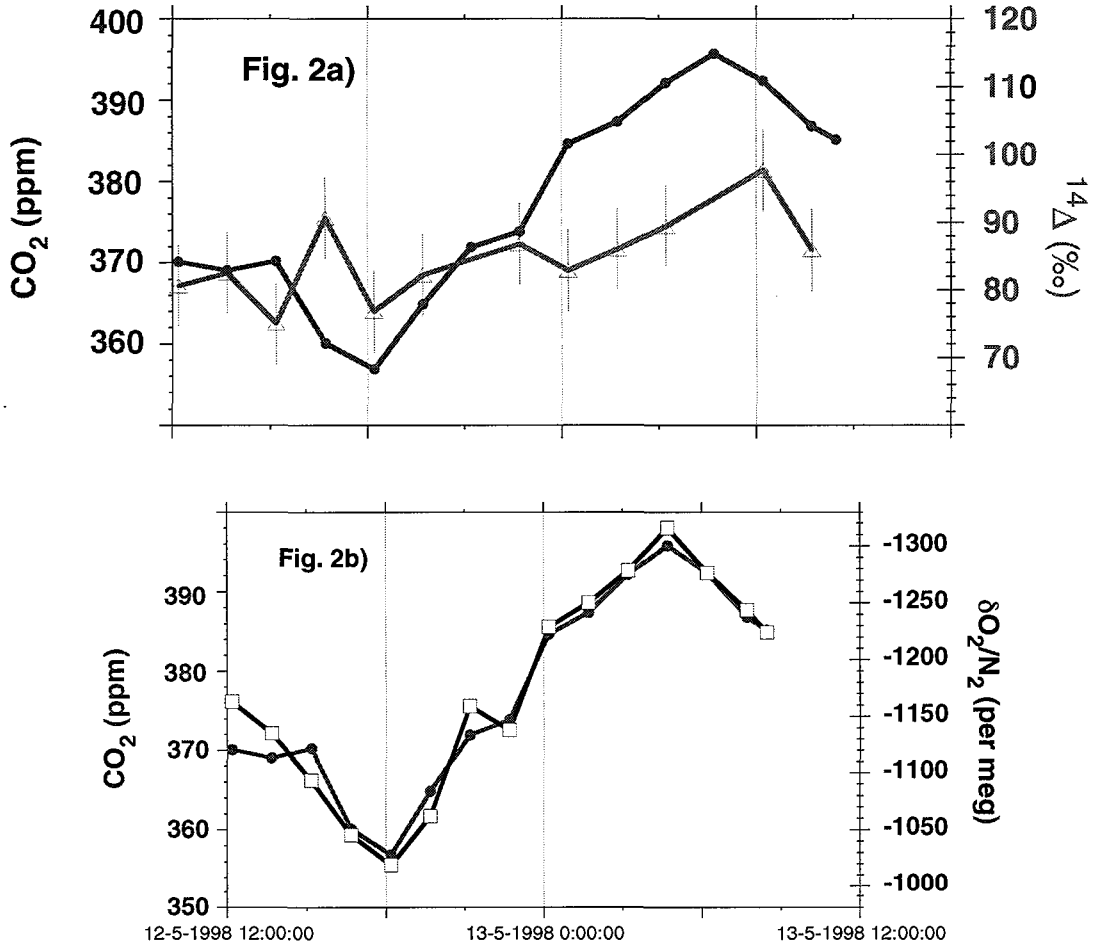

Figure 2 (a): The CO_2 concentration (circles) together with the $\Delta^{14}C$ (triangles) from the CO_2 in the glass bulbs. Since no significant variation in $\Delta^{14}C$ is observed, we conclude that all CO_2 in this diurnal cycle is biogenic. (b): The CO_2 concentration (circles) compared to the results of our oxygen concentration measurements (squares), given as $\delta O_2/N_2$, the deviation of the ratio O_2/N_2 from the ratio of our working standard. Note that the oxygen scale is reversed, in order to make the anti-parallel behavior more obvious, as an increase of CO_2 means a decrease of O_2.

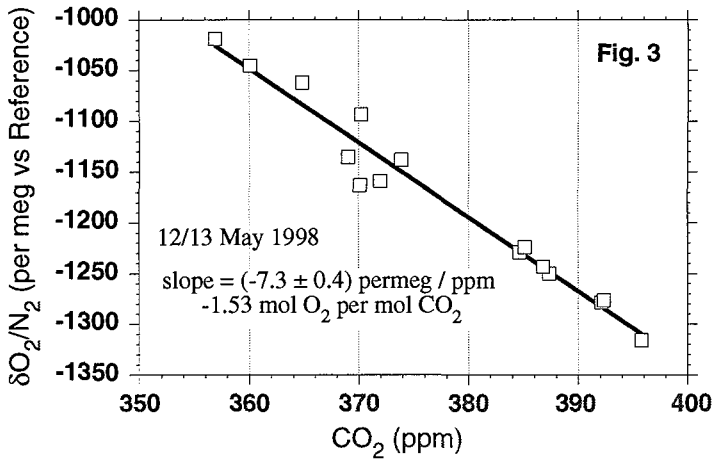

Figure 3: The correlation between CO_2 and O_2 concentrations. We find a slope of (-7.3 ± 0.4) permeg O_2 per ppm CO_2, which means a stoichiometric ratio of 1.53 mol O_2 used up per mol CO_2 produced.

4. CONCLUSION AND PERSPECTIVES

The mass spectrometric O_2/N_2 measurement technique has been adopted by CIO. The regular whole air sample volume has been reduced to 2.5 litres now. At present the technique is in full use for analysis of vertical profiles in the EU-project Eurosiberian Carbonflux. Furthermore, we are working on the establishment of an international network, of which one of the sites is meant to act as intercomparison site with some of the other O_2/N_2 programs running concurrently.

Finally, we are establishing the regional monitoring station Lutjewad, situated directly on the sea-dike 25 km north-west of Groningen (53°23' N, 6°22' E, with a 60 m mast), at which we will, a/o, perform investigations of the apparent atmospheric stoichiometry CO_2: O_2. By means of $^{14}CO_2$ (AMS-) measurements we are able to divide night-time CO_2 increases into biogenic and fossil-fuel-derived parts and thus can establish a regional mean stoichiometry climatology for both these parts separately.

REFERENCES

[1] KEELING, C.D., BACASTOW, R.B., BAINBRIDGE, A.E., EKDAHL Jr., C.A., 1976, Atmospheric carbon dioxide variations at Mauna Loa Observatory, Hawaii, Tellus 28, 538-551

[2] MOOK, W.G., KOOPMANS, M., CARTER, A.F., KEELING, C.D., 1983, Seasonal, Latitudinal and Secular Variations in the abundance and isotopic ratios of atmospheric carbon dioxide. 1. Results from land stations, Journal of Geophysical Research, 88, 10915-10933

[3] KEELING, C.D., WHORF, T.P., WAHLEN, M., VAN DER PLICHT, J., 1995, Interannual extremes in the rate of rise of atmospheric carbon dioxide since 1980, Nature, 375, 666-670

[4] FRANCEY, R.J., TANS, P.P., ALLISON, C.E., ENTING, I.G., WHITE, J.W.C., TROLIER, M., 1995, Changes in oceanic and terrestrial carbon uptake since 1982, Nature, 373, 326-330

[5] FRANCEY, R.J., TANS, P.P., 1987, Latitudinal variation in oxygen-18 of atmospheric CO_2, Nature, 327, 495-497

[6] CIAIS, P., TANS, P.P., DENNING, A.S., FRANCEY, R.J., TROLIER, M., MEIJER, H.A.J., WHITE, J.W.C., BERRY, J.A., RANDALL, D.A., COLLATZ, G.J., SELLERS, P.J., MONFRAY, P., HEIMANN, M., 1997b, A three-dimension synthesis study of $d^{18}O$ in atmospheric CO_2. II Simulations with the TM2 transport model. J. Geoph. Res. D 102, 5873-5883

[7] CIAIS, P., MEIJER, H.A.J., 1998. The $^{18}O/^{16}O$ isotope ratio of atmospheric CO_2 and its role in global carbon cycle research. In: Stable Isotopes, Integration of Biological ecological and geochemical processes, H. Griffiths (ed.),Bios Scientific Publishers ltd. Oxford,409-431

[8] LEVIN, I., BÖSINGER, R., BONANI, G., FRANCEY, R.J., KROMER, B., MÜNNICH, K.O., SUTER, M., TRIVETT, N.B.A., WÖLFLI, W., 1992, Radiocarbon in atmospheric carbon dioxide and methane: global distribution and trends, in: Radiocarbon After Four Decades, An Interdisciplinary Perspective, Springer (Heidelberg), 503-518

[9] MEIJER, H.A.J., VAN DER PLICHT, J., GISLEFOSS, J.S., NYDAL, R., 1995, Comparing long-term atmospheric ^{14}C and ^{3}H records near Groningen, the Netherlands with Fruholmen, Norway and Izana, Canary Islands ^{14}C stations, Radiocarbon, 37, 39-50

[10] ROTTY, R.M., 1987, Estimates of seasonal variation in fossil fuel CO_2 emissions, Tellus, 39B, 184-202

[11] BODEN, T., MARLAND, G., ANDRES, R.J.,1995, Estimates of Global, Regional, and National Annual CO_2 Emissions from Fossil-Fuel Burning, Hydraulic Cement Production, and Gas Flaring: 1950-1992, ORNL/CDIAC Report 90, Oak Ridge National Laboratory, Oak Ridge, USA

[12] ANDRES, R.J., MARLAND, G., BODEN, T., BISCHOF, S., 1996, Carbon Dioxide Emissions from Fossil Fuel Consumption and Cement Manufacture, 1751-1991; and an Estimate of Their Isotopic Composition and Latitutinal Distribution, in: The Carbon Cycle, Cambridge University Press, 53-62

[13] BATTLE, M., BENDER, M., SOWERS, T., TANS, P.P., BUTLER, J.H., ELKINS, J.W., ELLIS, J.T., CONWAY, T., ZHANG, N., LANG, P., CLARKE, A.D., 1996, Atmospheric gas concentrations over the past century measured in air from firn at the South Pole, Nature 383, 231-235

[14] CIAIS, P., TANS, P.P., WHITE, J.W.C., TROLIER, M., FRANCEY, R.F., BERRY, J.A., RANDALL, D.R., SELLERS, P.J., COLLATZ, J.G., SCHIMEL, D.S., 1995a, Partitioning of ocean and land uptake of CO_2 as inferred by delta-13C measurements from the NOAA climate monitoring and diagnostics laboratory global air sampling network, Journal of Geophysical Research, 100, 5051-5070

[15] CIAIS, P., TANS, P.P., TROLIER, M., WHITE, J.W.C., FRANCEY, R.J., 1995b, A large Northern hemisphere terrestrial CO_2 sink indicated by the $^{13}C/^{12}C$ ratio of atmospheric CO_2, Science, 269, 1098-1102

[16] HESSHAIMER, V., HEIMANN, M., LEVIN, I., 1994, Radiocarbon evidence for a smaller oceanic carbon dioxide sink than previously believed, Nature, 370, 201-203

[17] KEELING, R.F., 1988, Measuring correlations between atmospheric oxygen and carbon dioxide mole fractions: a preliminary study in urban air, Journal of Atmospheric Chemistry, 7, 153-176

[18] KEELING, R.F., NAJJAR, R.G., BENDER, M.L., TANS, P.P., 1993, What atmospheric oxygen measurements can tell us about the global carbon cycle, Global Biogeochemical Cycles, 7, 37-67

[19] KEELING, R.F., PIPER, S.C., HEIMANN, M., 1996, Global and hemispheric CO2 sinks deduced from changes in atmospheric O_2 concentration, Nature, 381, 218-221

[20] BENDER, M.L. TANS, P.P. ELLIS, J.T. ORCHARDO, J. HABFAST, K., 1994, A high-precision isotope ratio mass spectrometry method for measuring the O_2/N_2 ratio of air, Geochimica et Cosmochimica Acta **58**, 4751-4758

[21] KEELING, R.F., 1995. The atmospheric oxygen cycle: the oxygen isotopes of atmospheric CO_2 and O_2 and the O_2/N_2 ratio, Reviews of Geophysics, 1253-1262

[22] MEIJER, H.A.J., NEUBERT, R., 1998. The atmospheric CO_2 monitoring activities in the Netherlands, In: Report of the 9th WMO meeting of experts on carbon dioxide concentration and related tracer measurement techniques. (Endorsed by the IAEA), R. Francey, ed. (Aspendale, Australia) WMO-TD No. 952.

[23] ZONDERVAN, A., MEIJER, H.A.J., 1996. Isotopic composition of CO_2 sources during regional pollution events using isotopic and radiocarbon analysis. Tellus **48B**, 601-612.

[24] MEIJER, H.A.J.,SMID,H.M., PEREZ, E., KEIZER, M.G., 1996. Isotopic characterisation of anthropogenic CO_2 emissions using isotopic and radiocarbon analysis., Phys. Chem. of the Earth **21**, 483-487.

THE DETERMINATION OF $\delta^{13}C$ IN ATMOSPHERIC METHANE IN THE SOUTHERN HEMISPHERE

D.C. LOWE, M.R. MANNING
National Institute of Water and Atmospheric Research (NIWA),
Wellington, New Zealand

Abstract. A technique to make measurements of $\delta^{13}C$ in atmospheric methane ($\delta^{13}CH_4$) to a precision of 0.02‰ (1 sigma) is presented. Measurements of the mixing ratio and $\delta^{13}CH_4$ from Baring Head, New Zealand and Scott Base, Antarctica are reviewed for the period 1989 to 1998. The data show persistent but irregular seasonal cycles in $\delta^{13}CH_4$ ranging from 0.1 - 0.3‰ superimposed on an increasing secular trend of about 0.04‰.year^{-1}. In 1990/91 a 0.2‰ positive anomaly appeared in this trend. The causes of the anomaly remain unresolved but, during 1992 when it disappeared, the decrease in $\delta^{13}C$ was approximately coincident with a decrease in growth rate consistent with a decrease in biomass burning sources, which are relatively enriched in $^{13}CH_4$. $\delta^{13}CH_4$ data are also reported from large clean air samples collected every 2.5° to 5° of latitude on four voyages across the Pacific between New Zealand and the West Coast of the USA in 1996 and 1997. These data show that the inter-hemispheric gradient for $\delta^{13}CH_4$ was highly dependent on season, and varied from less than 0.1‰ in June 1996 to more than 0.5‰ in November 1996 with an estimated annual mean of 0.2–0.3‰.

1. INTRODUCTION

Atmospheric methane mixing ratios have increased rapidly over the last 200 years due to an excess of sources over sinks [1, 2]. Methane is released to the atmosphere by many kinds of anaerobic sources e.g. ruminant animals, rice paddies and wetlands, leakage and venting of natural gas and biomass burning, especially in the tropics [3, 4]. The major sink for atmospheric methane is oxidation by hydroxyl, OH, radicals and the current loss rate by this process, which depends strongly on OH mixing rates and the reaction rate constant with methane, is estimated at 400–600 Tg year^{-1} [4]. Soils are believed to be a minor sink for atmospheric methane and may account for a further 5–58 Tg year^{-1} [5].

Extensive mixing ratio measurements made over several years at a number of sites in the northern and southern hemispheres have been used to develop a consistent picture of the global methane budget using atmospheric chemistry and transport models [4, 6, 7]. In addition measurements of variations in the isotopic composition of atmospheric methane have provided additional constraints on the budget because several of the sources can be distinguished by characteristic ^{14}C, ^{13}C and ^{2}H signatures [8–12]. For example, methane produced by methanogenesis under anaerobic conditions is depleted in ^{13}C [13] whereas methane released from biomass burning is relatively enriched in ^{13}C, retaining values close to that of the parent carbon in the fuel [14, 15]

In this work we provide a brief review of ^{13}C measurements made in atmospheric methane at various sites in the Pacific. These include Baring Head, New Zealand, 41°S, Scott Base, Antarctica, 78°S and measurements made from air samples collected on board of container ships crossing the Pacific between New Zealand and the US west coast (see Figure 1). The data are used to determine the inter-hemispheric gradient of $\delta^{13}C$ in atmospheric methane and its seasonal variations and to provide a better understanding of methane transport into the extra-tropical Southern Hemisphere. In addition a primary purpose of this work is to provide a comprehensive description of the techniques used to make the measurements.

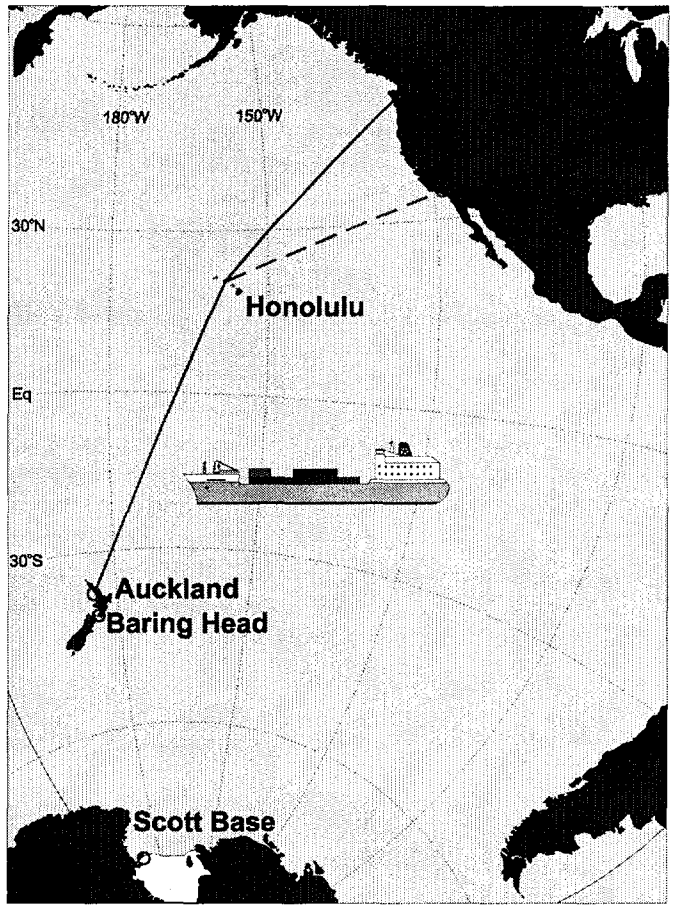

Figure 1: Location of the ground sites and typical container ship voyage tracks used to collect large clean air samples for $\delta^{13}CH_4$ analysis.

2. EXPERIMENTAL

The $^{13}CH_4$ measurements are made using dry whole air samples collected at Baring Head, Scott Base and aboard Blue Star Line (now part of P&O Nedlloyd) container ships, the "Melbourne Star" and the "Argentina Star" which make frequent voyages between New Zealand and the West Coast of the United States. A typical voyage track, ("Melbourne Star" in June 1996) is shown in Figure 1 as well as the positions of the Baring Head and Scott Base sites. Sampling techniques at the two sites and on the ships have been described by *Lowe et al.* [16, 17]

Mixing ratio determinations of the methane in the air samples are made using gas chromatography with flame ionisation detection and all results are reported as ppb (nmole.mole^{-1}), in dry air. The primary standard reference materials are prepared by the US National Institute of Standards and Technology (NIST) and laboratory working standards are calibrated against these. Full details of the gas chromatography used have been reported by *Lowe et al.* [17]

To determine $^{13}C/^{12}C$ ratios in methane from the large air samples, we use a gas source isotope ratio mass spectrometer (IRMS). However, the methane must first be quantitatively extracted from the air samples and converted to CO_2. This is done on a vacuum conversion line using a modification of a "flow through" procedure developed by *Lowe et al.* [18] and inspired by the early work of *Stevens and Krout* [19]. Briefly the air sample is stripped of remaining water, CO_2, N_2O, and NMHC by passage at 1 liter.min^{-1} (controlled by an

integrating mass flow controller) through a series of cryogenic traps held at liquid nitrogen temperature. In addition CO is removed from the stream by passage through a 350 g bed of Schütze reagent where the active reagent is iodine pentoxide on a silica gel support. Subsequently, methane in the air sample is combusted at 790°C in a furnace containing 100 g of 1% platinum catalyst supported on 3 mm alumina pellets. The resulting CO_2, which retains the $^{13}C/^{12}C$ and $^{14}C/^{12}C$ ratios from the methane in the air samples, and water from the combustion are collected in cryogenic traps immediately after the furnace. The water is removed at –80°C in alcohol dry ice traps by triple vacuum distilling the CO_2 from the cryogenic traps into small pyrex bottles or flame sealed pyrex tubes. This CO_2 is analyzed for ^{13}C by IRMS and the same gas may be used for ^{14}C determinations by conversion into graphite targets for accelerator mass spectrometry [18].

$^{13}C/^{12}C$ ratio measurements of the CO_2 derived from the methane are made at NIWA using a Finnigan MAT (Bremen, Germany) 252 IRMS running in dual inlet mode. The sample inlet side of the IRMS has been modified by inserting a 500 µl cold finger stainless steel volume at the head of the sample capillary with the inlet isolated by a pneumatically actuated gold seated dual valve (Finnigan MAT, Bremen). This allows the direct introduction of 10–80 µl CO_2 samples from volumes of either 0.5 or 2.5 ml into the IRMS ion source. With this inlet system m/z = 44 signals are typically 4 volts (collector resistance 3×10^8 Ω) for the atmospheric methane samples and the internal precision of individual $\delta^{13}C$ determinations (10 changeovers between sample and working reference) is typically 0.01‰.

We use the standard notation:

$$\delta^{13}C = (R_s/R_r - 1) \times 1000 \text{ [in ‰]}$$

to calculate $^{13}C/^{12}C$ ratios as parts per mille (‰), where R_s and R_r are the $^{13}C/^{12}C$ ratios of the unknown sample and a working reference gas respectively. The working reference is dry CO_2 stored in a 25 liter glass flask at 1.1 bar and is metered as required via 3 mm OD stainless steel lines and Nupro high vacuum valves into the variable volume bellows on the reference side of the MAT 252. The reference CO_2 was made from combusted, purified, land fill methane and mixed with CO_2 derived from marine carbonates to produce a $\delta^{13}C \approx -47‰$, which is in the middle of the range expected for atmospheric methane samples. Two working references denoted CH4WR1 and CH4WR2 were prepared in this fashion. These isotopically "light" CO_2 working reference gases are compared with CO_2 evolved every 6–12 months from NBS-19 carbonate supplied by the International Atomic Energy Agency (IAEA), Vienna, Austria [20]. This provides the link to the V-PDB scale widely used in the literature and all measurements reported here are as ‰ deviations from V-PDB. CH4WR1 and CH4WR2 were first determined at $\delta^{13}C = -47.07 \pm 0.01‰$ and $-47.02 \pm 0.01‰$ V-PDB respectively versus NBS-19 in January 1995 and repeated comparisons since then show that any drift in these values is less than 0.005‰ in more than 4 years. As a control, the two light working reference gases are compared against each other on the MAT 252 IRMS at the start of each day that $\delta^{13}C$ in methane analyses are made. In this work, we will refer to the $\delta^{13}C$ of the carbon in methane as "$\delta^{13}CH_4$", noting that this is for ease of nomenclature only.

An additional assurance of calibration is provided by a light barium carbonate reference material supplied by the IAEA in Vienna, IAEA-CO-9, also known as NZCH [18, 20]. The published stable isotope values for this material are $\delta^{13}C = -47.119 \pm 0.149‰$ and $\delta^{18}O = -15.282 \pm 0.093‰$. CO_2 from this material is evolved and compared with NBS19 and the working references, CH4WR1 and CH4WR2, as described above. Quality assurance is also provided by the routine measurement of $\delta^{13}CH_4$ in methane mixtures in synthetic air and ambient methane in dry air samples collected at Baring Head, New Zealand and stored or "archived" in stainless steel tanks as described by *Lowe et al.* [16]. These controls provide

confidence in the sample preparation and analysis techniques and the $\delta^{13}CH_4$ data reported here and a series of tests are shown in the regression line in figure 2. The overall precision of the technique, 1 sigma, as determined by $\delta^{13}CH_4$ analyses of sets of duplicate air samples collected at Baring Head, is 0.02‰. Inter-calibration has also routinely been carried out with other laboratories making $\delta^{13}CH_4$ measurements in air. For example, a set of 15 air samples exchanged between Paul Quay, University of Washington, Seattle and NIWA and analysed for $\delta^{13}CH_4$ by both labs showed a mean difference of 0.01±0.05‰ [16]. A similar inter-calibration exercise is currently in progress with the Geosciences Department, University of California, Irvine and a set of 16 samples exchanged between the two labs from early 1995 to mid 1998 shows a mean analysis difference for $\delta^{13}CH_4$ of 0.01±0.06‰.

3. RESULTS AND DISCUSSION

Time series for CH_4 mixing ratio and $\delta^{13}CH_4$ are shown in Figure 2 for Baring Head and Scott Base. Both series show considerable secular and seasonal variability. The seasonal variations in mixing ratio are attributed to variations in the strength of the OH sink. OH is a maximum in summer when its production by UV photolysis of water and ozone is greatest and methane mixing ratios at both Baring Head and Scott Base both show corresponding minima in February March. The secular growth rate caused by the imbalance of sources and sinks is quite variable from 1989 to 1998 with a maximum growth rate of 16 ppb/year observed in 1991 and a minimum of close to zero in 1993. $\delta^{13}CH_4$ data at both sites also shows a variable seasonal cycle with an amplitude of 0.1–0.3‰ superimposed on a rather variable increasing secular trend of about 0.04‰ $\cdot year^{-1}$. This cycle is approximately six months out of phase with the corresponding methane mixing ratio cycle. In 1990/91 a large positive anomaly of about 0.2‰ was observed in $\delta^{13}CH_4$ at both Baring Head and Scott Base. The causes of the anomaly remain unresolved but, during 1992 when it disappeared, the decrease in $\delta^{13}C$ was approximately coincident with a decrease in growth rate. This is consistent with a decrease in biomass burning sources which are relatively enriched in $^{13}CH_4$ [21].

Methane mixing ratio measurements for air samples collected on four container ship voyages are plotted as a function of sine of latitude in Figure 3. The voyages took place in June and November 1996 ("Melbourne Star") and February and September 1997 ("Argentina Star"). Time coincident data from Suva, Fiji, 17°S, Baring Head, New Zealand, 41°S, Scott Base, Antarctica, 78°S, and data from a C130 flight in the troposphere between Christchurch, New Zealand, 43°S, and McMurdo Sound, Antarctica, 78°S in February 1997 are also plotted in Figure 3. All data sets show relatively uniform mixing ratios between 78°S and about 30°S indicative of a well mixed extra-tropical southern hemisphere. However, north of 15°S, a typical position for the South Pacific Convergence Zone (SPCZ) at 170°W [22] (see Figure 1), mixing ratio data from the voyages showed quite different trends.

For example, the voyages in November 1996 and February 1997 showed a steady increase from about 1710 to 1740 ppb between 10°S and 10°N, the position of the Inter Tropical Convergence Zone (ITCZ). Here there was an abrupt transition to much higher and more variable values ranging from 1740 to 1840 ppb indicative of the extra-tropical northern hemisphere. Higher methane mixing ratios are expected north of the ITCZ because most methane sources are in the Northern Hemisphere. For the June 1996 voyage, however, a local minimum of 1710 ppb occurred at the position of the SPCZ, 10°S, followed by a rapid rise to 1740 ppb by 5°S.Thereafter the mixing ratio was fairly uniform up to the ITCZ located at about 10°N. Thus on the voyage route in June 1996, a well defined SPCZ and ITCZ led to a confined region of well mixed air in the equatorial Pacific showing methane mixing ratios midway between the extra tropical southern and northern hemispheres.

The $\delta^{13}CH_4$ data for the four container ship voyages are also shown in Figure 3 with equivalent data from the other sites and the aircraft flight described above. In the June 1996 voyage from Auckland to Seattle, we measured a relatively uniform decrease in $\delta^{13}C$ from –47.15‰ at 35°S to a minimum value of –47.35‰ at the equator. However, there was a sharp increase in $\delta^{13}CH_4$ to –47.15‰ at 10°S, which anti-correlated with a minimum in methane concentration and coincided with the position of the SPCZ. In the Northern Hemisphere, $\delta^{13}CH_4$ decreased gradually to about –47.30‰ at 20°N. No abrupt change was observed at the ITCZ, located at about 10°N, and the observed average gradient in $\delta^{13}CH_4$ between the hemispheres was relatively small, less than 0.1‰. In November 1996, however, a large gradient between the hemispheres was measured in $\delta^{13}CH_4$ with relatively small variations ranging from about –47.00 to –47.10‰ up to about 5°N followed by a rapid drop to about –47.50‰ at about 30°N. In February 1997 $\delta^{13}CH_4$ showed a virtually monotonic decrease from about –47.05‰ at 78°S to –47.35‰ at 30°N with most values falling midway between the June and November 1996 data. The September 1997 voyage, however, featured a broad but pronounced maximum in $\delta^{13}CH_4$ at about 10°S with minimum values in the mid-latitudes of both hemispheres.

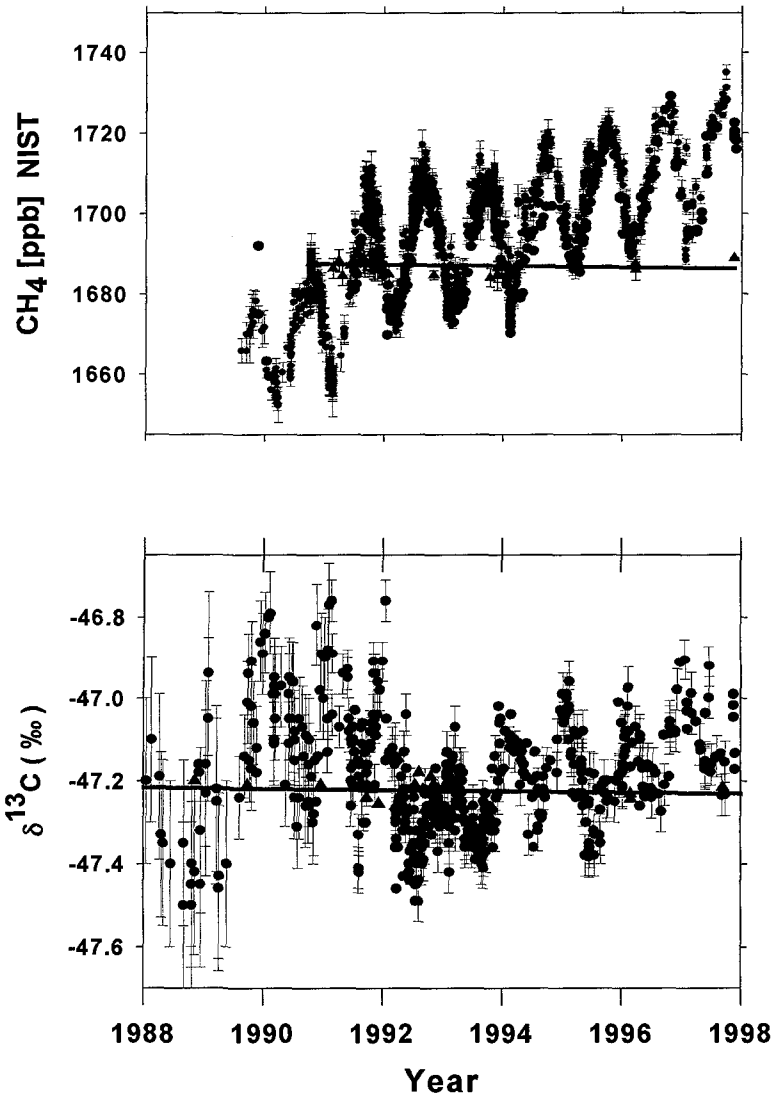

Figure 2: Atmospheric mixing ratio and ^{13}C data from Baring Head and Scott Base are shown as the solid circles with vertical error bars (1 sigma). The horizontal solid lines are regression lines fitted through the quality control "archive" tanks (triangles) referred to in the text.

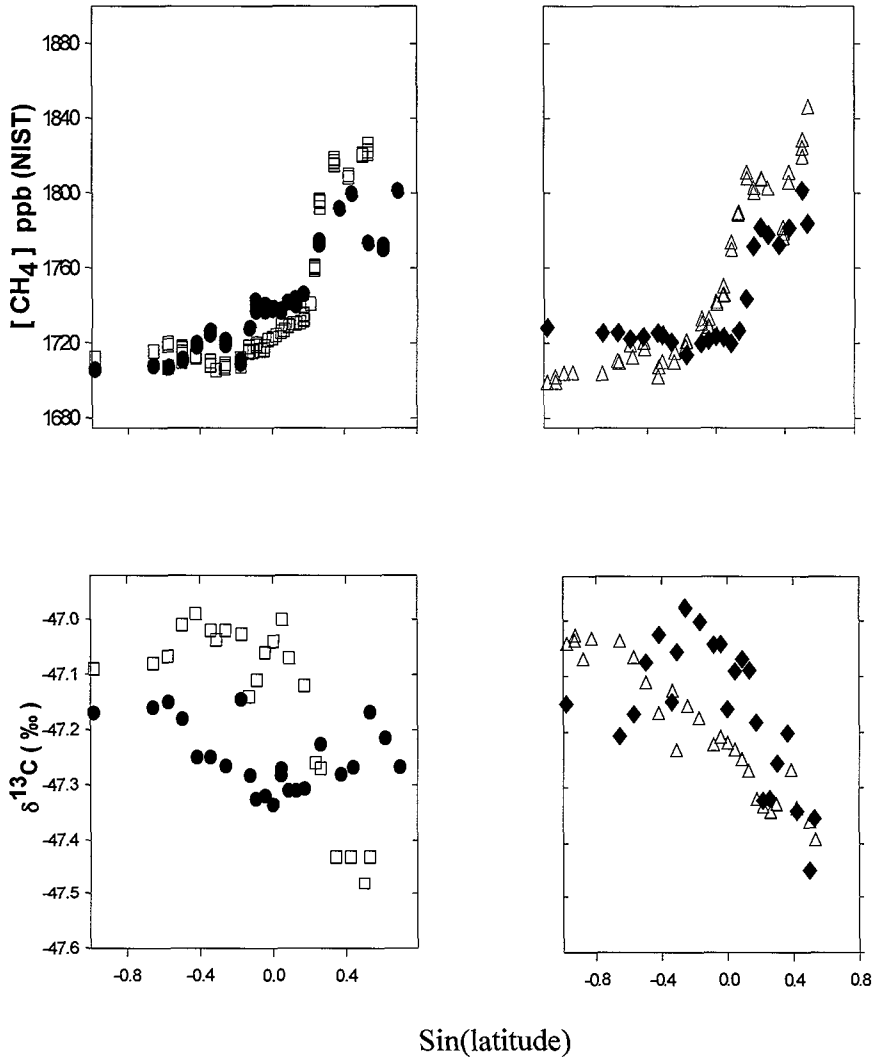

Figure 3: Adapted from [21] Methane mixing ratio and $\delta^{13}CH_4$ data from clean air samples collected on four Pacific voyages. The left hand panels show data from June 1996 (filled circles) and November 1996 (open squares) and the right hand panels show data from February 1997 (open triangles) and September 1997 (filled diamonds). For clarity data from Scott Base and Baring Head are not marked differently, but they can be located on the plot by their latitude.

The $\delta^{13}CH_4$ data shown in Figure 3 clearly exhibit marked seasonal behaviour with cycles quite unlike those observed for the concurrent methane mixing ratio data or similar shipboard atmospheric methane mixing ratio data reported for the Pacific by *Dlugokencky et al.* [6]. Examination of the data shows that the maximum of a cycle at 33°N in June 1996 is about –47.25‰ which is similar in magnitude to the seasonal minimum observed at Baring Head and Scott Base. Since the tropical data show a minimum of about –47.30‰ at this time, no pronounced inter-hemispheric gradient in $\delta^{13}CH_4$ data on the voyage in June 1996 was observed. For the November 1996 voyage, however, the situation was quite different with the minimum of seasonal cycles in the northern Pacific coinciding with maximum values in the Southern Hemisphere. This, coupled with the fact that, on average, $\delta^{13}CH_4$ is lower in the Northern than the Southern Hemisphere, led to a relatively large inter-hemispheric gradient of 0.5‰. Interpolation of data from all four voyages suggests that the annual average inter-hemispheric gradient in $\delta^{13}CH_4$ in the Pacific is about 0.2–0.3‰.

The principal removal mechanism for methane from the atmosphere is believed to be chemical destruction by the OH radical and hence, because $^{12}CH_4$ reacts faster with OH than $^{13}CH_4$, methane remaining in the atmosphere becomes enriched in ^{13}C relative to the global source. This process has been investigated under laboratory conditions and a kinetic isotope effect (KIE) defined as the ratio of the rate constants of the reaction of OH with $^{12}CH_4$ and with $^{13}CH_4$ has been measured at 1.0054, or 5.4‰, by *Cantrell et al.* [23] and recently by *Saueressig et al.* [24] at 3.9‰ at 296K. Consequently as methane "ages" after emission to the atmosphere, it becomes progressively enriched in ^{13}C as it is oxidised by OH. Hence an inter-hemispheric exchange time of about 1 year, 1/10 of the atmospheric methane lifetime, implies that methane reaching the southern hemisphere from the northern hemisphere will be enriched in ^{13}C by about 0.5‰. When contributions by southern hemisphere sources of methane are taken into account, this enrichment is consistent with the average inter-hemispheric gradient, 0.2–0.3‰, deduced from the data in shown in Figure 3.

Large-scale biomass burning occurs in the tropics and subtropics, particularly the southern tropics during the dry period of August to October [15, 25, 26]. These regions contain tropical rain forests comprising C3 plants with $\delta^{13}C$ about –28‰, and Savannah regions with C4 plants, $\delta^{13}C$ about –13‰ [14]. Methane produced during biomass burning is known to have a $\delta^{13}C$ value near that of the carbon in the parent material [13] and is therefore considerably more enriched in ^{13}C than atmospheric methane. The $\delta^{13}CH_4$ data from the voyage of September 1997 show a large broad peak in the southern tropics with a maximum at about 12°S consistent with the release of methane enriched in ^{13}C from biomass burning in the dry season in the Southern Hemisphere. These data were coincident with large fires and wide spread areas of smoke reported from Kalimantan to Sumatra caused by an intense El Nino induced drought in the latter part of 1997 [27] and similar to the situation caused in the El Nino southern oscillation event of 1991 [28].

4. CONCLUSIONS

Measurements of methane $\delta^{13}C$ and mixing ratio at Baring Head, New Zealand, and Scott Base, Antarctica, from 1989 to 1998 show both seasonal and secular variability. The secular growth rate caused by the imbalance of methane sources and sinks is quite variable with a maximum growth rate of 16 ppb.year^{-1} observed in 1991 and a minimum of close to zero in 1993. $\delta^{13}CH_4$ data at both sites show a variable seasonal cycle with an amplitude of 0.1–0.3‰ superimposed on a rather variable increasing secular trend of about 0.04‰.year^{-1}. This cycle is approximately six months out of phase with the corresponding methane mixing ratio cycle. In 1990/91 a large positive anomaly of about 0.2‰ was observed in $\delta^{13}CH_4$ at both Baring Head and Scott Base. The causes of the anomaly remain unresolved but, during 1992 when it disappeared, the decrease in $\delta^{13}C$ was approximately coincident with a decrease in growth rate consistent with a decrease in biomass burning sources that are relatively enriched in $^{13}CH_4$.

The shipboard data reported here show that the methane distribution in the Southern Hemisphere appears to be largely determined by inter-hemispheric transport with about a 5% difference in mixing ratio between the hemispheres and an abrupt gradient at the ITCZ. Significant variations in mixing ratio distributions between the ITCZ and the SPCZ were observed on the 4 voyages reported here and related to the intensity and position of the SPCZ. In June 1996, a well defined SPCZ and ITCZ led to a confined region of well mixed air around the equator showing methane mixing ratios midway between the extra tropical southern and northern hemispheres. However a relatively weak SPCZ in September 1997 led

to uniform mixing ratios extending throughout the extra tropical southern hemisphere and SPCZ to the ITCZ region. Complex tropical meteorology which results in changes in the intensity and position of the convergence zones clearly plays a major role in the distribution of atmospheric methane in tropical regions and its transport to the extra-tropical southern hemisphere.

The inter-hemispheric gradient for $\delta^{13}CH_4$ is highly dependent on season, varying from a minimum of less than 0.1‰ in June 1996 to a maximum of more than 0.5‰ in November 1996. Lower values for $\delta^{13}CH_4$ were observed in the Northern Hemisphere north of the ITCZ. Interpolation of the data suggests that the average inter-hemispheric gradient in $\delta^{13}CH_4$ in the Pacific is 0.2–0.3‰.

The small gradients between the ITCZ and 35°S as well as the broad peak observed in $\delta^{13}CH_4$ in the southern tropics in September 1997 suggest that the seasonal cycles observed in the extra tropical southern hemisphere are influenced by the southward transport of ^{13}C enriched methane from tropical biomass burning.

The cycles in the extra tropical southern hemisphere can be used to estimate a value for the apparent KIE of methane oxidation of 12–15‰ which is much larger than current laboratory measurements of the KIE of $CH_4 + OH$.

The data reported here demonstrate the value of simultaneous high precision measurements of $\delta^{13}CH_4$ and methane mixing ratios as tools to probe latitudinal and seasonal structures in the Pacific region. However, far more high precision $\delta^{13}CH_4$ data are needed to increase the scope of the method and to constrain 3-D chemical tracer models used to predict the global distribution of atmospheric methane.

REFERENCES

[1] ETHERIDGE, D.M., G.I. PEARMAN, P.J. FRASER, Changes in tropospheric methane between 1841 and 1978 from a high accumulation-rate Antarctic ice core. Tellus, 1992. **44B**: p. 282–294.

[2] ETHERIDGE, D.M., L.P. STEELE, R.J. FRANCEY, R.L. LANGENFELDS, Atmospheric methane between 1000 A.D. and present: Evidence of anthropogenic emissions and climatic variability. Journal of Geophysical Research, 1998. **103**(D13): p. 15,979-15,993.

[3] CICERONE, R.J., R.S. OREMLAND, Biogeochemical aspects of atmospheric methane. Global Biogeochemal. Cycles, 1988. **2**: p. 299–327.

[4] FUNG, I., J. JOHN, J. LERNER, E. MATTHEWS, M. PRATHER, L.P. STEELE, P.J. FRASER, Three-dimensional model synthesis of the global methane cycle. Journal of Geophysical Research, 1991. **96**(D7): p. 13,033–13,065.

[5] BORN, M., H. DÖRR, I. LEVIN, Methane consumption in aerated soils of the temperate zone. Tellus, 1990. **42B**: p. 2–8.

[6] DLUGOKENCKY, E.J., L.P. STEELE, P.M. LANG, K.A. MASARIE, The growth rate and distribution of atmospheric methane. Journal of Geophysical Research, 1994. **99**(D8): p. 17,021–17,043.

[7] HEIN, R., P.J. CRUTZEN, M. HEIMANN, An inverse modeling approach to investigate the global atmospheric methane cycle. Global Biogeochemical Cycles, 1997. **11**(1): p. 43–76.

[8] LOWE, D.C., C.A.M. BRENNINKMEIJER, M.R. MANNING, R.J. SPARKS, G.W. WALLACE, Radiocarbon determination of atmospheric methane at Baring Head, New Zealand. Nature, 1988. **372**: p. 522–525.

[9] WAHLEN, M., N. TANAKA, R. HENRY, B. DECK, J. ZEGLEN, J.S. VOGEL, J. SOUTHON, A. SHEMESH, A. FAIRBANKS, W. BROECKER, Carbon-14 in methane sources and in atmospheric methane: The contribution from fossil carbon. Science, 1989. **245**: p. 286–290.

[10] TYLER, S.C., Kinetic isotope effects and their use in studying atmospheric trace species: Case study CH_4 + OH. American Chemical Society Symposium Series, 1992. **502**: p. 390–408.

[11] CONNY, J.M., L.A. CURRIE, The isotopic characterization of methane, non-methane hydrocarbons and formaldehyde in the troposphere. Atmospheric Environment, 1996. **30**(4): p. 621–638.

[12] BERGAMASCHI, P., C.A.M. BRENNINKMEIJER, P.J. CRUTZEN, N.F. ELANSKY, I.B. BELIKOV, N.B.A. TRIVETT, D.E.J. WORTHY, Isotopic analysis based source identification for atmospheric CH_4 and CO sampled across Russia using the Trans-Siberian railroad. Journal of Geophysical Research, 1998. **103**(D7): p. 8227–8235.

[13] STEVENS, C.M., A. ENGELKEMEIR, Stable carbon isotopic composition of methane from some natural and anthropogenic sources. Journal of Geophysical Research, 1988. **93**(D1): p. 725–733.

[14] BENDER, M.M., Variations in the $^{13}C/^{12}C$ ratios of plants in relation to the pathway of photosynthetic carbon dioxide fixation. Phytochemistry, 1971. **10**: p. 1239–1244.

[15] HAO, W.M., D.E. WARD, Methane production from global biomass burning. Journal of Geophysical Research, 1993. **98**: p. 20,657–20,661.

[16] LOWE, D.C., C.A.M. BRENNINKMEIJER, G.W. BRAILSFORD, K.R. LASSEY, A.J. GOMEZ, E.G. NISBET, Concentration and ^{13}C records of atmospheric methane in New Zealand and Antarctica: Evidence for changes in methane sources. Journal of Geophysical Research, 1994. **99**(D8): p. 16,913–16,925.

[17] LOWE, D.C., W. ALLAN, M.R. MANNING, A.M. BROMLEY, G.W. BRAILSFORD, D.F. FERRETTI, A. GOMEZ, R.K. KNOBBEN, R.M. MARTIN, M. ZHU, R. MOSS, K. KOSHY, M. MAARTA, Shipboard determinations of the distribution of ^{13}C in atmospheric methane in the Pacific. Journal of Geophysical Research, 1999. 104 (D21), 26,125–26,135, 1999.

[18] LOWE, D.C., C.A.M. BRENNINKMEIJER, S.C. TYLER, E.J. DLUGOKENCKY, Determination of the isotopic composition of atmospheric methane and its application in the Antarctic. Journal of Geophysical Research, 1991. **96**(D8): p. 15,455–15,467.

[19] STEVENS, C.S., L. KROUT, Method for the determination of the concentration and the carbon and oxygen isotopic composition of atmospheric carbon monoxide. International Journal of Mass Spectrometry and Ion Physics, 1972. **8**: p. 265–275.

[20] GONFIANTINI, R., W. STICHLER, K. ROZANSKI. Standards and intercomparison materials distributed by the International Atomic Energy Agency for stable isotope measurements. In: Reference and intercomparison materials for stable isotopes of light elements. IAEA, Vienna, 1995. TECDOC-825, p. 13–29.

[21] LOWE, D.C., M.R. MANNING, G.W. BRAILSFORD, A.M. BROMLEY, The 1991–1992 atmospheric methane anomaly: Southern hemisphere ^{13}C decrease and growth rate fluctuations. Geophysical Research Letters, 1997. **24**(8): p. 857–860.

[22] TRENBERTH, K.E., General characteristics of El Nino-southern oscillation, in Teleconnections Linking Worldwide Climate Anomalies, M. Glantz, R.W. Katz, and N. Nicholls, Editors. 1991, Cambridge University Press. p. 13–41.

[23] CANTRELL, C.A., R.E. SHETTER, A.H. MCDANIEL, J.G. CALVERT, J.A. DAVIDSON, D.C. LOWE, S.C. TYLER, R.J. CICERONE, J.P. GREENBERG, Carbon kinetic isotope effect in the oxidation of methane by the hydroxyl radical. Journal of Geophysical Research, 1990. **95**(D13): p. 22,455–22,462.

[24] SAUERESSIG, G., P. BERGAMASCHI, J.N. CROWLEY, C. BRUHL, H. FISCHER, Carbon and hydrogen kinetic isotope effects (KIE) of methane in its atmospheric chemical sink processes: New results for the reaction $CH_4 + OH$ (abstract). EGS Annales Geophysicae, 1999.

[25] FISHMAN, J., K. FAKHRUZZAMAN, B. CROS, D. NGANGA, Identification of widespread pollution in the southern hemisphere deduced from satellite analysis. Science, 1991. **252**: p. 1693–1696.

[26] HAO, W.M., M.H. LIU, Spatial and temporal distribution of tropical biomass burning. Global Biogeochemical Cycles, 1994. **8**(4): p. 495–503.

[27] SWINBANKS, D., Forest fires cause pollution crisis in Asia. Nature, 1997. **389**(6649): p. 321.

[28] SALAFSKY, N., Drought in the rain forest: Effects of the 1991 El Nino-southern oscillation event on a rural economy in West Kalimantan, Indonesia. Climatic Change, 1994. **27**: p. 373–396.

ISOTOPIC DISCRIMINATION DURING NITROUS OXIDE LOSS PROCESSES: AN IMPORTANT PIECE OF THE N_2O GLOBAL ATMOSPHERIC BUDGET

T. RAHN, M. WAHLEN
Scripps Institution of Oceanography, University of California San Diego,
La Jolla, California, United States of America

HUI ZHANG, G. BLAKE
Division of Geological and Planetary Sciences, California Institute of Technology,
Pasadena, California, United States of America

Abstract. Nitrous oxide plays an important role in greenhouse forcing and stratospheric ozone regulation. It is destructed in the stratosphere mainly by UV photolysis. Laboratory studies of N_2O-N_2 mixtures irradiated at 193 and 207 nm reveal a significant enrichment of the residual heavy nitrous oxide isotopomers. The isotopic signatures are well described by an irreversible Rayleigh distillation process, with large enrichment factors of $\varepsilon_{15,18}$ (193 nm) = –18.4, –14.5 per mil and $\varepsilon_{15,18}$(207 nm) = –48.7, –46.0 per mil. These results, when combined with diffusive mixing processes might help to explain the stratospheric enrichments previously observed.

1. INTRODUCTION

There are five species of interest when analyzing N_2O isotopes; the abundant isotopomer $^{14}N^{14}N^{16}O$ and the rare isotopomers $^{14}N^{15}N^{16}O$, $^{15}N^{14}N^{16}O$, $^{14}N^{14}N^{17}O$ and $^{14}N^{14}N^{18}O$. The two ^{15}N species are indistinguishable with current mass spectrometric techniques. The two rare oxygen species have in the past been assumed to be mass-dependently related although it has recently been shown that there is a slight mass-independent enrichment of ^{17}O in tropospheric samples [1] which is as yet unaccounted for. Isotopic values are typically reported as ratios of the heavy-to-light species relative to the those in a standard such that $\delta = [(R_{samp}/R_{std}) - 1] \times 1000$ (expressed in units of per mil).

Because the isotopomers of interest are isobaric with those of CO_2 (masses 44, 45, and 46) and since CO_2 in natural environments is generally ~1000 times more abundant, traditional methods of isotopic analysis employed techniques involving selective decomposition of N_2O and subsequent analysis of products. For this reason, the isotopic standards for N_2O have been atmospheric N_2 for ^{15}N and either atmospheric O_2 or Standard Mean Ocean Water for the oxygen isotopes. (Atmospheric O_2 has become the de facto standard for the oxygen isotopes due to its negligible isotopic variations.) In the case of current analytical techniques (with the exception of ^{17}O analyses), N_2O is now routinely separated from CO_2 and introduced directly into a mass spectrometer. It is then referenced to a nitrous oxide gas standard with known isotopic values relative to N_2 and O_2.

Nitrous oxide is a trace gas that is produced during microbial energy exchange reactions involving both reduced (NH_3) and oxidized (NO_3^-) forms of nitrogen. A portion of the N_2O that is produced escapes to the troposphere where it is chemically inert. The commonly accepted model holds that nitrous oxide ascends to the stratosphere where it is photolyzed by ultraviolet radiation (90% of the total loss), oxidized by excited atomic oxygen (10% of loss), or returned to the troposphere during stratosphere/troposphere exchange processes. The bulk of the N_2O photolysis, as demonstrated in Fig. 1, occurs on the shoulder of the cross section spectrum, between the Schumann-Runge bands and Herzberg continuum of O_2 absorption, rather than at the peak. While in the atmosphere, N_2O actively absorbs infrared radiation and thereby contributes to greenhouse warming. A portion of the N_2O destroyed by the reaction with $O(^1D)$ provides the principle natural source of NO, which

initiates the catalytic NO_x cycling of stratospheric ozone. The current tropospheric concentration of N_2O, which is increasing at a rate of ~0.25% per year, is about 313 ppbv and the estimated atmospheric lifetime is approximately 120 years. Because of its influence on the Earth's radiative budget and its increasing concentration, nitrous oxide has been selected as one of the six gases slated for regulation by the Kyoto Protocol of 1997.

Despite the importance of nitrous oxide and its incorporation in the Kyoto Protocol, its global budget is poorly characterized. Estimates of the natural sources of N_2O range from 1 to 5 Tg N/a for oceanic sources and 3.3 to 9.7 Tg N/a from tropical and temperate soils [2]. The atmospheric increase is considered to arise primarily from application of fertilizers to cultivated soils but animal waste, biomass burning, fuel combustion, and industrial processes also contribute. The estimated range of the sum of the anthropogenic sources is 3.7 to 7.7 Tg N/a [2]. In an effort to reduce the error in these estimates, investigations of the stable isotopic signatures of the various sources and sinks have been carried out by several research groups [see: 3–11].

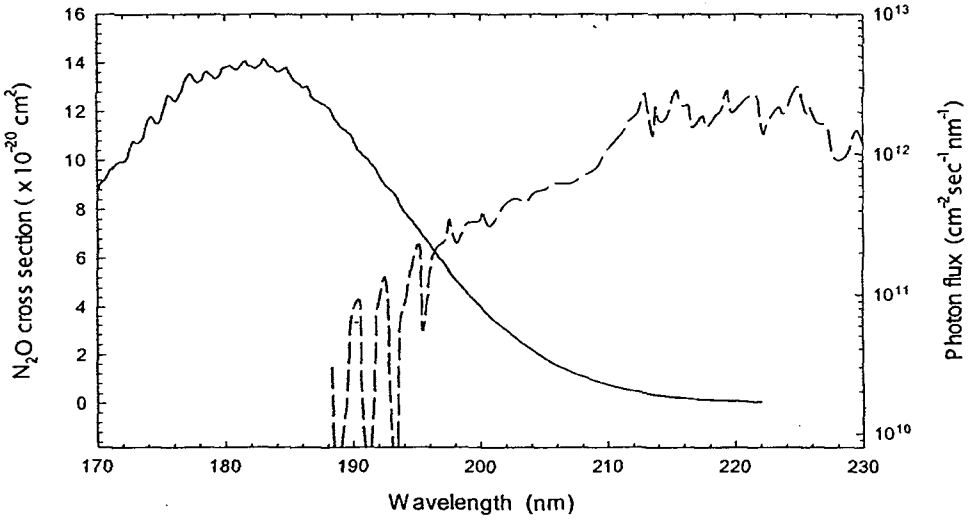

Figure 1. High resolution N_2O cross section (solid) from Yoshino, et al., [25] and the actinic flux (dashed) as measured at 40 km by Herman and Mentall 26] (0.21 nm resolution).

2. ISOTOPIC CONSIDERATIONS

The stable isotopic composition of atmospheric trace gases provides information about their origin and fate that cannot be determined from concentration alone. Biological source and loss processes, such as bacterial production of CH_4 or photosynthetic consumption of CO_2, are typically accompanied by isotopic selectivity associated with the kinetics of bond formation and destruction. Thermodynamic considerations also predict isotopic differentiation between phases and/or reactants under equilibrium conditions. Of the three important biologically mediated greenhouse gases, our understanding of the isotopic budget of nitrous oxide lags far behind that of carbon dioxide and methane. This is due in part to problems inherent in collection and analytical techniques which hamper our ability to make measurements of very high precision. It is also due to the fact that a limited data base and a wide range of observed isotopic values for each of the major natural sources of N_2O has made it difficult to assign unique values to each of the source terms.

The isotopic ratios of tropospheric N_2O are commonly reported as $\delta^{15}N$ = 7.0 ‰ and $\delta^{18}O$ = 20.7‰ [7] although inter-laboratory averages vary by 3 and 4 ‰ for $\delta^{15}N$ and $\delta^{18}O$,

respectively [see: 1,3,4,5,7,12,13]. The measured isotopic ratio of N_2O emitted from terrestrial environments is nearly everywhere depleted relative to the tropospheric average. The averages of known measurements from terrestrial sources, including fertilized lands, are -14.6 ± 11.9 ‰ for $\delta^{15}N$; and 8.2 ± 7.1 ‰ for $\delta^{18}O$ [8,14]. Oceanic surface waters are observed to be typically depleted in both ^{15}N and ^{18}O [7,11,12] although it is proposed that, in certain upwelling areas, isotopically enriched deep waters may be introduced to the surface [9]. The observation that the source terms are depleted relative to the tropospheric reservoir lead Kim and Craig [8] to propose that the enrichments which they observed in the stratosphere might provide the necessary balance. A conundrum resulted when it was shown by Johnston [15] that the fractionations associated with the major N_2O loss terms, photolysis and photooxidation, were not great enough to account for the observed stratospheric values. Rahn and Wahlen [13] subsequently verified that stratospheric N_2O is indeed enriched in the heavy stable isotopes of both N and O (Fig. 2). These stratospheric results have lead to speculation that the anomalous enrichment might provide evidence of novel excited state photochemical sources of nitrous oxide [16,17,18,19]. In particular, Zipf and Prasad [19] suggest that highly vibrationally excited O_3 could react with N_2 to form N_2O and O_2 and that this reaction could account for as much as 8% of the global source of nitrous oxide. Such photochemical sources would significantly alter our understanding of the geochemical cycle of N_2O. The results of Rahn and Wahlen [13], however, are in good agreement with a Rayleigh distillation loss model indicating that no significant source products are interfering with the isotopic signature of the destruction mechanism. Source processes, should they exist, would therefore have to be able to mimic the Rayleigh distillation model or be associated with negligible fractionation or represent a very minor portion of the global budget.

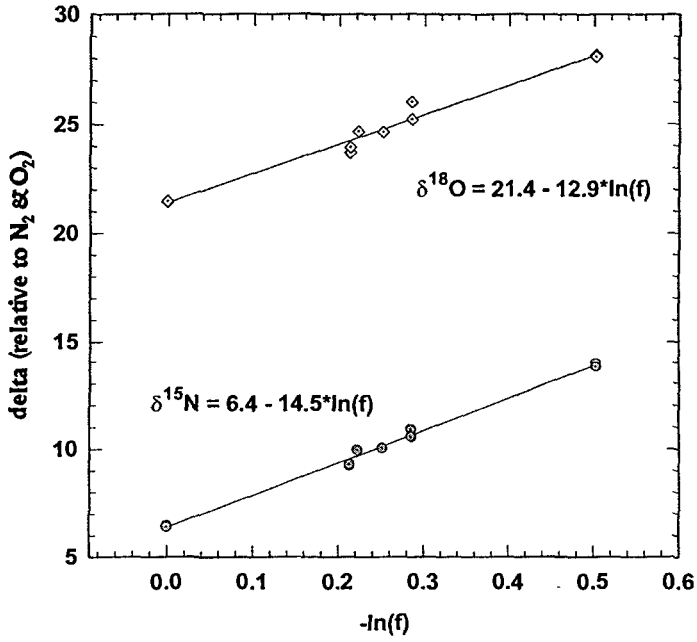

Figure 2. Lower stratosphere (between 14 and 19 km) isotopic enrichments of ^{15}N and ^{18}O. The results compare favorably with a Rayleigh distillation model where $R = R_o f^{(\alpha-1)}$: with R and R_o equal to the residual and initial heavy-to-light isotope ratios; f, the fraction of tropospheric N_2O remaining; and α, the ratio of heavy-to-light destruction rates. Note that the regressions pass through tropospheric values at ln(f) = 0. A single sample from 22.4 km (not shown) shows reasonable agreement for ^{18}O and an increased enrichment for ^{15}N indicating the possibility of competing processes at higher altitudes.

3. PHOTOLYTIC FRACTIONATION

An alternative explanation for the isotopic enrichment of stratospheric N_2O has been provided by Yung and Miller [20]. They have proposed a wavelength-dependent mechanism for the photolytic fractionation of N_2O based on subtle shifts in the zero point energy with isotopic substitution. The wavelength dependence allows for the minimal fractionation observed by Johnston, et al. [15] near the peak of the absorption cross section at 184.9 nm yet predicts increasing fractionation at longer wavelengths where the bulk of the stratospheric N_2O photolysis takes place. This principle is demonstrated graphically in Fig. 3 using the absorption cross section spectral function recommended by Selwyn, et al.[21]. The curve representing the ^{18}O substituted species (dashed curve) is slightly blue shifted, by –27.5 cm^{-1} [20], relative to the normal curve (both calculated at 300 K). Cross sections are nearly equal in the region of the curve crossing at the absorption peak but a clear separation is observed on both shoulders.

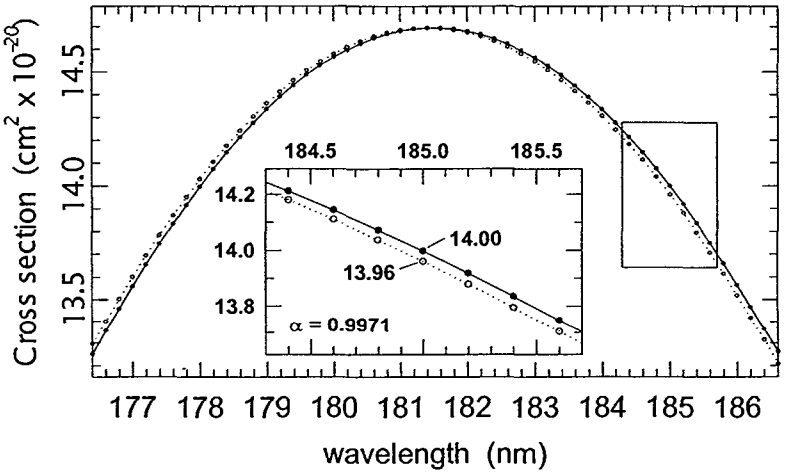

Figure 3. Representation of the theoretical shift in cross section with ^{18}O substitution according to Yung and Miller [20]. The inset plot is a detail of the highlighted section between 184 and 187 nm.

The insert plot of Fig. 3 details the section on the higher wavelength shoulder and shows that for $N_2{}^{16}O$ the cross section is 14.00×10^{-20} cm^2 at 185 nm in contrast to 13.96×10^{-20} cm^2 for $N_2{}^{18}O$. Analogous to determining the kinetic fractionation for a chemical reaction, the photolytic fractionation factor will be equal to the ratio of the heavy to light cross sections or α=0.9971. This can be expressed as an enrichment factor ε, where $\varepsilon=1000 \times (\alpha-1)$, and its value is ε_{185}= –2.9 ‰. Following this procedure, the enrichment factors can be calculated and plotted as a function of wavelength.

As can be seen in Fig. 4, the wavelength dependant enrichment factor, ε_λ, is initially positive at shorter wavelengths, passes through zero at the cross section maximum, and gets progressively more negative with increasing wavelength.

Similar constructs can be developed for each of the remaining isotopic species, all of which exhibit similar behavior with varying magnitude. However, the asymmetry of nitrous oxide leads to complications in the ^{15}N analyses because the two isotopomers, $^{14}N^{15}NO$ and $^{15}N^{14}NO$, have different predicted blue shifts. Yung and Miller [20] account for this complexity by averaging the predicted enrichment of the two ^{15}N species. If the averaged ^{15}N value and the ^{18}O value are taken as a ratio ($\varepsilon_{15N}/\varepsilon_{18O}$), a fairly uniform value between 1.1 and 1.2 is calculated over all wavelengths. This is in good agreement with the ratio observed in the stratosphere by Rahn and Wahlen [13] where $\varepsilon_{15N}/\varepsilon_{18O} = -14.5/-12.9 = 1.12$.

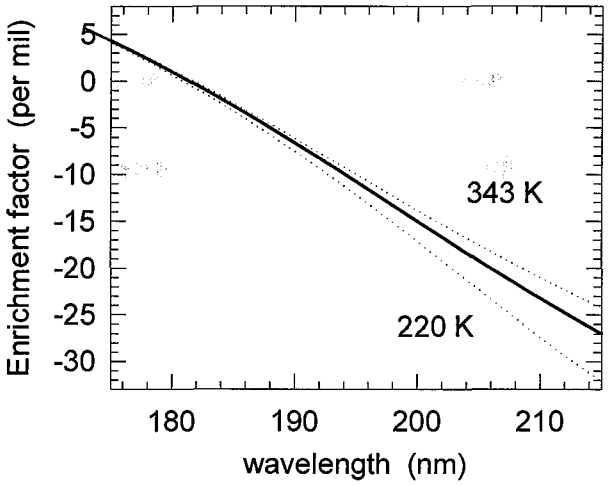

Figure 4. Theoretical wavelength dependence of the photolytic fractionation of $N_2{}^{18}O$ as predicted according to Yung and Miller [20]. Solid curve calculated at 300 K, dashed curves calculated at temperatures indicated.

In reality, the situation is complicated even further by vibrational structure in the absorption continuum. If we apply the same treatment as described above to the cross section curves of Selwyn and Johnston [22], we see that there are multiple curve crossings causing ε_λ to change sign several times over the cross section spectrum (Fig. 5). Included in Fig. 5 are the results of Rahn, et al. [23] for laser induced photolysis at two discrete wavelengths. The results compare favorably with the predicted ε_λ value at 193 nm but the data of Selwyn and Johnston [22] do not extend to wavelengths greater than 197 nm making a comparison of the 207 nm data impossible.

The results shown in Fig. 5 are approximately double that predicted by the theory of Yung and Miller [20]. While the absolute magnitudes of the observed and predicted fractionation are significantly different, the general concept of enrichment being caused by spectral shifts induced by isotopic substitution is still a valid and likely mechanism. A more rigorous treatment of the model, including non-Born-Oppenheimer effects and dipole moment surface variations, might yield better quantitative agreement.

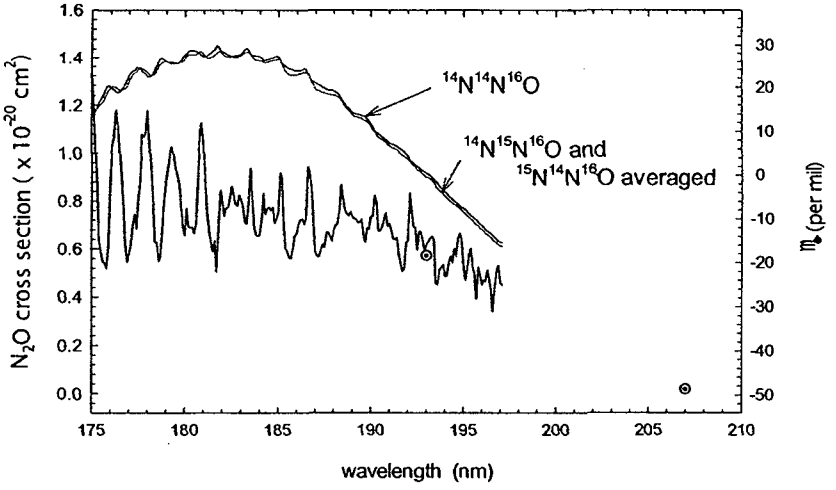

Figure 5. Top two curves show absorption cross sections for the N_2O species as indicated (reproduced from [22]). Bottom curve indicates the spectral enrichment factor calculated as described in the text. The two symbols at 193 and 207 nm are the laboratory results from Rahn, et al., [23].

The laboratory results are also significantly greater, on average, than the values observed in the stratosphere by Rahn and Wahlen [13]. It has been shown however that the standard Rayleigh fractionation model scales with $(\alpha^{1/2} - 1)$ rather than $(\alpha - 1)$ in a purely diffusive regime [24]. Exchange of air between troposphere and stratosphere occurs by advection and eddy diffusion. The former (exporting tropospheric air through the equatorial Hadley cells, with return fluxes at mid-latitudes (seasonal) and over polar regions) does not fractionate, but diffusion does. Vertical one-dimensional eddy diffusion can be used to approximate how stratospheric mixing might influence isotopic enrichment factors. For a tracer A (such as N_2O) with a chemical decay constant λ_A and no *in situ* production the steady state continuity equation can be expressed as $K_D(\partial^2[A]/\partial z^2) - \lambda_A(\partial[A]/\partial z) = 0$, with K_D being the eddy diffusion coefficient and z the height above the tropopause. With the boundary conditions $A = A_0$ at z(0) and $A = 0$ at $z(\infty)$, the solution becomes $A = A_0 \times \exp[-z\sqrt{(\lambda_A/K_D)}]$. If B is the isotopically substituted species then $R = B/A$ and $R/R_0 = \exp[-z\{(\sqrt{\lambda_B} - \sqrt{\lambda_A})/\sqrt{K_D}\}]$. With $f = A/A_0$ and $\ln(f) = -z[\sqrt{(\lambda_A/K_D)}]$ one obtains $R = R_0 f^{[\{\sqrt{(\lambda B/\lambda A)}\}-1]}$, a Rayleigh type equation with an $\alpha_{eff} = \sqrt{(\lambda B/\lambda A)}$, or $\alpha_{eff} = \sqrt{\alpha}$. Therefore in such a diffusive system $\varepsilon_{eff} \sim \varepsilon/2$. If we consider the fractionation at 205 nm to be representative of the integrated stratospheric fractionation (as in [20]) and assume that the laboratory results at 193 and 207 nm can be linearly interpolated, then the laboratory observations are in much better agreement with the stratospheric observations.

If the integrated fractionation factors under stratospheric conditions can be determined, this result may prove useful in models dealing with stratospheric transport processes and troposphere/stratosphere exchange.

4. CONCLUSIONS

Since photolysis is the most important sink of atmospheric nitrous oxide, any attempts at constructing a global N_2O budget incorporating isotopic results must take into account this photolytic fractionation. In order to determine the integrated stratospheric fractionation, enrichment factors at high spectral resolution will have to be determined and convoluted with models of stratospheric actinic flux. This will be an essential parameter if we are to advance our understanding of the global nitrous oxide isotopic budget and could also provide a new tool for examining issues of troposphere/stratosphere exchange.

Fractionation associated with the minor sink, reaction with excited atomic oxygen, must also be taken into account. The fractionation due to this reaction has been determined for the oxygen species, ^{17}O and ^{18}O, and has been shown to be mass dependent with $\varepsilon_{18O} = -6 \pm 1$ ‰ [15]. The fractionation due to photooxidation for the N species has yet to be determined. Finally, we note that the asymmetry of N_2O presents a unique opportunity to investigate an additional set of parameters with which we can constrain the N_2O budget. The fractionation for the two ^{15}N isotopomers is predicted to be significantly different according to the theory of Yung and Miller [20]. It will be interesting to determine if the biologically mediated source terms have unique ^{15}N position signatures as well.

REFERENCES

[1] Cliff, S. S., and M. H. Thiemens, The $^{18}O/^{16}O$ and $^{17}O/^{16}O$ ratios in atmospheric nitrous oxide: A mass-independent anomaly. Science, 278, 1774–1776, 1997.

[2] IPCC, (Intergovernmental Panel on Climate Change), Climate change, 1994 : radiative forcing of climate change and an evaluation of the IPCC IS92 emission scenarios, J.T. Houghton, [et al.], Ed., Cambridge [England]; New York: Cambridge University Press, 1995.

[3] Moore, H., Isotopic measurement of atmospheric nitrogen compounds, Tellus, XXVI, 169–174, 1974.
[4] Yoshida, N., and S. Matsuo, Nitrogen isotope ratio of atmospheric N_2O as a key to the global cycle of N_2O, Geochemical Journal, **17**, 231–239, 1983.
[5] Wahlen, M. and T. Yoshinari, Oxygen isotope ratios in N_2O from different environments, Nature, **313**, 780–782, 1985.
[6] Yoshinari, T., and M. Wahlen, Oxygen isotope ratios in N_2O from nitrification at a wastewater treatment facility, Nature, 317, 349–350, 1985.
[7] Kim, K.-R., and H. Craig, Two isotope characterization of N_2O in the Pacific Ocean and constraints on its origin in deep water, Nature, 347, 58–61, 1990.
[8] Kim, K.-R., and H. Craig, Nitrogen-15 and oxygen-18 characteristics of nitrous oxide: A global perspective, Science, 262, 1855–1857, 1993.
[9] Yoshinari, T., M. A. Altabet, S. W. A. Naqvi, L. Codispoti, A, Jayakumar, M. Kuhland, andA. Devol, Nitrogen and oxygen isotopic composition of N_2O from suboxic waters of the eastern tropical North Pacific and the Arabian Sea — measurement by continuous-flow isotope-ratio monitoring, Marine Chem., 56, 253–264 1997.
[10] Naqvi, S. W. A., T. Yoshinari, D. A. Jayakumar, P. V. Narvekar, A. H. Devol, J. A. Brandes, and L. A. Codispoti, Budgetary and biocheochemical implications of N_2O isotope signatures in the Arabian Sea, Nature, 394, 462–464, 1998.
[11] Dore, J. E., B. Popp, D. Karl, F. Sansone, A large source of atmospheric nitrous oxide from subtropical North Pacific surface waters, Nature, 396, 63–66, 1998.
[12] Yoshida, N., A. Hattori, T. Saino, S. Matsuo, and E. Wada, $^{15}N/^{14}N$ ratio of dissolved N_2O in the eastern tropical Pacific Ocean, Nature, 307, 442–444, 1984.
[13] Rahn, T., and M. Wahlen, Stable isotope enrichment in stratospheric nitrous oxide, Science, 278, 1776–1778, 1997.
[14] Casciotti, K., Rahn, T., Wahlen, M., Stable isotopes of N and O in nitrous oxide emissions from fertilized soil (abstract), Fall Meeting of Am. Geophys. U., San Francisco, Eos Supplement, F, 1997.
[15] Johnston, J. C., S. Cliff, and M. Thiemens, Measurement of multioxygen isotopic ($\delta^{18}O$ and $\delta^{17}O$) fractionation factors in the stratospheric sink reactions of nitrous oxide, J. Geophys. Res., 100, 16801–16804, 1995.
[16] McElroy, M. B., and D. B. A. Jones, Evidence for an additional source of atmospheric N_2O, Glob. Biogeochem. Cycles, 10, 651–659, 1996.
[17] Prasad, S. S., Potential atmospheric sources and sinks of nitrous oxide 2: Possibilities from excited O_2, "embryonic" O_3, and optically pumped excited O_3, J. Geophys. Res., 102, 21527–21536, 1997.
[18] Prasad, S. S., E. C. Zipf, and X. P. Zhao, Potential atmospheric sources and sinks of nitrous oxide 3: Consistency with the observed distributions of the mixing ratios, J. Geophys. Res., 102, 21537–21541, 1997.
[19] Zipf, E., and S. Prasad, Experimental evidence that excited ozone is a source of nitrous oxide, Geophys. Res. Lett., 25, 4333–4336, 1998.
[20] Yung, Y. L., and C. E. Miller, Isotopic fractionation of stratospheric nitrous oxide via photolysis, Science, 278, 1778–80, 1997.
[21] Selwyn, G., J. Podolske, H.S. Johnston, Nitrous oxide ultraviolet absorption spectrum at stratospheric tempertures, Geophys. Res. Lett., 4, 427–430, 1977.
[22] Selwyn, G., and H. S. Johnston, Ultraviolet absorption spectrum of nitrous oxide as function of temperature and isotopic substitution, J. Chem. Phys., 74, 3791–3803, 1981.
[23] Rahn, T, H. Zhang, M. Wahlen, G. Blake, Stable isotope fractionation during ultraviolet photolysis of N_2O, Geophys. Res. Lett., 25 , 4489–4492, 1998.

[24] Eriksson, E., Deuterium and oxygen-18 in precipitation and other natural waters: Some theoretical considerations, Tellus, XXVI, 498–512, 1965.
[25] Yoshino, K., D. E. Freeman, and W. H Parkinson, High resolution absorption cross section measurements of N_2O at 225–299 K in the wavelength region 170–222 nm, Planetary Space Science, 32, 1219–1222, 1984.
[26] Herman, J., and J. Mentall, The direct and scattered solar flux within the stratosphere, J. Geophys. Res., 87, 1319–1330, 1982.

THERMAL DIFFUSION: AN IMPORTANT ASPECT IN STUDIES OF STATIC AIR COLUMNS SUCH AS FIRN AIR, SAND DUNES AND SOIL AIR

M. LEUENBERGER, C. LANG
Climate and Environmental Physics, Physics Institute,
University of Bern, Switzerland

Abstract. Thermal diffusion induced by temperature gradients is an additional part of diffusional processes besides the ordinary or concentration diffusion. Heavier molecules normally migrate to the colder end of a static column hence leading to a slight separation in composition. Thermal diffusion can be most easily traced by isotopic ratios which are hardly exposed to changes in other processes, such as nitrogen and argon isotope ratios. Since only a limited number of thermal diffusion factors is measured up to now, it is important to have an idea how large they could be to check whether thermal diffusion effects have to be considered in interpreting corresponding isotope or elemental ratios. The Lennard-Jones (13,7) model is quite successful in estimating these factors as seen by comparison between measured and calculated values. However, there are still large uncertainties, particularly in assigning a correct critical temperature to a complex mixture such as air when considering only a ratio of two air components. It seems that the noble gas ratio Ne/Ar would be ideal to separate the gravitational enrichment from thermal diffusion due to a rather high thermal diffusion factor. However, as helium, neon has a high permeability in ice which strongly hampers this advantage. Therefore other noble gas ratios such as Ar/Kr and/or Ar/Xe are favoured for such experiments. For ice core studies the temporal variation of the thermal diffusion fractionation carries a large potential for reconstructing temperature variations over long time periods as well as synchronising gas and ice records with high precision based on very precise estimates of gas-ice age differences.

1. INTRODUCTION

Under the term "diffusion" one commonly understands the relative motion of components in a mixture of gases. Such relative motion is normally due to concentration gradients in composition within a given mixture. Diffusion as a transport process works towards removing these concentration gradients by a slow motion of the components along its concentration gradient. Diffusion originating in this way is called "ordinary" or "concentration" diffusion. However, diffusion may be caused by other inhomogeneities such as temperature gradients. This kind of diffusion is known as "thermal diffusion".

According to this understanding thermal diffusion defines the relative motion of components of a mixture arising from applied or present temperature differences within the mixture. This transport then leads progressively to concentration gradients of initially uniform composition. This, however, initiates ordinary diffusion, which will work as mentioned above to compensate these developed concentration gradients. In such a system an equilibrium means that the separating flux of thermal diffusion will be compensated by the flux of ordinary diffusion.

Thermal diffusion was first discovered in liquids in 1856 [1] and was investigated more in detail [2] some twenty years later (see for instance [3]). In gases the thermal diffusion effect was predicted before it was observed experimentally. These studies were mainly undertaken by [4, 5]. The thermal diffusion received great attention when it was shown [6] how thermal diffusion could be utilised to almost completely separate the components of a gas mixture.

An associated effect which was described first by [7] is the diffusion thermoeffect. It consists of a transport of heat as part of the process of diffusion in a gas mixture and is therefore dependent on the existence of a concentration gradient. The thermoeffect is hence connected with thermal diffusion as molecular transport of the developed temperature gradient. This temperature gradient will be produced such that the thermal diffusion will work op-

posite to the concentration or ordinary diffusion. This then normally will lead to rising temperatures for the part of lighter gas and a cooling where the heavier molecules are denser.

Both effects can be used to determine the thermal diffusion factor with advantages and disadvantages. Thermal diffusion experiments are concentration as well as temperature dependent and will give only indirect values of the thermal diffusion factor for a certain temperature. The diffusion thermoeffect on the other hand is dependent on the imperfection of gases which are interdiffusing, resulting in an additional transport of heat. Fortunately, this additional process is pressure dependent in contrast to the diffusion thermoeffect. Furthermore, to retrieve the thermal diffusion factor from diffusion thermoeffect experiments one requires thermal conductivity values of the gases used. However, this method allows one to get values for the thermal diffusion factor at a certain temperature and the sensitivity is independent of composition. Therefore, it is better suited to measure thermal diffusion factors for mixtures in which one component is rare.

Recently, [8, 9] have shown that thermal diffusion can significantly influence the air composition in a static air column such as it is present — at least during certain periods of the year — in sand dunes, firn ice and probably soil air. Based on these findings thermal diffusion effects on species otherwise constant such as nitrogen isotopes or noble gases are helpful tools in extracting information about temperature gradients in the respective air column. In case of firn air this effect will be "frozen" into the ice and can be determined as changes in the air composition extracted from bubbles in the ice. By doing this with a high resolution, one obtains a history of temperature gradients at an ice core drill site.

In this study, we are comparing different effects altering the air composition in static air columns, in particular firn air focussing on thermal diffusion. Based on models, we estimate the thermal diffusion factors of species not yet measured such as CFC's in air and Ne/Kr in air. Knowing the influential potential of thermal diffusion in contrast to other effects like to gravitational enrichment [10], we are able to disentangle these two effects and to get a better reconstruction of former temperature gradients which lead to a better calibration of the isotopic paleothermometer, i.e $^{18}O/^{16}O$ and D/H ratios in the ice.

2. RESULTS AND DISCUSSION

Thermal diffusion can be described as an additional term to the ordinary diffusion equation. For a binary mixture, no subject to external forces, this will read:

$$\bar{c}_1 - \bar{c}_2 = \overline{C}_1 - \overline{C}_2 = \frac{1}{n_{10} n_{20}} \left[D_{12} \frac{\partial n_{10}}{\partial r} + D_T \frac{1}{T} \frac{\partial T}{\partial r} \right] \tag{1}$$

where

$\bar{c}_1, \bar{c}_2$ = mean velocities of the two species of molecule, species (1) refers to the heavier molecule;

$\overline{C}_1, \overline{C}_2$ = mean thermal velocities;

n_{10}, n_{20} = volume fractions or concentrations of the two species (if n_1, n_2 are the number densities, and $n = n_1 + n_2$ then $n_{10} = {}^{n_1}\!/_{n}, n_{20} = {}^{n_2}\!/_{n}$);

D_{12} = coefficient of ordinary (concentration) diffusion;

D_T = coefficient of thermal diffusion;

$\frac{\partial n_{10}}{\partial r}, \frac{\partial T}{\partial r}$ = grad of n_{10} or T.

Both diffusion coefficients are complex functions of the relative masses, the concentrations of two molecular species, and of quantities which depend on the forces between the molecules. Since ordinary diffusion coefficients have been measured and reported more frequently in the literature, we express the thermal diffusion coefficient as $D_T = k_T D_{12}$, where k_T is the thermal to ordinary diffusion coefficient ratio. Since this factor depends very strongly on composition another parameter is introduced taking account of that — at least for our interest — negative fact, it is named thermal diffusion factor α. It is defined as:

$$\alpha = \frac{k_T}{n_{10} n_{20}} \tag{2}$$

The thermal diffusion factor α, as well as the thermal diffusion ratio k_T are dimensionless. From equation (1) it follows that for steady state condition (e.g. $\overline{C}_1 - \overline{C}_2 = 0$), the concentration gradient is only vanishing when no temperature gradient is present, if a temperature gradient exists there will be a concentration gradient of:

$$\frac{\partial n_{10}}{\partial r} = -k_T \frac{1}{T}\frac{\partial T}{\partial r} = -\alpha n_{10} n_{20} \frac{1}{T}\frac{\partial T}{\partial r} \tag{3}$$

Assuming that the temperature and concentration range are small, the thermal separation, q, can be described after integration of eq. (3) as a simple ratio of concentrations at the two temperature building the gradient:

$$q = \frac{\left[n_{10}/n_{20}\right]_{T_1}}{\left[n_{10}/n_{20}\right]_{T_2}} \tag{4}$$

In principal there are two methods available, the bulb and the swing-separator (Trennschaukel) method. For the bulb method a temperature gradient is build up by either heating one bulb or cooling the other bulb or applying both heating and cooling, which then leads to a separation of the formerly uniform distributed gas mixture. Similarly, a temperature gradient is applied to the swing-separator by heating or cooling different parts of the system. An important advantage of the swing-separator is that the thermal diffusion separation is multiplied by the number of tubes of the swing separator.

In the literature we found numerous studies of thermal diffusion during the three decades 1940 to 1970. This can be understood as separating gases became increasingly important since development of new technologies required pure materials and gases (e.g. semi-conductor industry etc.). In Table 1, we summarise the experimental results for the thermal diffusion factors, α, for mainly elemental and a few isotopic binary mixtures.

Many studies give only mean values for a certain temperature range and are therefore not directly applicable to a given temperature. As discussed below there are only a very limited number of studies — to our knowledge — which dealt with the temperature dependence of the thermal diffusion factor. In only a few studies the temperature of one bulb was fixed in their experimental setup resulting in a very precise determination of the temperature dependence.

TABLE 1. LIST OF BINARY MIXTURES EXAMINED EXPERIMENTALLY, ADAPTED FROM GREW AND IBBS [10]. FOR REFERENCES PLEASE REFER TO THIS PUBLICATION

Mixture	Temperature range [K]	Thermal diffusion factor
H_2-He	273-760	0.152
	292-90	0.137
	292-20	0.140
H_2-CH_4	300-523	0.288
	300-190	0.222
H_2-Ne	288-128	0.36
	290-90	0.28
	290-20	0.174
H_2-CO	288-373	0.330
	293-90	0.216
H_2-N_2	288-456	0.312
	288-373	0.340
	292-90	0.24
	293	0.28
H_2-C_2H_4	300-523	0.277
	200-190	0.241
	288-373	0.32
H_2-O_2	294-90	0.192
H_2-A	288-456	0.28
	286-108	0.22
	292-90	0.191
	293	0.28
H_2-C_3H_6	300-523	0.305
	232-376	0.284
H_2-C_3H_8	300-523	0.315
	231-375	0.291
H_2-CO_2	288-456	0.284
	288-373	0.298
	300-400	0.272
H_2-Rn	273-373	0.31
D_2-N_2	287-373	0.313
He-Ne	288-373	0.388
	300-400	0.364
	200-600	0.316
	293-90	0.330
	293-20	0.242
He-N_2	287-373	0.36
He-A	288-373	0.372
	300-400	0.42
	185	0.36
	293	0.38
	369	0.39
	273-90	0.31
He-Kr	288-373	0.40
	185	0.43
	293	0.448
	369	0.448
	465	0.448
He-Xe	288-373	0.403
	233	0.43
	293	0.434
	369	0.434
	465	0.434
He-Rn	273-373	0.64
N_2-A	288-373	0.181
	185	0.148
	293	0.174
	369	0.19
	465	0.191
Ne-Kr	288-373	0.267
	185	0.21
	293	0.29
	369	0.31
	465	0.32
Ne-Xe	288-373	0.253
	185	0.26
	293	0.30
	369	0.33
	465	0.37
Ne-Rn	273-373	0.23
N_2-O_2	293	0.018
	89	<0.001
N_2-A	293	0.071
	89	0.035
N_2-CO_2	288-400	0.05
	288-373	0.061
	283	0.036
	372	0.051
N_2-N_2O	288-400	0.048
O_2-A	283	0.050
A-CO_2	283	0.019
A-Kr	288-373	0.055
	185	0.038
	294	0.075
	370	0.104
	465	0.149
A-Xe	288-373	0.077
	185	0.063
	294	0.087
	369	0.139
	465	0.176

TABLE 1. (CONT.)

Mixture	Temperature range [K]	Thermal diffusion factor
A-Rn	273-373	0.024
Kr-Xe	288-373	0.016
H_2-D_2	288-373	0.173
	273-360	0.149 (20% D_2)
^{3}He-^{4}He	273-613	0.059
$^{12}CH_4$-$^{13}CH_4$	296-728	0.0080
	296-573	0.0074
^{36}A-^{40}A	638-835	0.025
	455-635	0.0218
	273-623	0.0182
	195-495	0.0146
	195-296	0.0116
	90-296	0.0071
	90-195	0.0031
$^{14}N_2$-$^{14,15}N_2$	195-623	0.0051
$^{16,16}O_2$-$^{16,18}O_2$	264	0.0099
	389	0.0128
	443	0.0145
	140-437	0.00507 to 0.0252 Ref[20]
$^{14}NH3$-$^{15}NH_3$	366	0.01
	268	-0.004
	239	-0.01
^{20}Ne-^{22}Ne	691-819	0.0346
	460-638	0.0318
	302-645	0.0302
	195-490	0.0254
	195-296	0.0233
	90-296	0.0187
	90-195	0.0162
$^{12}CO_2$-$^{13}CO_2$	239-502	-0.00085 to +0.00398 Ref[21]

Most of these mixtures had equal quantities, hence it is not easy to directly extrapolate this information to mixtures consisting of the same components but of different proportions. Some help comes from experiments discussing the dependence of the thermal diffusion factor on composition (see below).

Additionally, the thermal diffusion factor also depends on the pressure of the studied mixture.

In the following, these three important points will be discussed in more detail and documented by experimental data.

2.1. Temperature dependence

From experimental results, it is obvious that the thermal diffusion depend strongly on temperature. This is nicely documented with the thermal separation results q (see eq. (4)) obtained by [11] for $^{14}N^{15}N/^{14}N_2$, showing a distinct temperature dependence (Fig. 1). Since these authors fixed one bulb temperature during their experiments one can retrieve the thermal diffusion factor and its temperature dependence by approximating the values with a quadratic function as given in Fig. 1. This quadratic function is forced to pass through the origin (0,0) since a vanishing temperature gradient prohibits thermal separation.

Ref. [12] has shown that the slope of the measured curve at a certain temperature of the plot in Fig. 1 corresponds to the thermal diffusion factor at that temperature. Therefore, the derivation of this quadratic function is equivalent to the temperature dependence of the thermal diffusion factor, which is shown in Fig. 2. As comparison, we also give the temperature dependence obtained from the Lennard-Jones (13,7) model as described in the paragraph below "Comparison of experimental and model data". The temperature at which the thermal diffusion factor, α, changes sign is called critical temperature.

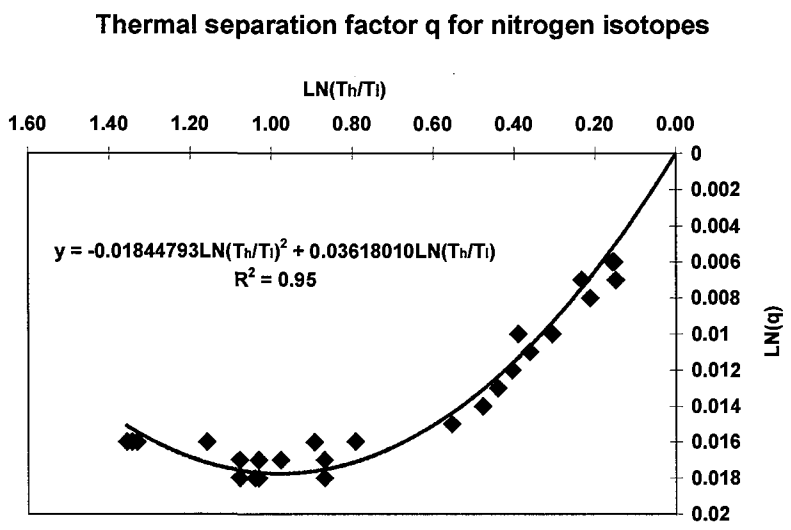

Fig. 1. Thermal diffusion separation factor q, here plotted as ln(q) as function of the logarithm naturalis of the two bulb temperatures (high, low) of the experiment.

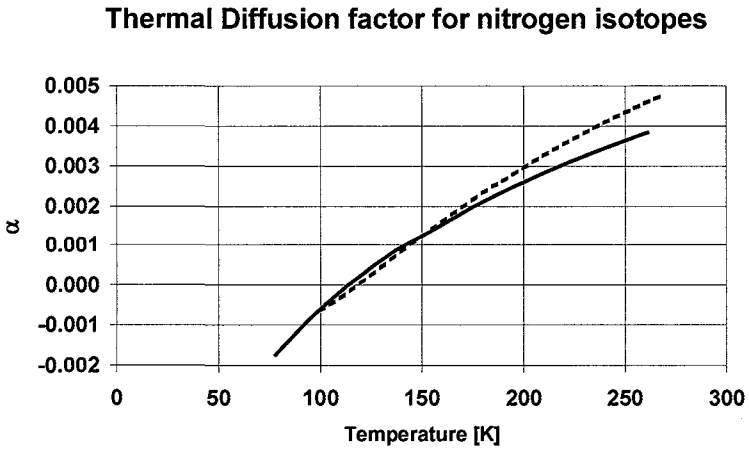

Fig. 2. Temperature dependence of the thermal diffusion factor for nitrogen isotopes as measured by [11](full line) and modelled using the Lennard-Jones (13,7) model (dashed line). The temperature at which the thermal diffusion factor, α, changes sign is called critical temperature.

Other measured values of the thermal diffusion factor for nitrogen isotopes are in good agreement with those of [11], except the values given by [13], which are offset towards higher values as is shown in Fig. 3. In this graph it is obvious that the result for higher temperatures document more or less constant thermal diffusion factors. This is the case for both isotopic mixtures for nitrogen (i.e. $^{15}N_2/^{14}N_2$ and $^{15}N^{14}N/^{14}N_2$).

2.2. Pressure dependence

From theory one would expect no dependence on pressure. In the literature, there are, however, contradicting studies. [14] have performed detailed studies in the pressure range of 3 to 80 atm and found a for all mixtures except nitrogen-methane increasing thermal diffusion factor with increasing pressure. The observed changes amounted to up to factor of eight. [14] also mentioned that the temperature and the concentration dependence (see below) were affected too. The authors explanation for such an alteration was mainly based on the imperfection of gas mixtures, since this will lead to an additional separation due to non-ideal diffusion behaviour in contrast to theory.

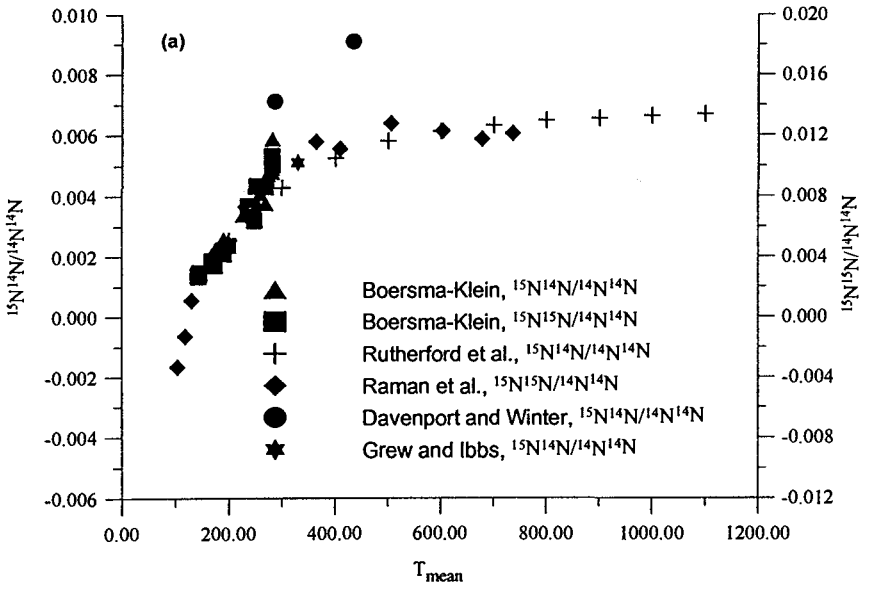

Fig. 3. Compilation of measured thermal diffusion factors.

2.3. Concentration dependence

The thermal diffusion factor is expected from theory — at least for isotopic mixtures — to decrease as the proportion of the heavier component increases and being more pronounced for high mass ratios. Experimental results as function of composition support this view, even for non-isotopic compositions, but are significantly larger than expected from theory.

For a given non-isotopic mixtures it is, however, very difficult to predict such a dependence safely because of the complex dependence of the theoretical thermal diffusion values on the relative gas proportions (see for instance [3]).

2.4. Comparison experiment and model data

A prerequisite of the comparison between experimental and model results is the existence of suitable models for description of atomic or molecular interactions based on which thermal diffusion effects can be calculated. There are — to the authors knowledge- five different model approaches which more or less capture the main effects of thermal diffusion. These are:

- Rigid elastic spheres
- Inverse-power repulsion ($F=kr^{-\nu}$)
- Lennard-Jones model ($F=kr^{-\nu}-k'r^{-\nu'}$)
- Sutherland model
- Buckingham model (exp-6 Potential)

F is the resulting force, k,ν and k',ν' refer to the repulsive force and to the attractive force, respectively.

The Lennard-Jones model is used with different sets of force indices such as (13,7) or (12,7) or (9,5). Of these 5 models listed above, the Lennard-Jones and the Buckingham model are the only ones showing a temperature dependence for the thermal diffusion factor. Since the Lennard-Jones model is widely used for instance for viscosity and ordinary diffusion coefficient calculations we used this model to estimate the thermal diffusion factors, which are not yet measured (for example: CFC-12, $\delta^{13}CH_4$ etc.). In our calculations we used the (13,7) model since this was tuned to match the viscosity data of several gases mixtures.

For calculation we used tabulated values for variables A, B and C according to *Grew and Ibbs* [3]. The most important point was to estimate the change of the critical temperature as the proportions of the two components of the regarded mixtures are very different (see Table II). As can be seen from Fig. 4, the differences in isotopic compared to elemental mixtures are large. There is a difference of a factor of 10 for the thermal diffusion factors between most of the elemental and isotope mixtures. But all of them show similar temperature dependencies with higher values for increasing temperatures. The values on the other hand can become negative at a certain temperature, the so-called critical temperature. For carbon dioxide this critical temperature is rather high at approximately 280K. This means that even at ambient temperatures we cannot definitely expect an increase of ^{13}C at the colder end for carbon dioxide. For nitrogen and oxygen isotope mixtures this is not a problem due to the much lower critical temperatures around 130 and 140K for turning to negative values.

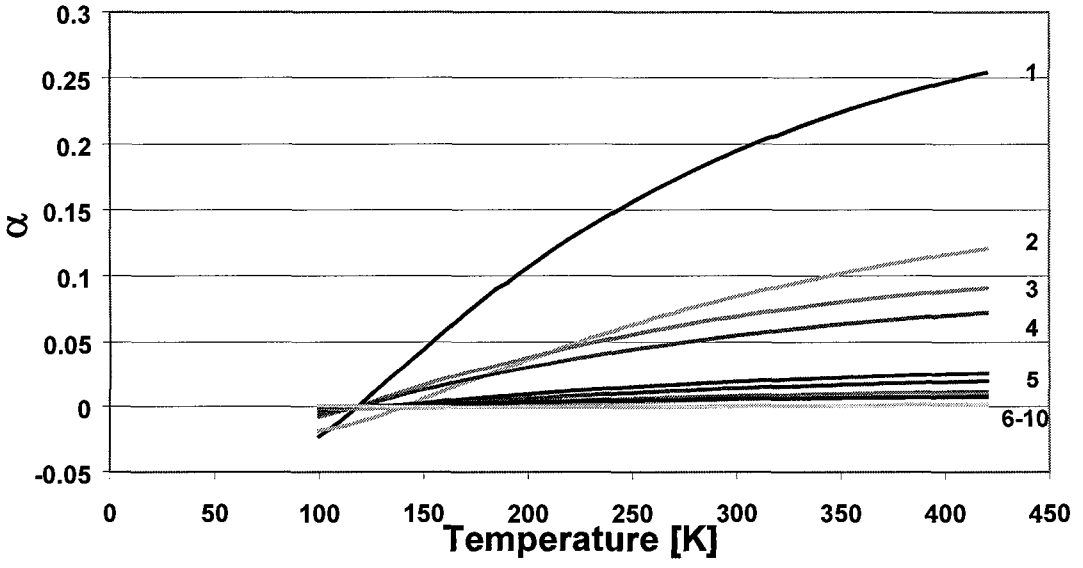

Fig. 4. Calculated thermal diffusion factors for isotopic and elemental mixtures based on Lennard-Jones (13,7) model.1: CFC-12/N_2; 2: Ar/Ne; 3: CO_2/N_2; 4: Ar/N_2; 5: O_2/N_2; 6: $^{40}Ar/^{36}Ar$; 7: $^{18}O/^{16}O$; 8: $^{13}C/^{12}C$ of CH_4; 9: $^{15}N/^{14}N$ of N_2; 10: $^{13}C/^{12}C$ of CO_2. Details for curves 6-10 see in Fig.5 .

However, one has to bear in mind that the calculation is based on an estimate of the critical temperature according to the proportions of the mixtures. Another approach would be to use geometric means of the critical temperatures of the mixtures components.

In Fig. 5, the thermal diffusion factor of several air components are given as calculated from the Lennard-Jones model. The main difference between the isotope and elemental mixtures originates from the mass dependencies of the thermal diffusion factor which is according to Chapman-Enskog theory given by

$$\alpha(T_c, M) = \alpha'(T_c) \cdot M = \alpha'(T_c) \cdot \frac{m_1 - m_2}{m_1 + m_2} \tag{4}$$

where $\alpha'(T_c)$ is mass-independent and m_1 and m_2 are the masses of the binary mixture.

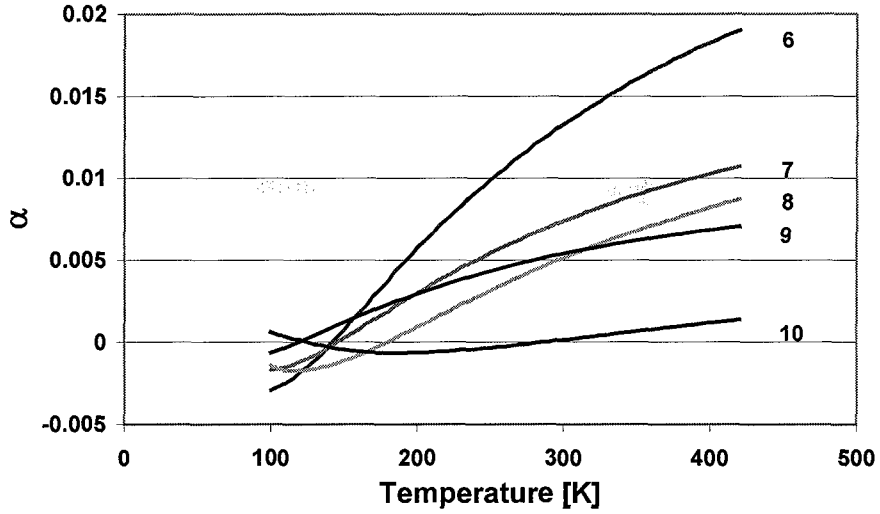

Fig. 5. Calculated thermal diffusion factors for isotope mixtures only based on the Lennard-Jones (13,7) model. 6: $^{40}Ar/^{36}Ar$; 7: $^{18}O/^{16}O$; 8: $^{13}C/^{12}C$ of CH_4; 9: $^{15}N/^{14}N$ of N_2; 10: $^{13}C/^{12}C$ of CO_2.

Therefore, the thermal diffusion increases linearly with the proportionate mass difference. This is indeed seen in Fig. 6, in which the calculated thermal diffusion factors are plotted against this mass difference, indicating that the influence of the critical temperature T_c is not very high. This certainly is a fact of the relative proportions of the mixtures components being close to 1 or close to zero, respectively, yielding very similar critical temperatures for binary mixtures of air components (see Table 2). The critical temperature influences mainly the temperature where α changes sign. Figure 5 becomes fully linear only when α is plotted against the reduced temperature, which is T/T_c. Experimental results show that the change in sign for a given binary mixture occurs at a slightly lower temperature than expected from the tabulated critical temperature in any physics handbook but slightly higher than the extracted temperature from the force constant ε (minimum potential energy of interaction of two molecules) based on viscosity measurements (see for example in [3]).

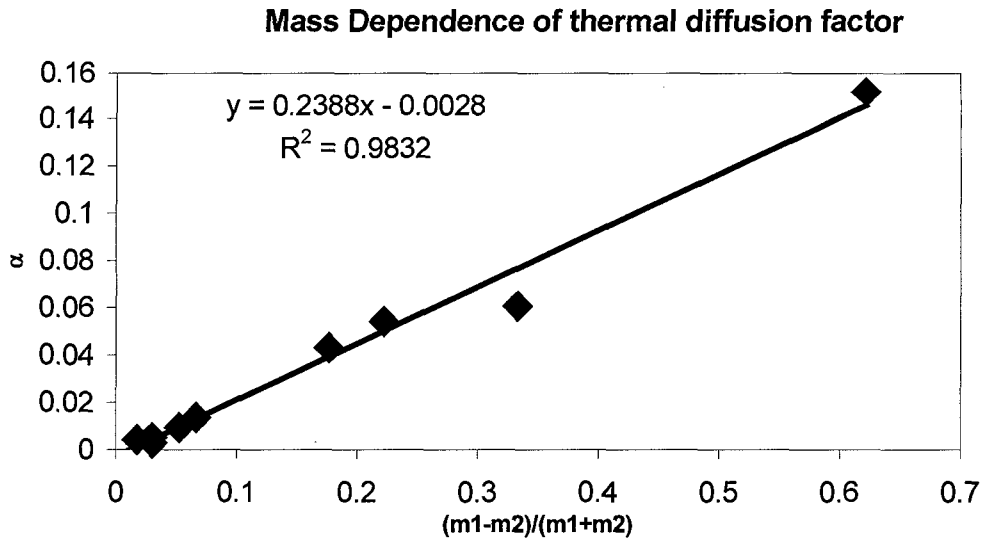

Fig. 6. Mass dependence of the calculated thermal diffusion factors for the Lennard-Jones (13,7) model.

TABLE 2. CALCULATED THERMAL DIFFUSION FACTORS FOR DIFFERENT BINARY MIXTURES. GRAVITATIONAL ENRICHMENT IS BASED ON A 70M THICK DIFFUSIVE FIRN ZONE

T0=245K	CO_2	CH_4	N_2	O_2	Ar40/Ar3	O_2/N_2	Ar/N_2	CO_2/N_2	Ar/Ne	CFC-12/N2
M=(m1-m2)/(m1+m2)	0.01124	0.0303	0.01754	0.0303	0.05263	0.06667	0.17647	0.22222	0.33333	0.6216216
α	-0.0004	0.00291	0.00421	0.00518	0.00948	0.01528	0.04305	0.05421	0.06076	0.1516397
Critical temperature K	304.15	190.85	126.25	154.761	150.86	132.06	126.55	126.3	150.66	126.25
Thermal effect for 10K grad	-0.0146	0.11651	0.16827	0.20741	0.37925	0.61147	1.72366	2.17102	2.43384	6.0848355
Gravitation effect (per mil)	0.3	0.3	0.3	0.6	1.2	1.2	3.6	4.8	6	27.6
Mass difference (in mass un	1	1	1	2	4	4	12	16	20	92
Gravitation/Thermoeffect	-20.539	2.57483	1.78282	2.89279	3.16418	1.96248	2.08858	2.21095	2.46524	4.5358663

Application of such models show that the estimates are better for isotopic ratios than for elemental ratios (see also concentration dependence above) and that the concentration dependence is simply assumed to be proportional to the concentration ratio of a specific mixture. The main difficulty is to assign a correct critical temperature to the mixture since the real mixture (air) consists of many more than only two components. Therefore, the estimates as given in Table 2 and Figs 4 and 5 have to be taken with care and a high uncertainty has to be assigned to them.

2.5. Thermal diffusion effect for a 10K temperature gradient

When using the calculated thermal diffusion factors from Table 2 and applying a 10K temperature gradient, which is rather large even in terms of climate change, the expected effect is always less than 1% for the binary mixtures presented here (Fig. 7). The isotope mixtures are clearly less affected than the elemental mixtures. However, since the precision of the isotope measurements (a few hundreds of a per mil) generally exceeds that of pure concentration determinations significantly (a few tens of a per cent), those smaller isotopic effects can be better traced. Since the precision of concentration measurements is of the same order of magnitude as the thermal diffusion effect for a rather large temperature gradient, it will not be very important for interpretation of the concentration variations of greenhouse

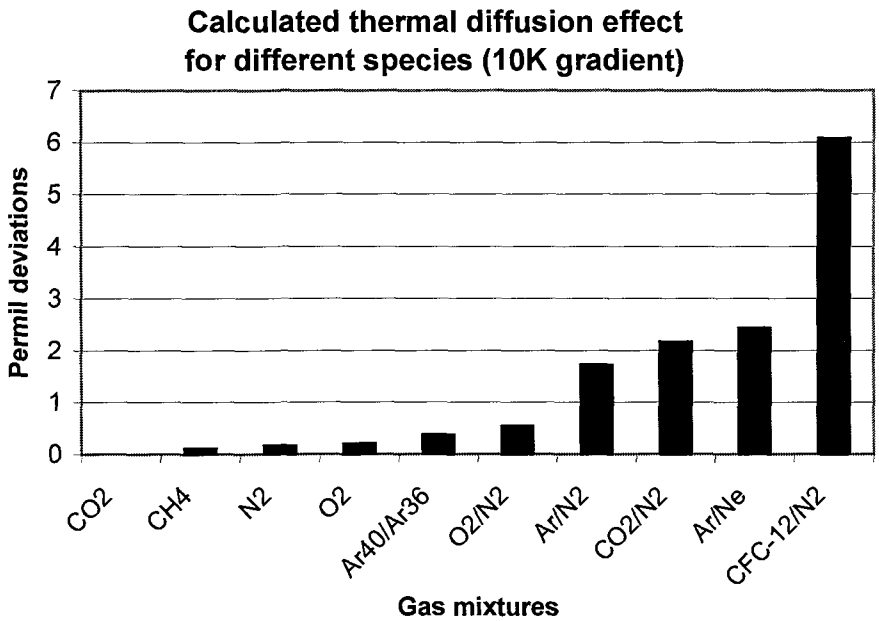

Fig. 7. Equilibrium per mil deviations for different binary mixtures as expected from thermal diffusion by applying a 10K temperature gradient.

gases, since their atmospheric concentration can change several ten percent over a period of a couple of thousand years [15, 16]. However, for noble gases and isotopes this effect has to be accounted for carefully since it is of the same order of magnitude as fractionation changes due to reservoir exchanges (e.g. $\delta^{13}CO_2$, $\delta^{18}O^{16}O$). Hence a good knowledge about the partitioning between the so-called firn column effects — the thermal diffusion and the gravitational enrichment (see below) — and the real atmospheric variations induced by exchanges of the gas species among the main reservoirs (the atmosphere, the biosphere, the ocean). Firn experiments — they were introduced by [10] — are very helpful in this respect since they allow us to study the firn specific effects which in turn will lead to an improvement of the firn modelling. This is essential for the interpretation of the ice core derived results.

2.6. Comparison thermal diffusion effect and gravitational enrichment

The thermal diffusion effect is a powerful tool in paleoclimatological studies in ice cores for estimating first the gas-ice age differences and improving therefore the synchronisation of gas and ice records. Secondly, and even more important, is the potential to use this effect to calibrate the paleothermometer as shown by [17, 18]. From Fig. 8, it is clear that both thermal diffusion as well as gravitation induced enrichment are increasing going from isotopic to elemental ratios, the latter effect is more important in absolute terms and should therefore also be considered for very large mass differences (e.g. CFC's etc). Both effects vary over time depending primarily on temperature variations, but is much more pronounced for thermal diffusion which even can change sign due to a reversal of the long-term temperature gradient. Changing from a cold to a warm state would induce an additional enrichment to the gravitational effect whereas a change from a warm to cold state would lower this enrichment. On a monthly basis one can easily observe the seasonal change in temperature due to thermal diffusion for example in the nitrogen isotopes in the uppermost firn [19]. In contrast, gravitational enrichment shows a much slower reaction to temperature and accumulation rate change (which again is a function of temperature) due to a slow response of these two parameters on the firn densification and hence on the close-off depth.

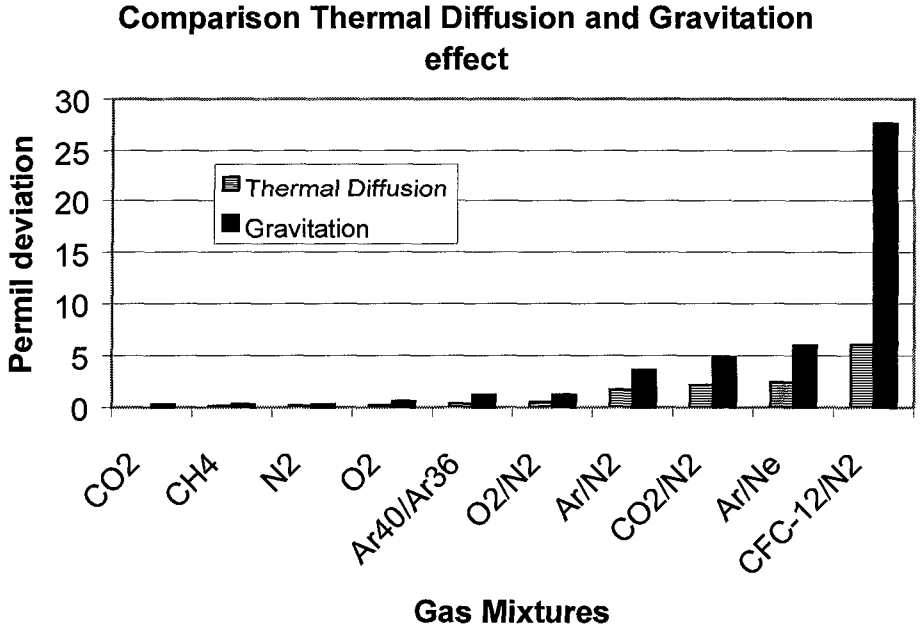

Fig. 8: Comparison of equilibrium thermal diffusion effect(10K temperature gradient) and gravitational enrichment for a 70 m thick diffusive column of the firn layer.

3. CONCLUSIONS

The temperature dependence of thermal diffusion can well be accounted for by the Lennard-Jones model. The theoretical estimates are in rather good agreement with measured thermal diffusion factors for binary isotopic mixtures. It is significantly less precise for binary elemental ratios. A further important difficulty is the estimation of such thermal diffusion factor for multi-gas mixtures such as air. This difficulty is mainly due to assigning a correct critical temperature to such a mixture. Nevertheless, the thermal diffusion effect seems to be small enough compared to the general precision of concentration measurements that this effect has not to be considered. However, for isotope ratios — for which the precision is far better- it is advisable to take this effect into account for their interpretation.

For ice core studies, thermal diffusion is an important effect mainly for isotopic compositions, with a contribution in the order of the gravitational enrichment. The advantage of this effect is that it varies strongly with time due to abrupt temperature changes. Since vertical temperature gradients within a static column can be either positive or negative the thermal diffusion values show also changes of sign. Therefore, fast variations of $\delta^{15}N$ as measured from ice cores document abrupt variations of temperature and are superimposed on the gravitational enrichment which changes at a lower rate.

ACKNOWLEDGEMENTS

We like to thank Jeff Severinghaus for helpful information regarding older thermal diffusion factor publications. We also would like to express our thank to an anonymous reviewer who's comments helped improving this paper. This work was supported by the EC Projects Mileclim, Firetracc/100 and Alpclim.

REFERENCES

[1] C. LUDWIG, S. B. Akad. Wiss. Wien, 20 (1856), 539.
[2] C. SORET, Arch. Sci. Phys. Nat. Genève, 2 (1879), 48.
[3] K. E. GREW, T. L. IBBS, Thermal Diffusion in Gases, University Press, Cambridge, 1952.
[4] D. ENSKOG, Ann. Phys. Lpz., 38 (1911), 731.
[5] S. CHAPMAN, T. G. COWLING, The Mathematical Theorie of Non-Uniform Gases, University Press, Cambridge, 1970.
[6] K. CLUSIUS, G. DICKEL, Naturwissenschaften, 28 (1938), 711.
[7] L. DUFOUR, On the diffusion of gases through porous partitions and the accompanying temperature changes, Pogg. Ann., 148 (1873), 490.
[8] J. P. SEVERINGHAUS, M. L. BENDER, R. F. KEELING, W. S. BROECKER, Fractionation of soil gases by diffusion of water vapor, gravitational settling and thermal diffusion, Geochimica and Cosmochimica Acta, 60 (1996), 1005-1018.
[9] J. P. SEVERINGHAUS, T. SOWERS, E. J. BROOK, R. B. ALLEY, M. L. BENDER, Timing of abrupt climate change at the end of the Younger Dryas interval from thermally fractionated gases in polar ice, Nature, 391 (1998), 141-146.
[10] J. SCHWANDER, J.-M. BARNOLA, C. ANDRIÉ, M. LEUENBERGER, A. LUDIN, D. RAYNAUD, B. STAUFFER, The age of the air in the firn and the ice at Summit, Greenland, J. Geophys. Res., 98 (1993), 2831-2838.
[11] V. BOERSMA-KLEIN, A. E. DE VRIES, The influence of the distribution of atomic masses within the molecule on thermal diffusion, Physica, 32 (1966), 717-733.

[12] K. E. GREW, Thermal diffusion in mixtures of the inert gases, Proc. Roy. Soc. A, 189 (1947), 402-414.
[13] A. N. DAVENPORT, E. R. S. WINTER, Diffusion properties of gases: part V. — The thermal diffusion of carbon monoxide, nitorgen, and methane, Trans. Faraday Soc., 47 (1951), 1160-1169.
[14] E. W. BECKER, Z. Naturforsch., 5a (1950), 457.
[15] T. BLUNIER, J. SCHWANDER, B. STAUFFER, T. STOCKER, A. DÄLLENBACH, J. INDERMÜHLE, J. TSCHUMI, D. CHAPPELLAZ, D. RAYNAUD, J.-M. BARNOLA, Timing of the Antarctic Cold Reversal and the atmospheric CO_2 increase with respect to the Younger Dryas event, Geophysical Research Letters, 24 (1997), 2683-2686.
[16] A. INDERMÜHLE, T. STOCKER, F. JOOS, H. FISCHER, H. J. SMITH, M. WHALEN, B. DECK, D. MASTROIANNI, J. TSCHUMI, T. BLUNIER, R. MEYER, B. STAUFFER, Holocene carbon-cycle dynamics based on CO_2 trapped in ice at Taylor Dome, Antarctica, Nature, 398 (1999), 121-126.
[17] M. LEUENBERGER, C. LANG, J. SCHWANDER, $\delta^{15}N$ measurements as a calibration tool for the paleothermometer and gas-ice age differences. A case study for the 8200 B.P. event on GRIP ice, JGR, 104 (1999), 22163-22170.
[18] C. LANG, M. LEUENBERGER, J. SCHWANDER, S. JOHNSEN, 16°C Rapid temperature variation in Central Greenland 70000 years ago, Science, 286 (1999), 934-937.
[19] M. LEUENBERGER, C. LANG, J. SCHWANDER, Seasonal thermal diffusion effects, (in preparation).
[20] B. P. MATHUR, W. W. WATSON, Thermal diffusion in isotopic $^{16}O_2$-$^{18}O_2$, Journal of Chemical Physics, 51 (1969), 2210-2214.
[21] B. P. MATHUR, W. W. WATSON, Isotopic thermal diffusion factor for CO2, Journal of Chemical Physics, 51 (1969), 5623-5625.

LIST OF PARTICIPANTS

Allison, C.	CSIRO-Atmospheric Research, P.O. Box 1, Aspendale, Victoria 3195, Australia
Bhattacharya, S.K.	Physical Research Laboratory, Ahmedabad 380 009, India
Ciais, P.	Laboratoire des Sciences du Climat et de l'Environnement, Centre d'Etudes de Saclay, F-91191-Gif-sur-Yvette, France
Florkowski, T.	Faculty of Physics and Nuclear Techniques, University of Mining and Metallurgy, Al. Mickiewicza 30, PO-30-059 Krakow, Poland
Francey, R.	CSIRO-Atmospheric Research, P.O. Box 1, Aspendale, Victoria 3195, Australia
Guevara, R.	Comision Ecuatoriana de Energia Atomica, Juan Larrea No. 534 y Riofrio, Quito, Ecuador
Holy, K.	Faculty of Mathematics and Physics, Comenius University, Mlynska Dolina, SK-842 15 Bratislava, Slovakia
Leuenberger, M.	Climate and Environmental Physics, Physics Institute, University of Bern, Sidlerstrasse 5, CH-3012 Bern, Switzerland
Levin, I.	Institut für Umweltphysik, Universität Heidelberg, Im Neuenheimer Feld 366, D-69120 Heidelberg, Germany
Lowe, D.	National Institute of Water and Atmospheric Research Ltd, 301 Evans Bay Parade, Greta Point, Wellington, New Zealand
Meijer, H.A.J.	Centrum voor Isotopen Onderzoek, Nijenborgh 4, NL-9747 AG Groningen, Netherlands
Tenu, A.	National Institute of Meteorology Hydrology & Water Management, Sos. Bucuresti Ploiesti 97, Bucharest, RO-71552, Romania
White, J.W.C.	Centre for Geochronological Research, INSTAAR, Campus Box 450, University of Colorado, Boulder, Colorado 80309-0450, United States of America
Wahlen, M.	Geological Research Division, Scripps Institution of Oceanography, University of California, La Jolla, California 82093, United States of America
Zouridakis, N.	NCSR Demokritos, Isotope Hydrology Laboratory II, Institute of Physical Chemistry, 53 10 Aghia Paraskevi, Athens, Greece